The effectiveness of an isolated slotted blade in delaying detachment of flow, with potential application to centrifugal compressor rotor blades

Fowler, H. S.; Bond, G. S.; Rudnitski, D.

Publisher's version / Version de l'éditeur:
https://doi.org/10.4224/40003824
Laboratory Memorandum (National Research Council Canada. Division of Mechanical Engineering. Engine Laboratory); no. NRC-ENG-68, 1971-06

L.O. 14560 A.
FILE M2-17-13.C-19
PREPARED BY H.S.F.
CHECKED BY J.C.

NATIONAL RESEARCH COUNCIL OF CANADA
DIVISION OF MECHANICAL ENGINEERING
OTTAWA, CANADA
LABORATORY MEMORANDUM
SECTION Engine Laboratory

NO. NRC-ENG-68
PAGE 1 OF 144
COPY NO. 27
DATE June 1971

SECURITY CLASSIFICATION Open

SUBJECT The Effectiveness of an Isolated Slotted Blade in Delaying Detachment of Flow, with Potential Application to Centrifugal Compressor Rotor Blades

PREPARED BY H.S. Fowler
G.S. Bond
D. Rudnitski

ISSUED TO Internal

Table of Contents

LIST OF ILLUSTRATIONS

1.0 INTRODUCTION

An experimental investigation on the flow in centrifugal impellers has been in progress in the Engine Laboratory since 1963. It has become very clear that the detachment of flow from the blade surfaces is one of the major influences on the poor distribution of flow in the impeller channels. From mid 1968 to mid 1969 a general exploration was carried out on this flow detachment in impeller channels and on isolated blades, and was reported in Lab Memo NRC-ENG-62 (Ref.1). It was there concluded that the most useful method of delaying this detachment in a compressor rotor appeared to be the use of slotted blades. Since that date, experiments have been carried out on the flow control obtainable from slotted blades under conditions simulating an impeller rotor. This Memo presents a report on this phase of the investigation.

2.0 AIM OF INVESTIGATION

It had been shown that slotted blades appear likely to present a practical method of delaying flow detachment in a centrifugal compressor impeller. It was, therefore, necessary to assess quantitatively the aerodynamic capabilities and penalties of such a system, and also to discover an optimum configuration for application to a rotor. The ultimate aim of the programme is to raise the efficiency and broaden the operating range of centrifugal compressors.

3.0 THE EXPERIMENTAL APPROACH USED

The impeller is usually considered as a group of rotating quasi-radial channels, and therefore a problem in diffusing channel flow, with superimposed inertial effects due to rotation. However, it is also valid to regard it as a space containing a number of aerofoils, moving in a flow whose natural path is radial (in absolute coordinates) or a spiral (relative to the rotating blades). The work done by the impeller through its blades is therefore characterised by the degree by which they deflect the flow out of this natural path. In the relative reference frame, this implies the deflection of the flow to a different spiral path, while in the absolute frame, the work of the impeller blading is measured by the amount the flow is deflected from its original (absolute) radial path. In such an absolute framework a stationary straight blade at 0° incidence would do no work. However, a cambered blade would deflect an initially straight flow, and give a valid simulation of a rotating impeller blade doing work on the fluid flowing past it. Hence it may properly be argued that the deflection of the flow produced by the blade will bear a relation to its effectiveness in the impeller, and the total pressure loss will be a measure of the inefficiency of the process. Furthermore, while the single blade will accord with the conception of the impeller as a set of rotating aerofoils, the flow on the left and right sides of the blade will correspond in a very real way to that on the right and left sides respectively of a rotating channel. Moreover, it was concluded in NRC Report ME229(2), from experimental evidence reported there, that even when discussing the impeller as a series of rotating channels, the exit-end interaction between flow in adjacent channels exerts a major effect on the flow in each channel. This interaction is, of course, fully reproduced in the "single-blade" experiment.

This model of the impeller as a set of rotating aerofoils is of additional merit, since it brings into play the well-developed body of information on axial flow cascades, with certain concepts such as the effects of incidence, spacing/chord ratio (or 1/solidity), camber angle, deflection and deviation angles, critical Mach number, the effect of aerofoil thickness and shape, and so on.

While the data accumulated in the axial flow field do not apply directly and quantitatively, the general concepts and tendencies certainly appear to have quite direct bearing on the centrifugal rotor blading.

It was therefore decided that the relative merits of various blade-slotting arrangements could be assessed quickly and simply by a straight two-dimensional wind-tunnel experiment, in which a single blade of considerable camber was placed at a series of incidences to an incoming air stream, and pitot-yawmeter traverses downstream of the blade measured the deflection and stream total pressure. The deficit of total pressure in the wake measured the loss suffered, and the measured turning angle of the air (camber minus deviation) gave the actual turning exerted by the blade of given camber angle. The incidence at which the blade "stalled" and the flow detached from it was naturally of critical importance, as this was considered to give some relative indication of the onset of stall in the compressor impeller.

The experiments were carried out at approximately constant air speed in a simple two-dimensional blowing tunnel with freedom of exit. The total pressure loss was divided by free-stream dynamic pressure at blade-inlet plane, and expressed as a non-dimensional Loss Factor, and the exit airflow angle was measured directly as the deviation from the exit blade direction, while the blades were set at a series of incidence angles between inlet blade direction and free stream direction.

A pitot-static probe was temporarily inserted into the tunnel one chord upstream of the blade to measure the inlet dynamic pressure before each run, and the outlet pressure and flow directions were measured at mid blade height by a combined pitot-arrowhead yaw-meter probe traversed just downstream of the blade trailing edge. The tunnel and traverse planes are shown in Fig. 1. A diagram of blade and flow-angle nomenclature is given in Fig. 2.

4.0 ARRANGEMENTS TESTED

An index of the arrangements tested is presented in Fig. 3; A summary of Loss Factors and Deviation Angles plotted on a base of Incidence Angle is presented in Figs. 4,5, 6 and 7. Details of blade and slot profiles, and traverse data are presented in Appendix "C".

4.1 Description of Blades

In all cases the blades tested were of C-4 Section (see Appendix "A") with max. thickness (at 30% C) equal to 12% C. The chord length (C) was in all cases 8.7", and the chord line was a straight line in blades A and B, and a circular arc of 6.6" radius, subtending 75°, in all other blades. The blades are therefore orthodox axial compressor aerofoils. The blades were all 5" in the spanwise direction.

4.2 Description of Slots

Four rules were proposed for the design of the slots as follows:

1) The slot must inhale with minimum loss and disturbance from flow parallel to the blade pressure surface.

2) The radius of curvature of the slot centreline must be kept as large as possible, and the rate of change of area shall be roughly constant through the slot.

3) The slot must eject flow as nearly parallel to the blade suction surface as possible, with as little disturbance as possible.

4) Total pressure loss in the slot must be a minimum.

Conditions 1, 2, and 3 control the slot centre-line geometry. Ideally, it should be formed by two circular arcs of equal radii. In practise it is made as near to this as possible.

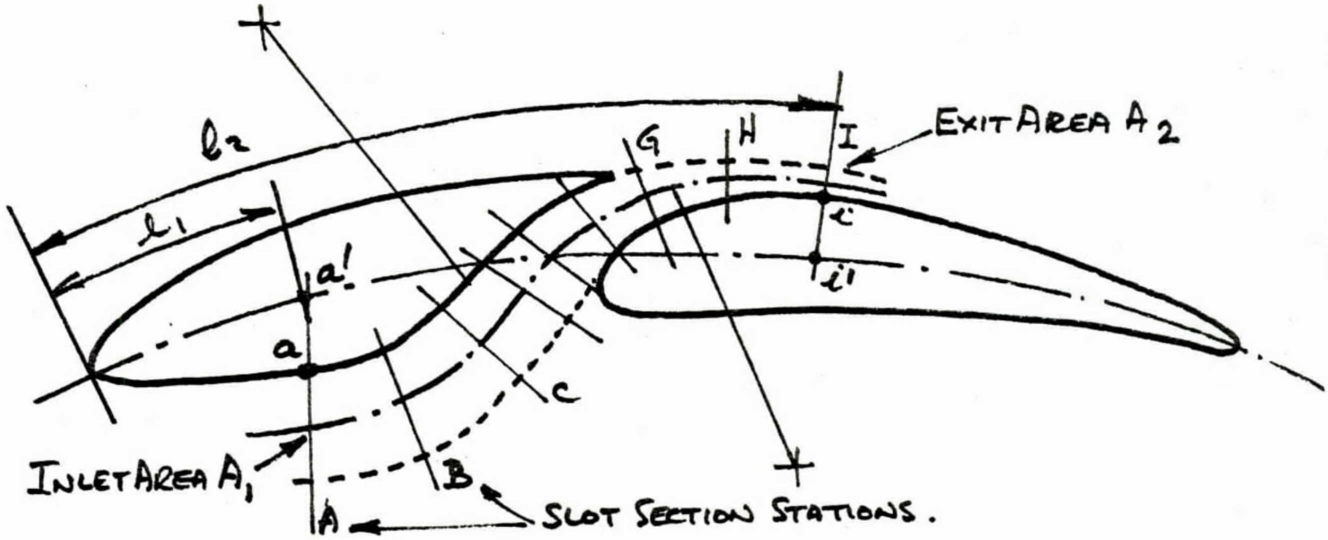

These slot centreline radii are controlled by the aerofoil thickness, the required area ratio (A_1/A_2) through the slot, and the points a & i on the surfaces, where flow is to enter and leave. These points are governed by the flow field round the aerofoil, and were determined experimentally. They are defined by the percentage of chord aft of the leading edge (l_1 and l_2, to stations a' & i' on the chord line). Condition 4 is complex. Ideally, the slot should admit air at the local velocity near the slot inlet, and accelerate it at a reasonably constant rate, so that it leaves the slot at the corresponding local velocity in the region of the slot exit, assuming ideal flow around the aerofoil. If a flow quantity through the slot is chosen, and the flow field round the aerofoil specified, the slot profile can then be defined.

In point of fact, the experiments reported in reference 1 gave sufficient indication of the size of slot required to give an effective flow, without letting too much of the total airflow "blow through the blades". Also, since the blade has to operate over a range of angles of incidence, which means a range of different velocity distributions round the blade, the degree of acceleration from slot inlet to outlet must be some compromise selected to cover a range of values. It was found that an Area Ratio A_1/A_2 of around 5.5 produced satisfactory results, with a Flap Gap (see Section 4.3) of from 2.0% to 2.5%.

Finally, the slot inlet lip is faired into the aerofoil pressure surface with radius to avoid detachment either from the slot wall or off the aerofoil surface downstream of the slot lip, as the incidence and local flow change.

The points on pressure and suction surfaces where the slot enters and leaves were initially chosen from inspection of boundary layer detachment points visualised by smoke; from then on the effects of slot shift, different numbers of slots, etc., were investigated in the experimental programme described herein.

The slots used were designed in a very empirical manner as the above rules were evolved. They are analysed in retrospect in Figs. 8, 9 and 10 on the basis of these rules.

4.3 Comparison with Foster's Paper (AIAA 71-96) (Ref.3)

A paper by Foster of RAE, ("The Flow round wing sections with high-lift devices") describing experiments on slots in wings became available in Jan. 1971. It discussed work directly comparable to the investigation described here, although with much lower camber and deflection angles. Foster uses "Flap Gap" $\equiv$ (slot throat width/chord) % as the parameter describing his geometries, and his results show a strong optimum over the range from 1.5% to 2.5%, with a peak at about 2.2%. It was observed with considerable interest that the two slots in the most successful arrangement described in the present paper (as typical of the slots tested in the present programme) have "Flap Gap" values of 2.42% and 2.06%.

The flow visualisations carried out in this programme also agree with Foster's conclusion, based on wake pressure surveys, (Foster's Fig.7) which is that:- "The optimum gap is at, or very near to, the smallest gap at which the boundary layer on the flap and the boundary layer on the wing lower surface are just separate". In other words, the gap must be wide enough to allow a jet of free-stream air from the pressure side of the aerofoil to be transferred onto the suction side downstream of the slot, so that the suction side is insulated from the low energy boundary layer which has built up upstream of the slot.

Such qualitative and quantitative agreement between results derived from very different sources was extremely encouraging. It also suggested that provided this conclusion was realised, the system should not be sensitive to Reynolds Number changes.

5.0 EXPERIMENTS AND ANALYSIS

5.1 Experimental Procedure

The blade was clamped between two transparent plastic discs with pins and screws, and the assembly placed in the tunnel, as shown in Fig. 1. A constant speed ½ H.P. electric motor drove the 20" d. axial fan at 1725 r.p.m., supplying an airstream at approximately 50 ft/second to the test section. The blade and disc assembly was rotated to the desired incidence angle and clamped, and the two loose inlet walls were set to give a parallel inlet channel of suitable width, and also clamped.

The inlet airspeed varied a little between tests due to different blockage at each incidence setting. A calibrated pitot-static probe was put into the tunnel on the centre-line upstream of the blade, and the inlet dynamic pressure measured. This probe was removed, and the traversing pitot-yawmeter probe inserted in the downstream traverse slide. This slide moved in a slot ½" downstream of the blade, in the upper plastic disc. The slot ran at right angles to the blade exit axis [i.e. to the exit flow direction assuming zero deviation] and the yaw scale was calibrated directly in deviation angles. Readings of total pressure and air exit angle were taken every .2" across a 7.2" arbitrary "passage", with extra readings each .1" where needed.

This process was repeated at a number of incidence angles. The flow was examined visually at each setting with a smoke plume from a standard Ammonia-Sulphur dioxide smoke probe. Unstable flow, points of detachment, stall-bubbles, etc. were clearly visible.

5.2 Analysis of Results

The total pressure and exit angle traverses were plotted (for example see Appendix "C"). It was clearly understood that this program aimed at a comparative evaluation of the various blade and slot configurations, and not at determining absolute values. It was therefore considered legitimate to refer all results to an arbitrary passage width of 7.2".

While inspections of the total pressure curve showed the width and character of the blade-wake, a simple graphical integration gave the mean total pressure loss across the blade-wake, and this mean loss divided by the inlet dynamic pressure was accepted as the Pressure Loss Factor for the configuration, after normal cascade practise. [See Appendix "B" - Calculation of Loss Factors].

A similar graphical integration gave a Mean Deviation Angle across the passage and blade-wake.

The complete data on blade profiles, pressure loss and exit angle traverse profiles, together with the plots of Loss Factor versus Incidence and Deviation versus Incidence derived from these mean values are given in Appendix "C".

6.0 DISCUSSION OF RESULTS

In the main, this discussion is based on the curves of Loss Factor and Deviation plotted against Incidence Angle in Figs. 4, 5, 6 and 7. These curves are arranged in two groups. Figs 4 and 5 compare the performance of blades A to E, showing basic simple blade and slot performance, and the difference of performance between unslotted and simple slotted blades. Figs. 6 and 7 then illustrate tests on a number of slot configurations, in an attempt to discover the optimum arrangement for testing on an actual rotor.

6.1 Blade "A" (0° camber, No slots)

This blade was tested to find the skin friction wake of the blade itself, without any loss due to turning of the air-stream. Losses above this would be due to turning work. Strictly, the above is true only at zero incidence, but the curve shows that the minimum loss holds over a ± 5° incidence range.

6.2 Blade "B" (0° Camber, 1 slot at 50% chord)

It was interesting to see that the presence of the slot made the blade-wake much thicker, and therefore increased the loss. At less than ± 4° incidence, slight instability increased the loss in this thick wake, and at around zero incidence a strong instability was setup, as flow reversed from side to side through the slot.

6.3 Blade "C" (75° camber, No slots)

This blade was the basic standard cambered aerofoil, to which all slot configurations were subsequently applied. In this (unslotted) configuration, the pressure side caused some turning of the air, but the flow was completely detached from the suction surface, at all incidences tested. The wake was extremely wide and severe, with a very high Loss Factor indeed.

6.4 Blade "D" (75° camber, 1 slot)

The presence of the single slot allows the blade to operate properly over a fair range of incidence, with a Loss Factor approaching that of a straight unslotted blade doing zero turning, although this blade is in fact turning the air through some 51°. (75 camber at 0° incidence minus 24° deviation). The blade reaches a stall point at + 2° incidence, after which it is bistable. Either attached flow or stalled flow could be induced up to the + 8° incidence test limit, but external interference was needed to change from stalled to attached flow, or vice-versa. The practical range was therefore limited to +2° incidence max.

The tremendous improvement due to the single slot gave hope of definite performance gains if the system could be applied to a compressor blade.

6.5 Blade "E" (75° camber, 2 slots)

This blade shows similar characteristics to the previous, single-slotted blade. The Loss Factor is on the whole a little lower, and the Deviation about 4° greater over the working range, but the working range is considerably improved. Stall does not occur until + 6° incidence, a 4° improvement. The same bistable attached flow or stall behaviour is noted.

This blade was considered to demonstrate considerable improvement over the unslotted standard blade. A series of further configurations was therefore compared with blade "E", to gain better understanding of slot behaviour, and approach an optimum configuration.

6.6 Blade "F" (75° camber, 4 slots)

This blade, with four slots in it, was considered to be about the reasonable mechanical limit which could be applied to a compressor, - and, in fact, probably beyond the economic limit.

Its performance was most interesting. It did not stall,in the normal sense, but as the incidence increased, the wake became broad and turbulent, showing that the blade was behaving in a quasi-porous manner, and "letting the wind blow through it" if the pressure drop across it was high enough. In view of the broad turbulent wake and the difficulty of producing such a blade, it was considered that four slots was above the useful range.

6.7 Blade "G" (75° camber, 3 slots)

This was in fact blade "F" with the front slot filled in. It performed poorly. The Loss Factor was very high, and although the deviation was a little lower than "E", blade "G" stalled at about + 4° incidence, 2° earlier than blade "E". The long unprotected front part of the suction side permitted early flow detachment, and the slots further aft did not pull the flow blade into the blade.

6.8 Blade "H" (75° camber, 2 slots)

This blade was identical to blade"E", except that the front slot was moved a little over one slot-width further forward. The performance was extremely poor. The wake generated was both wide, and of very high loss. It became unstable early in the incidence range, and stalled early at about + 3° incidence. There appeared to be a tendency for the jet from the front slot to blow the flow off the surface, rather than to attach it. It may well have injected flow at an unsuitable point in the pressure field.

6.9 Blade "I" (75° camber, 2 slots)

This blade was again identical to blade "E", except that in this case the forward slot was moved a little over one slot-width aft. It again behaved poorly, having a characteristic of high loss and early stall almost identical to that of blade "G". It appears to have been shown conclusively that the optimum position of the forward slot is as in Blade "E". The aft slot seems less critical, but blade "E" appears to be satisfactory.

6.10 Blade "J" (75° camber, 2 wide slots)

This blade was identical to blade "E", except that the front element was moved 1.2% C upwards, and the rear element 1.2% C down, widening both slots by about this amount. The characteristic was almost identical to that of blade "E".

6.11 Blade "K" (75° camber, 2 narrow slots)

This blade was again identical to blade "E", except that in this case both slots were narrowed, by moving the front element down 1.2% C, and the rear element 1.2% C up. Apart from a higher deviation, the performance was very like that of "E" or "J". However, the narrow slots would be more difficult and critical to manufacture, and more susceptible to blockage by dirt.

7.0 CONCLUSIONS

It is concluded that slotted blades might well be used in a centifugal blower impeller with the intention of increasing the operating range before reaching the stall point.

Of the blades tested, the configuration "E" appears to represent the optimum slot arrangement.

The slot design criteria are described in detail in Section 4.2 and Figs. 8,9 and 10. They are in agreement with the findings of Foster (Ref.3).

Blades with slots designed on the basis of this Memo should be tested in a rotor on the Low Speed Centrifugal Compressor' Rig, and their performance compared with that of similar blades without slots.

8.0 REFERENCES

1. Fowler, H.S. "Attempts to Delay Flow-Detachment with Potential Application to Centrifugal Compressor Rotor Blades". Lab. Memorandum, NRC-ENG-62, April 1969.

2. Fowler, H.S. "Experiments on the Flow Process in Simple Rotating Channels". NRC Mechanical Engineering Report ME-229, Jan. 1969.

3. Foster, D.N. "The Flow Around Wing Sections with High-Lift Devices". AIAA Paper No. 71-96, Jan. 1970.

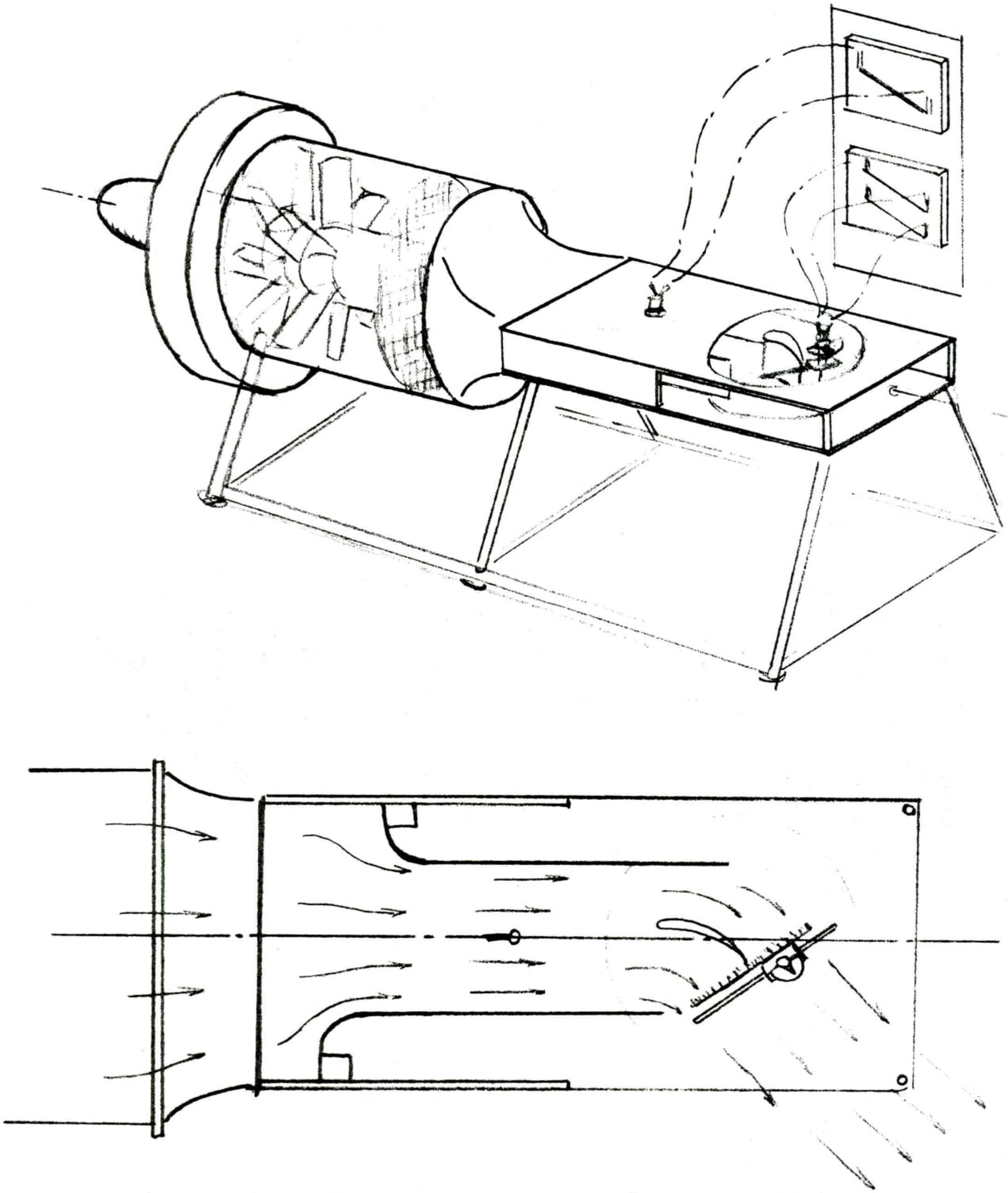

DIAGRAM OF TWO-DIMENSIONAL AEROFOIL TEST WIND TUNNEL.

FIG 1.

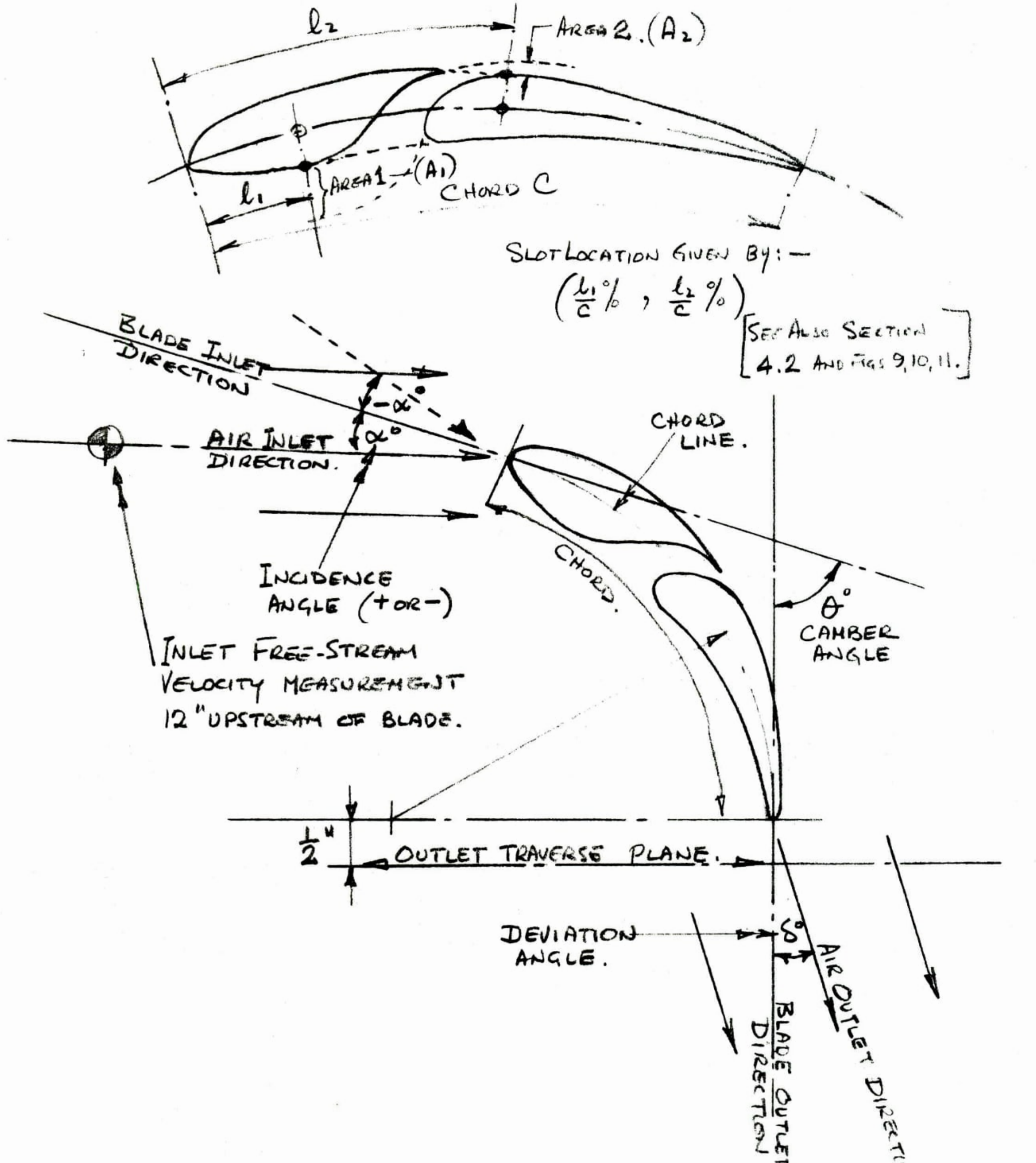

DIAGRAM - SHOWING BLADE AND FLOW NOMENCLATURE

FIG. 2.

INDEX OF BLADES TESTED

All blades were C-4 aerofoil section, 12% max.thickness/chord, of 8.7" chord. The cambered blades were all based on a circular-arc camber line.

BLADE	CAMBER	SLOTS	SLOT POSITIONS (% of chord)
A	0°	None	-
B	0°	1	symmetrical at 50% C.
C	75°	None	-
D	75°	1	(21% - 63%)
E	75°	2	(11% - 43%) & (40% - 77%)
F	75°	4	(4% - 31%),(21% - 63%),(63% - 84%), and (76% - 92%).
G	75°	3	Blade 'F', with (4% - 31%) slot filled in.
H	75°	2	(4% - 31%) & (40% - 77%) (Blade 'E' with front slot moved forward).
I	75°	2	(17% - 49%), & (40% - 77%) (Blade 'E" with front slot moved aft).
J	75°	2	Blade 'E', with front element 1.2% C up, and rear element 1.2% C down, relative to mid-element, opening up both slots.
K	75°	2	Blade 'E', with front element 1.2% C down, and rear element 1.2% C up, relative to mid-element, reducing both slots.

[The system of slot position dimensioning is shown in Fig. 2]

FIG. 3

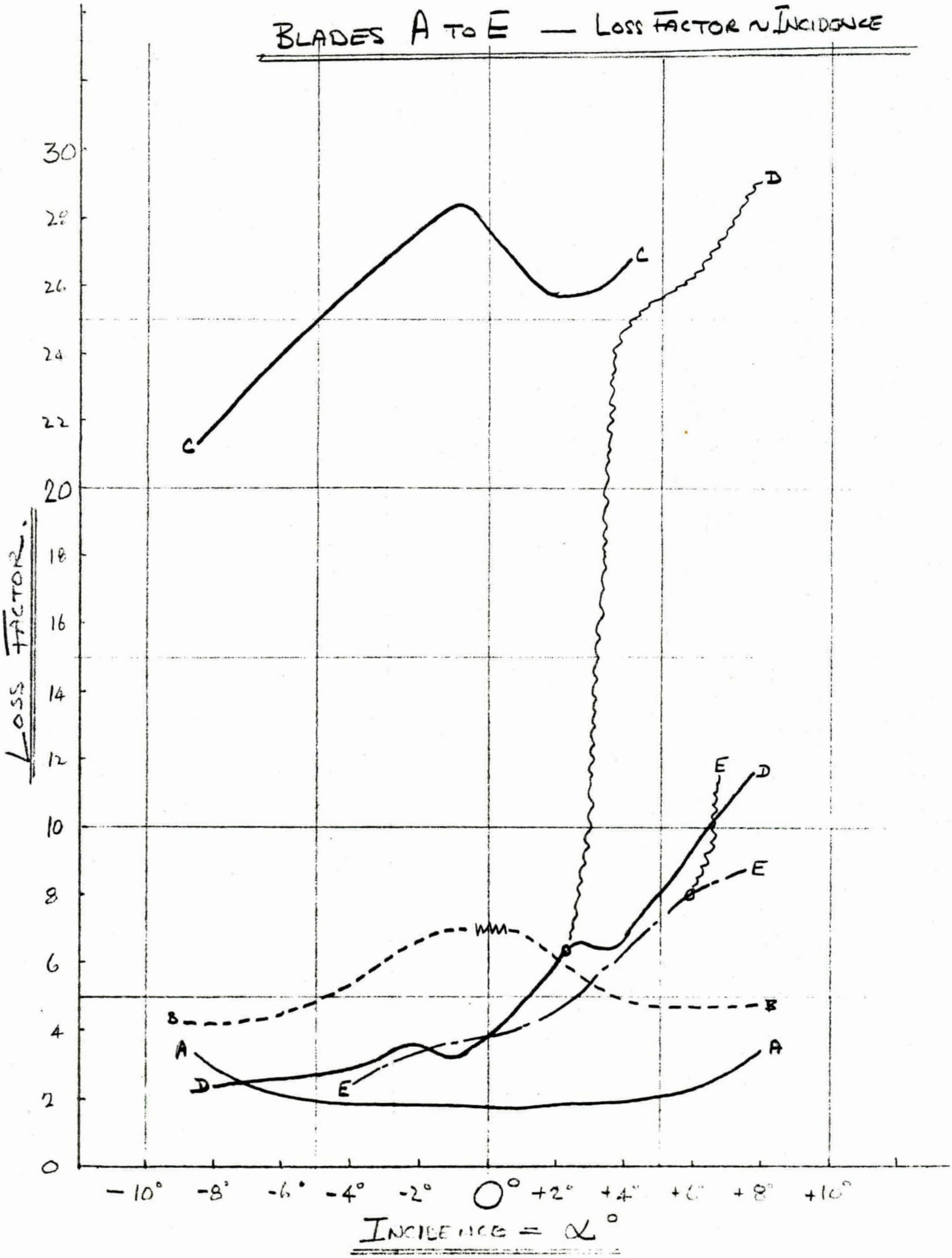
BLADES A TO E — LOSS FACTOR ~ INCIDENCE
LOSS FACTOR
30
28
26
24
22
20
18
16
14
12
10
8
6
4
2
0
−10° −8° −6° −4° −2° 0° +2° +4° +6° +8° +10°
INCIDENCE = α°
A
B
C
D
E

Fig 4

BLADES A TO E — DEVIATION v INCIDENCE.

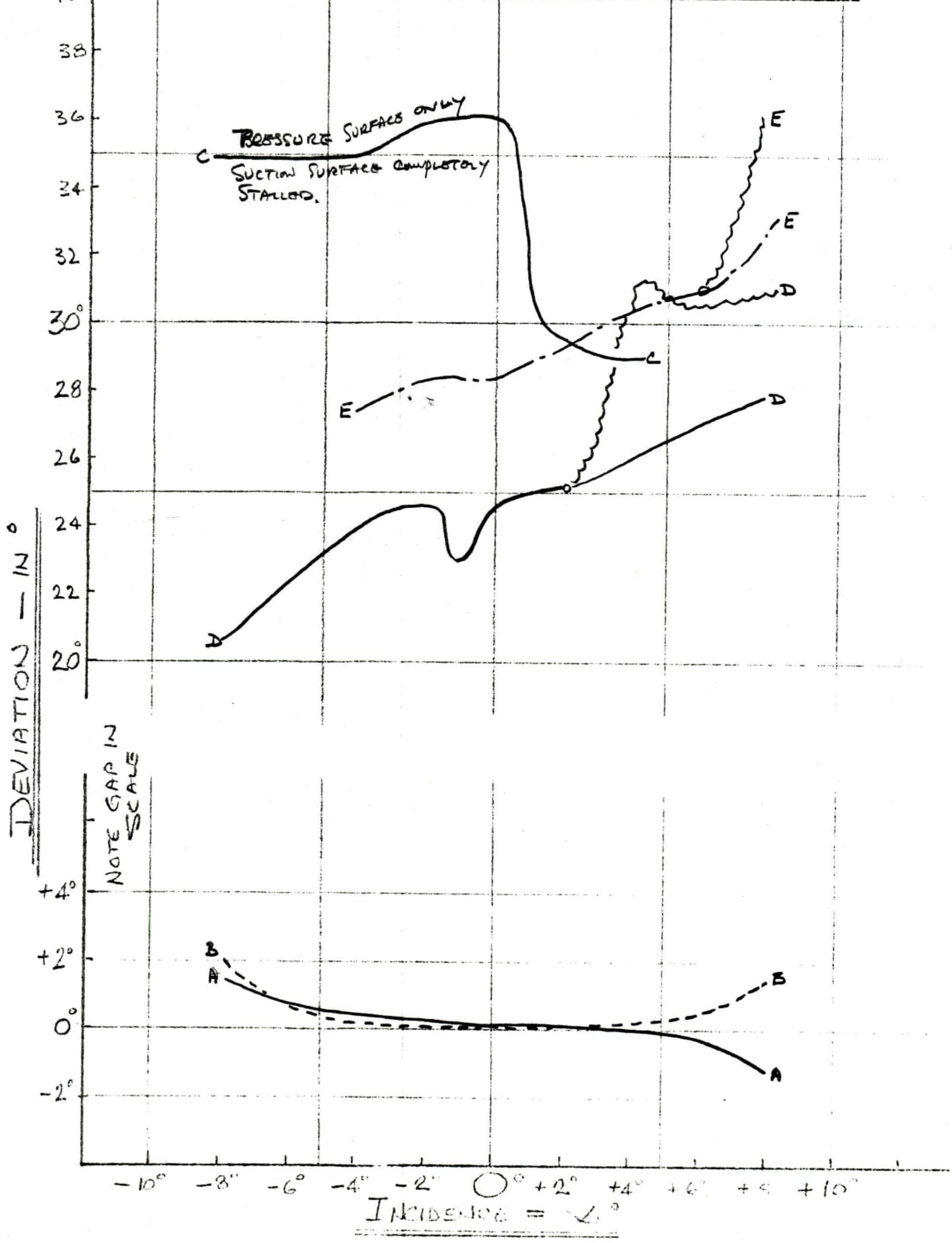

Fig 5

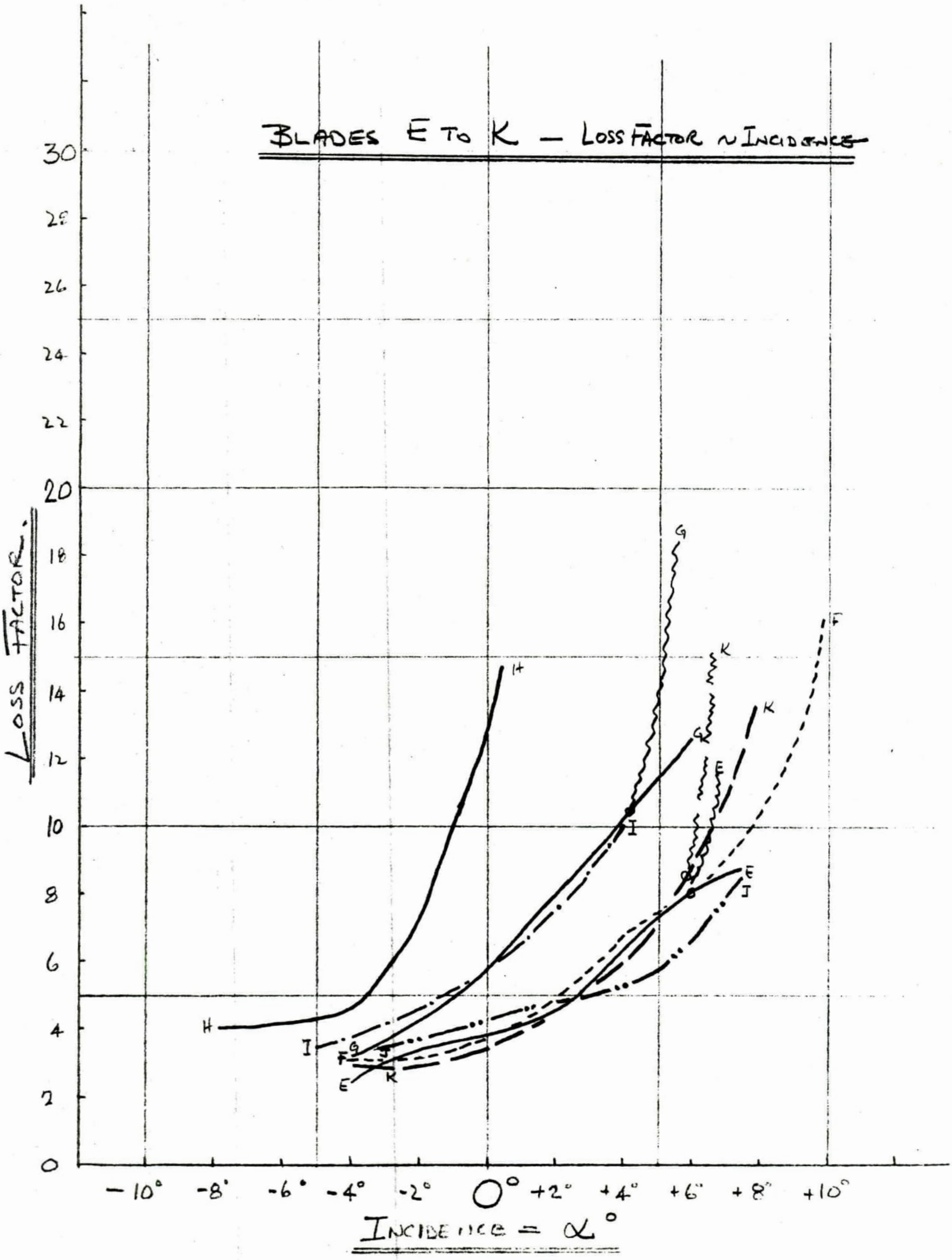

BLADES E TO K — LOSS FACTOR ~ INCIDENCE
LOSS FACTOR
INCIDENCE = α°
30
28
26
24
22
20
18
16
14
12
10
8
6
4
2
0
−10°
−8°
−6°
−4°
−2°
0°
+2°
+4°
+6°
+8°
+10°
H
I
G
F
J
E
K

Fig 6

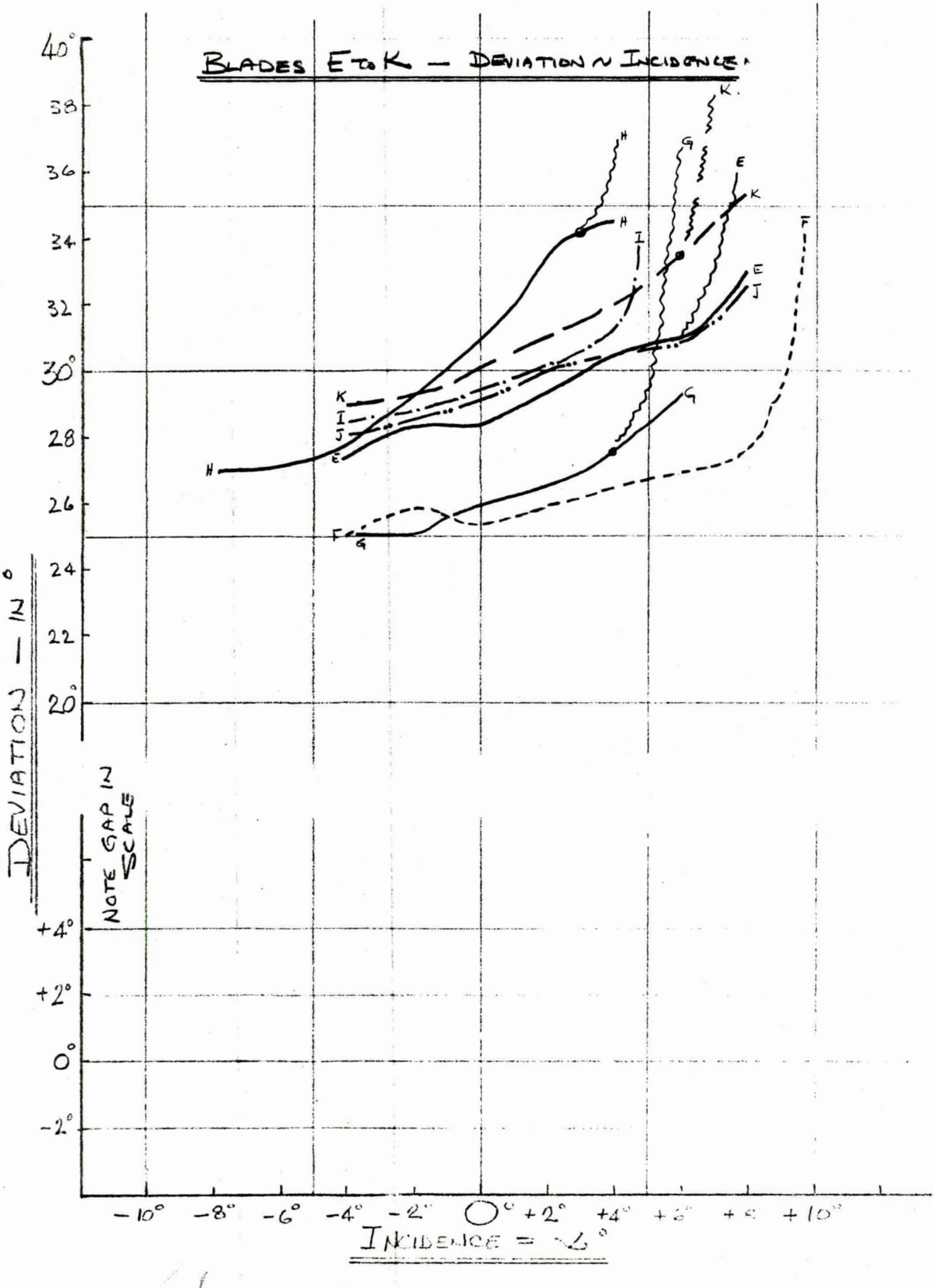

BLADES E to K — DEVIATION ~ INCIDENCE
DEVIATION — IN °
NOTE GAP IN SCALE
INCIDENCE = ∠°

Fig 7

BLADE "D" – SINGLE SLOT.

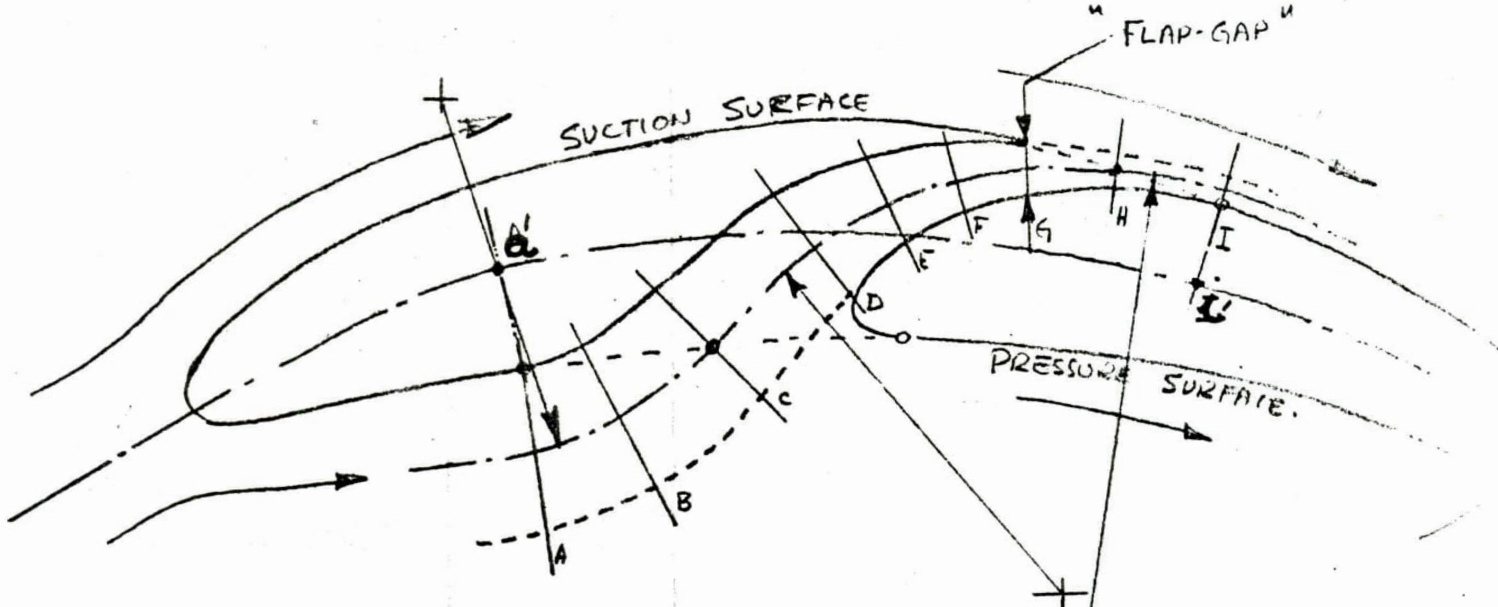

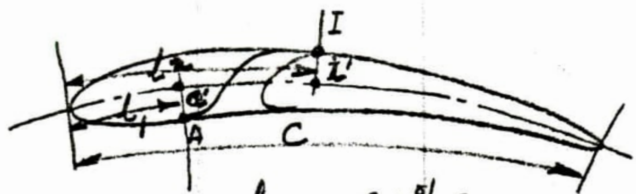

$l_1 = 21\%C.$

$l_2 = 63\%C.$

AREA RATIO, $\equiv A_1/A_2 = 5.8.$

FLAP GAP $\equiv$ GAP/CHORD $= 2.35\%$

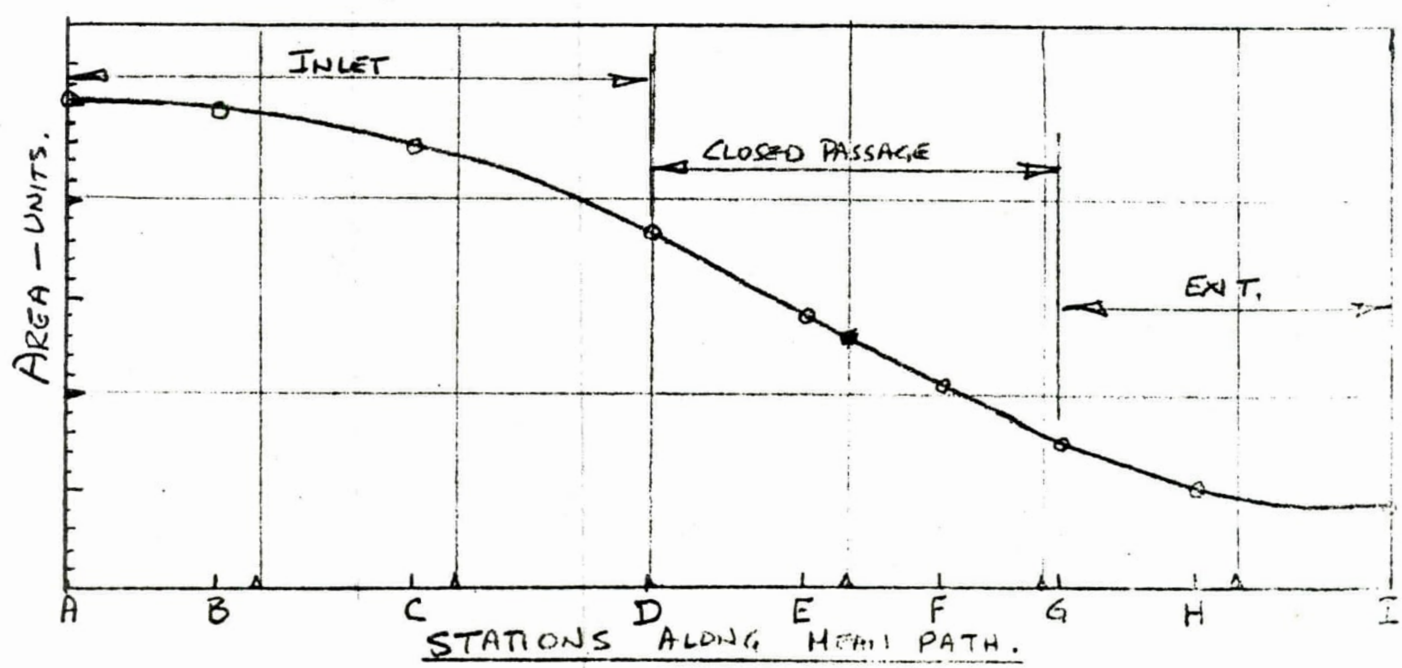

Fig 8

BLADE "E" — TWO SLOTS.

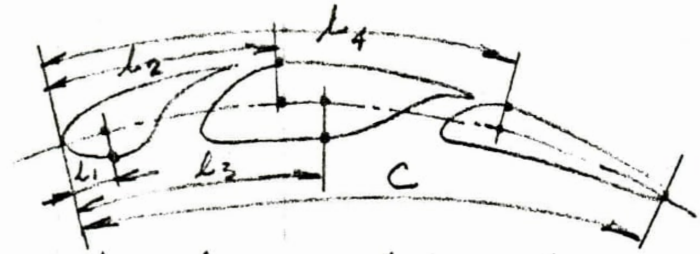

SLOT 1 $l_1 = 10{\cdot}7\%\,C$ $l_2 = 42{\cdot}5\%\,C$

AREA RATIO = 5·3 FLAP-GAP = 2·42 %.

SLOT 2 $l_3 = 40{\cdot}0\%\,C$ $l_4 = 77{\cdot}0\%\,C$

AREA RATIO = 5·7 FLAP GAP = 2·06 %

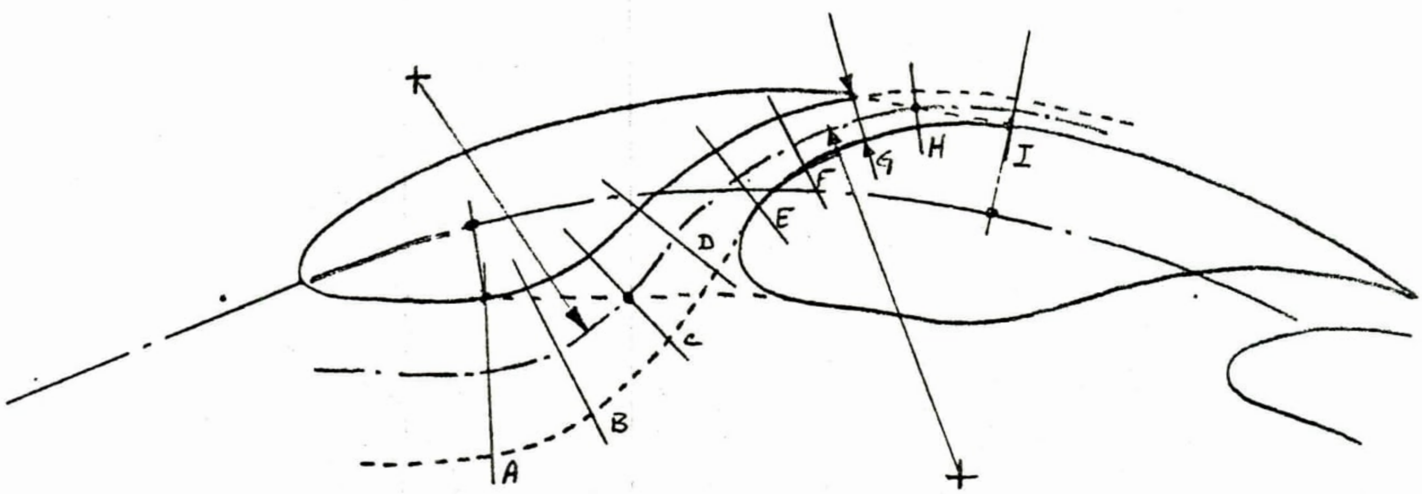

SLOT E 1

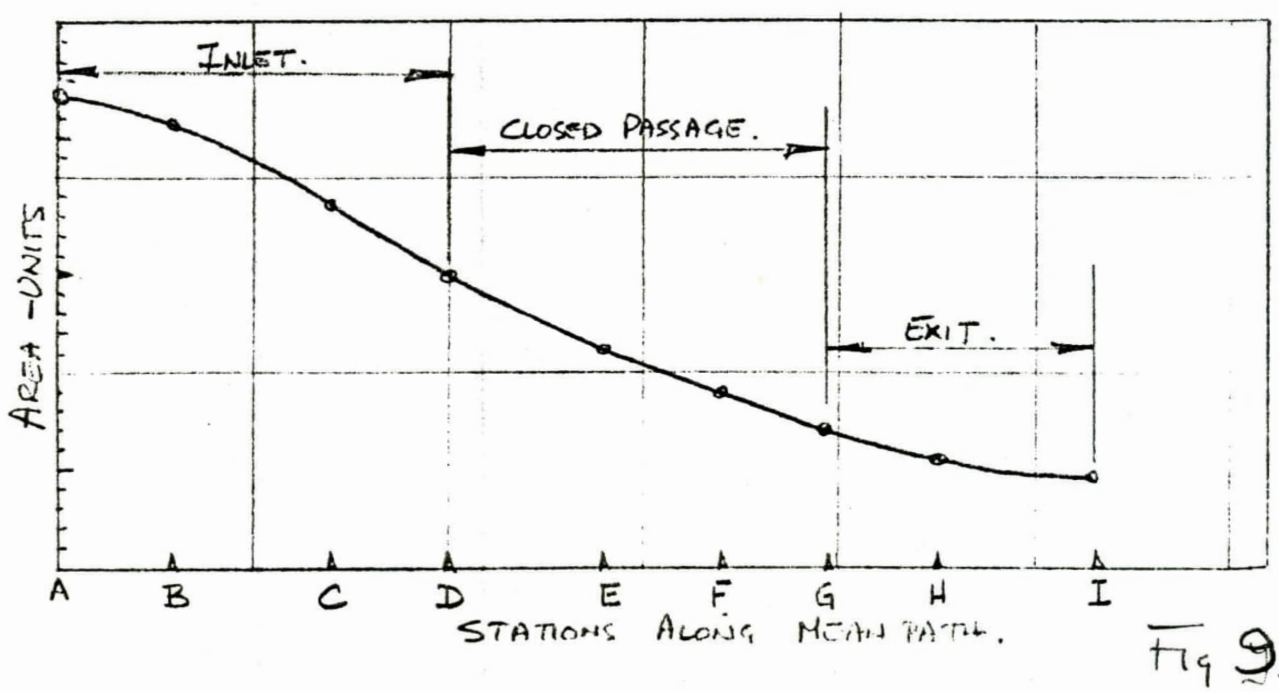

Fig 9

BLADE "E" (CONTINUED.)

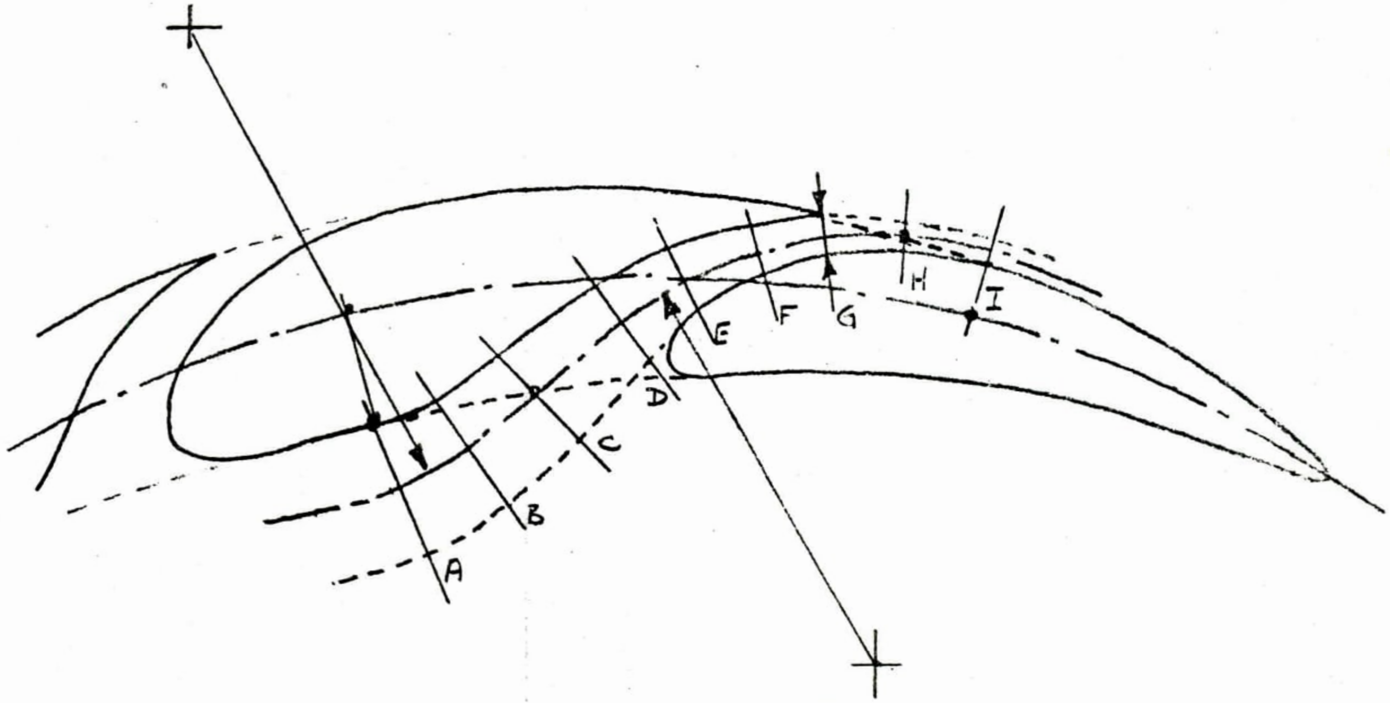

SLOT E 2

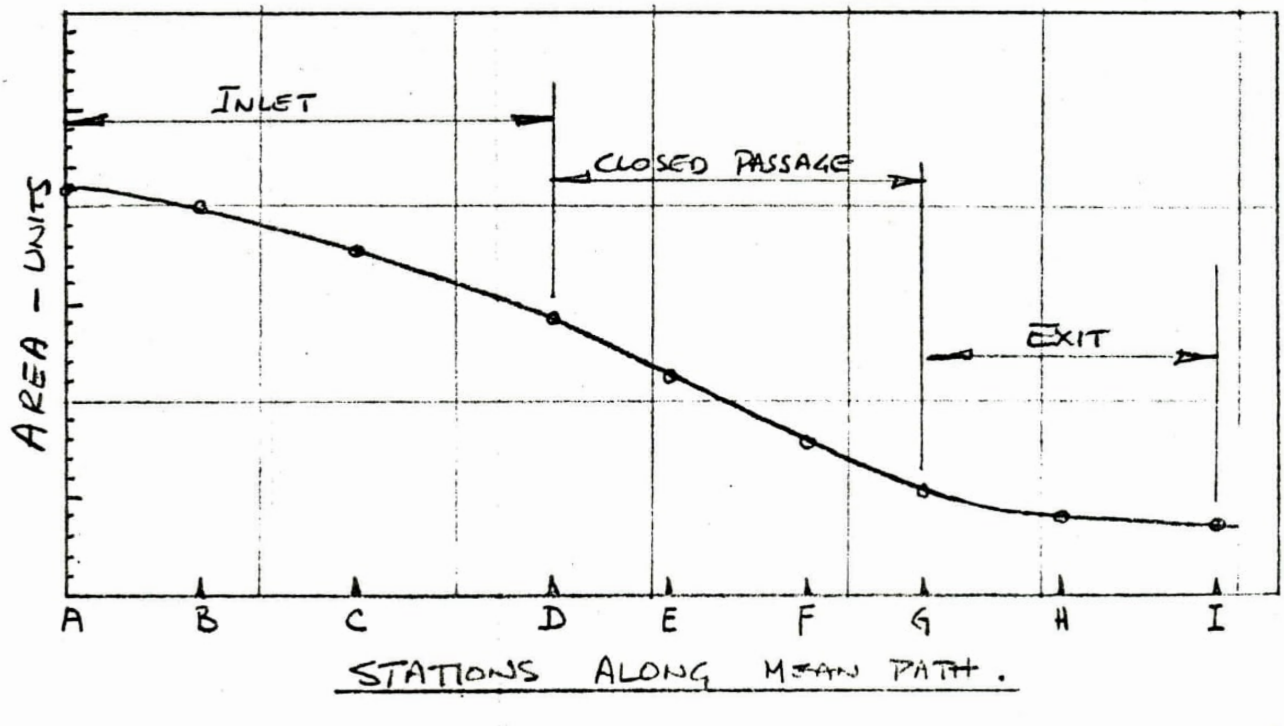

Fig 10.

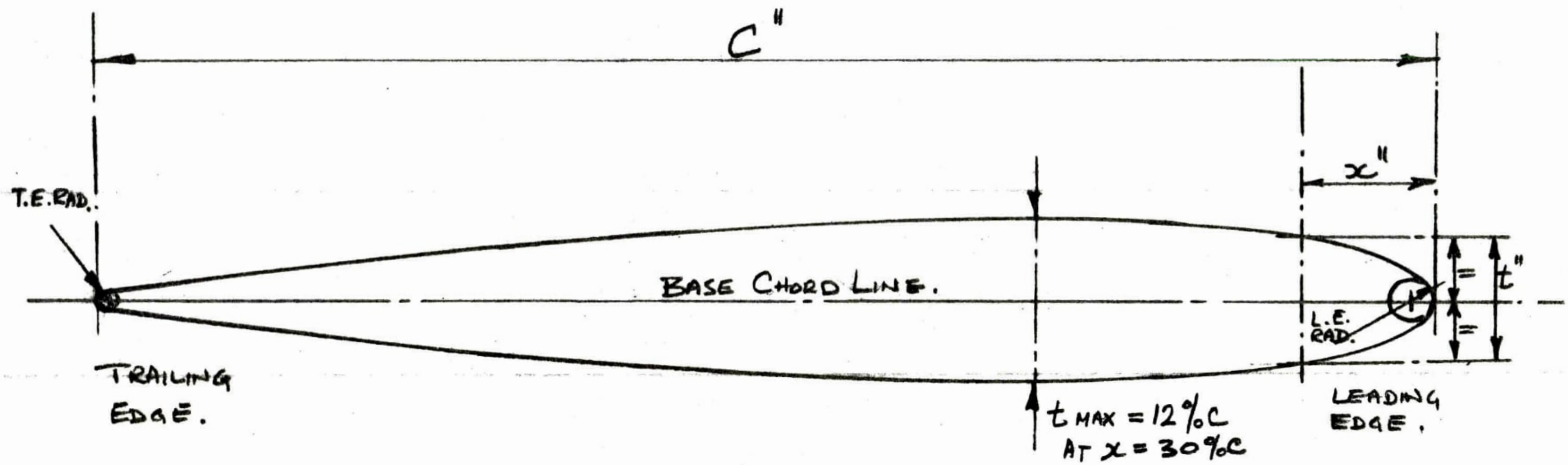

ORDINATES FOR C-4 AEROFOIL [t/c = 12%]

	L.E.													T.E.
$\frac{x}{c}$%	0	2·5	5	7·5	10	20	30	40	50	60	70	80	90	100
$\frac{t}{c}$%	0	5·45	7·40	8·70	9·65	11·60	12·00	11·73	10·97	9·73	8·10	6·10	3·84	0

LE RAD = 1·4%c

TE RAD = ·70%c

C-4 AEROFOIL DATA.

CALCULATION OF LOSS FACTOR

It must be clearly understood that the purpose of this program is to compare various blade and slot configurations being tested in a very simple two-dimensional tunnel. No attempt has been made to obtain absolute values.

Since in every case the thickness and chord of the blade was the same, it was considered that the area-based quantity, the sum of the elemental pressure losses, gives a fair comparative measure of the total magnitude of the wake, accounting in a single number for both its severity of total pressure loss and width. If this is non-dimensionalised by dividing it by the free-stream velocity head ($\frac{1}{2}\rho V^2$) upstream of the blade, then the resulting "Loss Factor" is of a similar form to that normally used in internal aerodynamics.

It must be remembered that this represents the Loss Factor of the wake of one blade. In cascade test results, the Loss Coefficient $\Delta P/\frac{1}{2}\rho V^2$ refers to the loss over one channel or blade pitch, and includes the very small loss over the part of the channel not affected by the blade wake. If it was wished to compare the above Loss Factors with this Cascade Loss Coefficient, the total loss would have to be that across the whole of the arbitrarily selected pitch (of 7.2" in this case), and the Loss Factor would be calculated, using 36 elements of .2" width each, in the 7.2" pitch, as:-

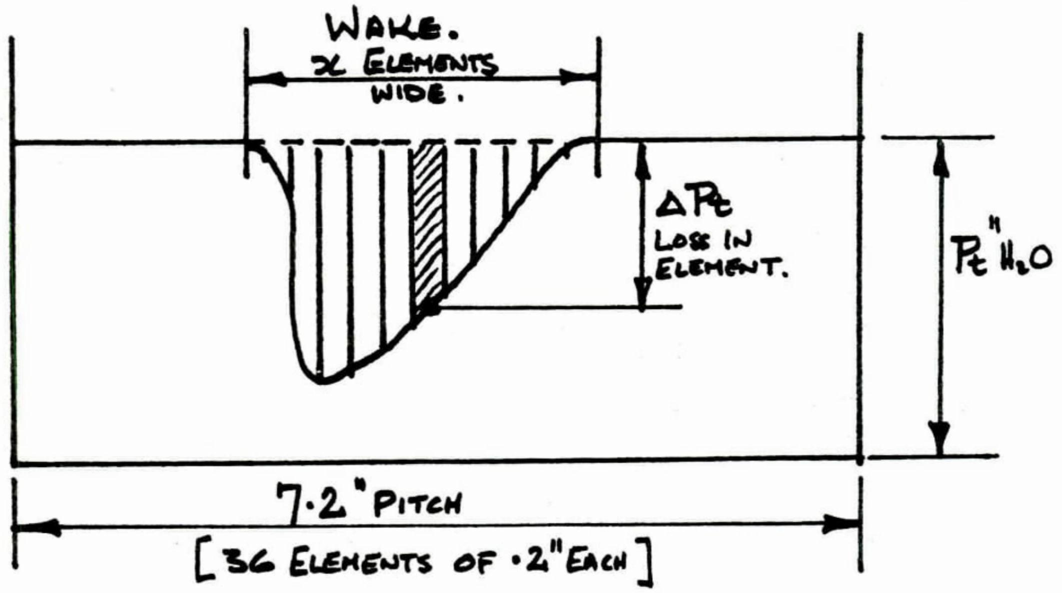

Loss in one element = $\Delta Pt \times 1$ element

$\therefore$ Loss in wake x elements wide = $\sum_{o}^{x} \Delta Pt \times 1$.

Loss in other (36-x) elements is zero.

$\therefore$ Total Loss in 36 element pitch = $\sum_{o}^{x} \Delta Pt \times 1 + \sum_{o}^{36-x} \text{zero} \times 1$.

$$\therefore \text{Mean Loss} = \frac{\sum_{o}^{x} \Delta Pt + 0}{36}$$

$$\therefore \text{Mean Loss Factor for whole pitch} = \frac{\sum_{o}^{x} \Delta Pt}{\frac{1}{2}\rho V^2 \times 36}.$$

(which is the Cascade Loss Coefficient)

However, in the present case, as explained above, the Loss Factor for the blade wake alone has been calculated, as:-

$$\text{Loss Factor in Wake} = \frac{\sum_{o}^{x} \Delta Pt}{\frac{1}{2}\rho V^2}.$$

The values thus obtained are in the convenient range of around 1 to 30, whereas the more usual Cascade Loss Coefficients, besides involving the arbitrary choice of a rather mythical pitch, would have fallen in the less convenient range of .027 to .85.

The deviation angles, however, represent the angle of the exit flow, not the wake. They are therefore given in their simplest form, as the arithmetic mean of the 36 elementary exit angle readings taken during the traverse.

DETAILS OF TRAVERSE DATA

[BLADES "A" - "K"]

BLADE "A"

NO SLOTS

0° CAMBER

[12%t/c C-4]

A.

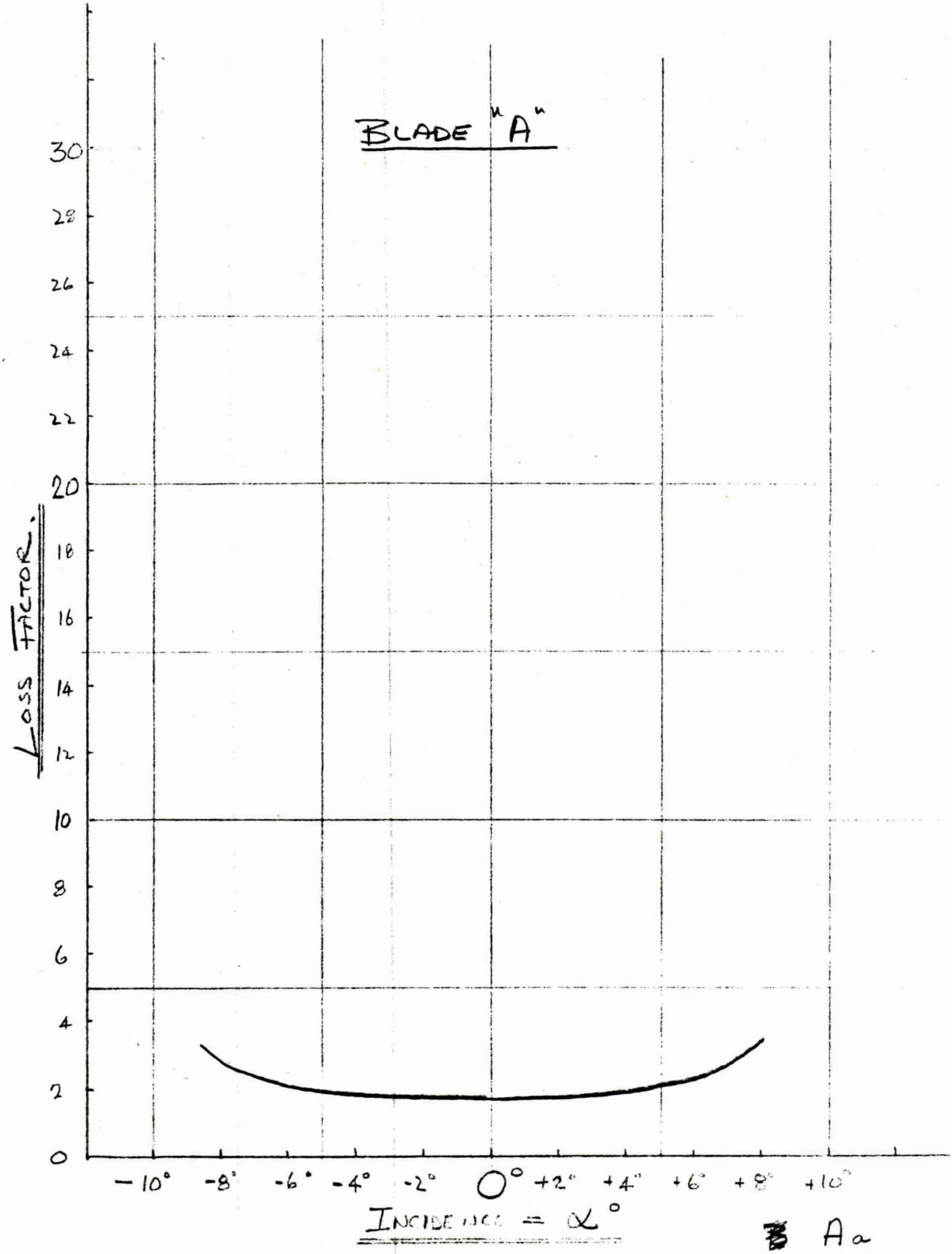

BLADE "A"
LOSS FACTOR.
30
28
26
24
22
20
18
16
14
12
10
8
6
4
2
0
−10° -8° -6° -4° -2° 0° +2° +4° +6° +8° +10°
INCIDENCE = α°

A a

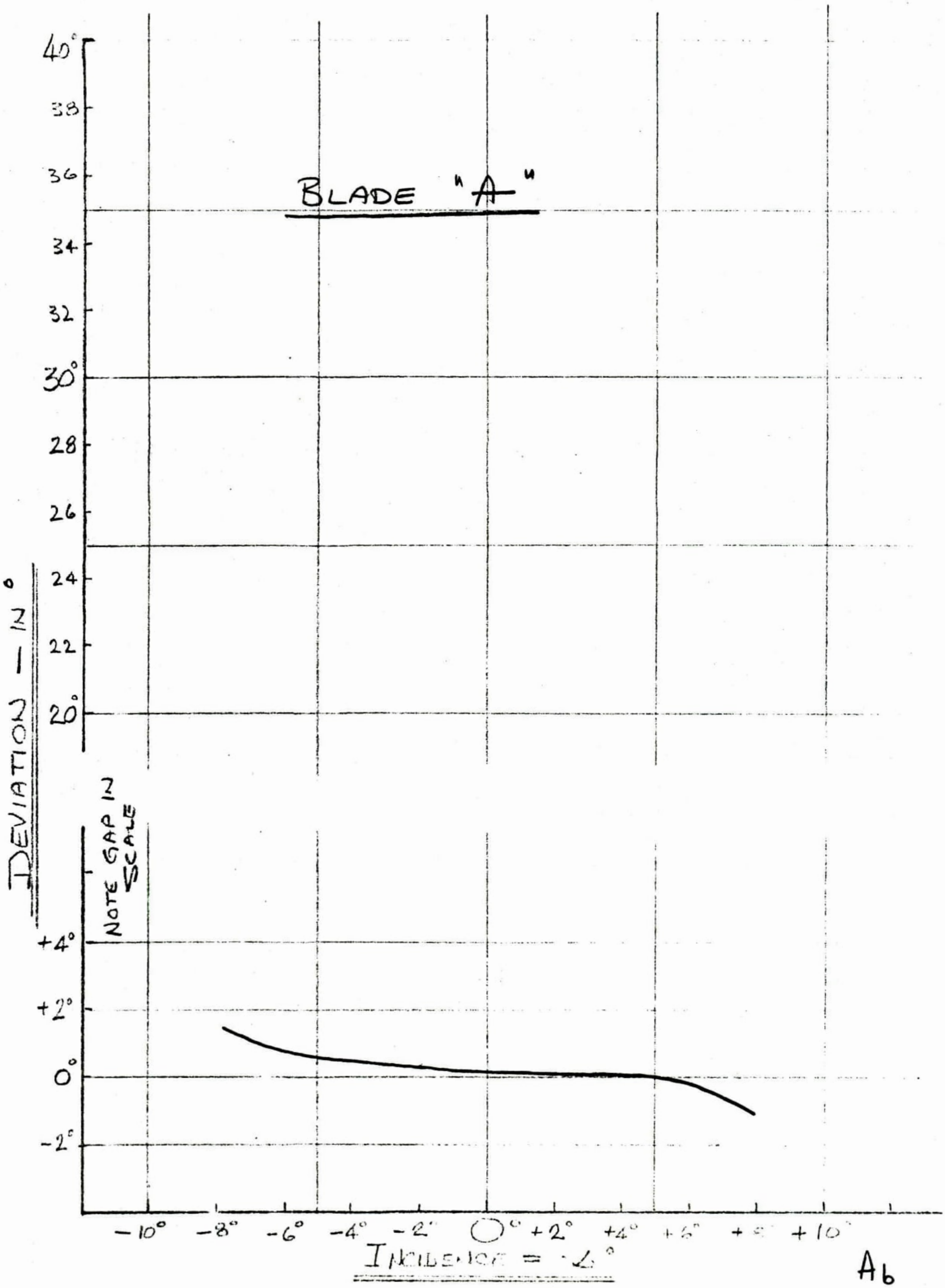

BLADE "A"
40°
38
36
34
32
30°
28
26
24
22
20°
+4°
+2°
0°
-2°
DEVIATION – IN °
NOTE GAP IN SCALE
-10°
-8°
-6°
-4°
-2°
0°
+2°
+4°
+10°

Ab

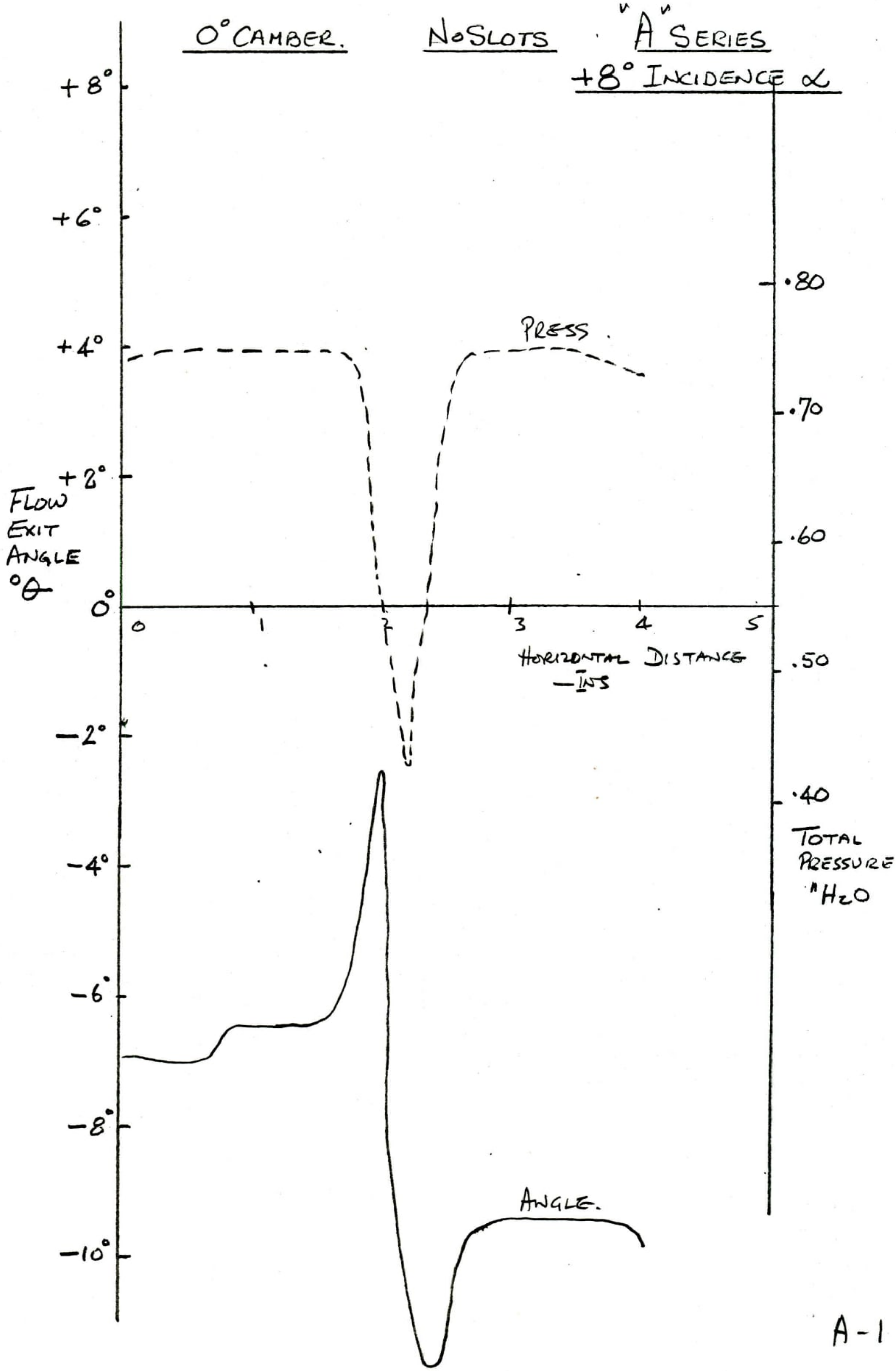

O° CAMBER.
NO SLOTS
"A" SERIES
+8° INCIDENCE α
+8°
+6°
+4°
+2°
0°
−2°
−4°
−6°
−8°
−10°
FLOW EXIT ANGLE °θ
PRESS.
ANGLE.
0
1
2
3
4
5
HORIZONTAL DISTANCE — INS
·80
·70
·60
·50
·40
TOTAL PRESSURE "H_2O

A-1

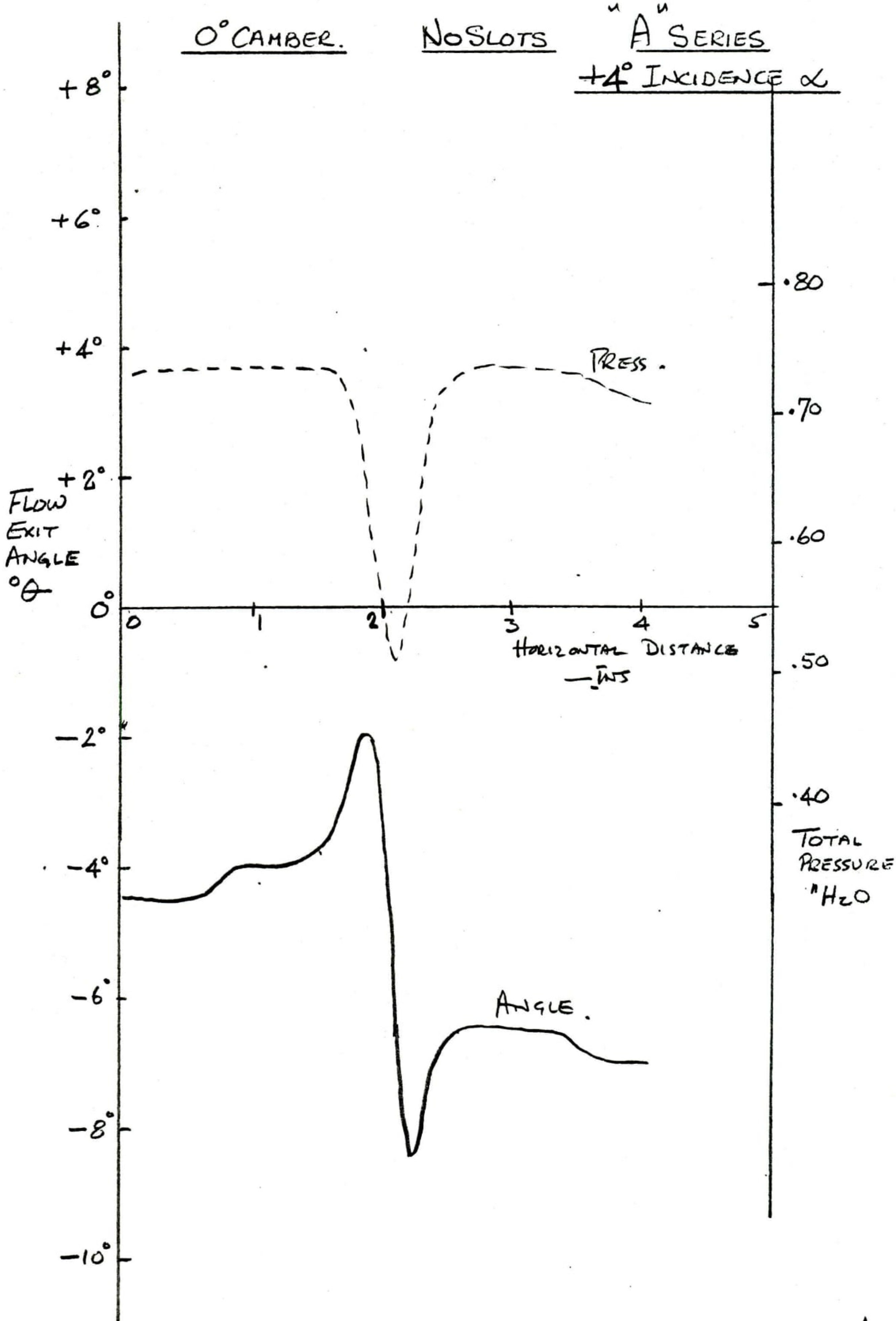

O° CAMBER.
NO SLOTS
"A" SERIES
+4° INCIDENCE α
+8°
+6°
+4°
+2°
0°
−2°
−4°
−6°
−8°
−10°
FLOW EXIT ANGLE °θ
·80
·70
·60
·50
·40
TOTAL PRESSURE "H₂O
PRESS.
ANGLE.
0
1
2
3
4
5
HORIZONTAL DISTANCE — INS

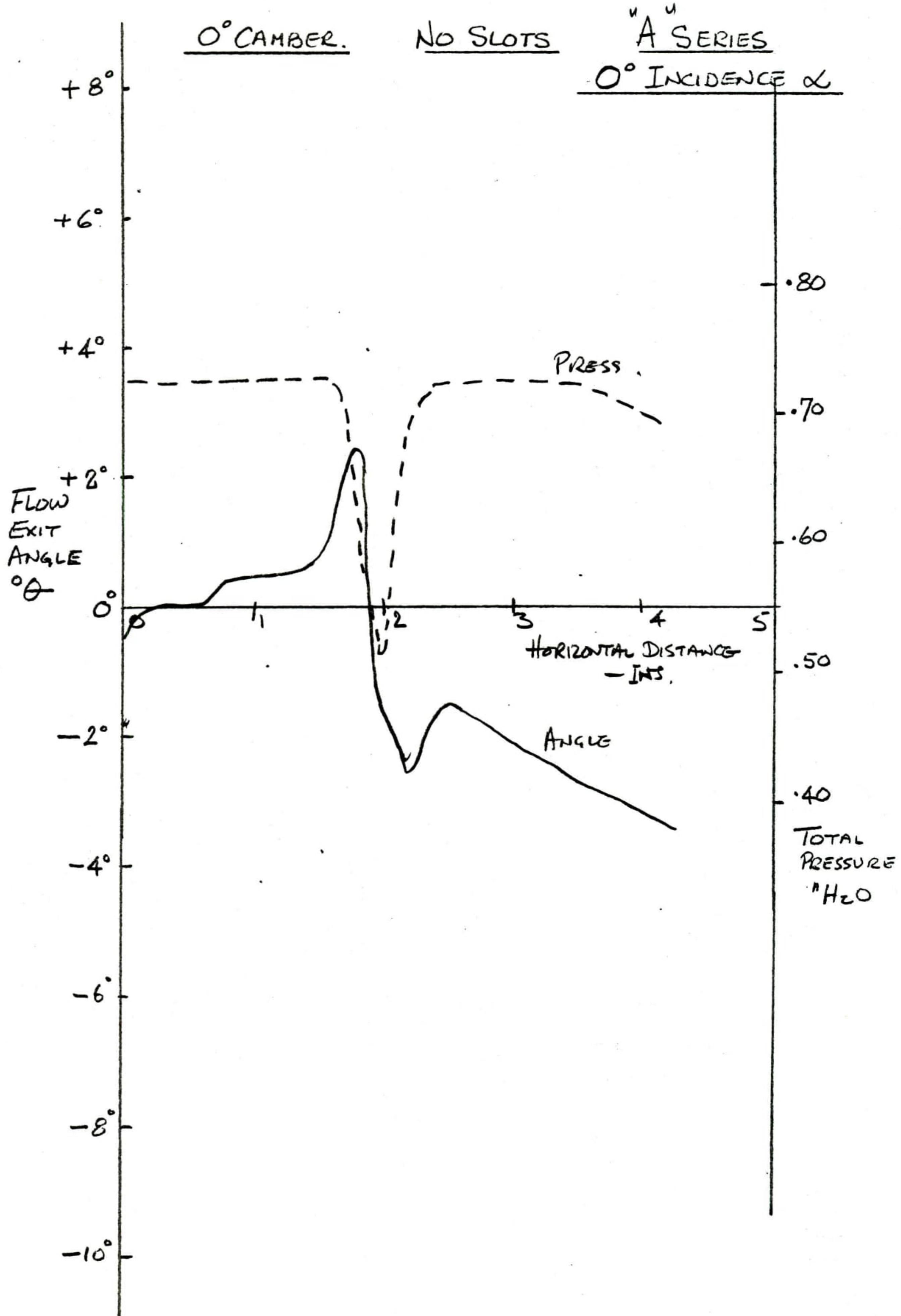

O° CAMBER.
NO SLOTS
"A" SERIES
0° INCIDENCE α
+8°
+6°
+4°
+2°
0°
−2°
−4°
−6°
−8°
−10°
FLOW EXIT ANGLE °θ
.80
.70
.60
.50
.40
TOTAL PRESSURE "H2O
PRESS.
ANGLE
0
1
2
3
4
5
HORIZONTAL DISTANCE — INS.

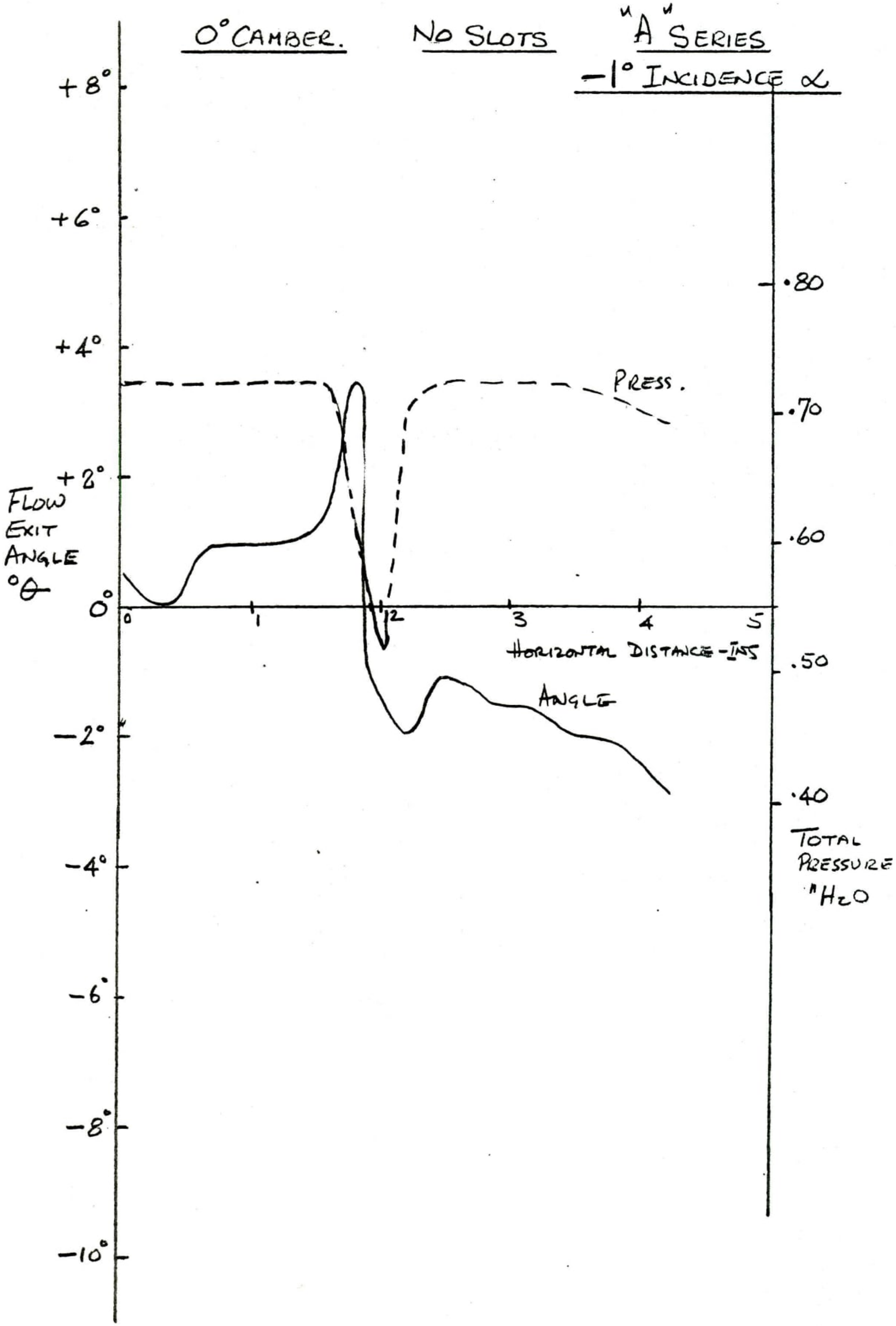

0° CAMBER.
NO SLOTS
"A" SERIES
−1° INCIDENCE α
+8°
+6°
+4°
+2°
0°
−2°
−4°
−6°
−8°
−10°
FLOW EXIT ANGLE °θ
·80
·70
·60
·50
·40
TOTAL PRESSURE "H_2O
0
1
2
3
4
5
HORIZONTAL DISTANCE - INS
PRESS.
ANGLE

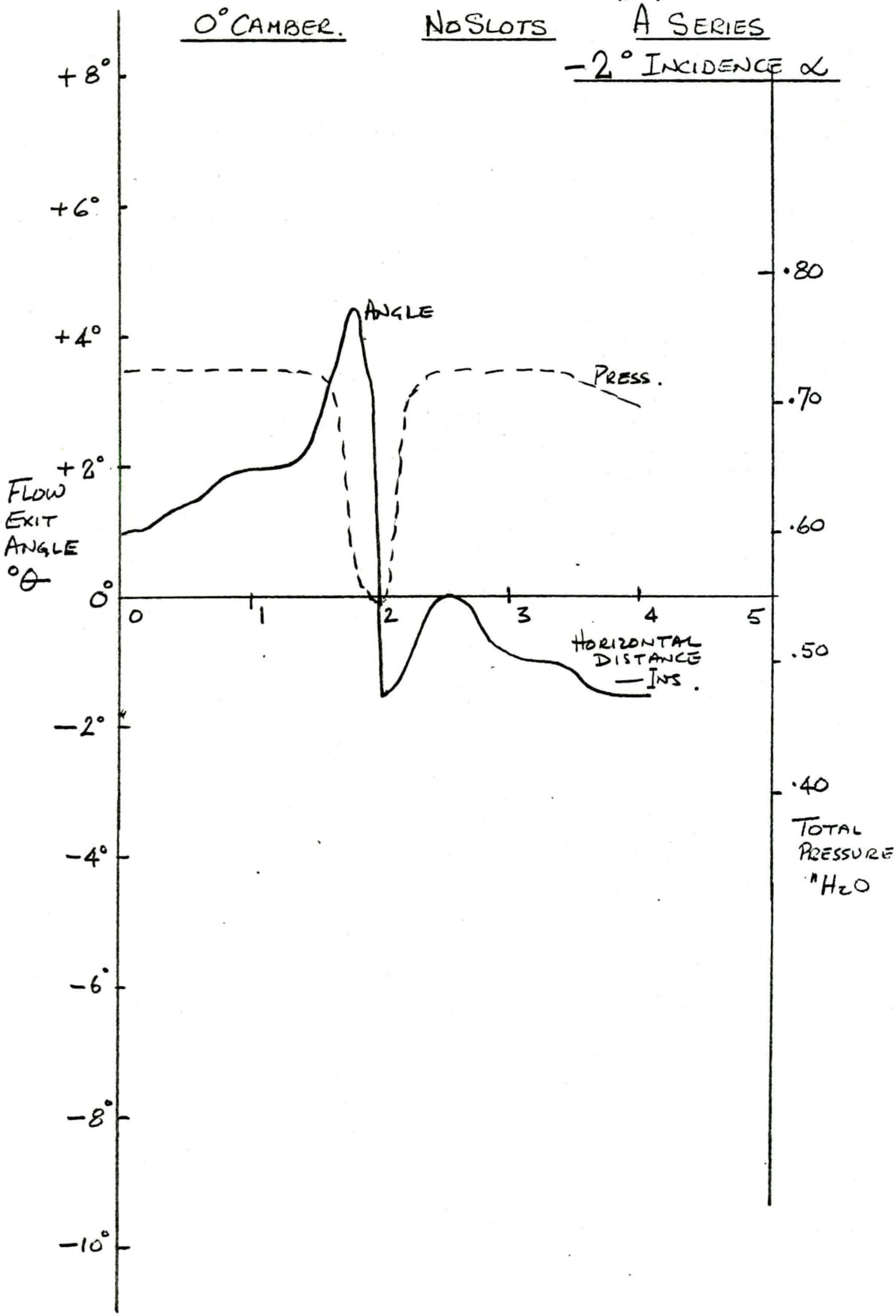

O° CAMBER.
NO SLOTS
"A" SERIES
-2° INCIDENCE α
+8°
+6°
+4°
+2°
0°
-2°
-4°
-6°
-8°
-10°
FLOW EXIT ANGLE °θ
ANGLE
PRESS.
.80
.70
.60
.50
.40
TOTAL PRESSURE "H_2O
0
1
2
3
4
5
HORIZONTAL DISTANCE — INS.

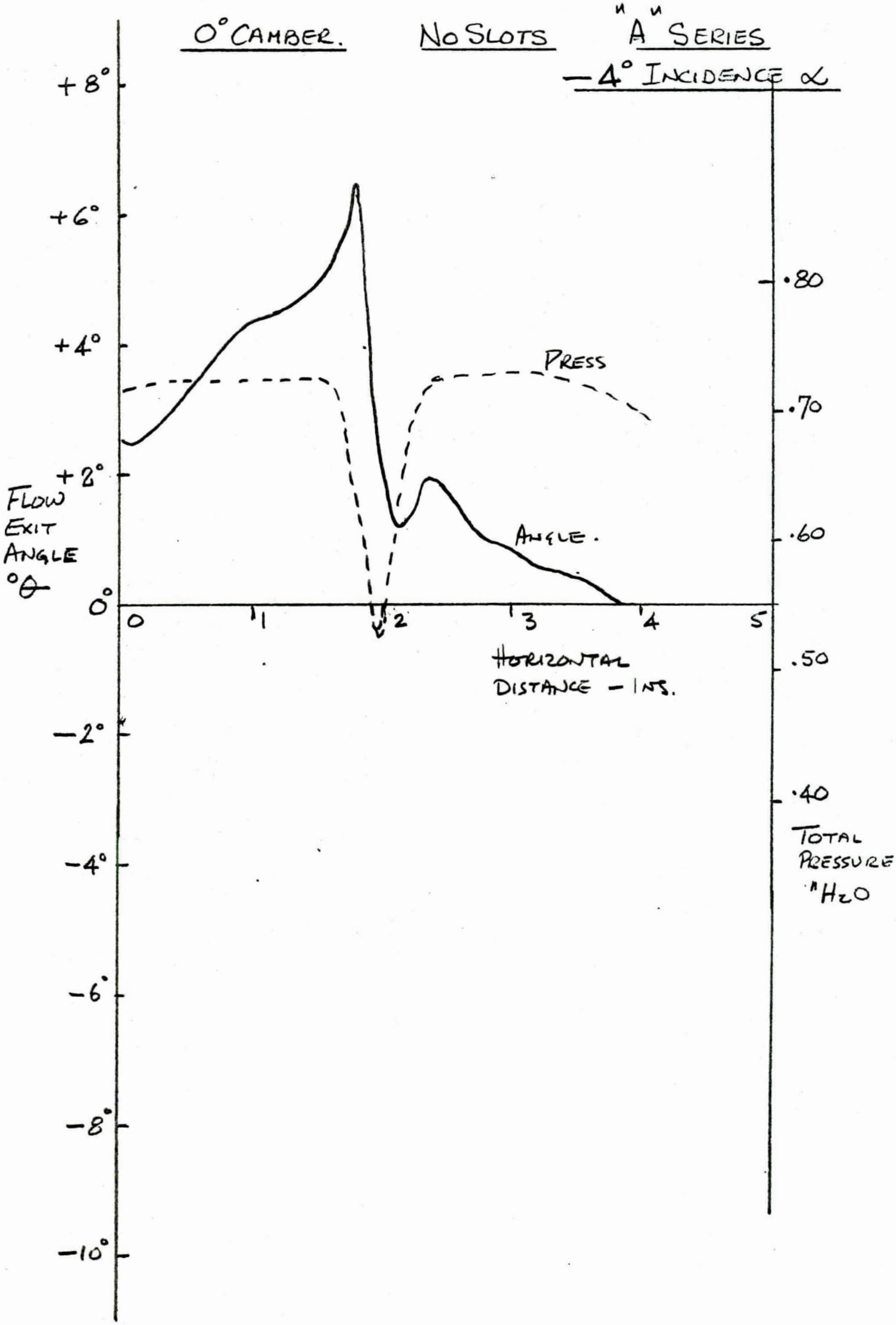

0° CAMBER. NO SLOTS "A" SERIES
−4° INCIDENCE α
+8°
+6°
+4°
+2°
0°
−2°
−4°
−6°
−8°
−10°
FLOW EXIT ANGLE °θ
PRESS
ANGLE.
0
1
2
3
4
5
HORIZONTAL DISTANCE − INS.
·80
·70
·60
·50
·40
TOTAL PRESSURE "H_2O

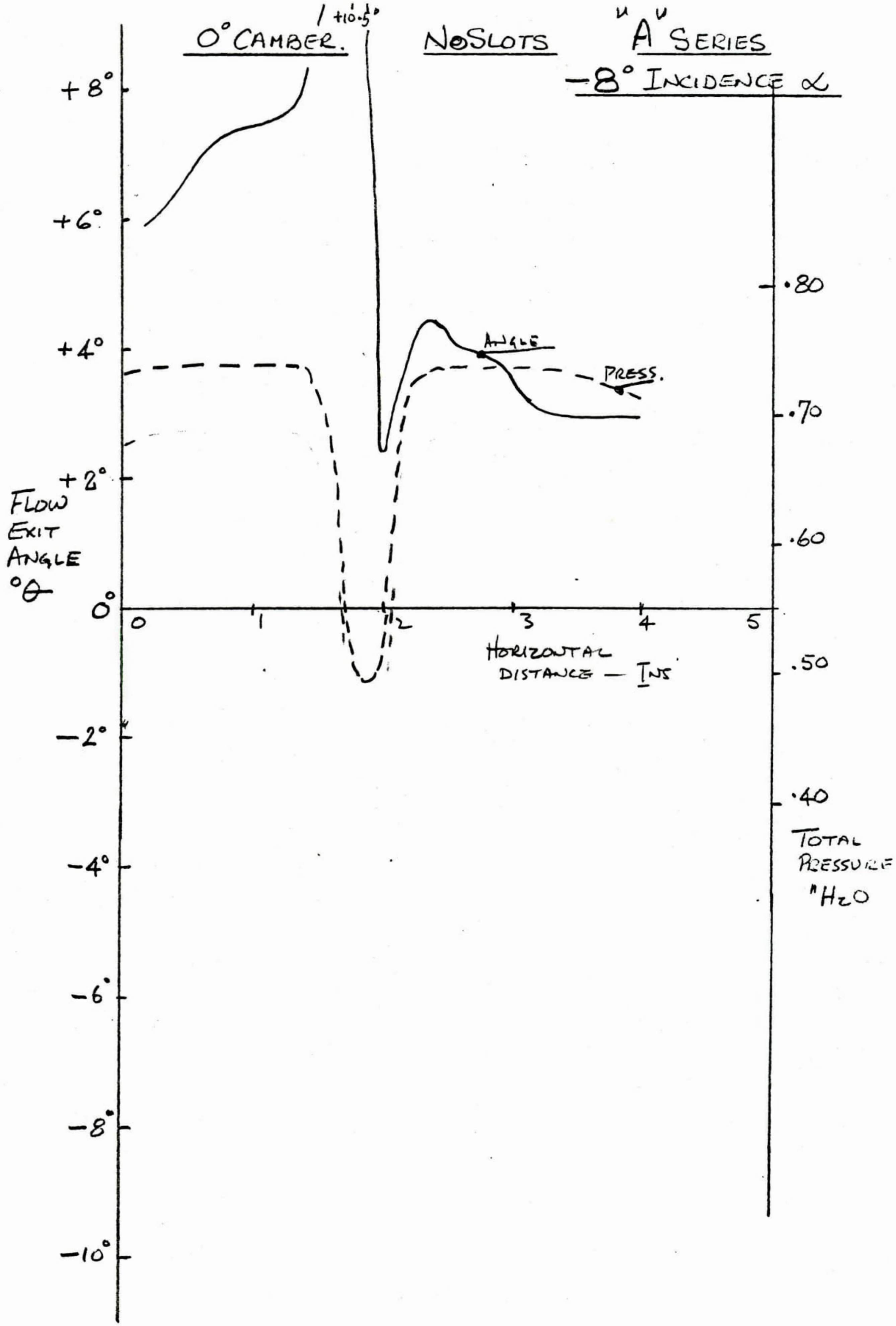
0° CAMBER.
NO SLOTS
"A" SERIES
-8° INCIDENCE α
+10.5°
+8°
+6°
+4°
+2°
0°
-2°
-4°
-6°
-8°
-10°
FLOW EXIT ANGLE °θ
ANGLE
PRESS.
0
1
2
3
4
5
HORIZONTAL DISTANCE — INS
.80
.70
.60
.50
.40
TOTAL PRESSURE "H₂O

BLADE "B"

1 SLOT

0° CAMBER

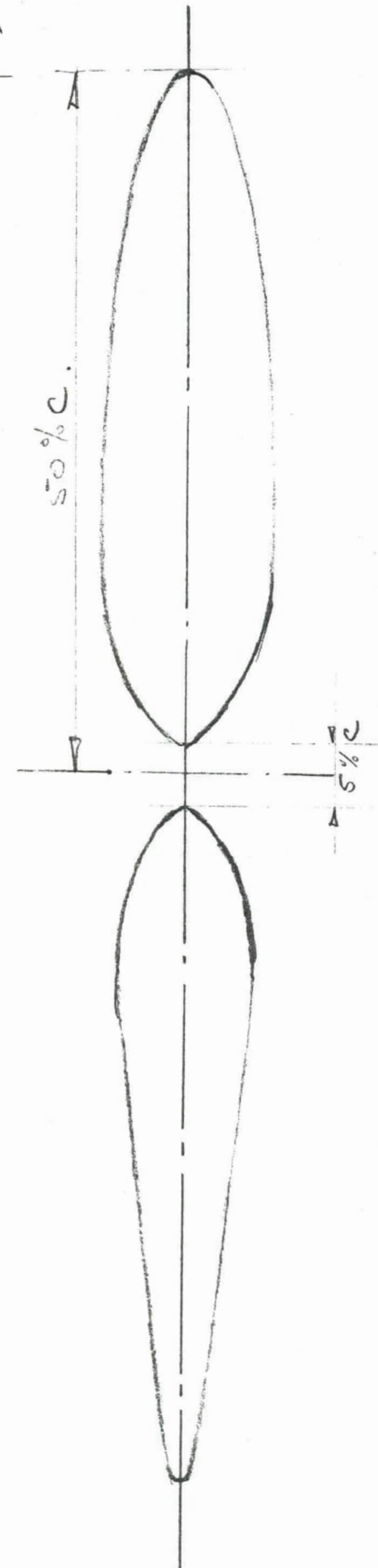

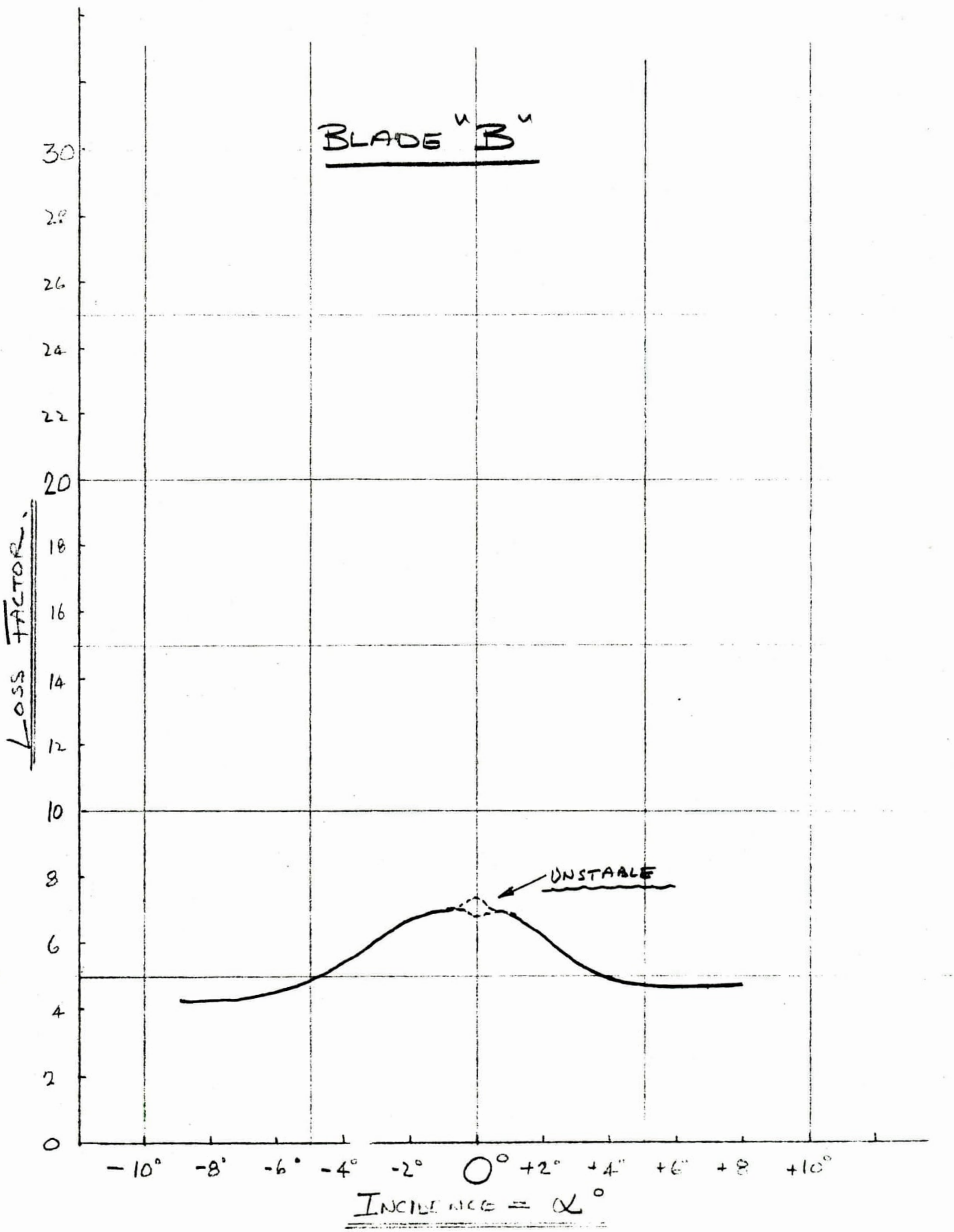

BLADE "B"
LOSS FACTOR
30
28
26
24
22
20
18
16
14
12
10
8
6
4
2
0
UNSTABLE
-10° -8° -6° -4° -2° 0° +2° +4° +6° +8 +10°
INCIDENCE = α°

Bb

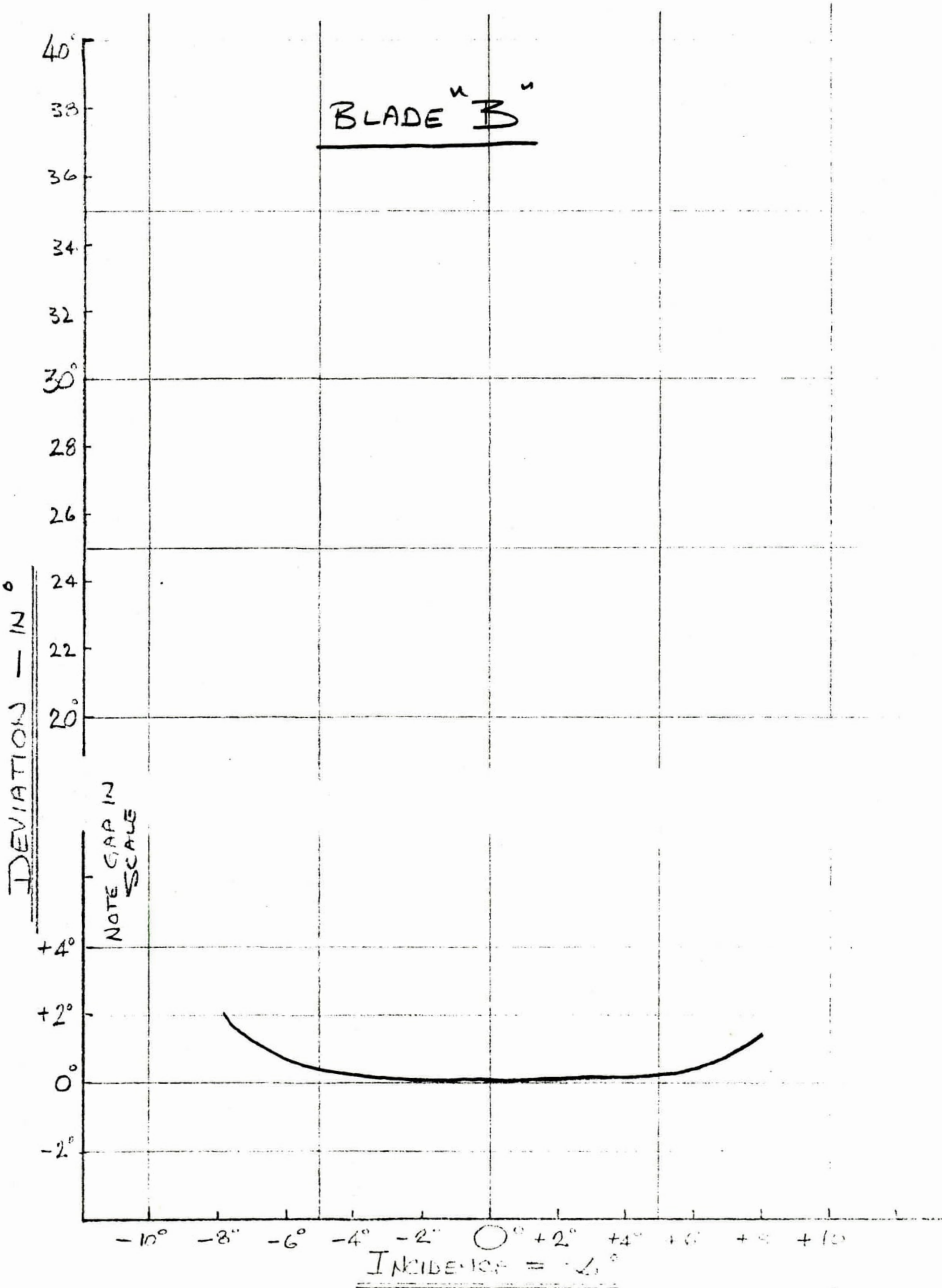

BLADE "B"
DEVIATION – IN °
NOTE GAP IN SCALE
40°
38
36
34
32
30°
28
26
24
22
20°
+4°
+2°
0°
-2°
-10°
-8°
-6°
-4°
-2°
0°
+2°
+4°
+10
INCIDENCE

B_b

0° CAMBER. 1 SLOTS "B" SERIES

+8° INCIDENCE α

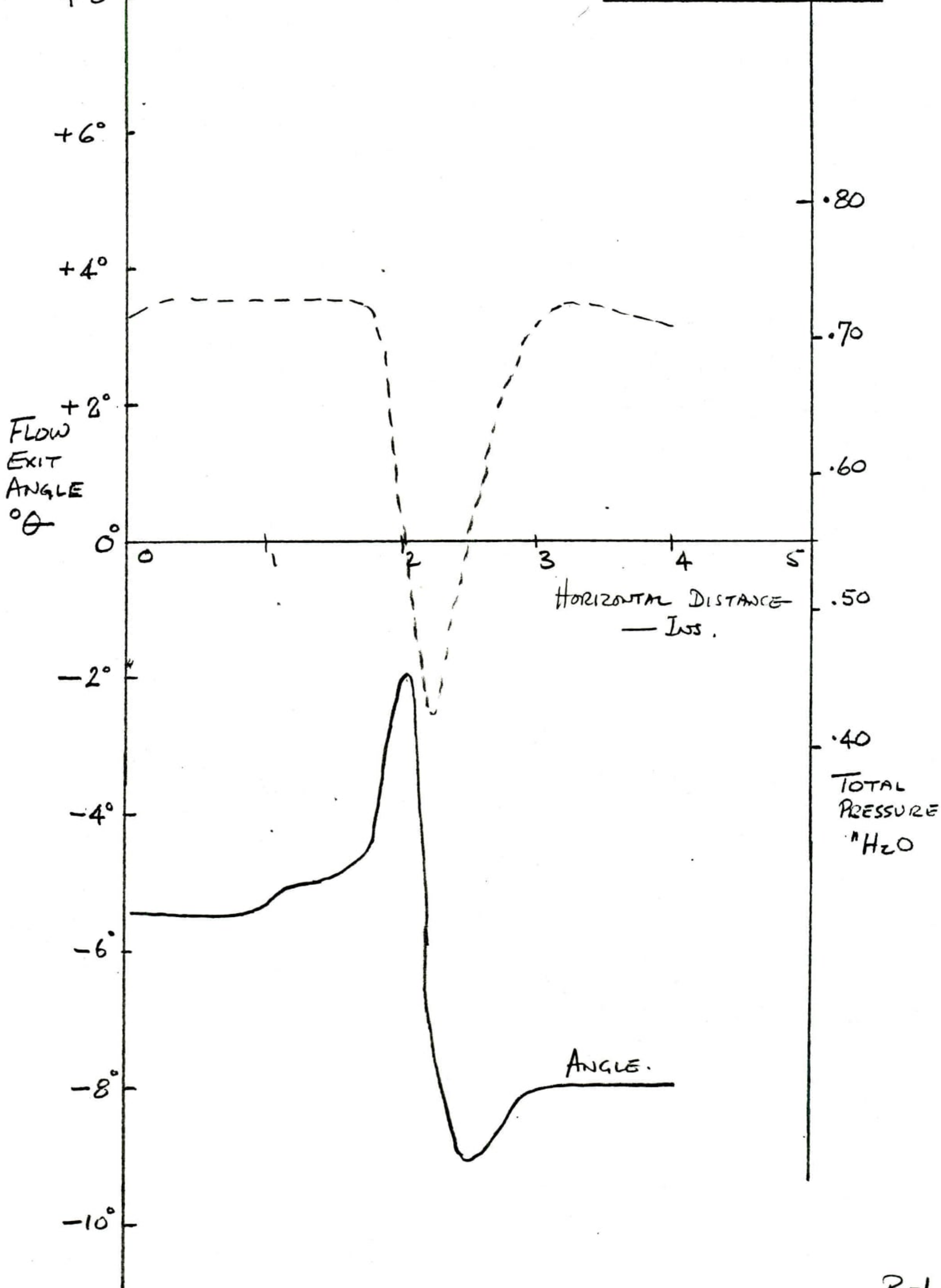

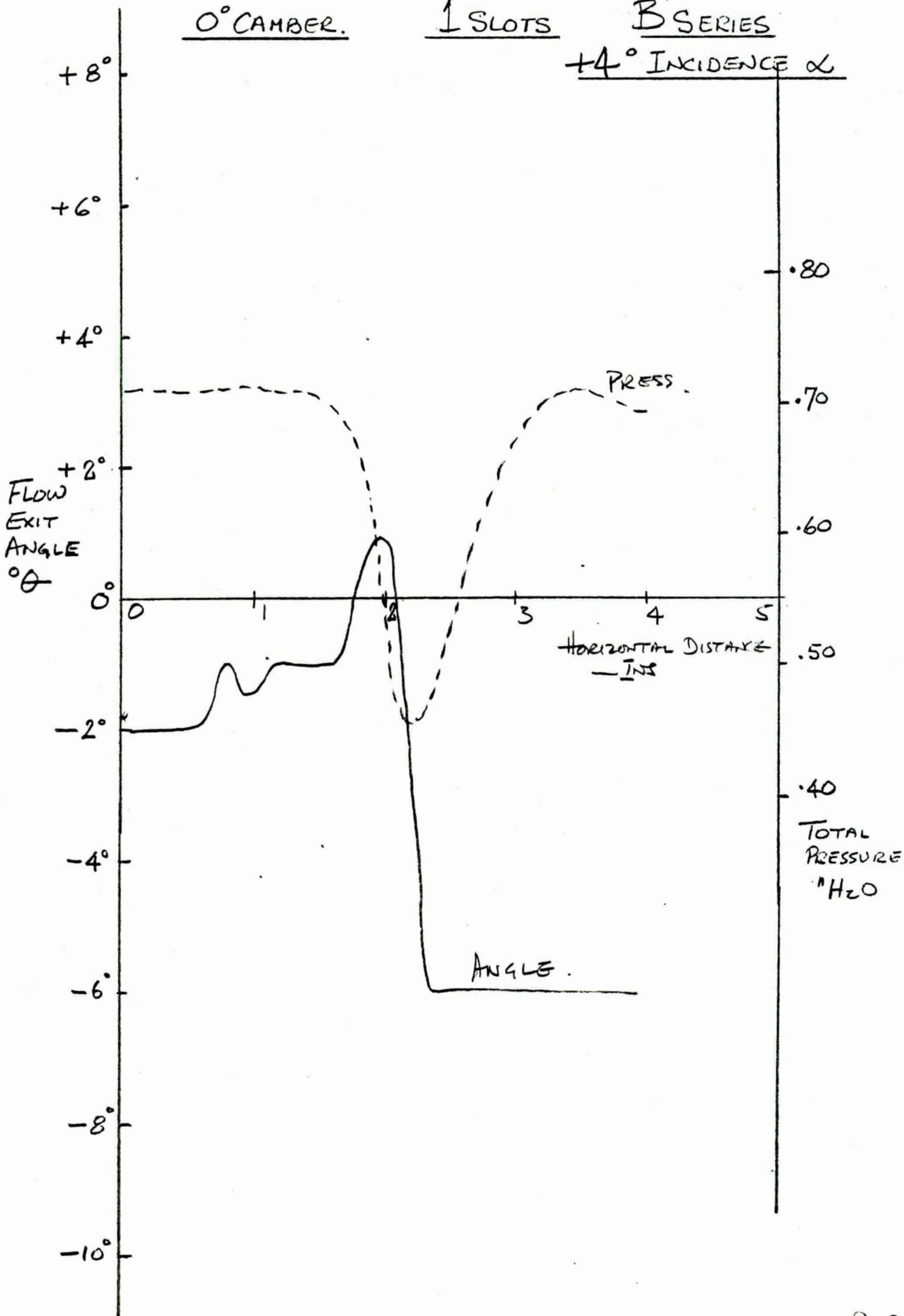

O° CAMBER.
1 SLOTS
"B" SERIES
+4° INCIDENCE α
+8°
+6°
+4°
+2°
0°
−2°
−4°
−6°
−8°
−10°
FLOW EXIT ANGLE °θ
.80
.70
.60
.50
.40
TOTAL PRESSURE "H2O
0
1
2
3
4
5
HORIZONTAL DISTANCE — INS
PRESS.
ANGLE.

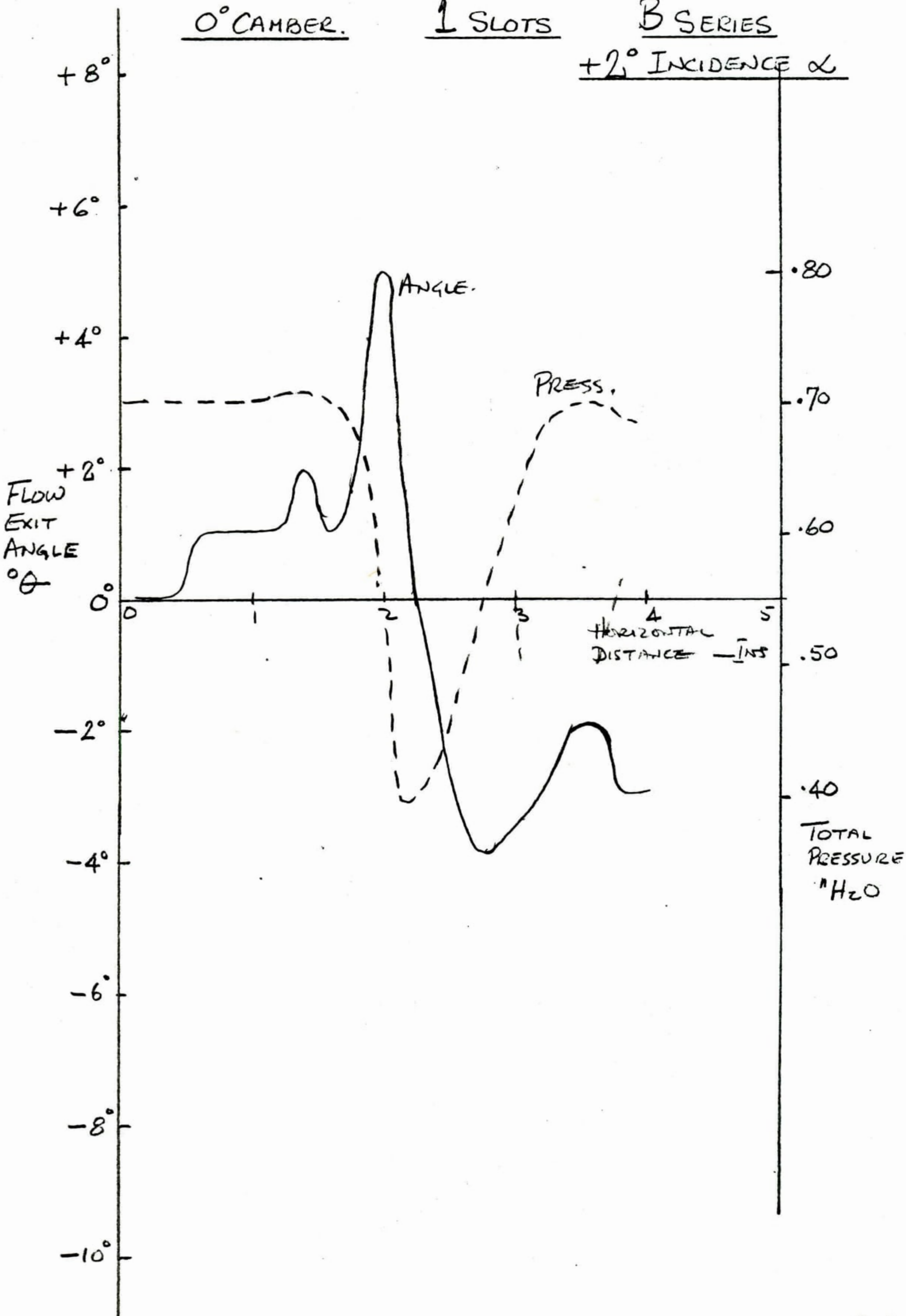
O° CAMBER.
1 SLOTS
"B" SERIES
+2° INCIDENCE α
+8°
+6°
+4°
+2°
0°
−2°
−4°
−6°
−8°
−10°
FLOW EXIT ANGLE °θ
ANGLE.
PRESS.
0
1
2
3
4
5
HORIZONTAL DISTANCE — INS
.80
.70
.60
.50
.40
TOTAL PRESSURE "H₂O

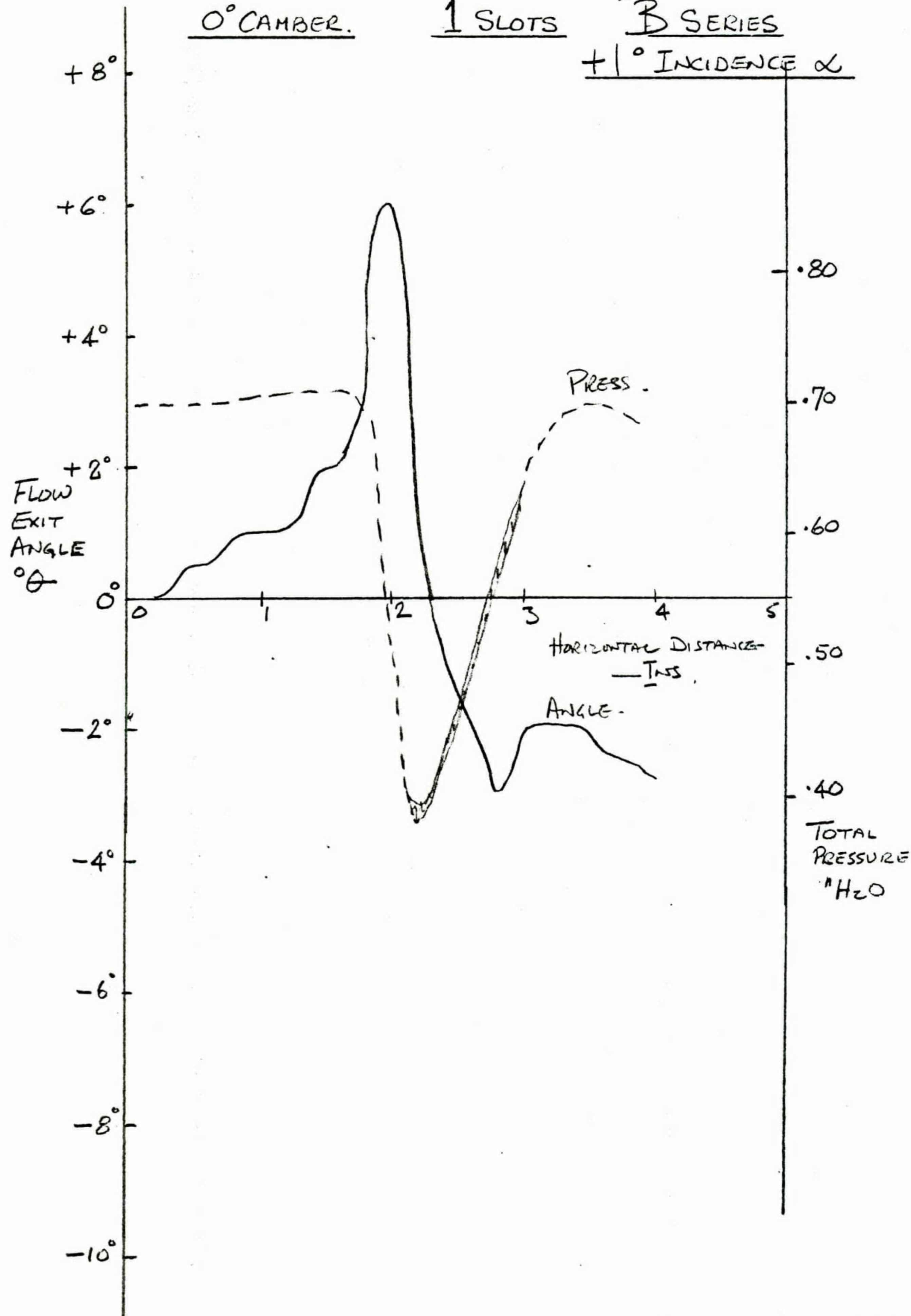

O° CAMBER.
1 SLOTS
"B" SERIES
+1° INCIDENCE α
+8°
+6°
+4°
+2°
0°
−2°
−4°
−6°
−8°
−10°
FLOW
EXIT
ANGLE
°θ
0
1
2
3
4
5
HORIZONTAL DISTANCE
— INS.
PRESS.
ANGLE.
·80
·70
·60
.50
·40
TOTAL
PRESSURE
"H₂O

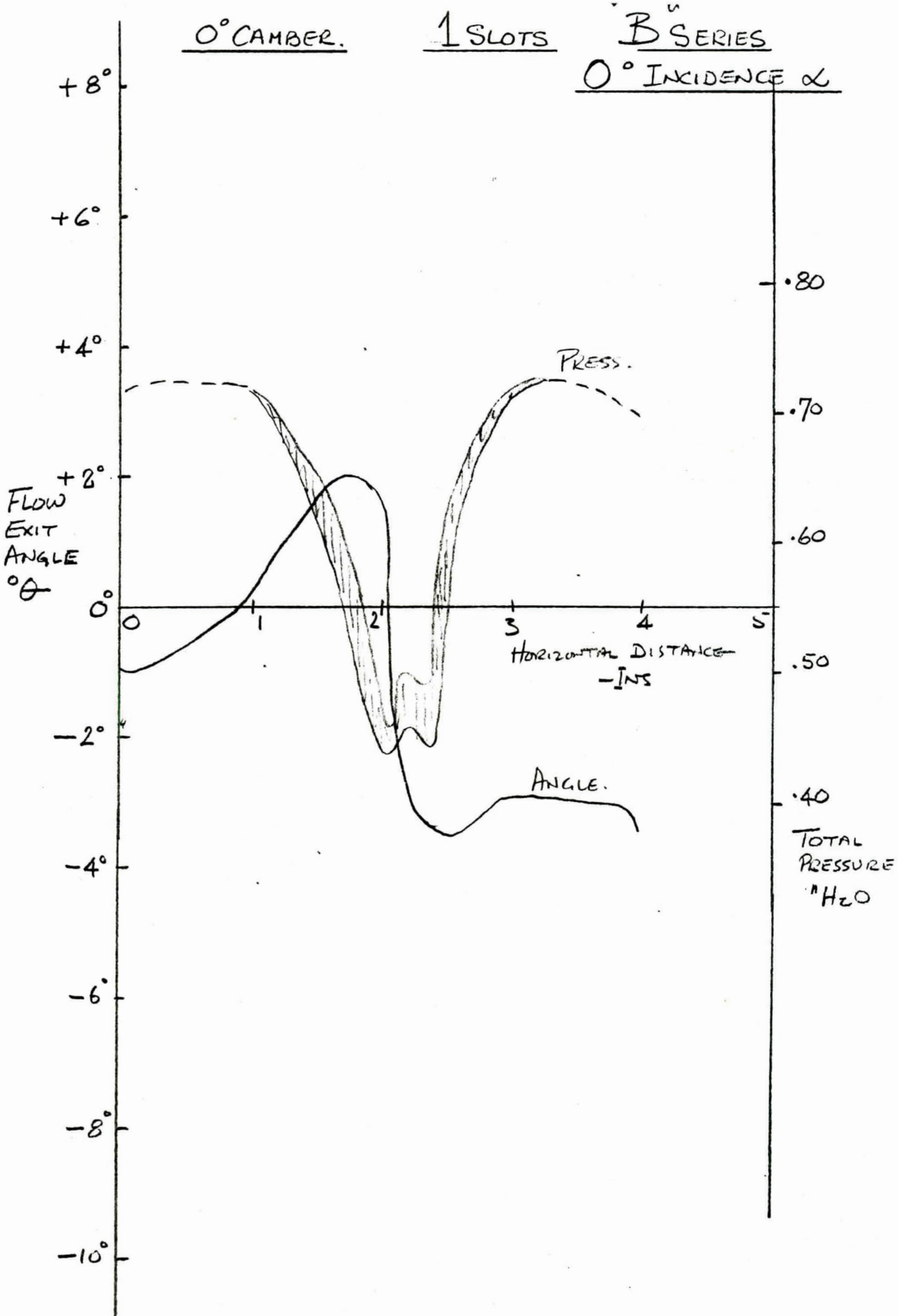

O° CAMBER.
1 SLOTS
"B" SERIES
0° INCIDENCE α
+8°
+6°
+4°
+2°
0°
−2°
−4°
−6°
−8°
−10°
FLOW EXIT ANGLE °θ
PRESS.
ANGLE.
0
1
2
3
4
5
HORIZONTAL DISTANCE −INS
·80
·70
·60
·50
·40
TOTAL PRESSURE "H_2O

B-5

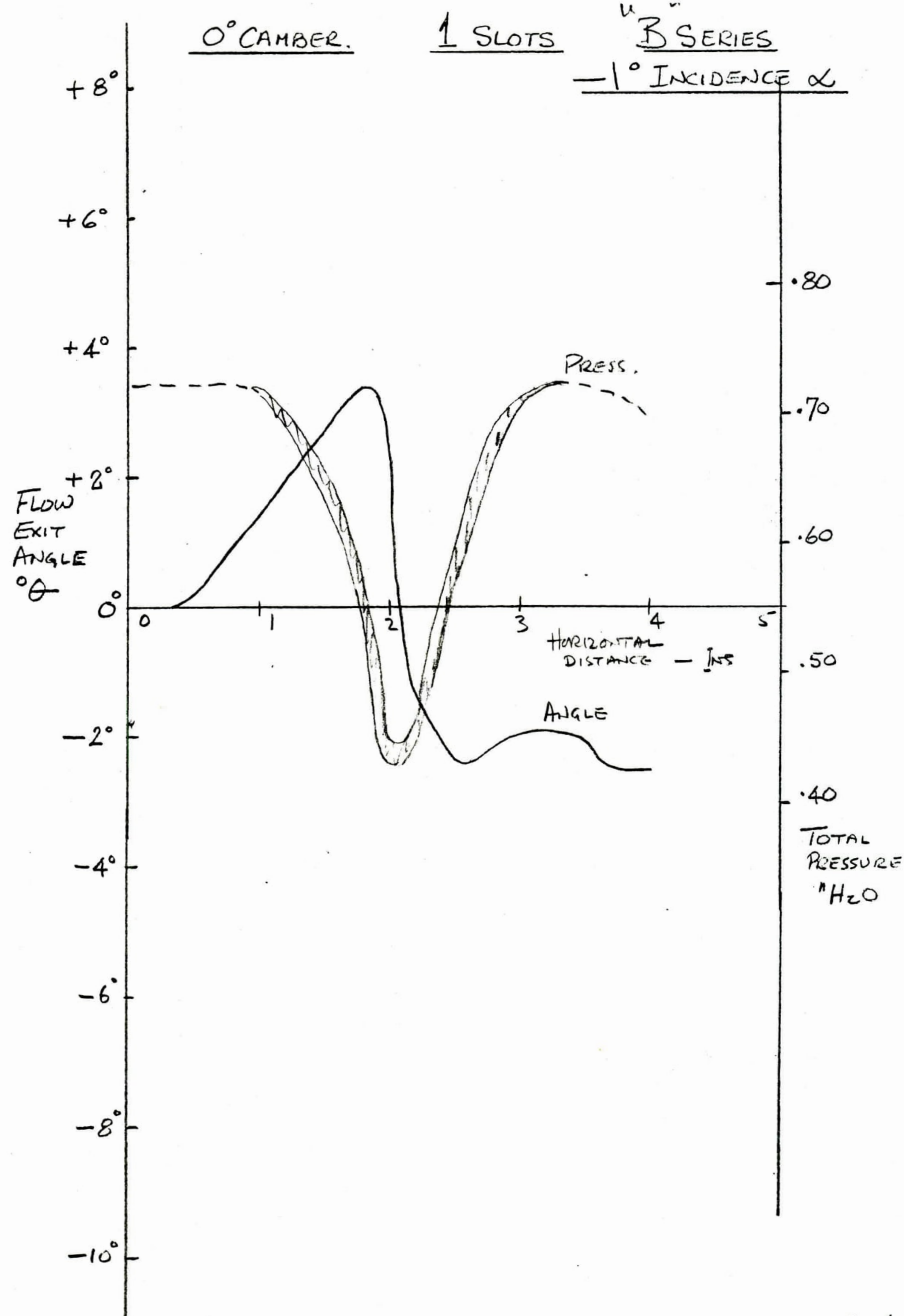
O° CAMBER. 1 SLOTS "B" SERIES
—1° INCIDENCE α
+8°
+6°
+4°
+2°
0°
−2°
−4°
−6°
−8°
−10°
FLOW EXIT ANGLE °θ
0
1
2
3
4
5
HORIZONTAL DISTANCE — INS
.80
.70
.60
.50
.40
TOTAL PRESSURE "H₂O
PRESS.
ANGLE

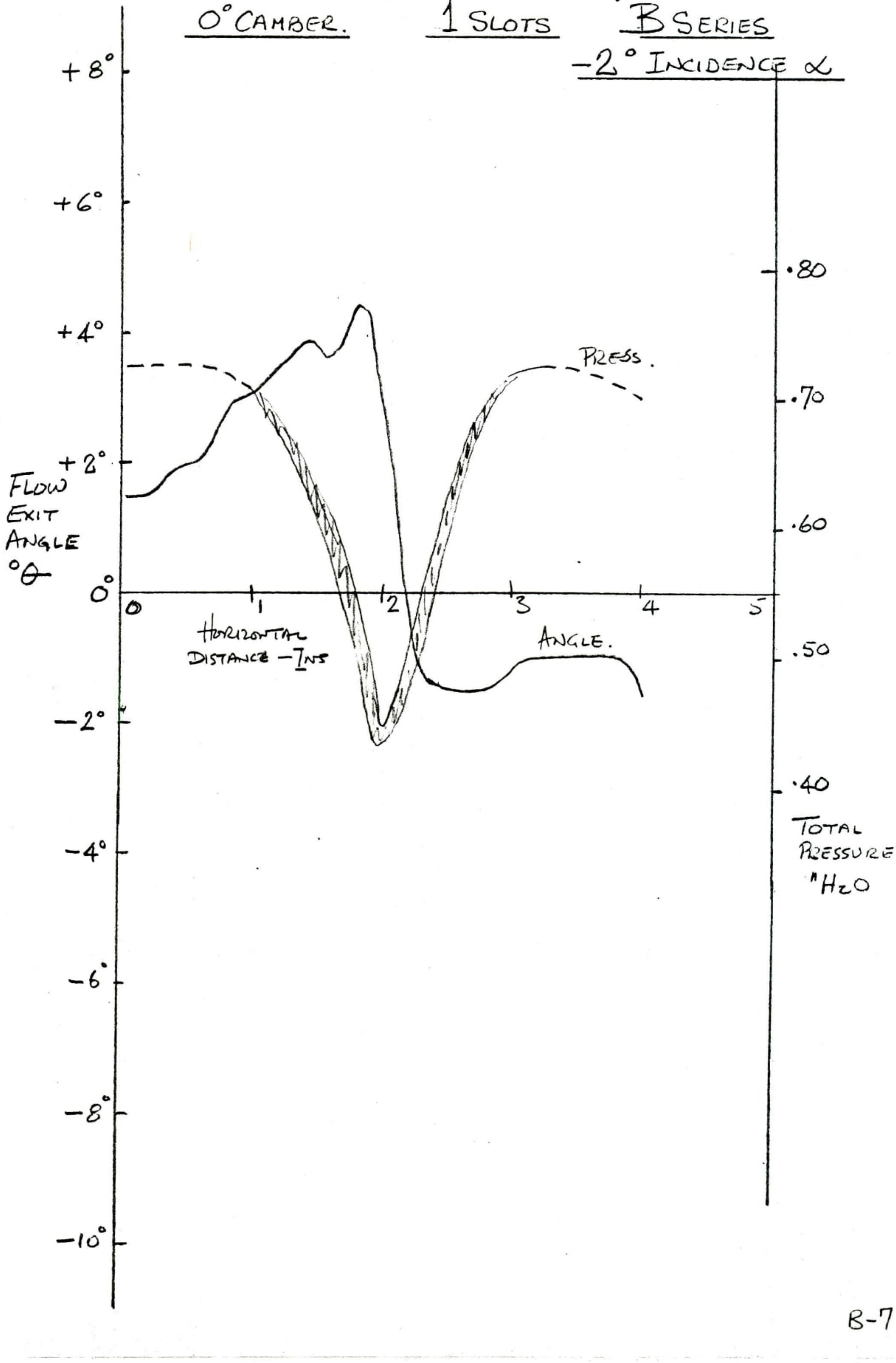

0° CAMBER.
1 SLOTS
"B" SERIES
-2° INCIDENCE α
+8°
+6°
+4°
+2°
0°
-2°
-4°
-6°
-8°
-10°
FLOW EXIT ANGLE °θ
0
1
2
3
4
5
HORIZONTAL DISTANCE - INS
PRESS.
ANGLE.
.80
.70
.60
.50
.40
TOTAL PRESSURE "H2O

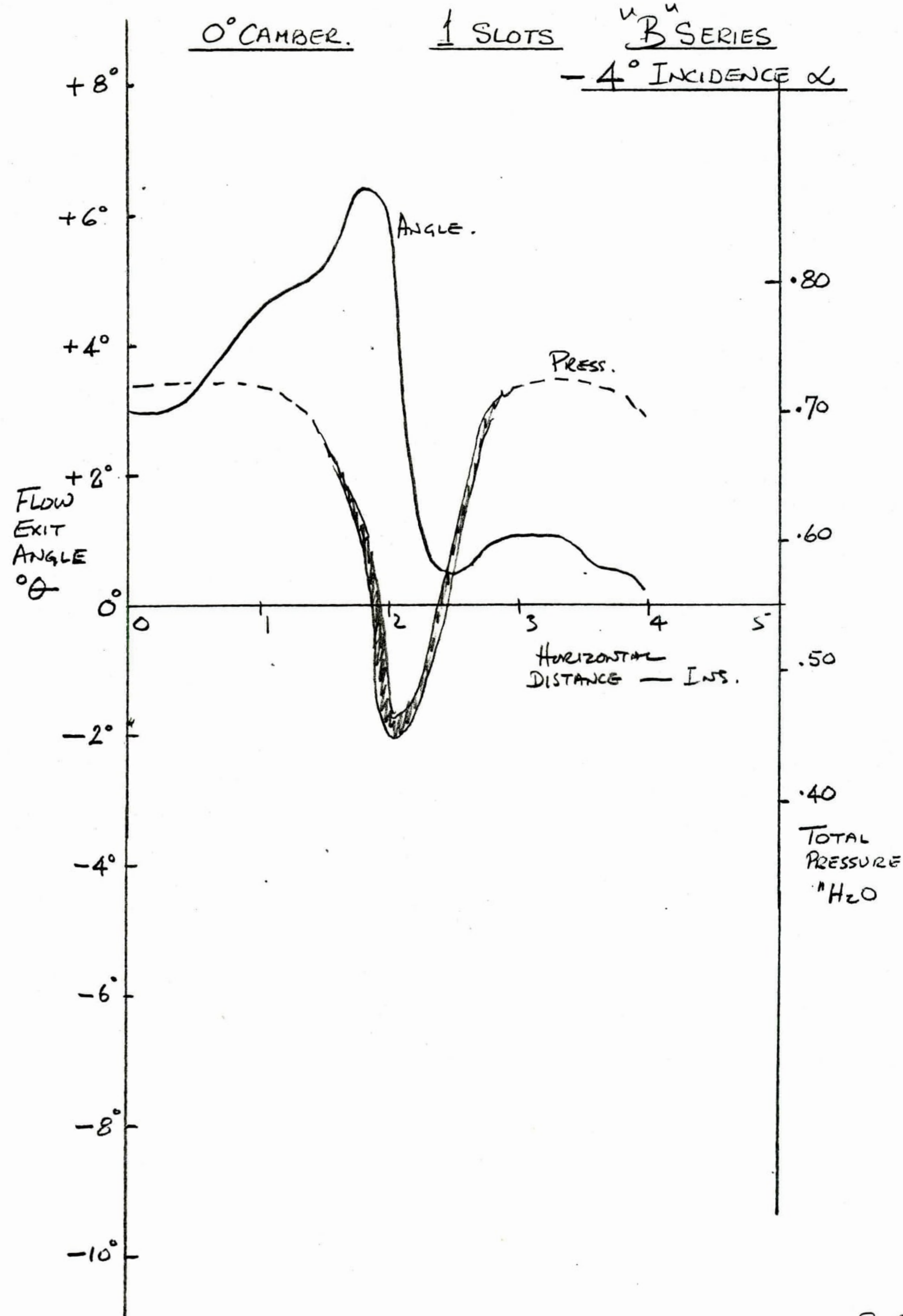

O° CAMBER.
1 SLOTS
"B" SERIES
− 4° INCIDENCE α
+8°
+6°
+4°
+2°
0°
−2°
−4°
−6°
−8°
−10°
FLOW
EXIT
ANGLE
°θ
ANGLE.
PRESS.
0
1
2
3
4
5
HORIZONTAL
DISTANCE — INS.
·80
·70
·60
·50
·40
TOTAL
PRESSURE
"H_2O

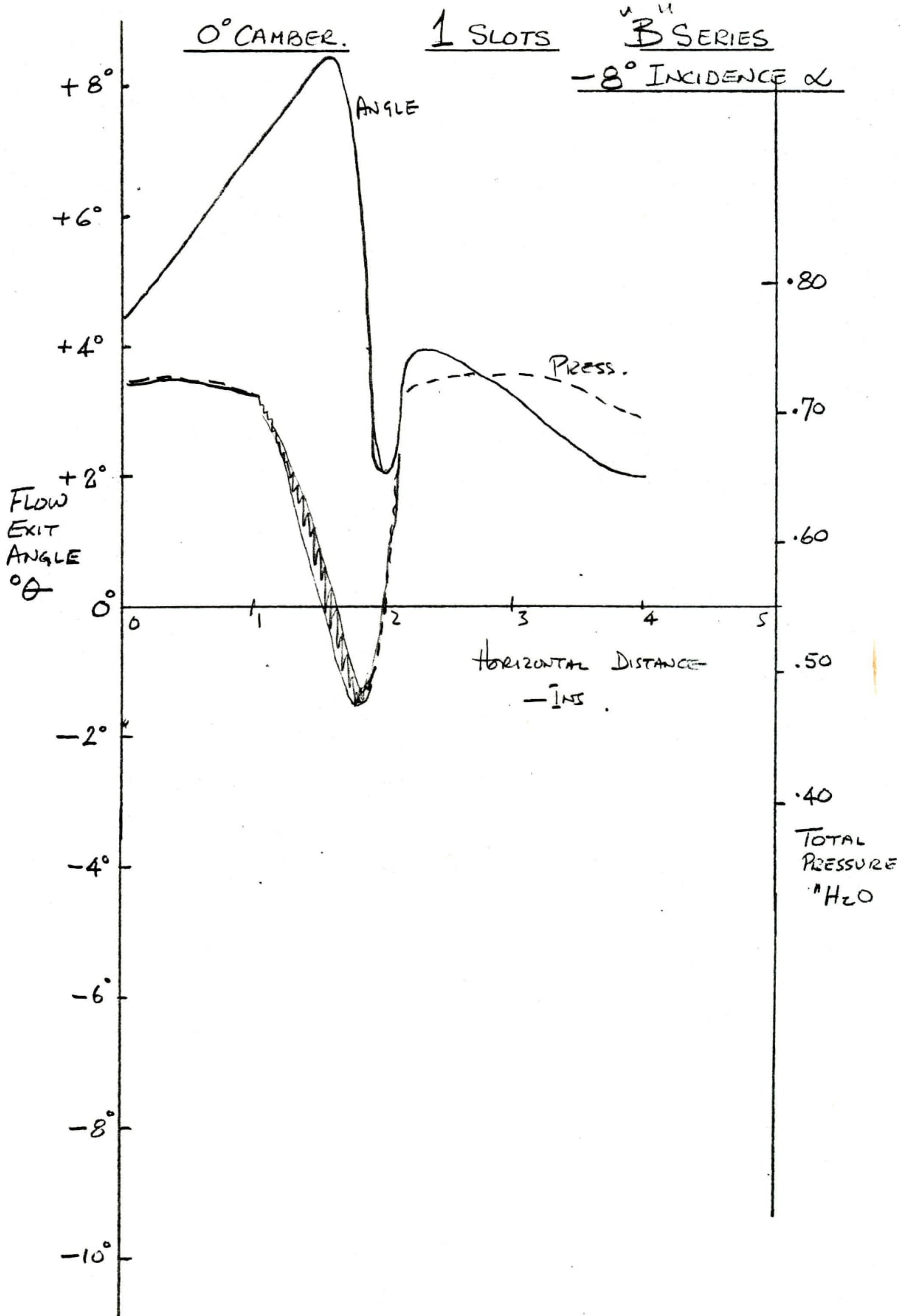

0° CAMBER.
1 SLOTS
"B" SERIES
−8° INCIDENCE α
ANGLE
PRESS.
+8°
+6°
+4°
+2°
0°
−2°
−4°
−6°
−8°
−10°
FLOW EXIT ANGLE °θ
0
1
2
3
4
5
HORIZONTAL DISTANCE — INS.
·80
·70
·60
·50
·40
TOTAL PRESSURE "H_2O

BLADE "C" NO SLOTS

75° CAMBER.

12% t/c C-4

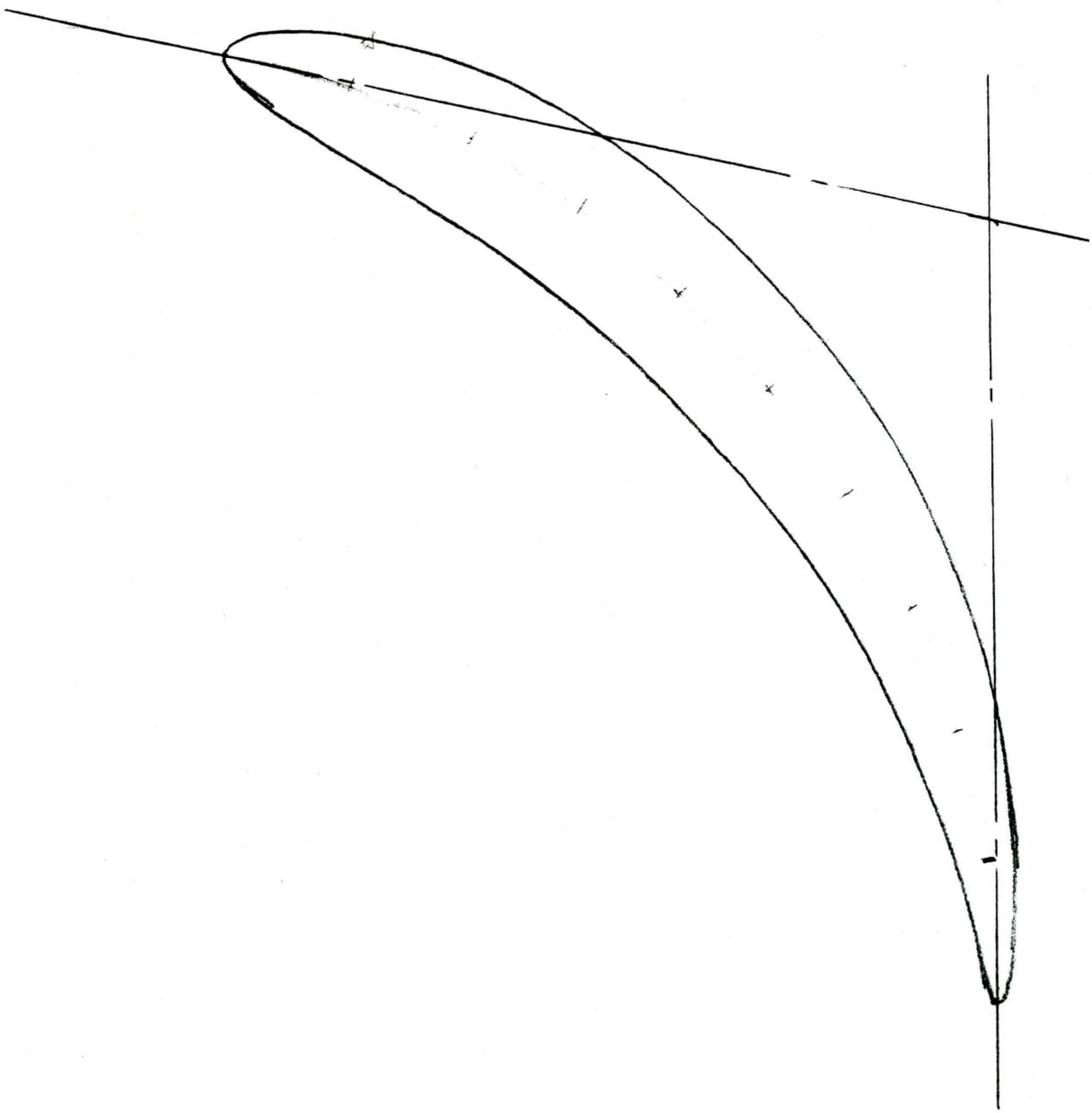

C6

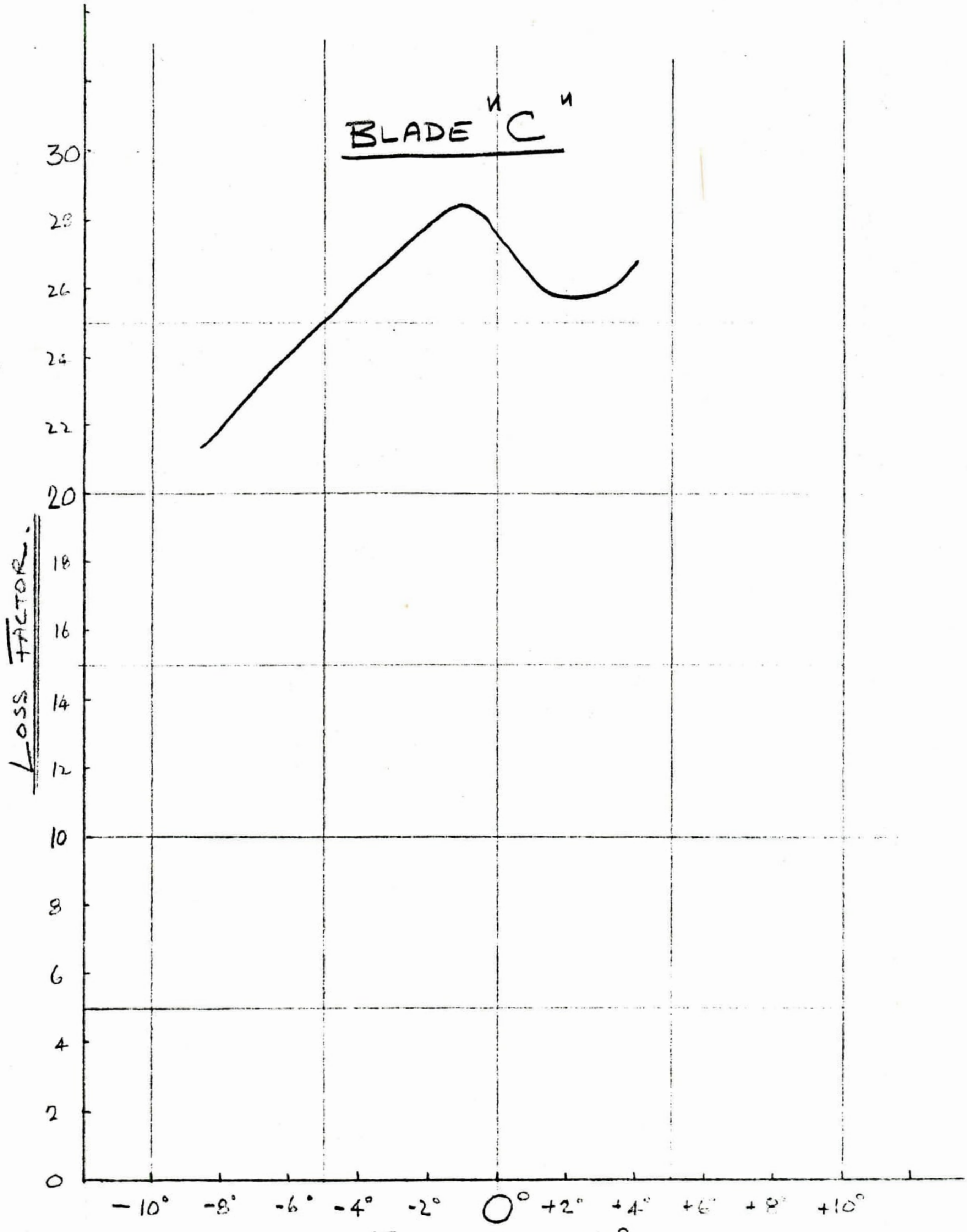
BLADE "C"
LOSS FACTOR
30
28
26
24
22
20
18
16
14
12
10
8
6
4
2
0
−10°
-8°
-6°
-4°
-2°
0°
+2°
+4°
+6°
+8°
+10°
INCIDENCE = α°

Ca

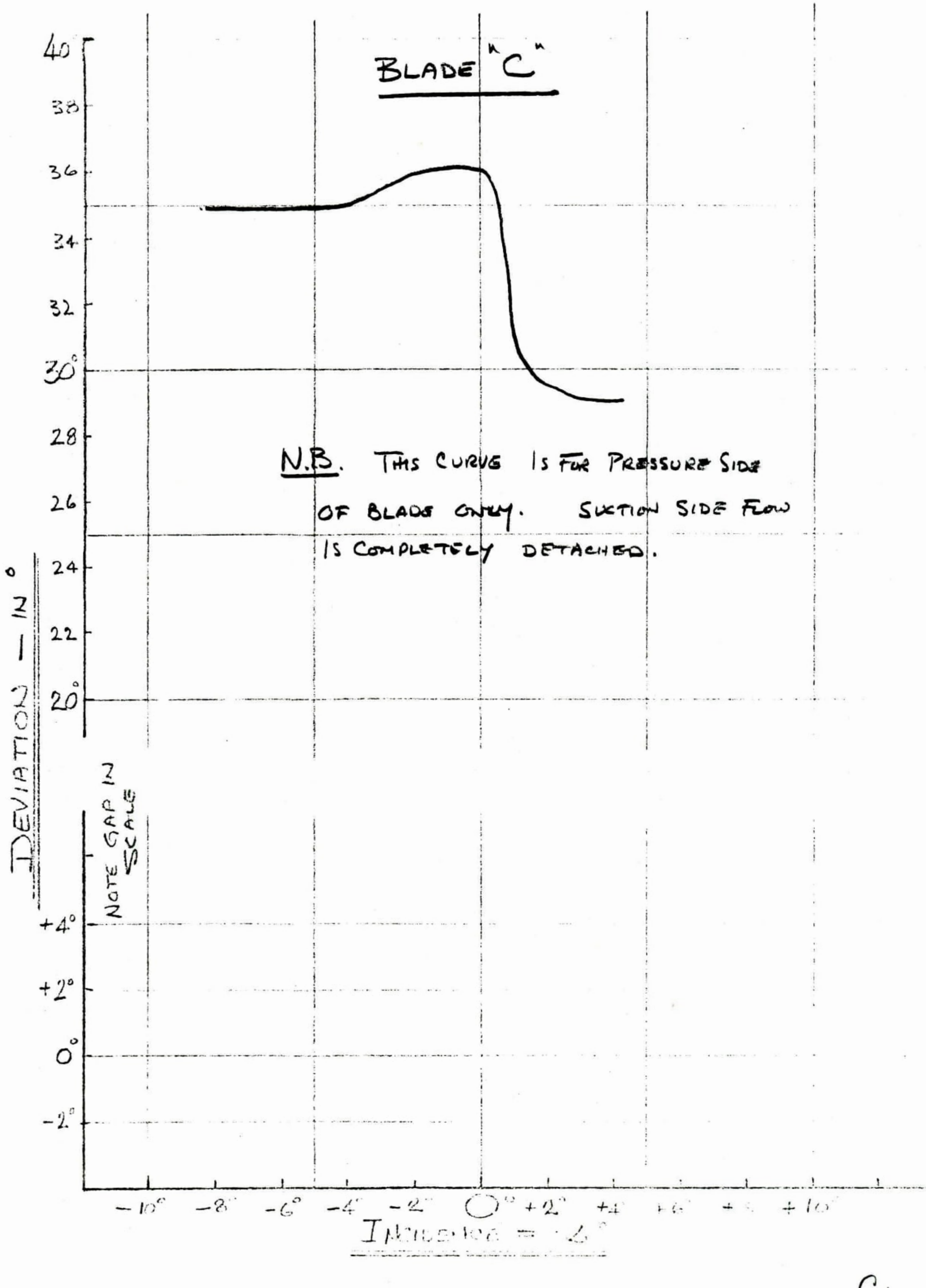
BLADE "C"
N.B. THIS CURVE IS FOR PRESSURE SIDE OF BLADE ONLY. SUCTION SIDE FLOW IS COMPLETELY DETACHED.
DEVIATION — IN °
NOTE GAP IN SCALE
40
38
36
34
32
30°
28
26
24
22
20°
+4°
+2°
0°
-2°
-10°
-8°
-6°
-4°
-2°
0°
+2°
+10°

Cb

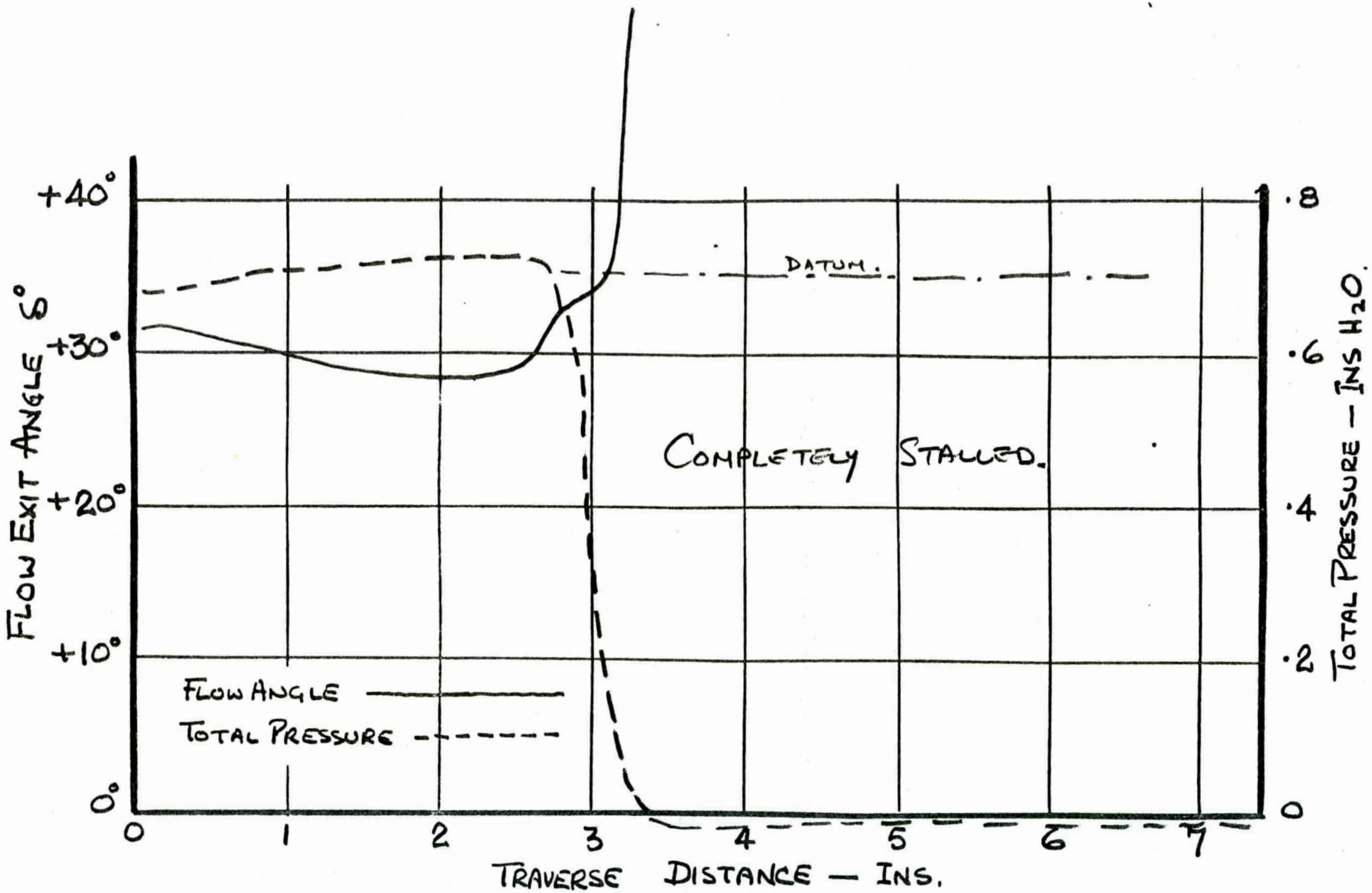

75° CAMBER. NO SLOTS. BLADE "C". +4° α

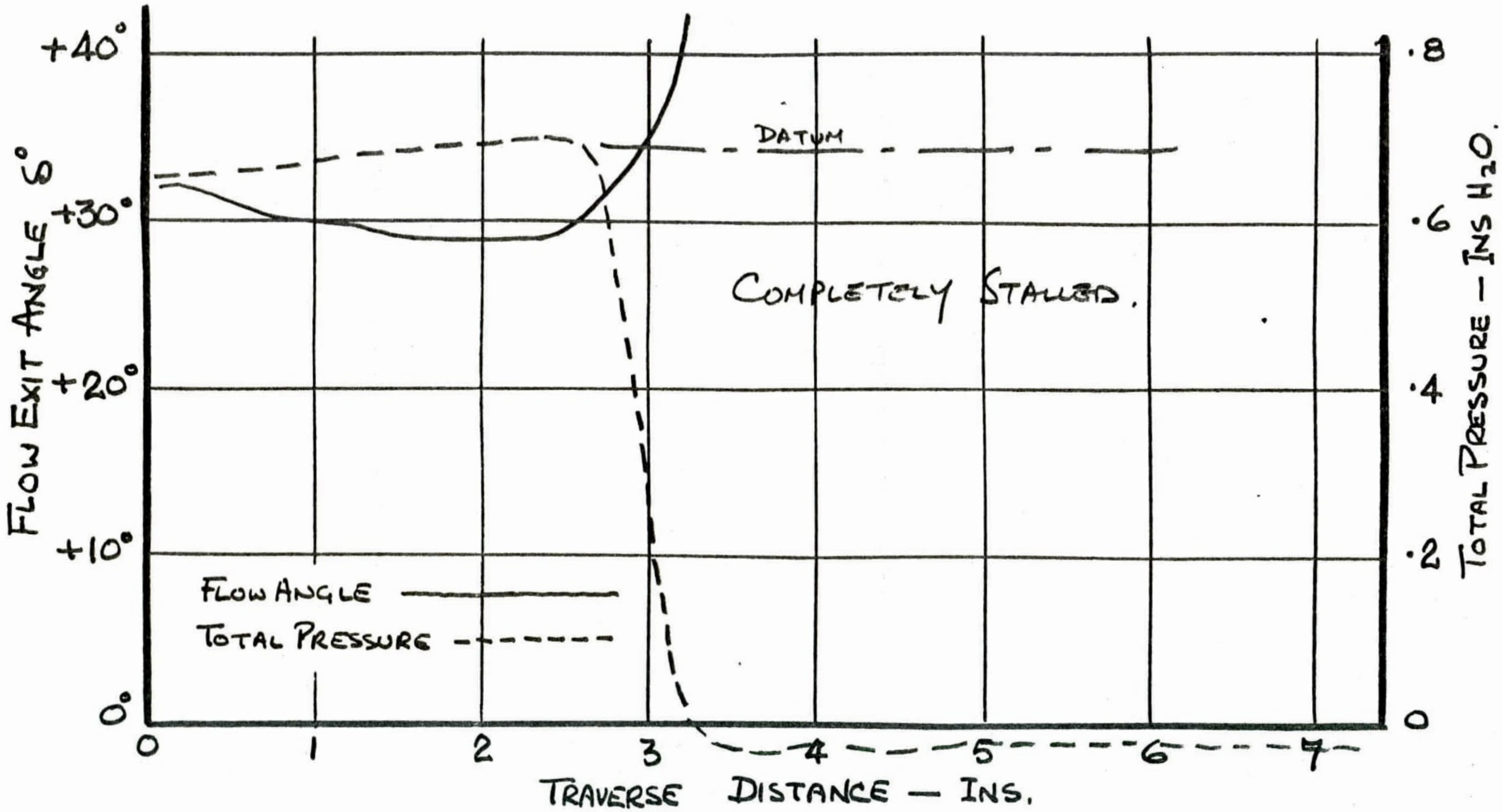

75° CAMBER. NO SLOTS. BLADE "C". +2 °α

C2

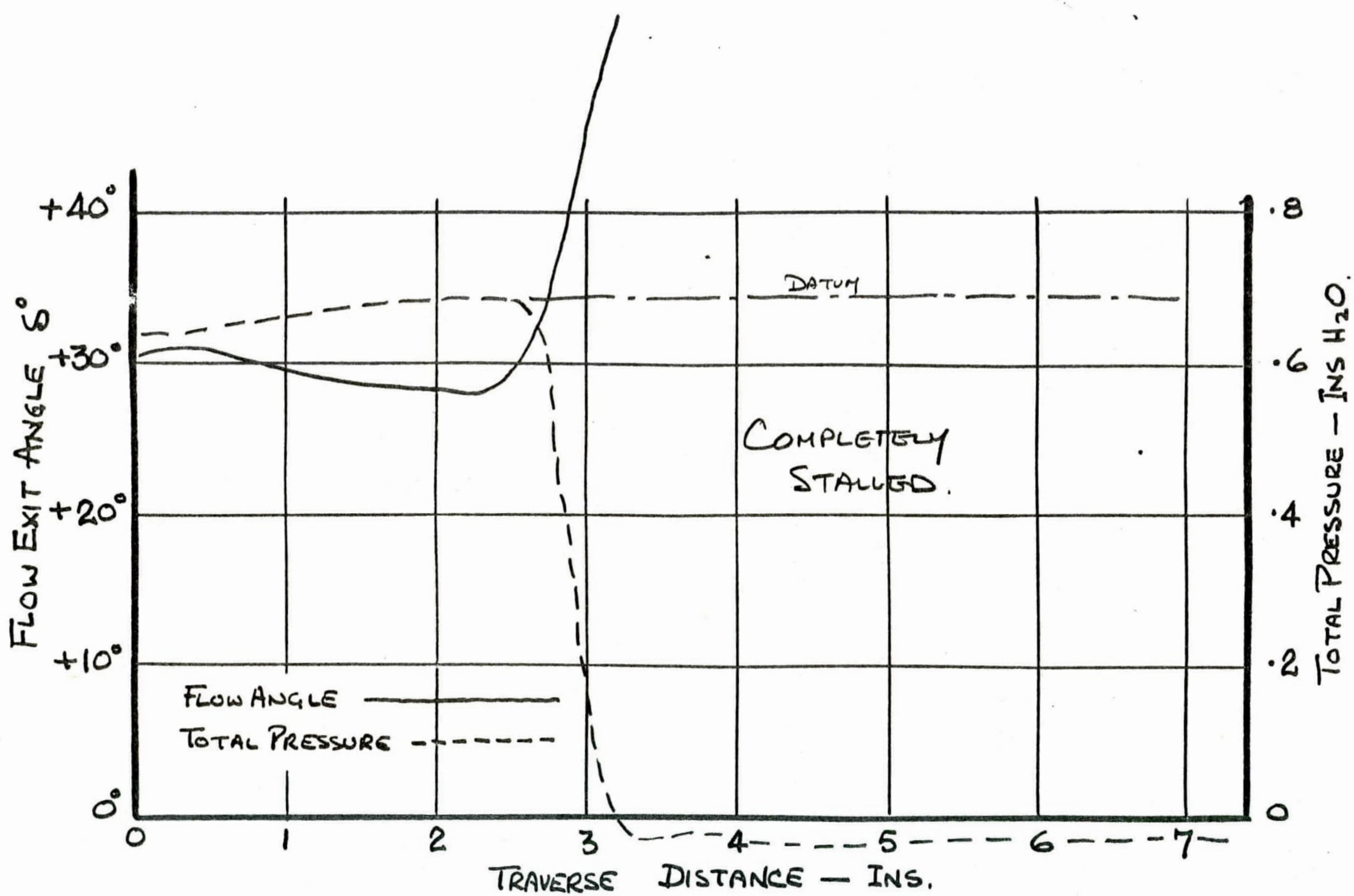

75° Camber. No Slots. Blade "C". +1 °α

C3

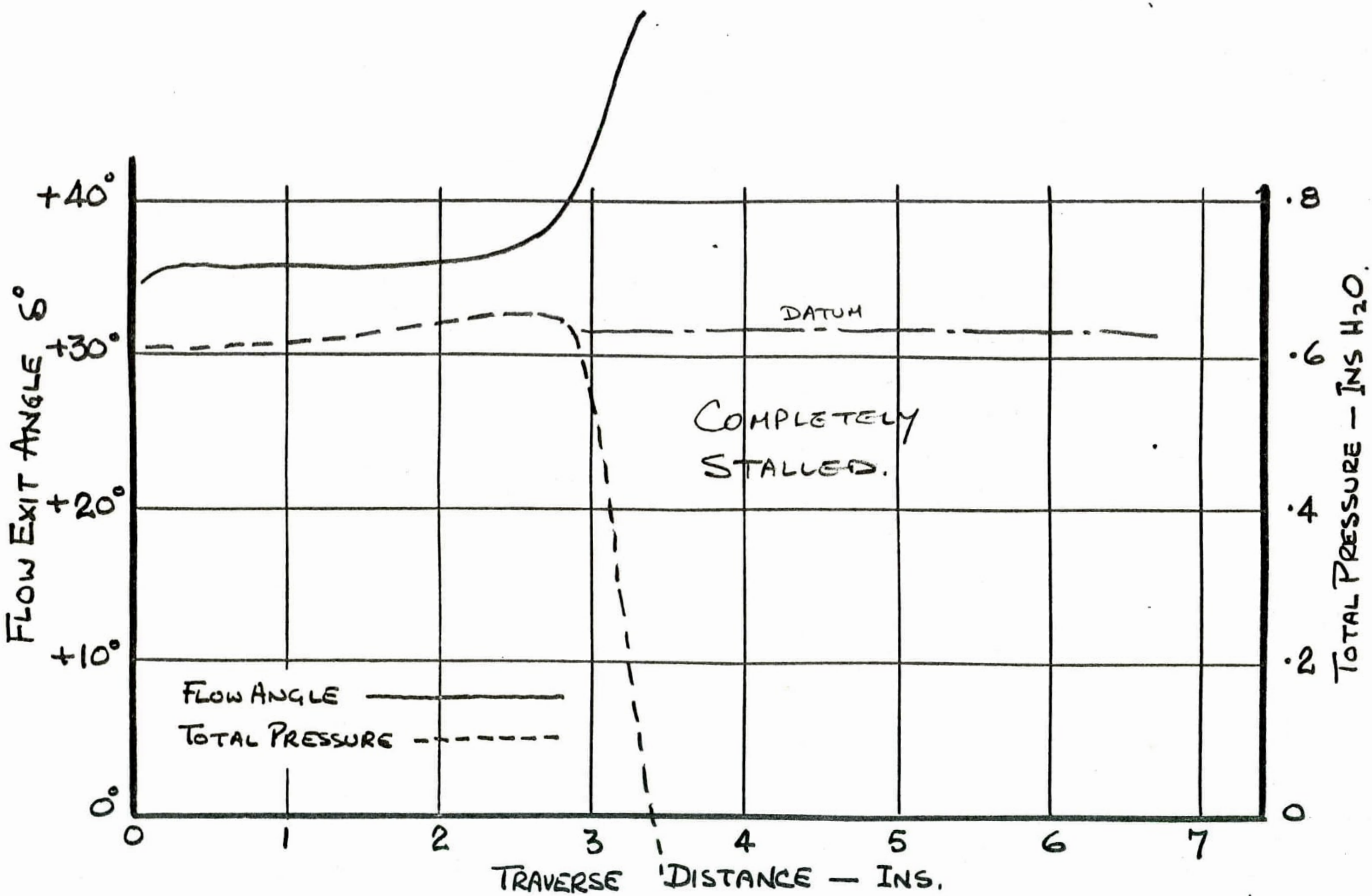

75° CAMBER. NO SLOTS. BLADE "C". 0°α

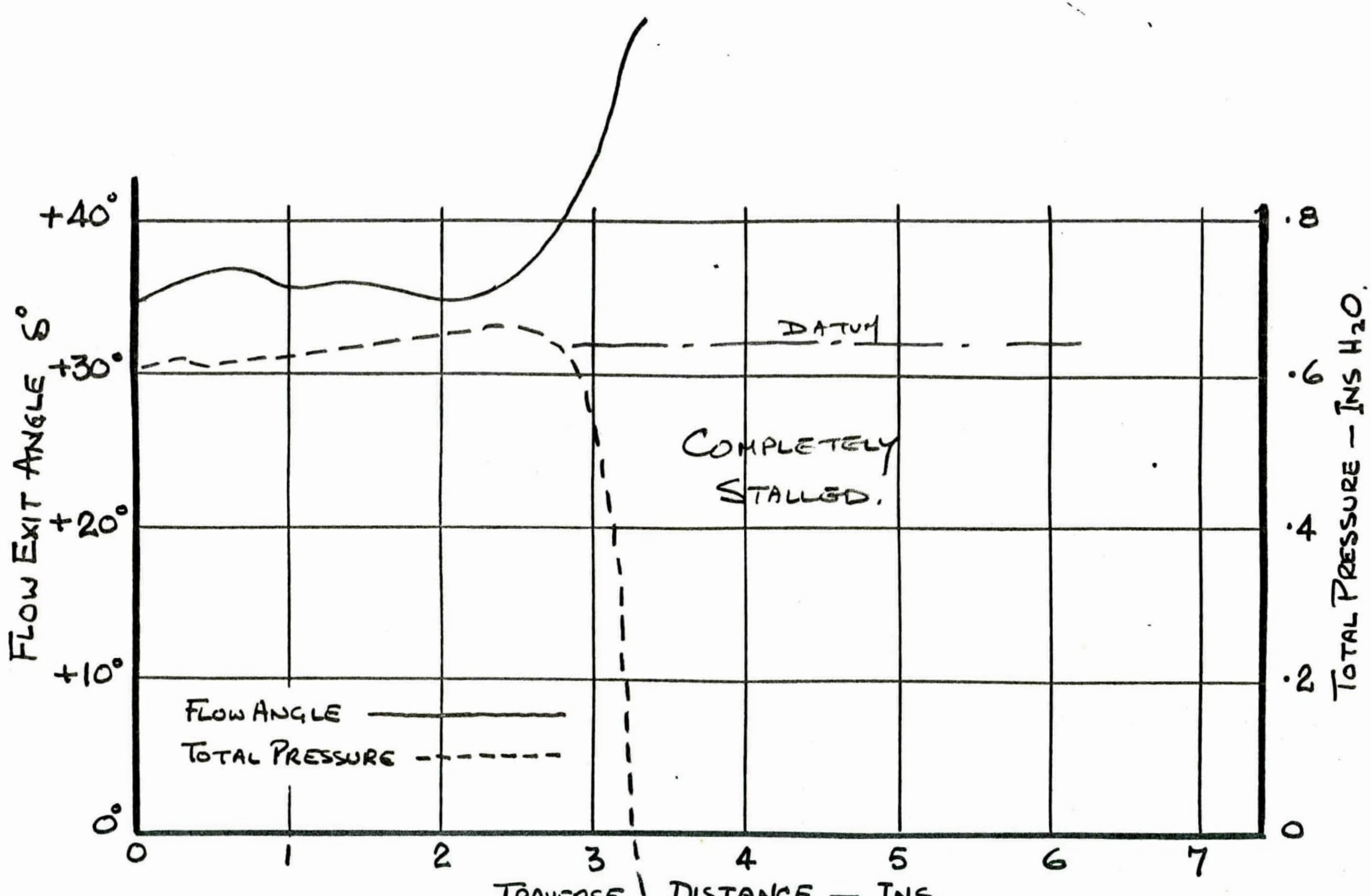

75° CAMBER. NO SLOTS. BLADE "C". −1 °α

C5

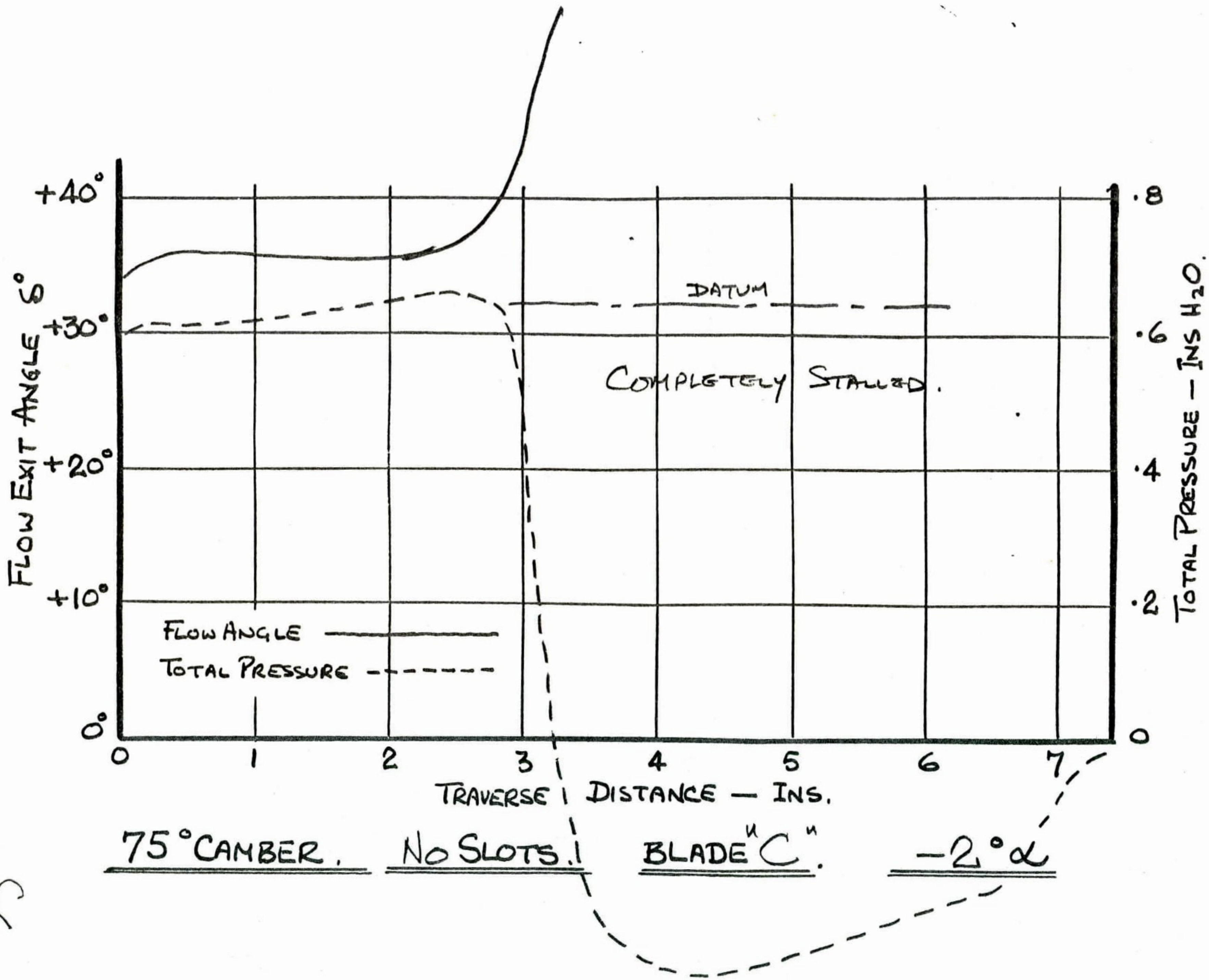

75° CAMBER. NO SLOTS. BLADE "C". −2° α

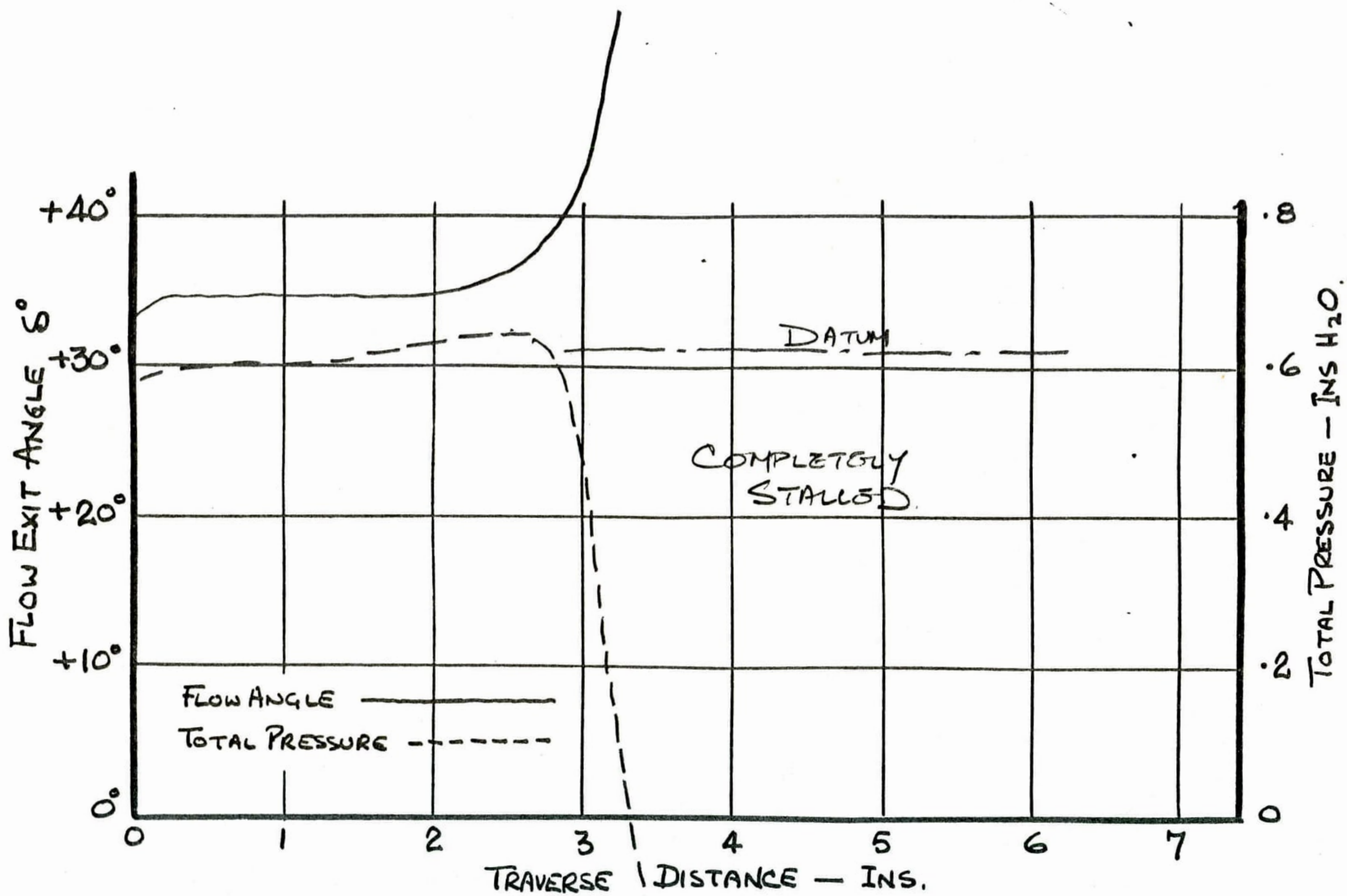

75° CAMBER. NO SLOTS. BLADE "C". −4°α

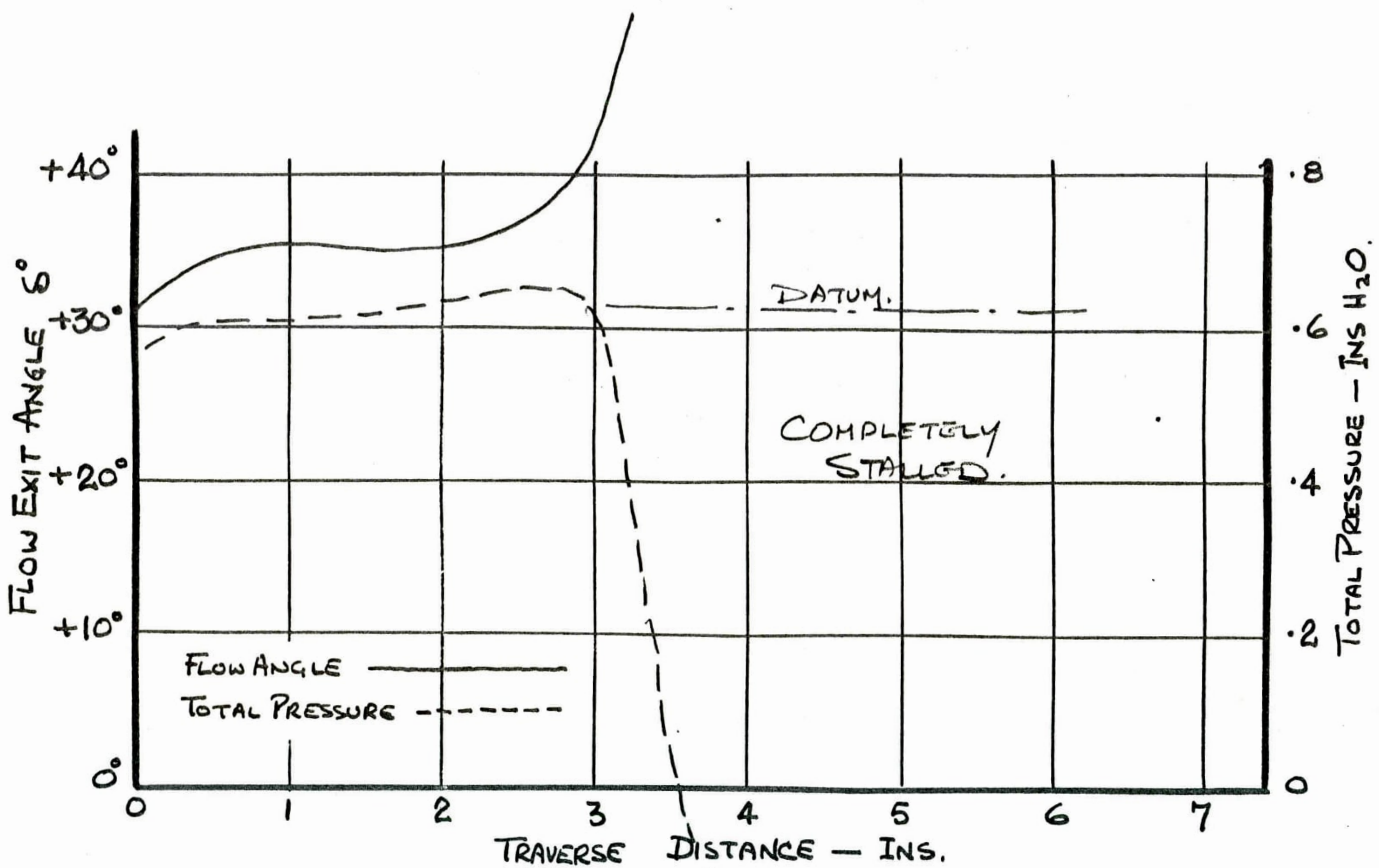

75° CAMBER. NO SLOTS. BLADE "C" −8°α

BLADE "D" N. 1 SLOT

75° CAMBER

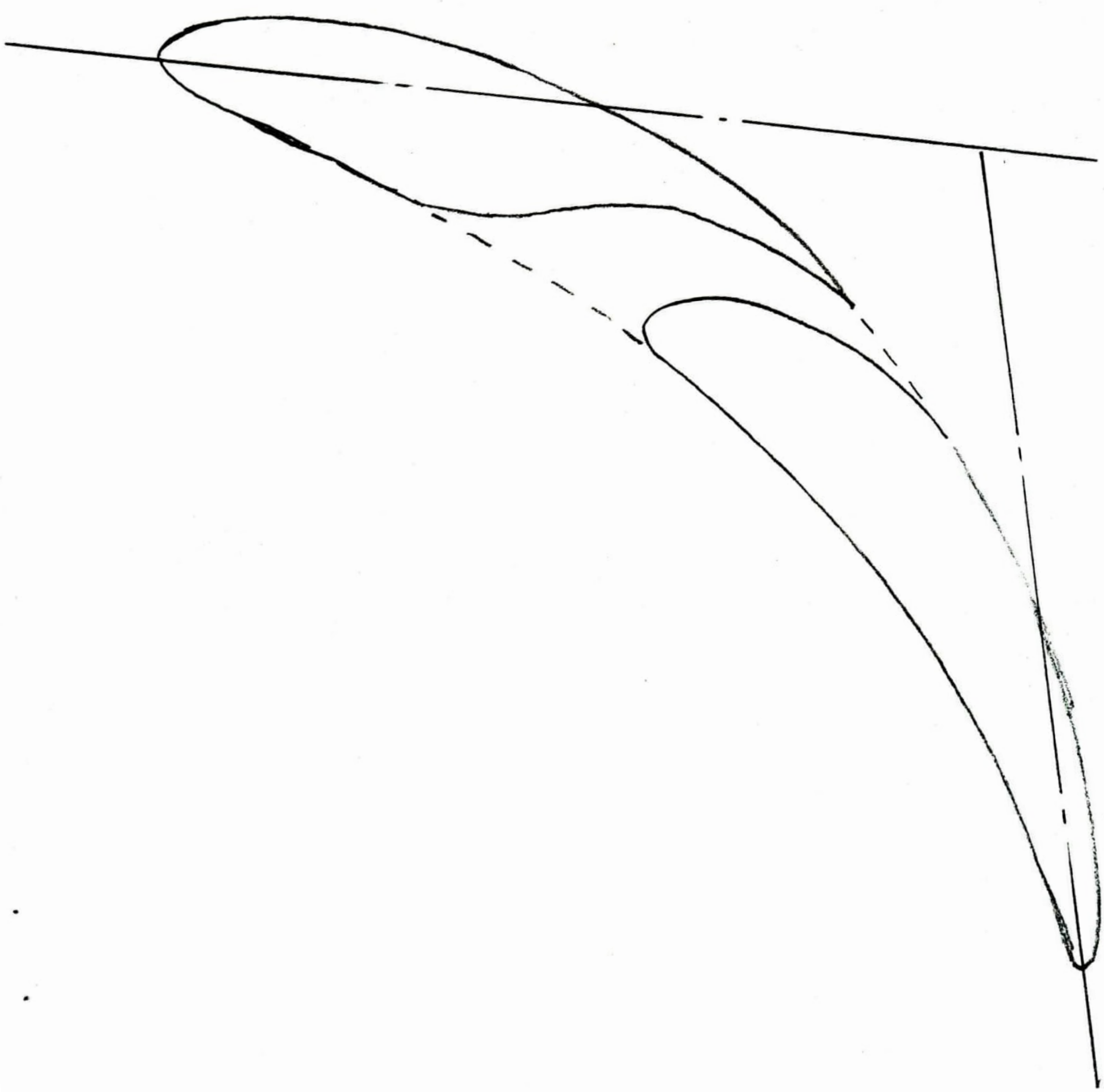

D

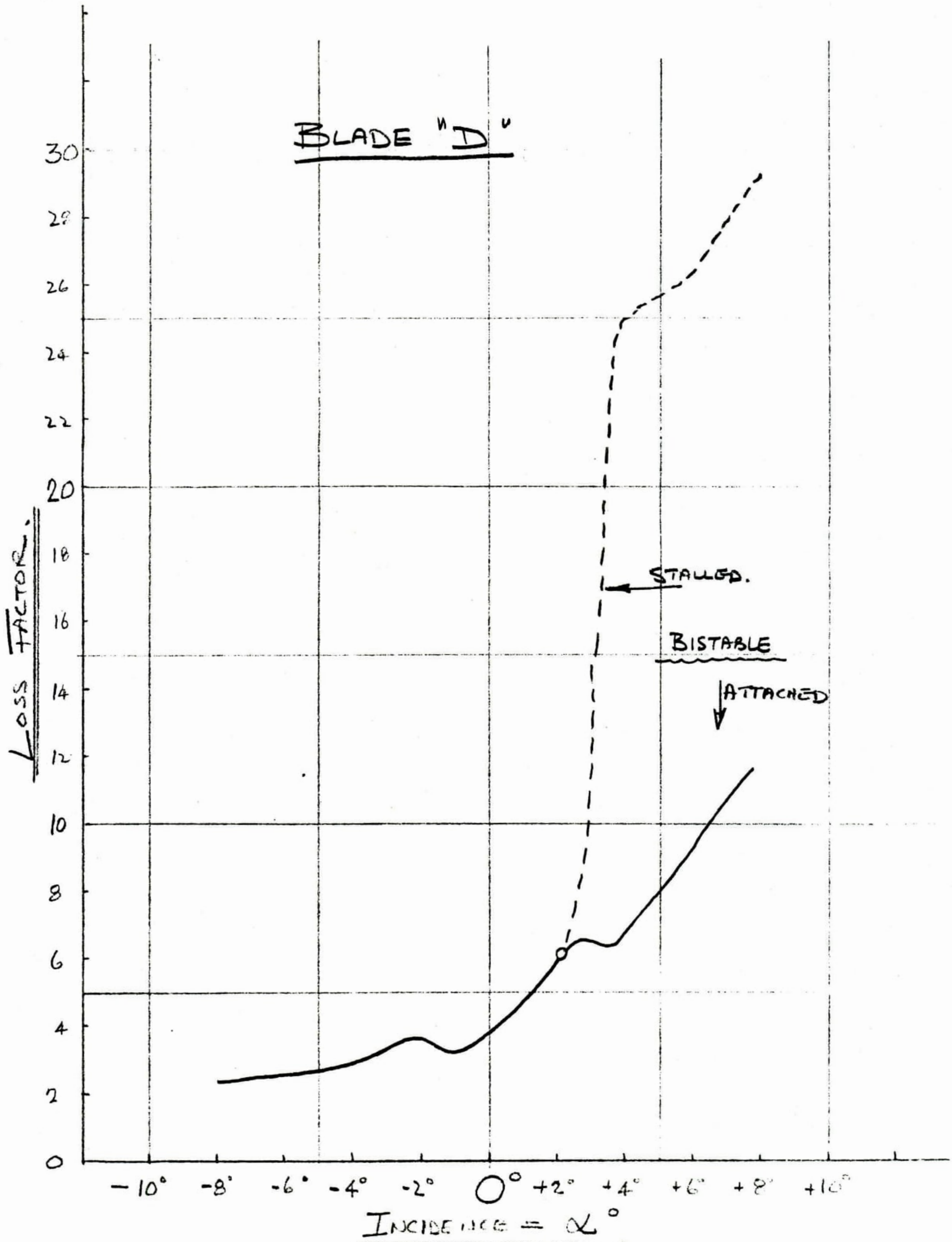

BLADE "D"
30
28
26
24
22
20
18
16
14
12
10
8
6
4
2
0
LOSS FACTOR.
STALLED.
BISTABLE
ATTACHED
−10°
-8°
-6°
-4°
-2°
0°
+2°
+4°
+6°
+8°
+10°
INCIDENCE = α°

Da

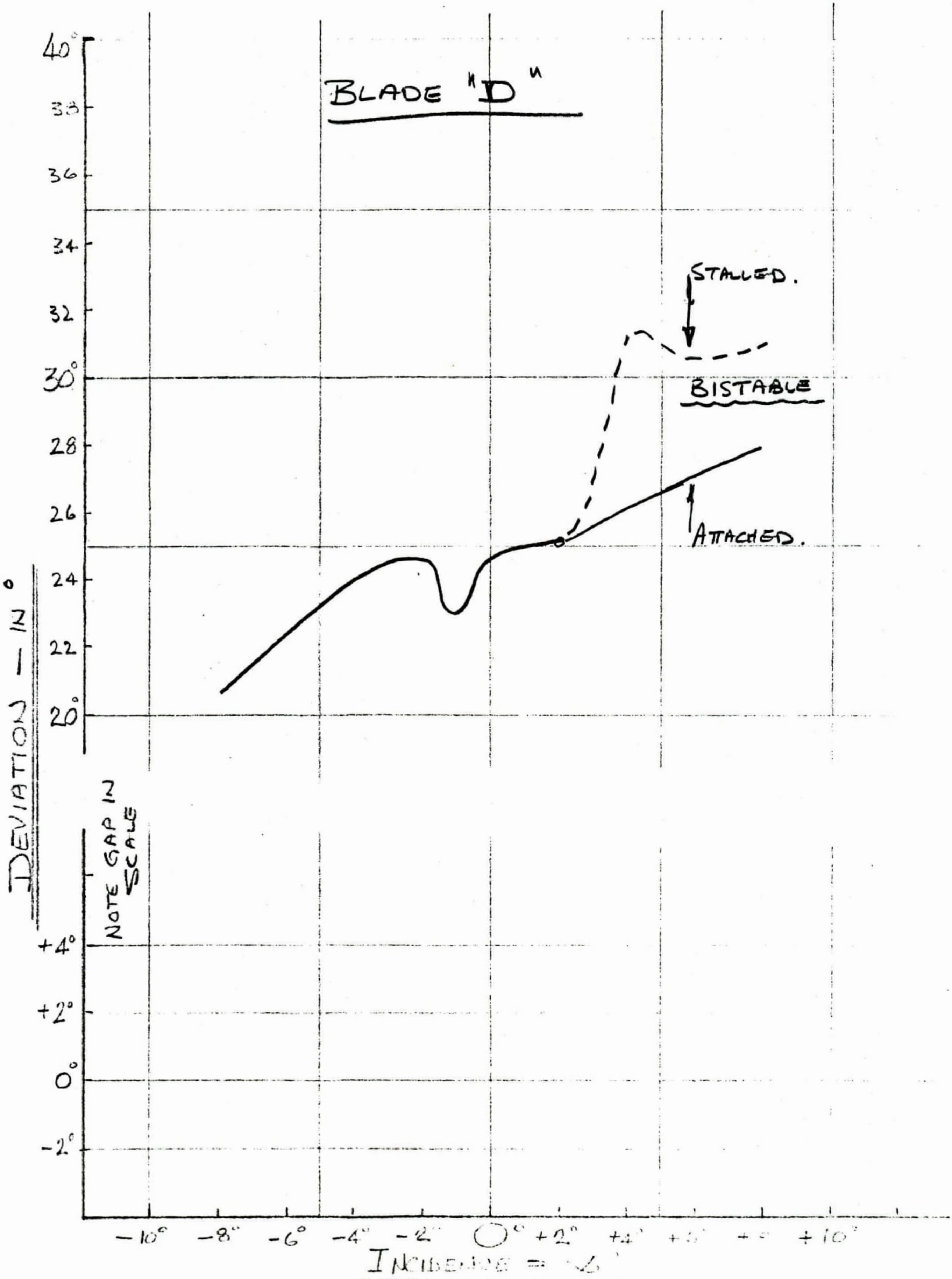

BLADE "D"
STALLED.
BISTABLE
ATTACHED.
DEVIATION - IN °
NOTE GAP IN SCALE
40°
38
36
34
32
30°
28
26
24
22
20°
+4°
+2°
0°
-2°
-10°
-8°
-6°
-4°
-2°
0°
+2°
+10°

Db

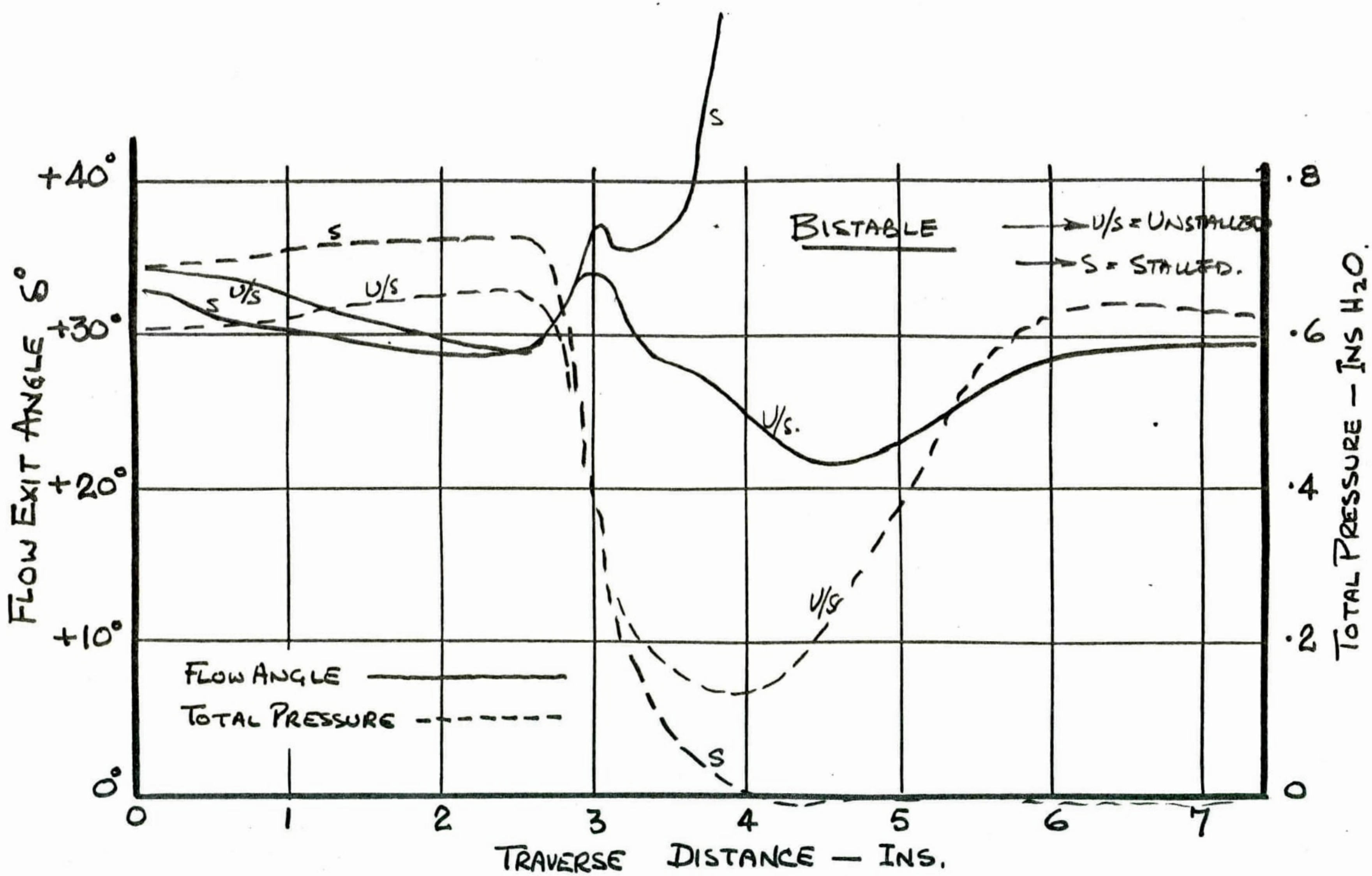

75° CAMBER. 1 SLOTS. BLADE "D". + 8° α

D

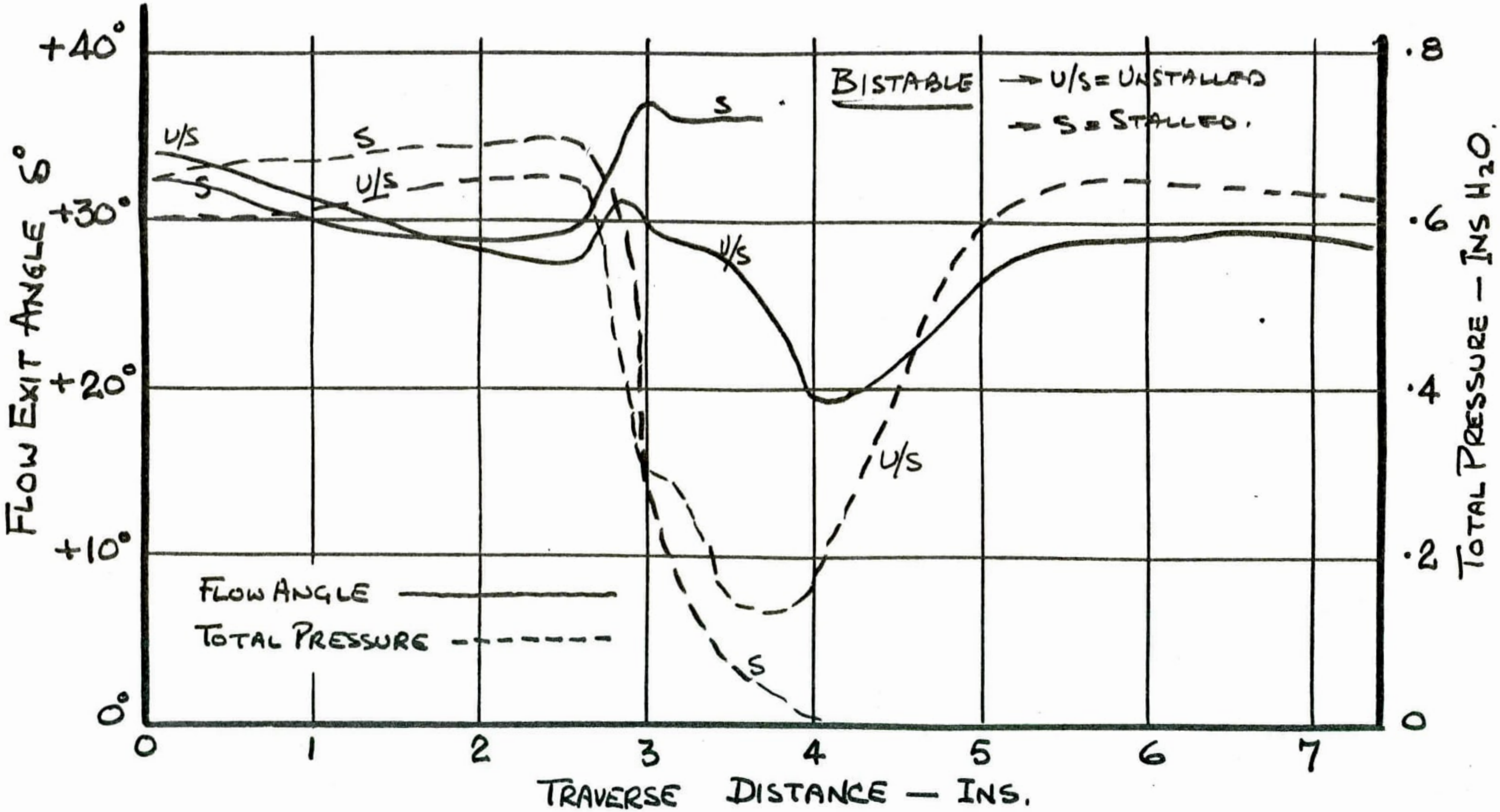

75° CAMBER. 1 SLOTS. BLADE "D". +6° α

D2

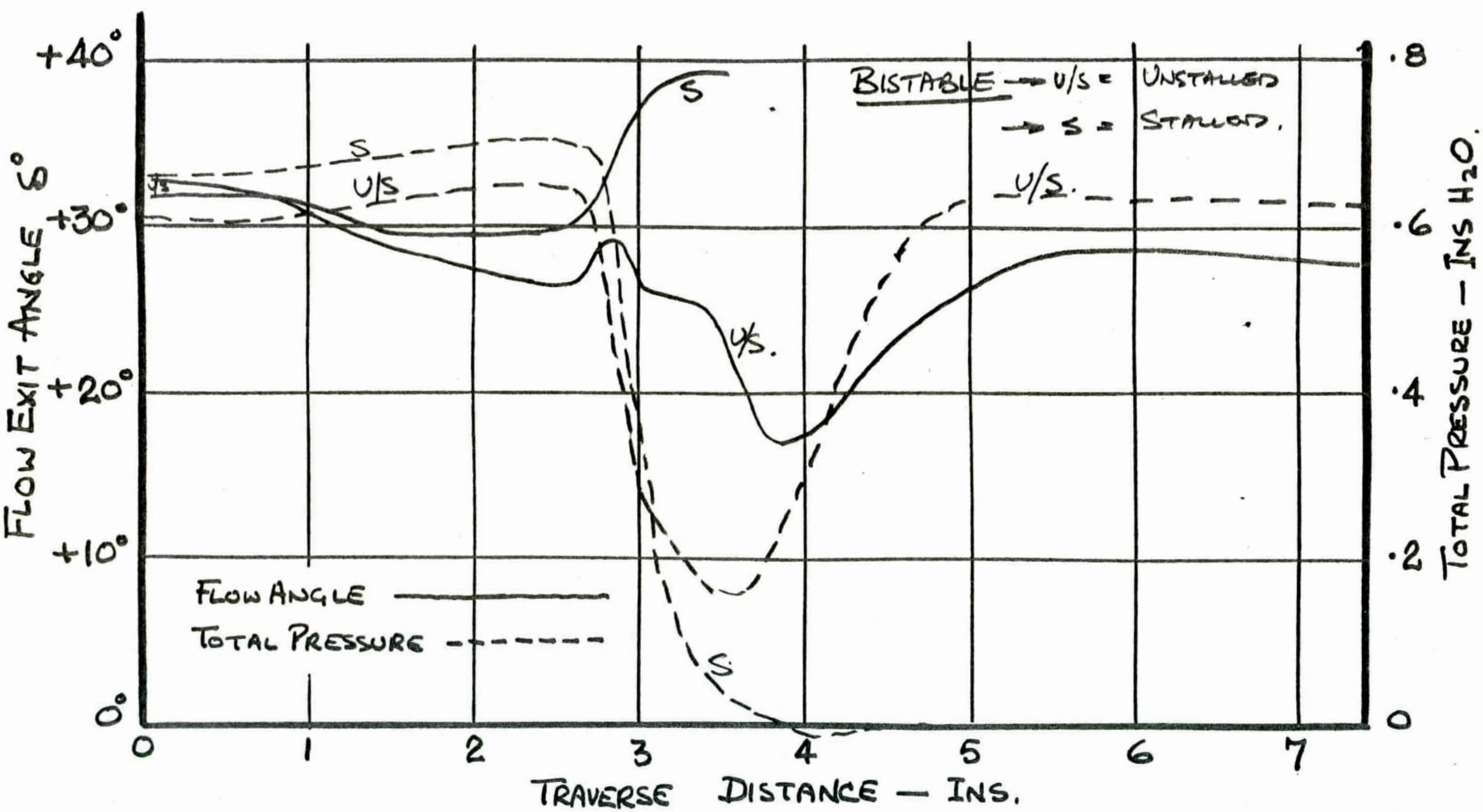

75° CAMBER. 1 SLOTS. BLADE "D". +4° α

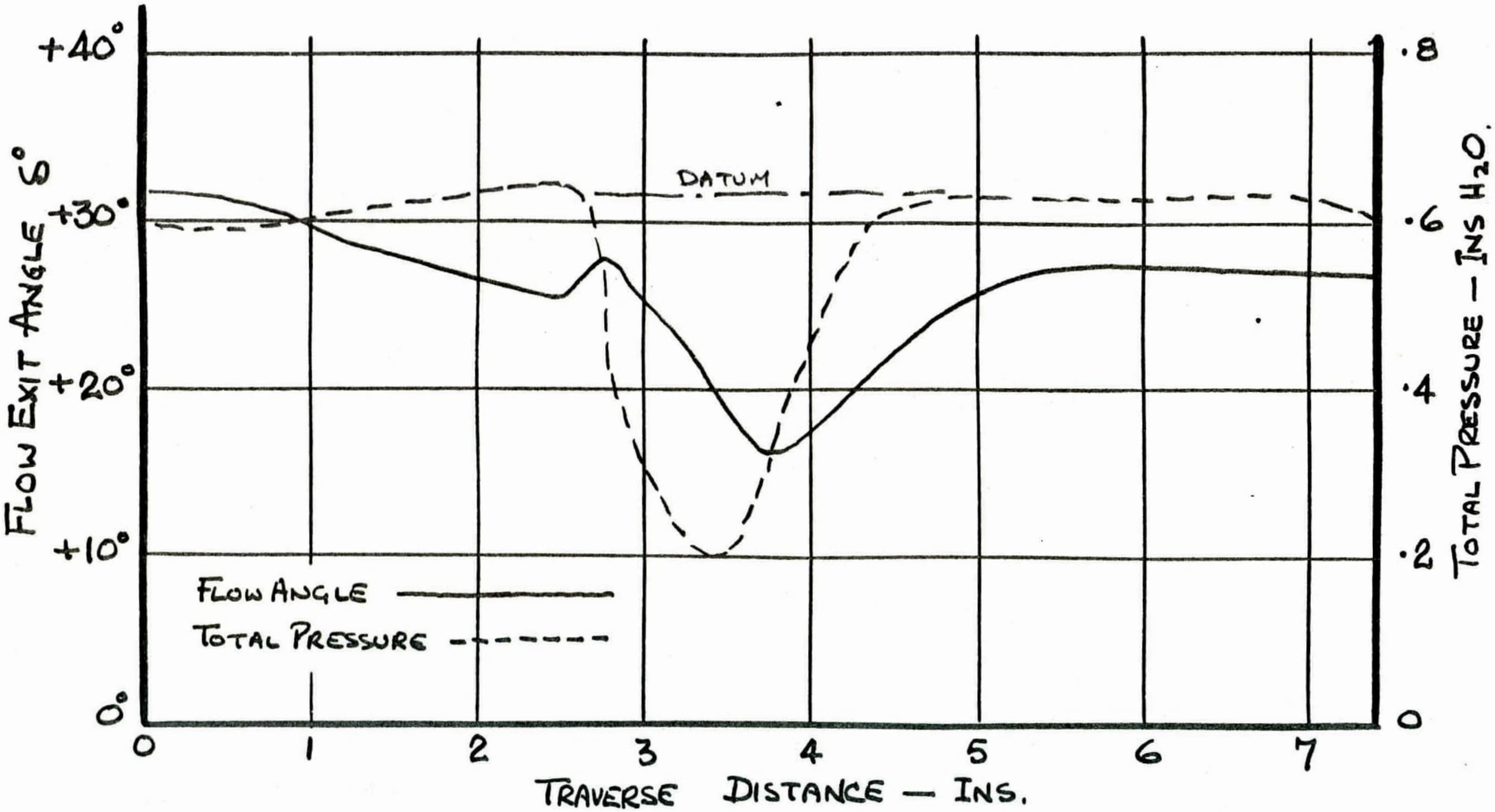

75° CAMBER. 1 SLOTS. BLADE "D". +2° α

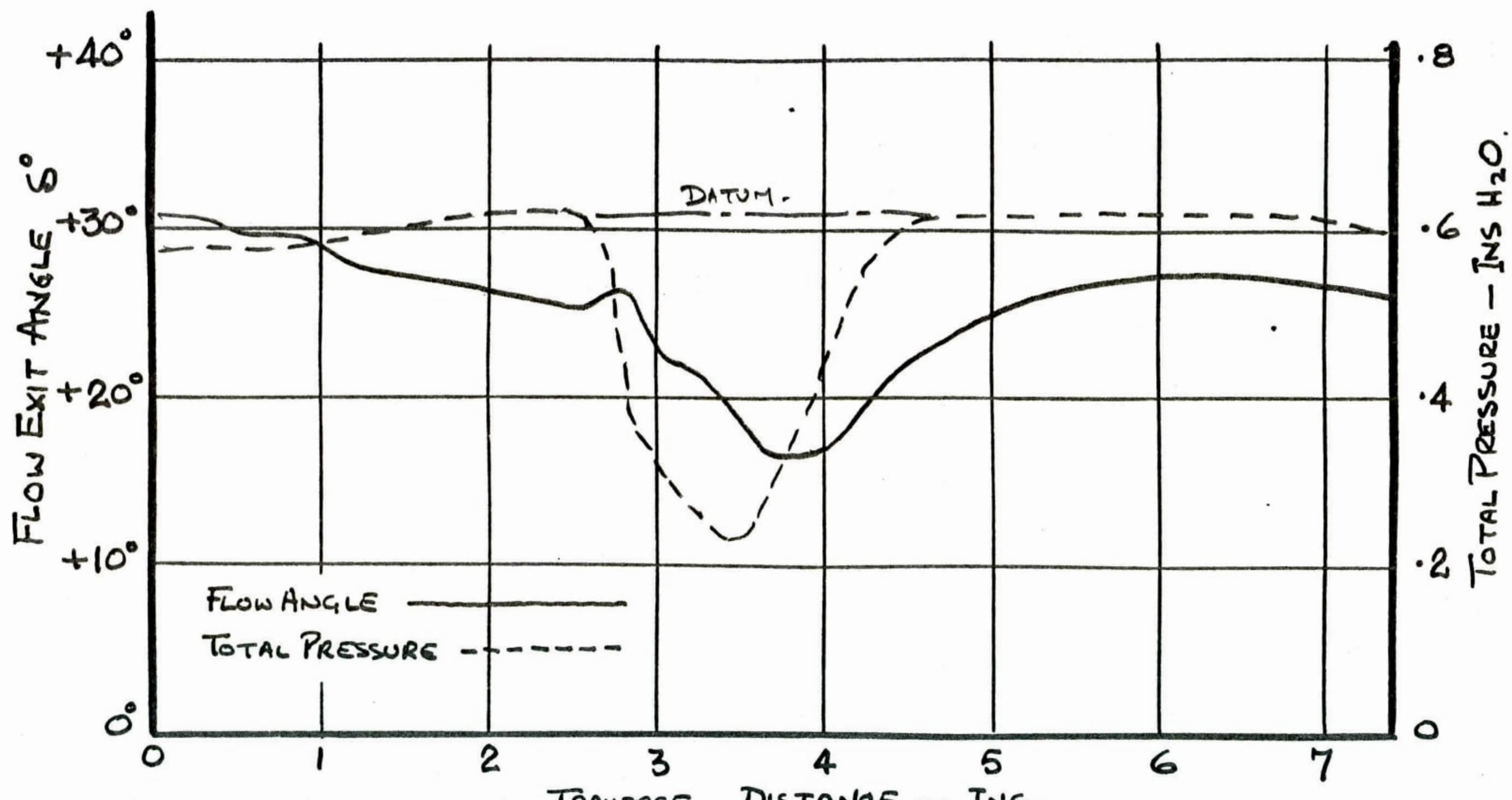

75° CAMBER. 1 SLOTS. BLADE "D". +1° α

D5

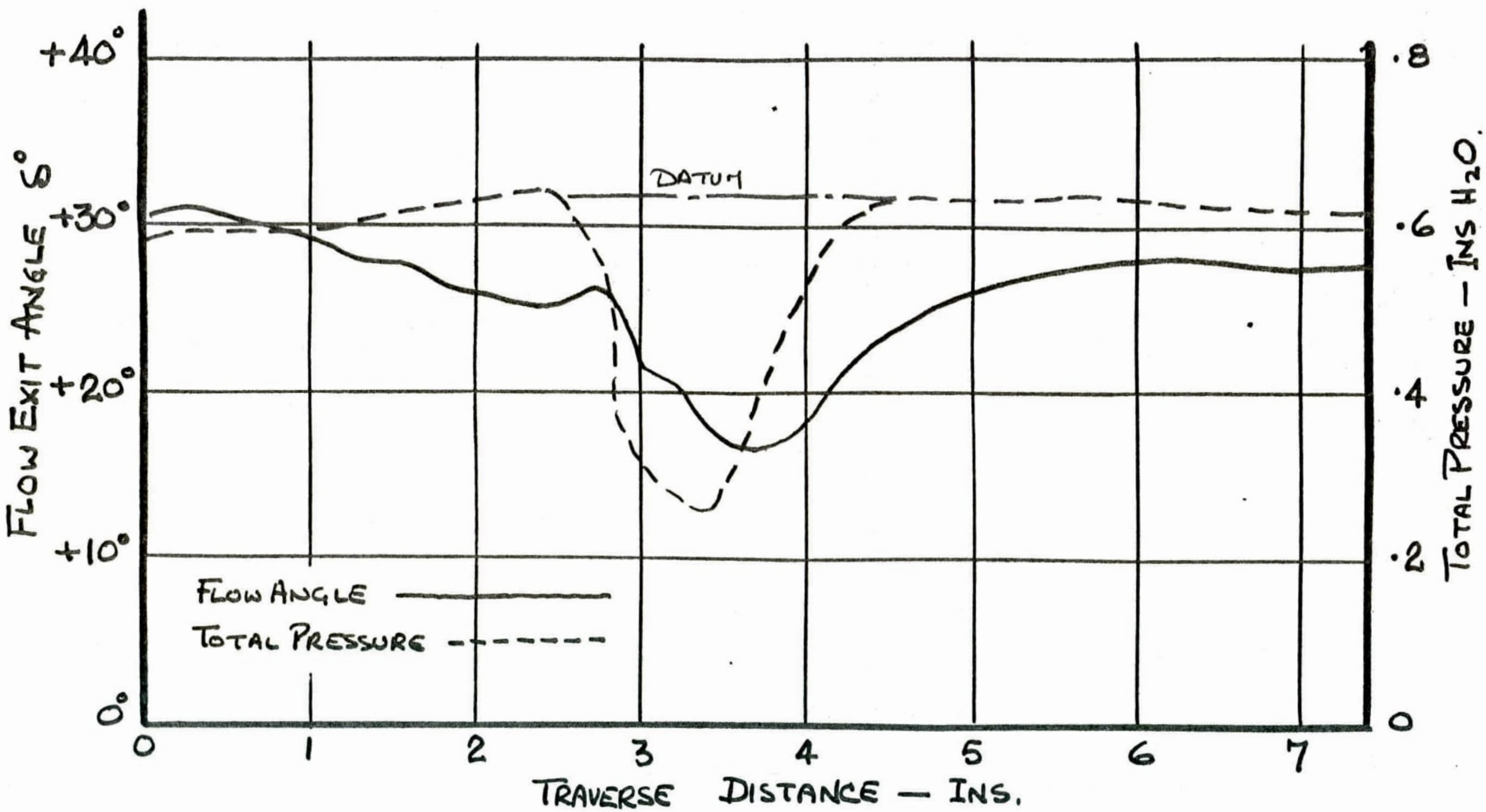

75°CAMBER. 1 SLOTS. BLADE "D". 0 °α

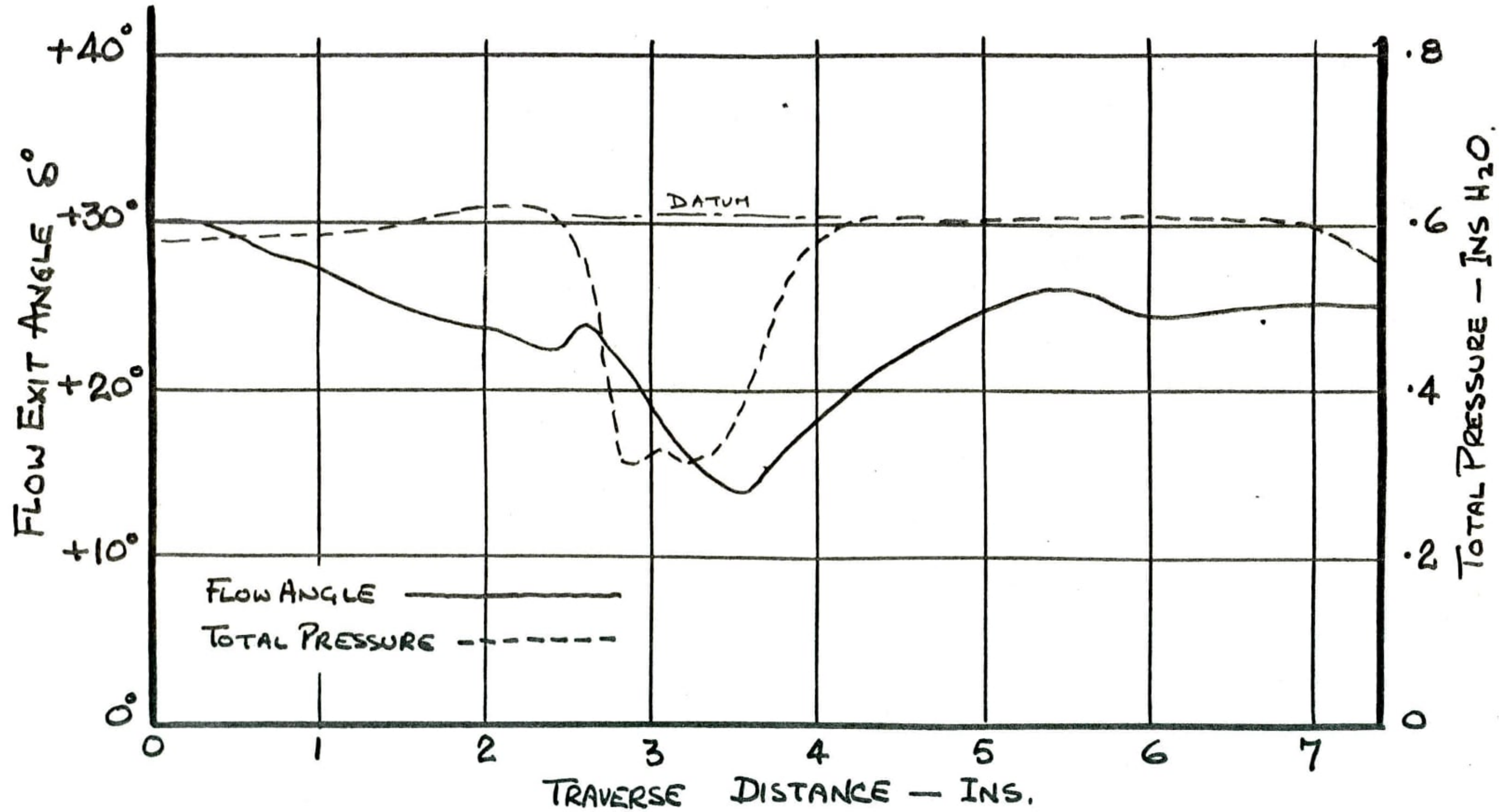

75° CAMBER. 1 SLOTS. BLADE "D". –1°α

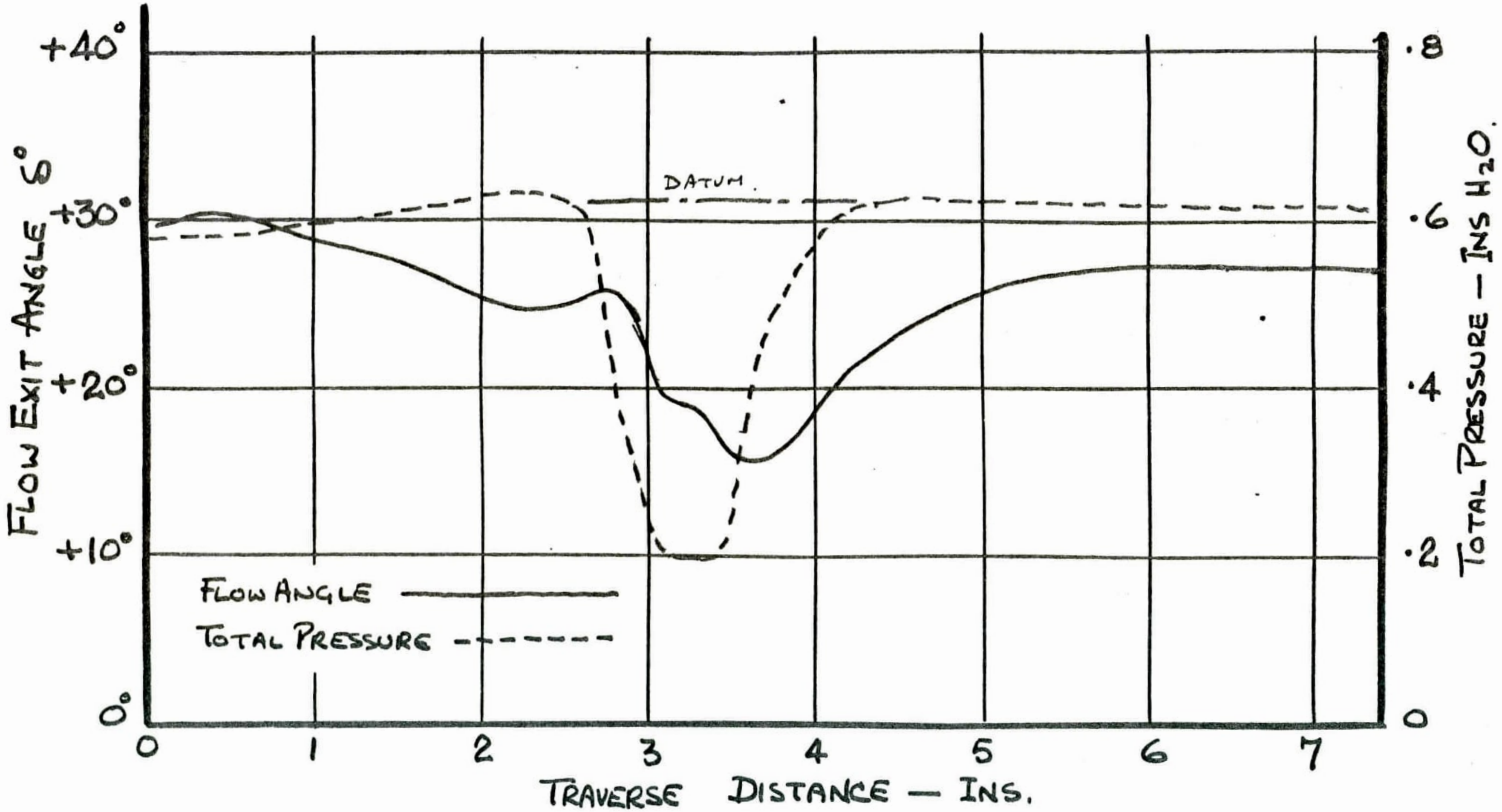

75° CAMBER. 1 SLOTS. BLADE "D". −2 °α

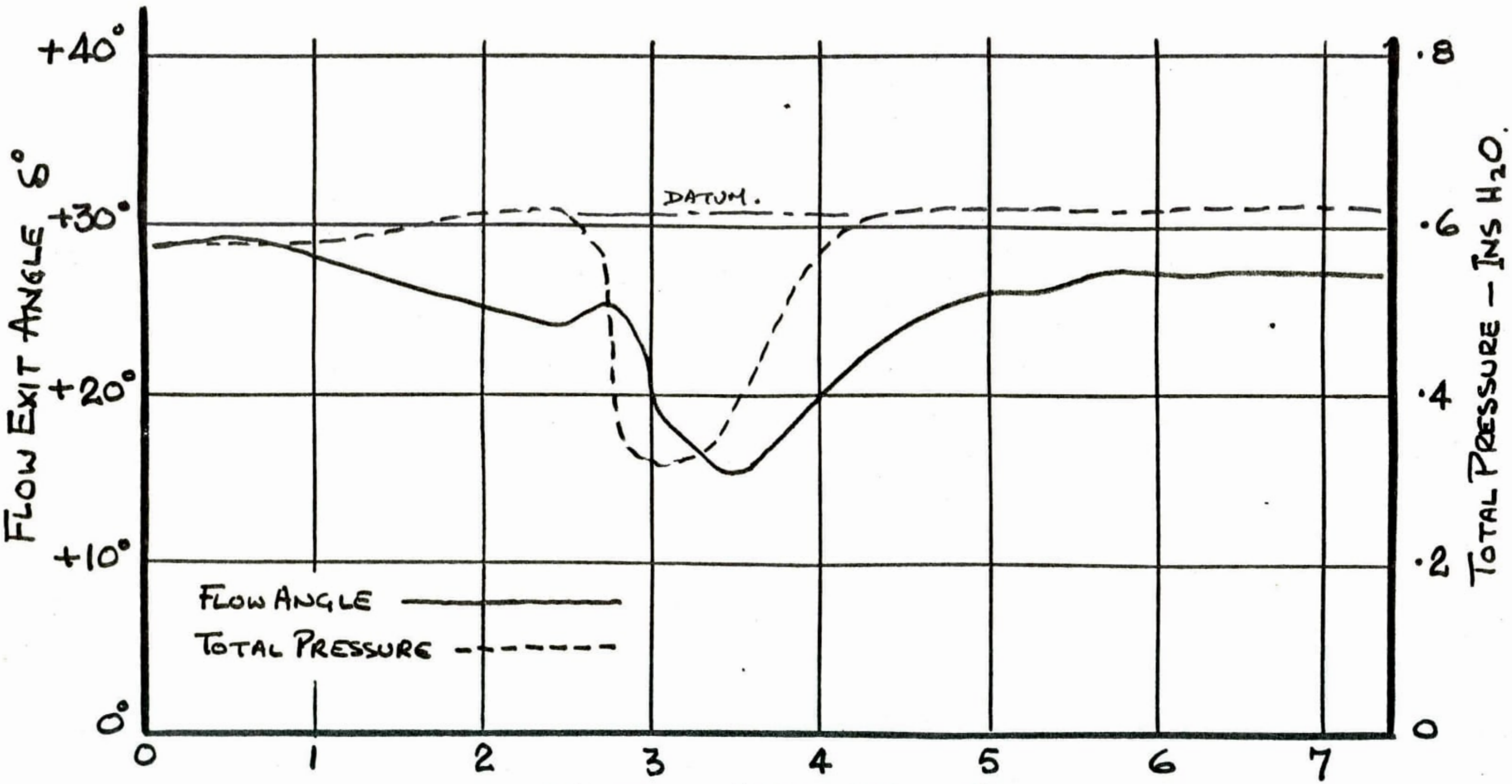

75° CAMBER. 1 SLOTS. BLADE "D". −4 °α

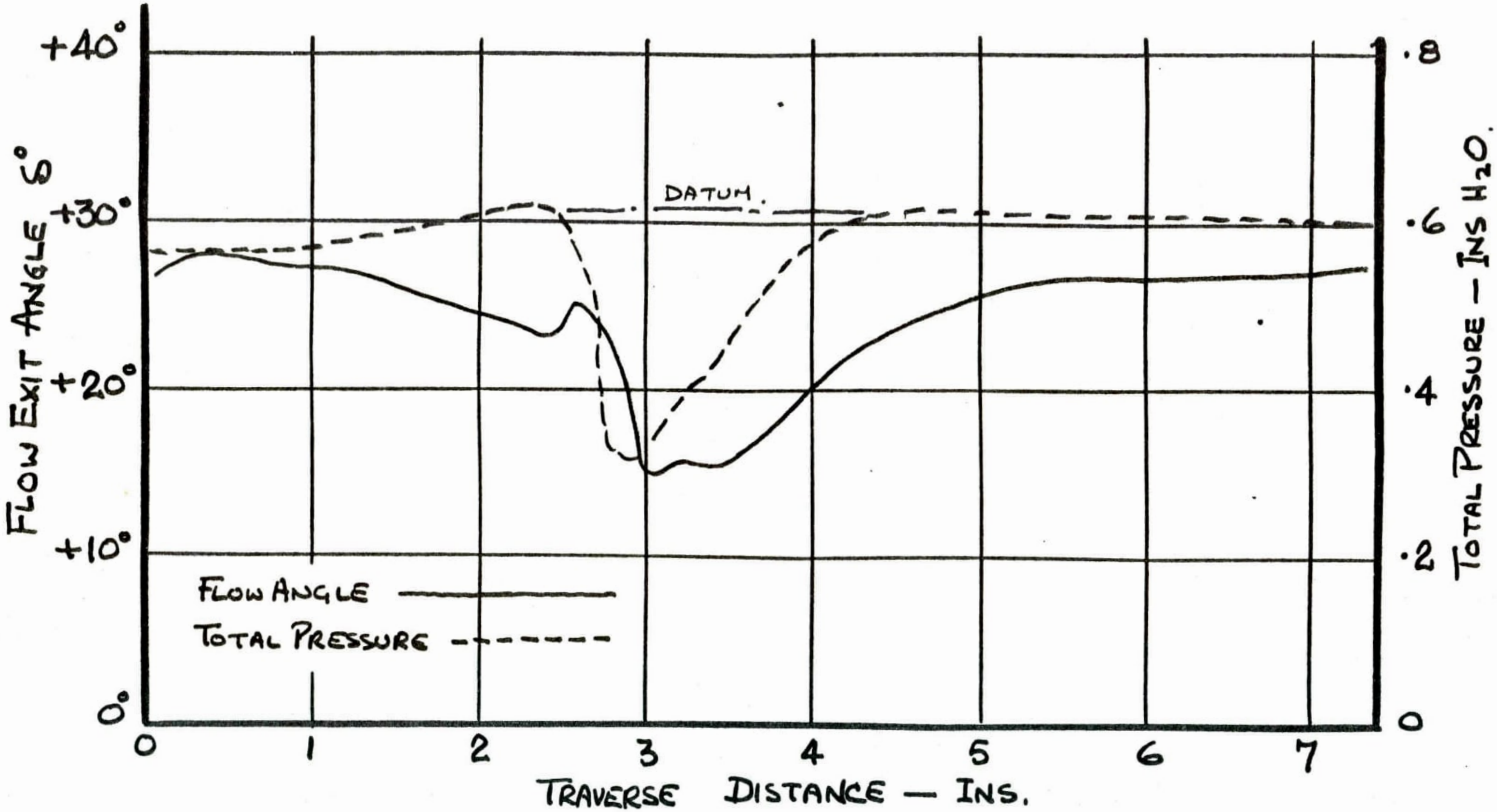

75° CAMBER. 1 SLOTS. BLADE "D". −8° α

BLADE "E" 2 SLOTS

75° CAMBER

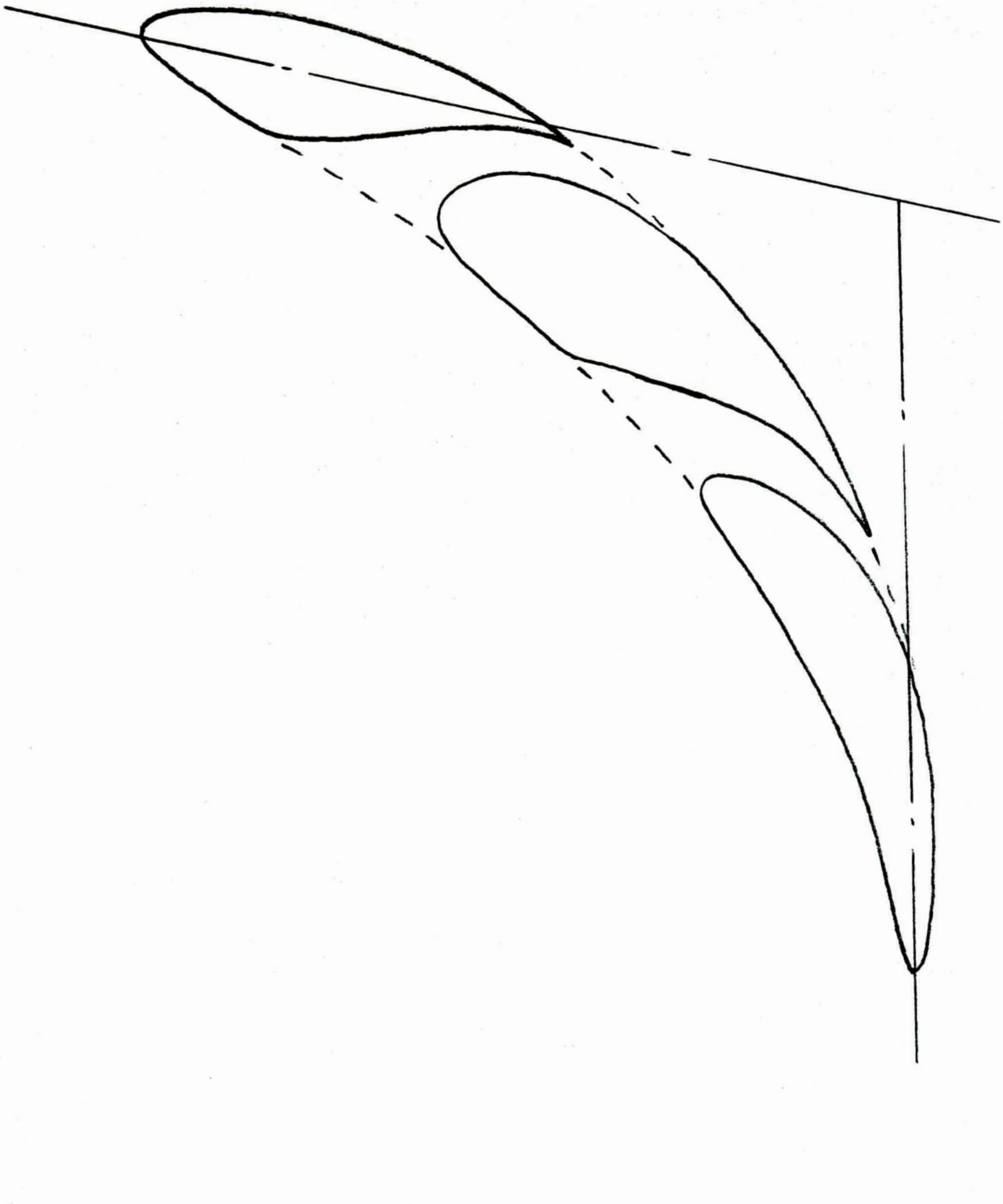

E

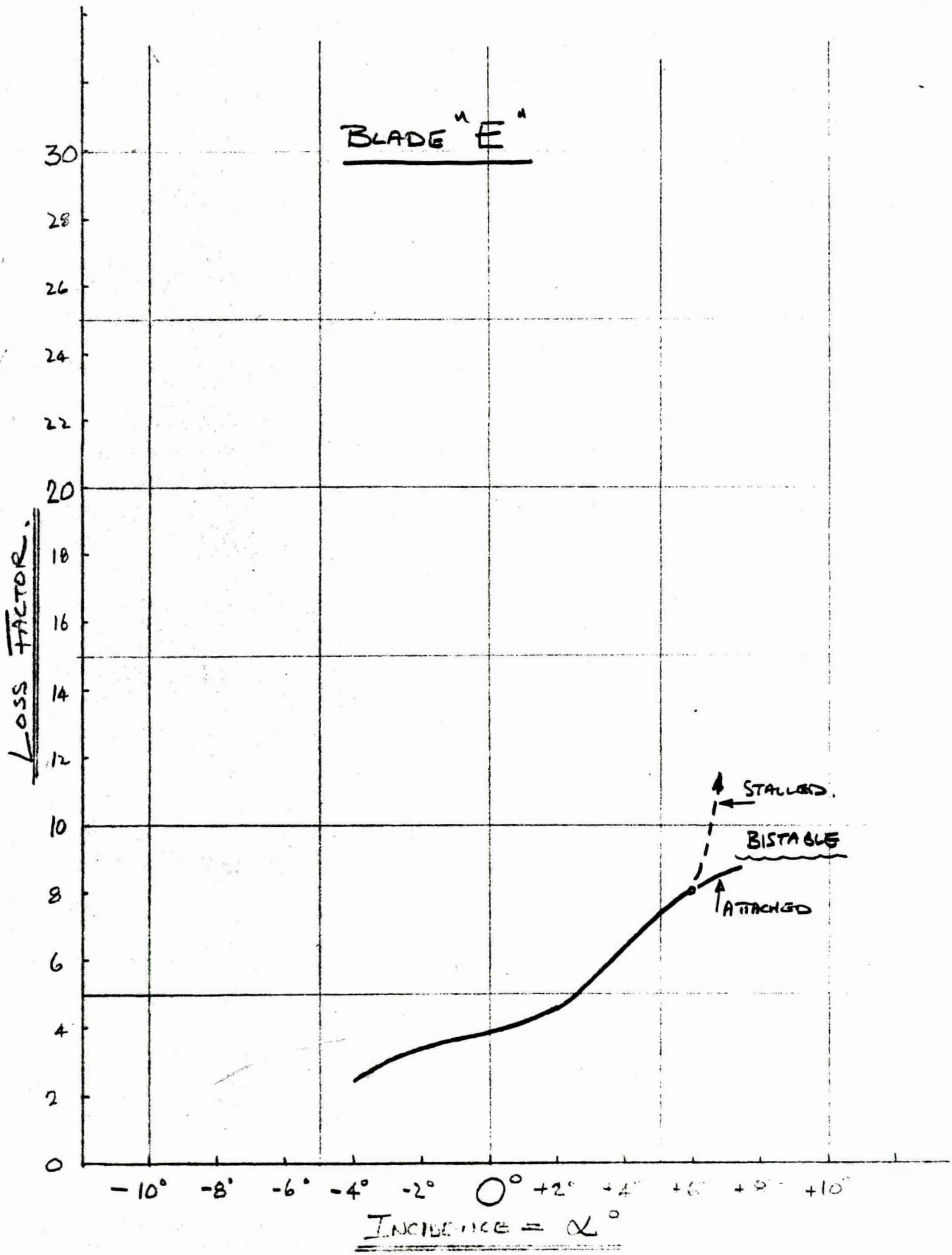

BLADE "E"
30
28
26
24
22
20
18
16
14
12
10
8
6
4
2
0
LOSS FACTOR.
STALLED.
BISTABLE
ATTACHED
− 10° -8° -6° -4° -2° 0° +2° +4° +6° +8° +10°
INCIDENCE = α°

Ea

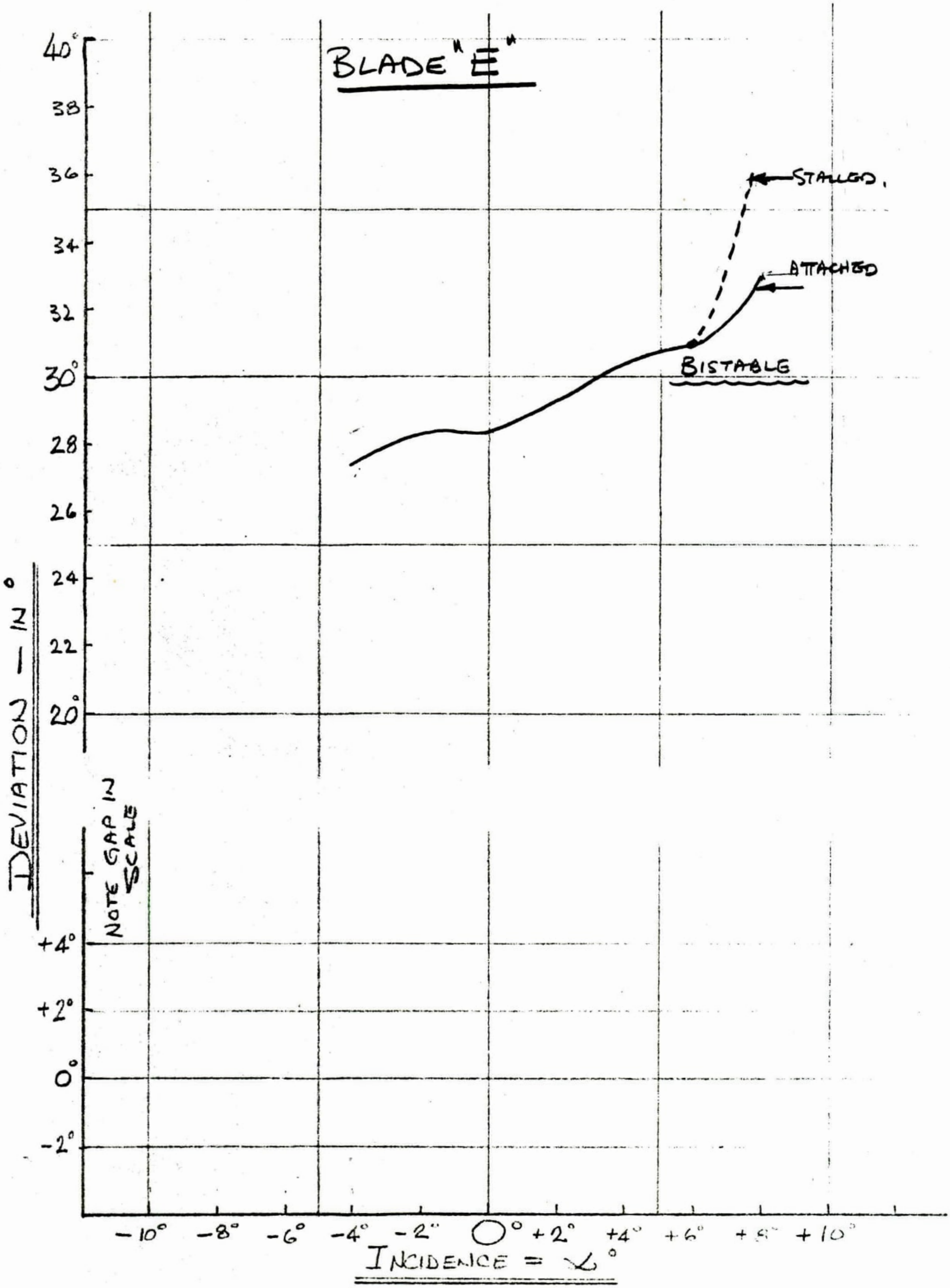

BLADE "E"
40°
38
36
34
32
30°
28
26
24
22
20°
+4°
+2°
0°
-2°
STALLED.
ATTACHED
BISTABLE
DEVIATION — IN °
NOTE GAP IN SCALE
-10° -8° -6° -4° -2° 0° +2° +4° +6° +8° +10°
INCIDENCE = α°

Eb

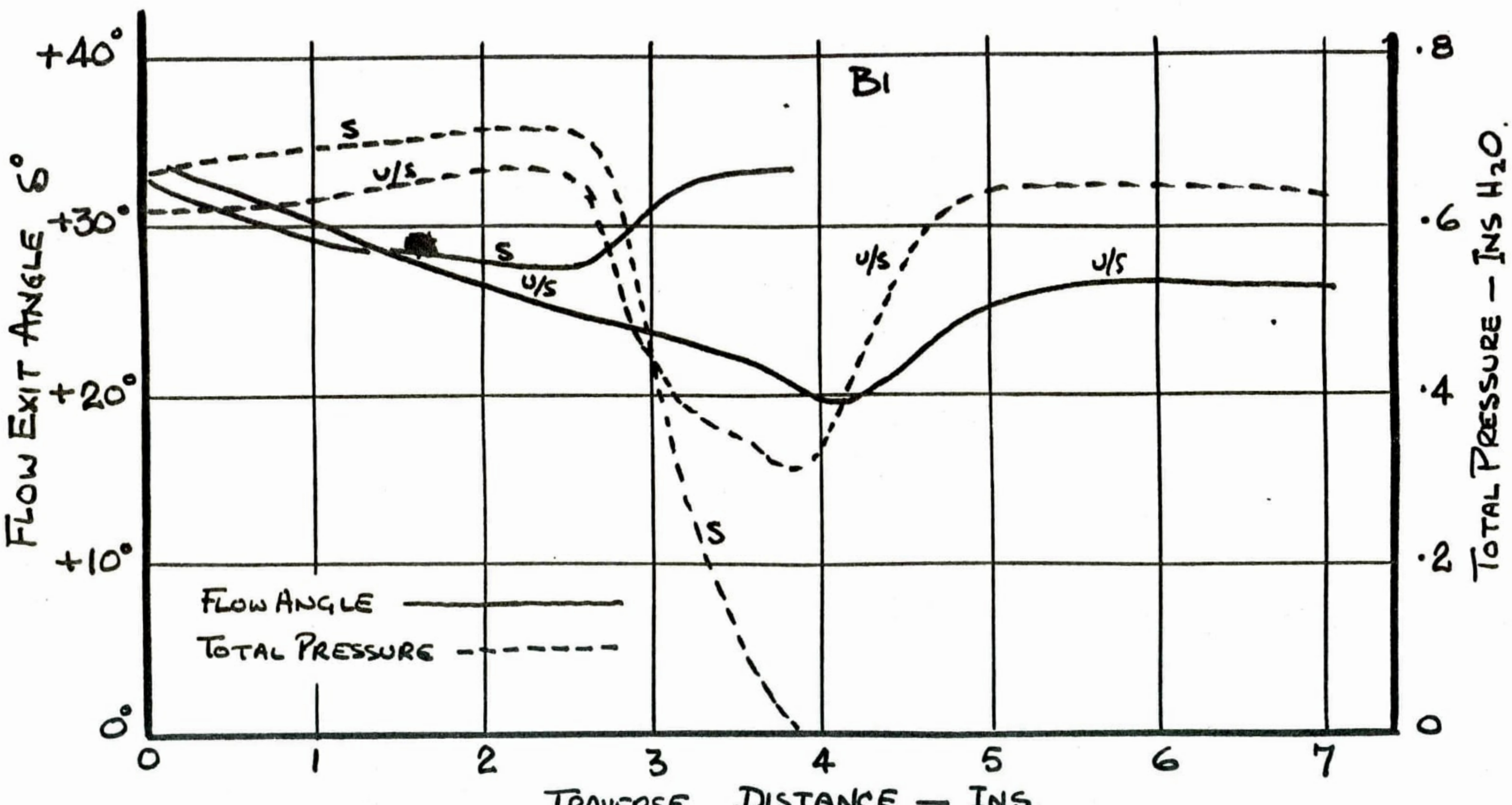

75° CAMBER. 2 SLOTS. BLADE "E". + 8° α

E1

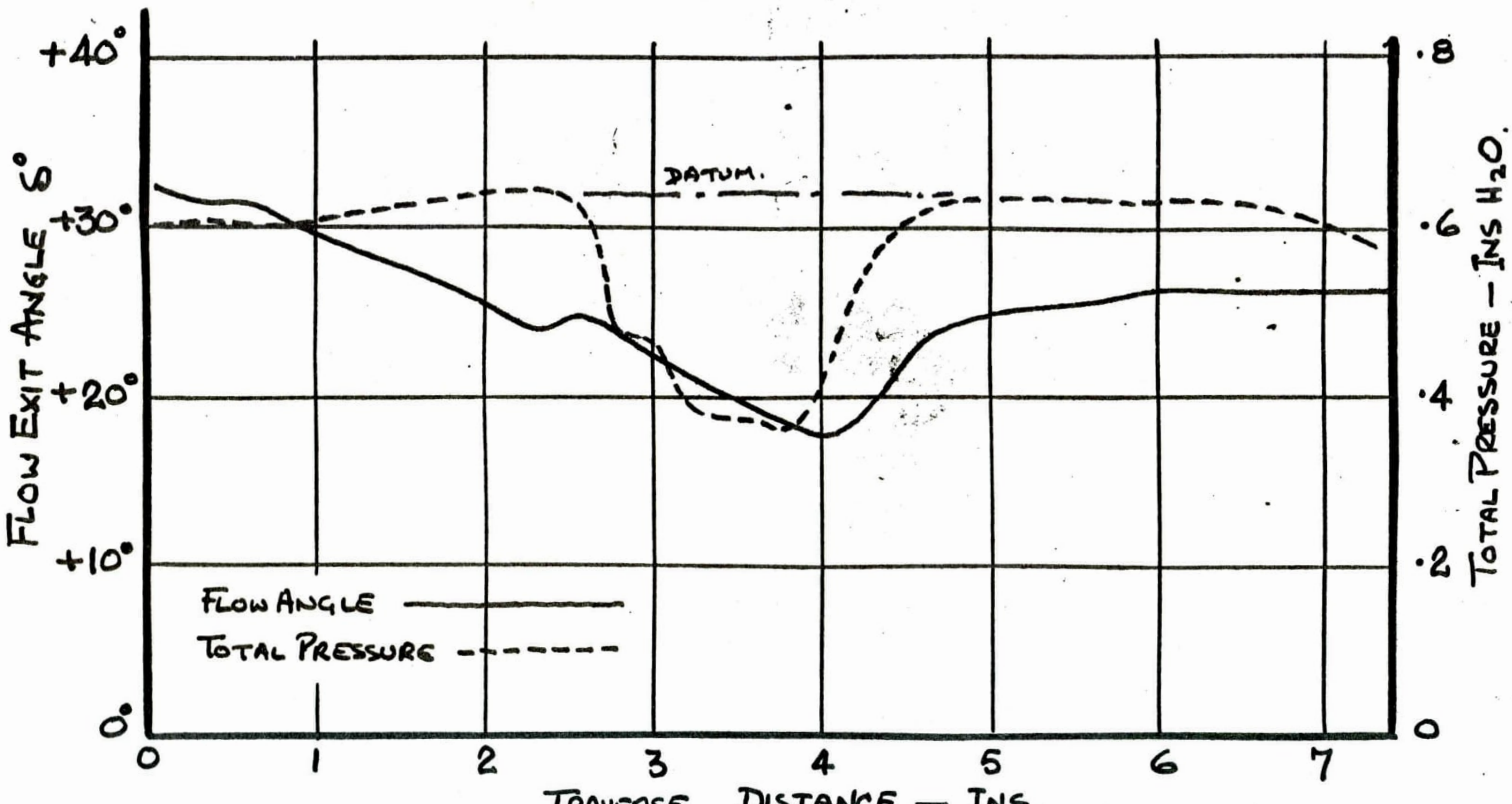

75°CAMBER. 2 SLOTS. BLADE "E". +6°α

E2

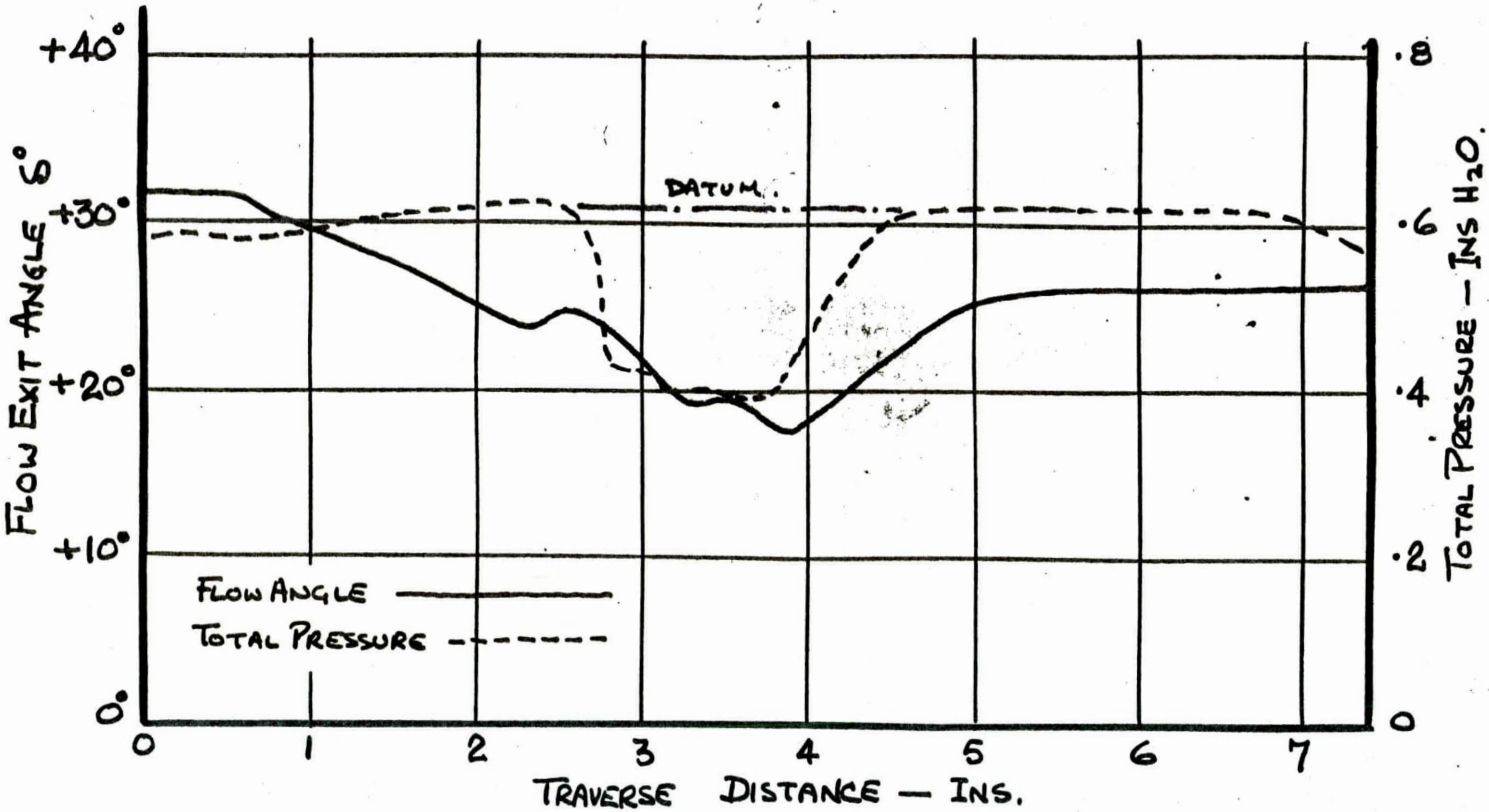

75° CAMBER. 2 SLOTS. BLADE "E". +4 °α

E3

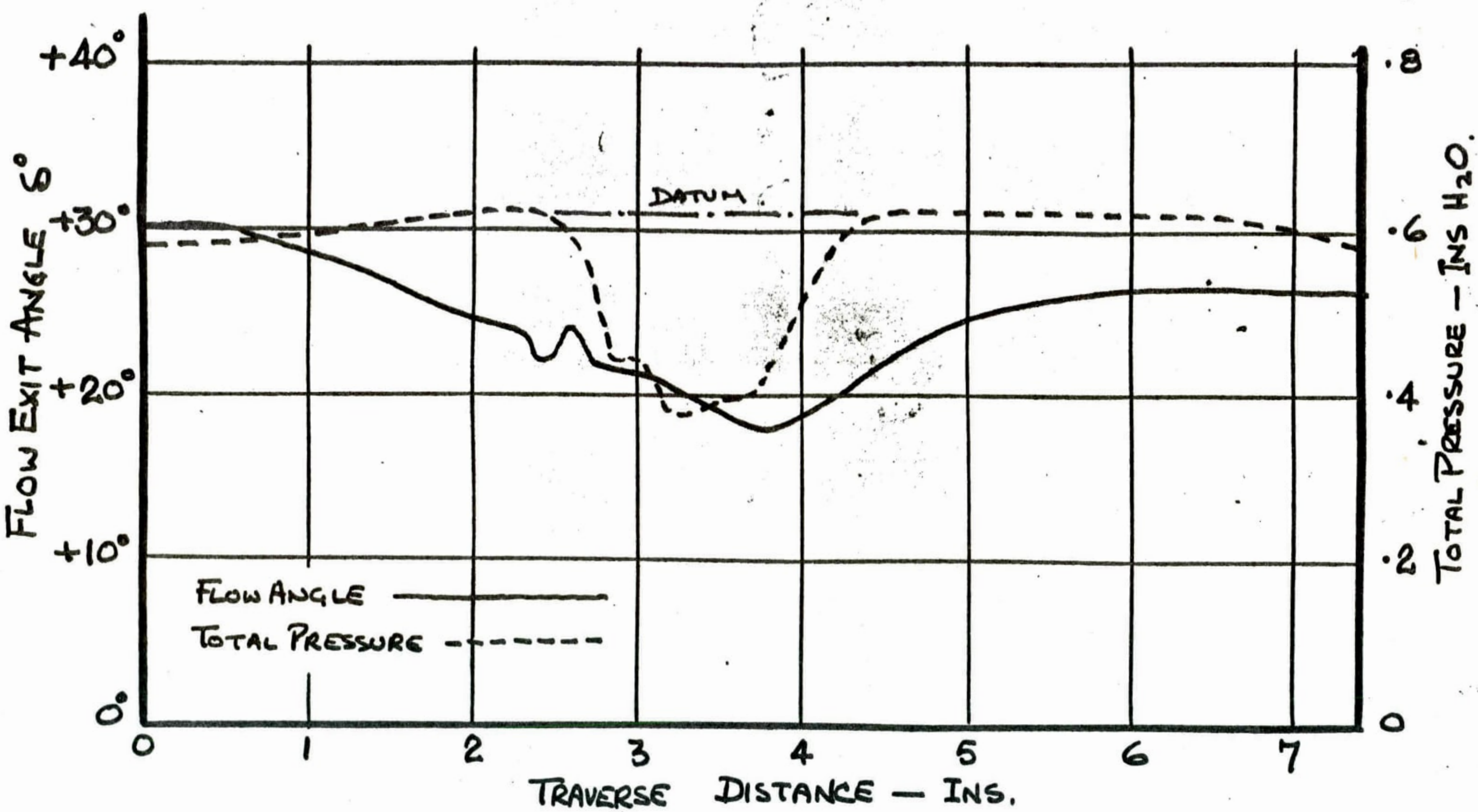

75° CAMBER. 2 SLOTS. BLADE "E". +2°α

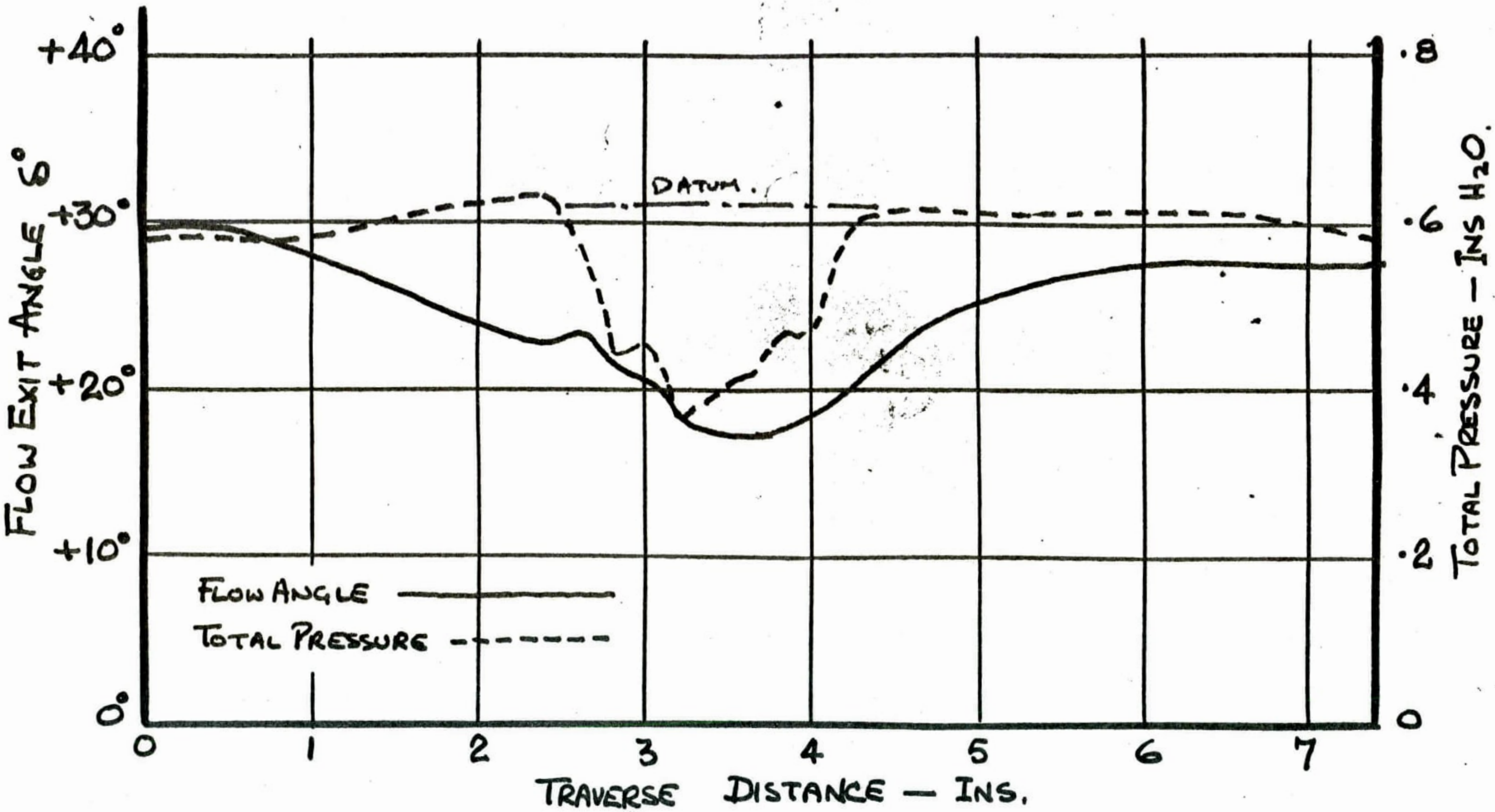

75° CAMBER. 2 SLOTS. BLADE "E". +1°α

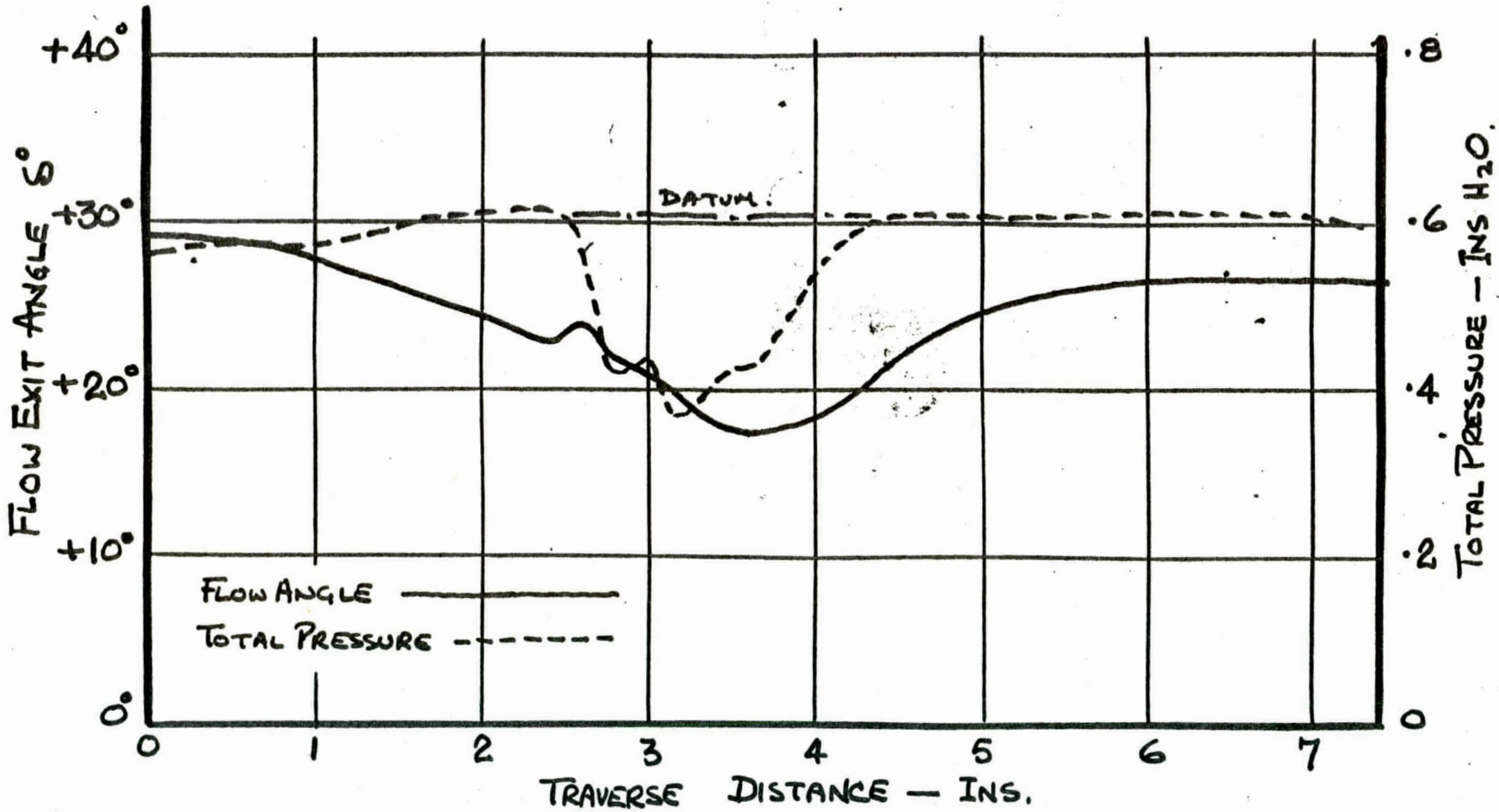

75° CAMBER. 2 SLOTS. BLADE "E". 0 °α

E6

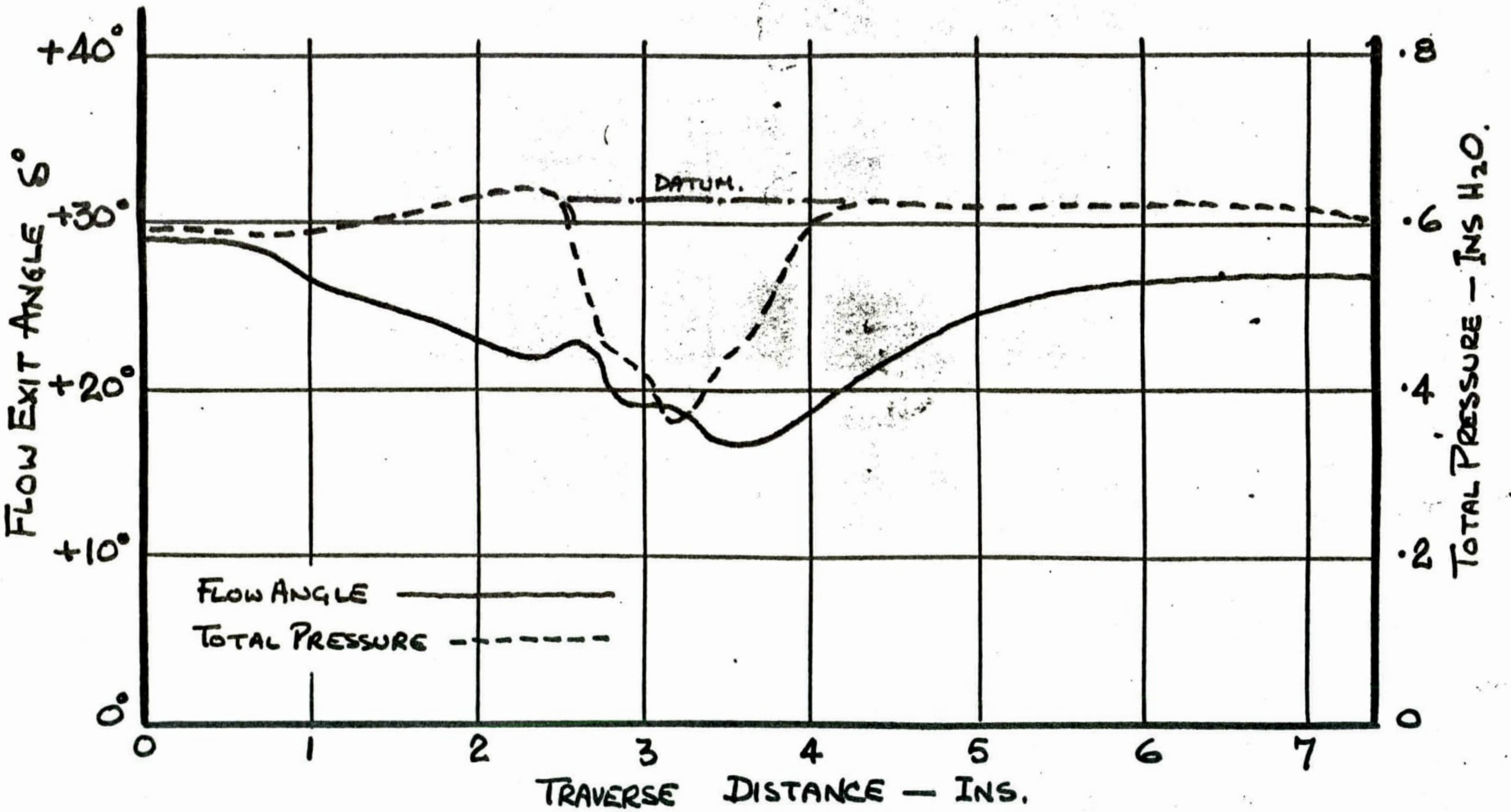

75°CAMBER. 2 SLOTS. BLADE "E". −1 °α

E7

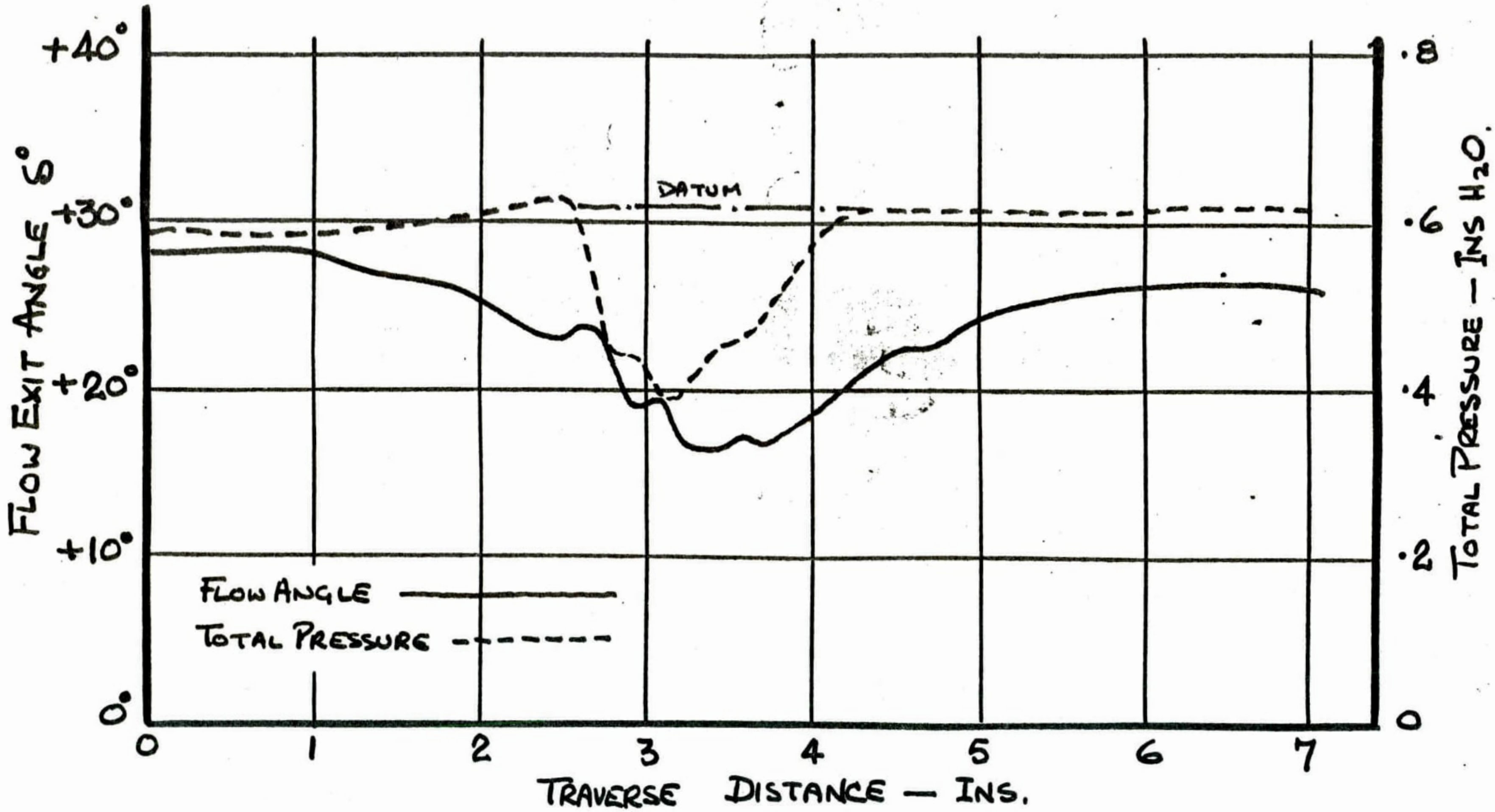

75° CAMBER. 2 SLOTS. BLADE "E". −2°α

E8

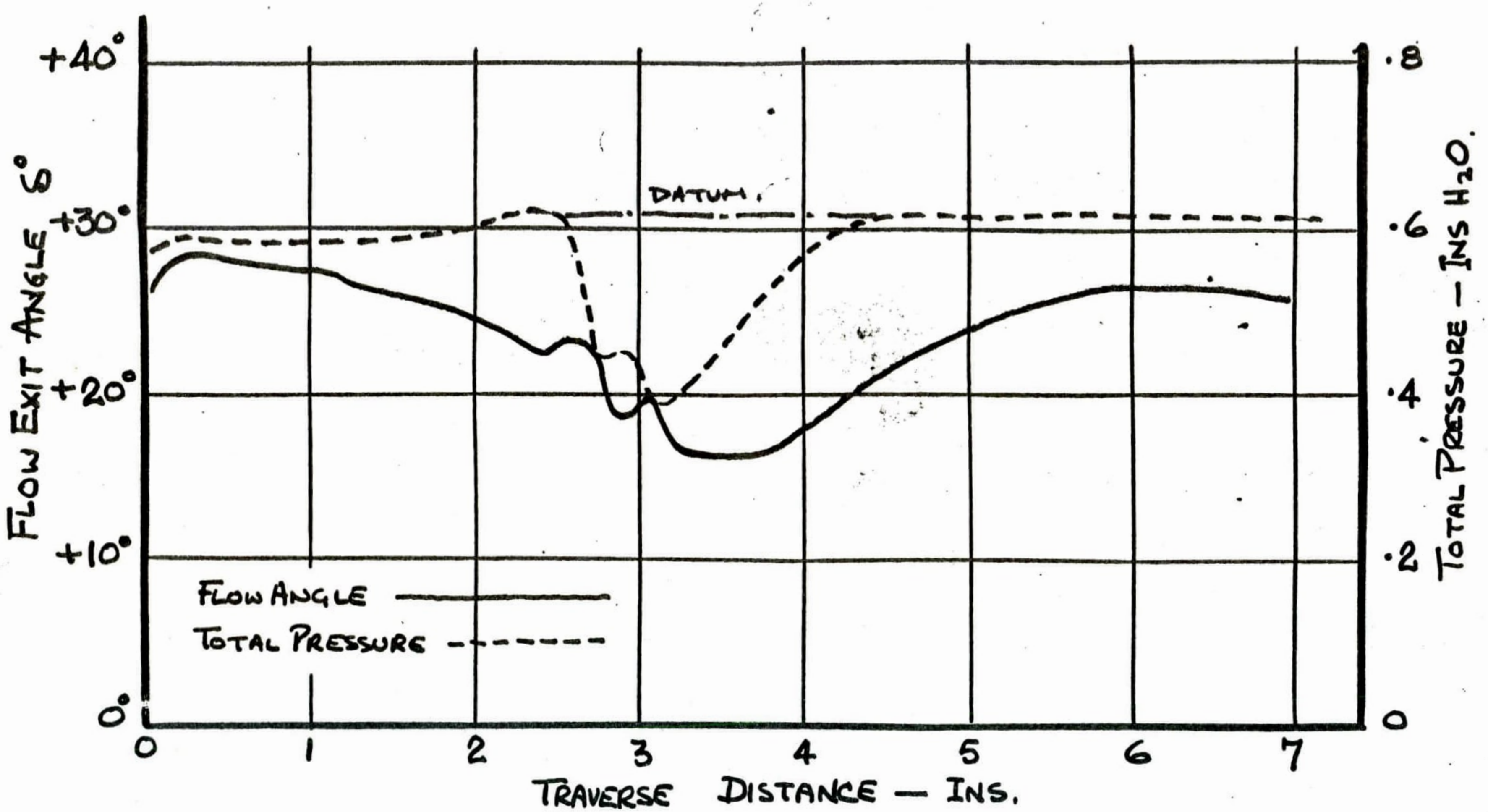

75°CAMBER. 2 SLOTS. BLADE "E". −4 °α

E9

BLADE "F" 4 SLOTS.

75° CAMBER.

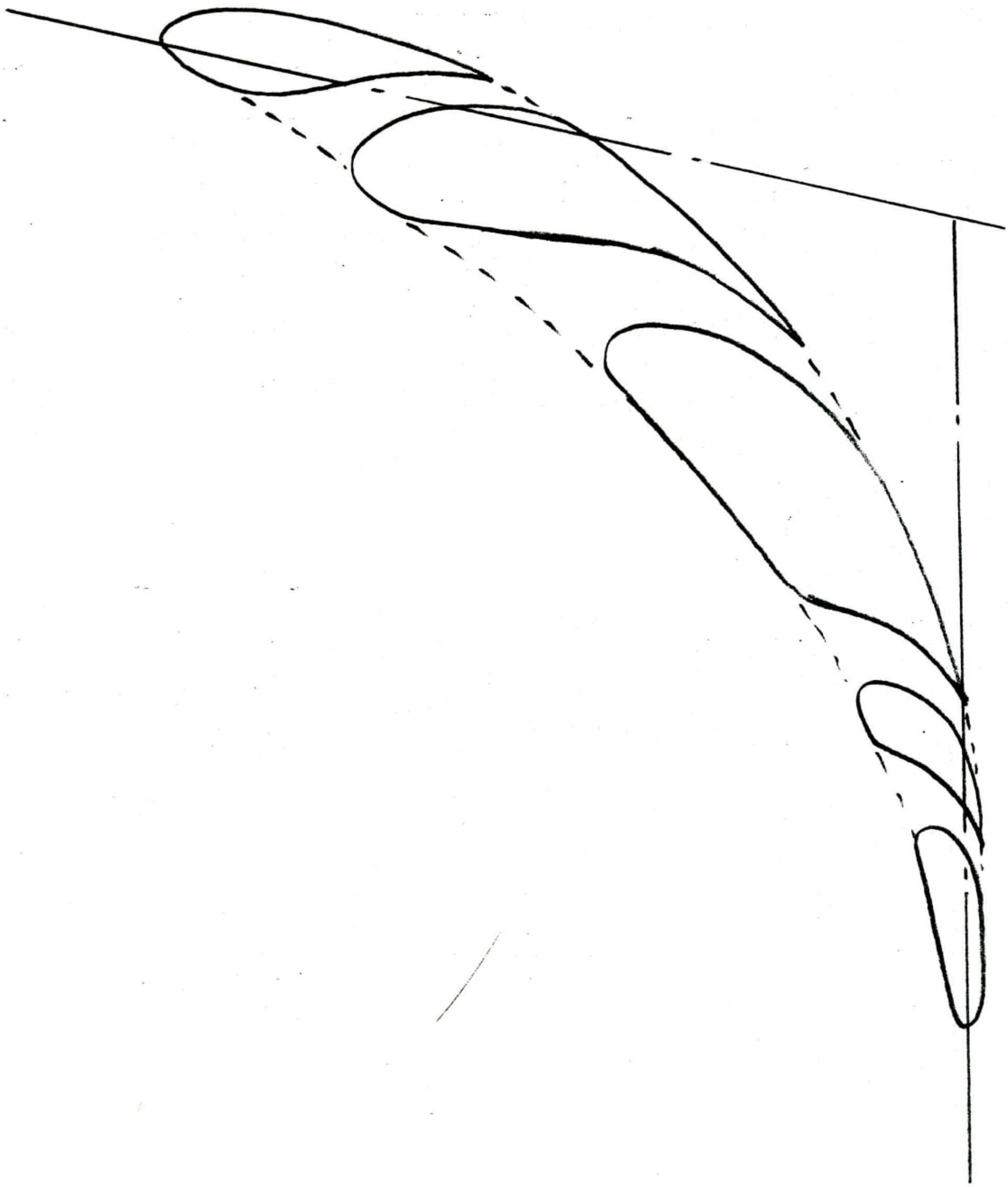

F.

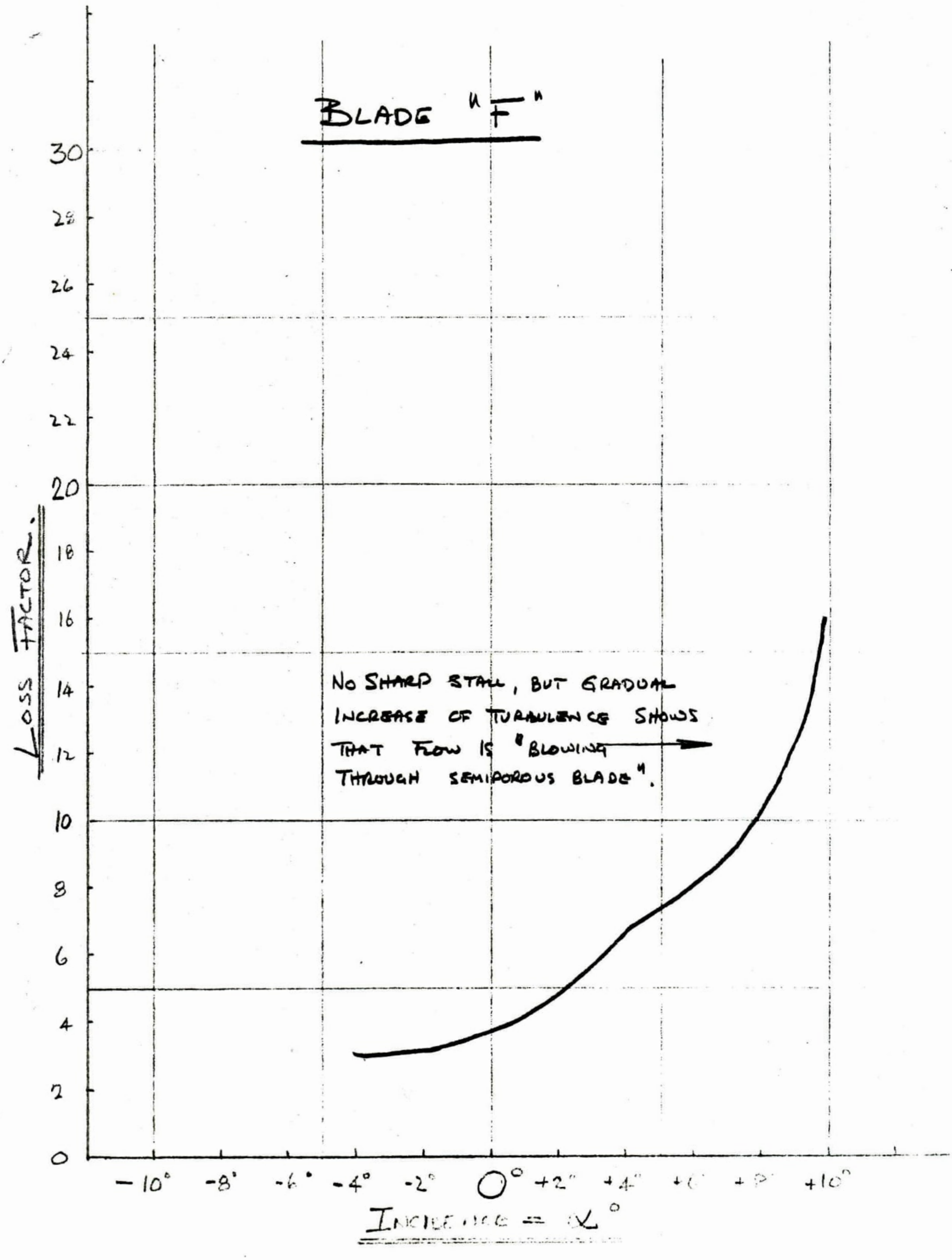

BLADE "F"
LOSS FACTOR.
30
28
26
24
22
20
18
16
14
12
10
8
6
4
2
0
NO SHARP STALL, BUT GRADUAL INCREASE OF TURBULENCE SHOWS THAT FLOW IS "BLOWING THROUGH SEMIPOROUS BLADE".
-10°
-8°
-6°
-4°
-2°
0°
+2°
+4°
+10°
INCIDENCE = α°

Fa

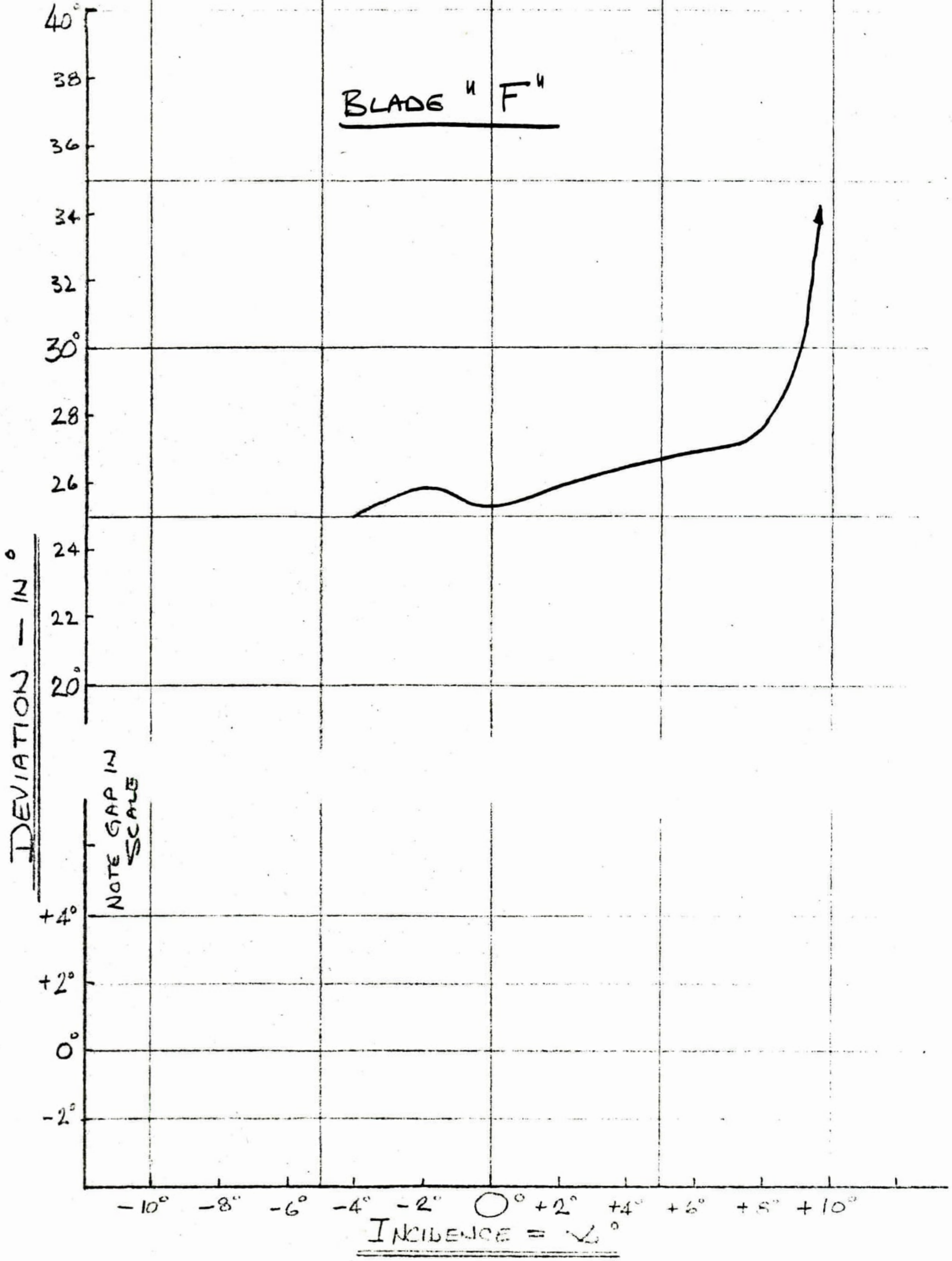

BLADE "F"
DEVIATION — IN °
NOTE GAP IN SCALE
40°
38
36
34
32
30°
28
26
24
22
20°
+4°
+2°
0°
-2°
-10°
-8°
-6°
-4°
-2°
0°
+2°
+4°
+6°
+8°
+10°
INCIDENCE = α °

Fb

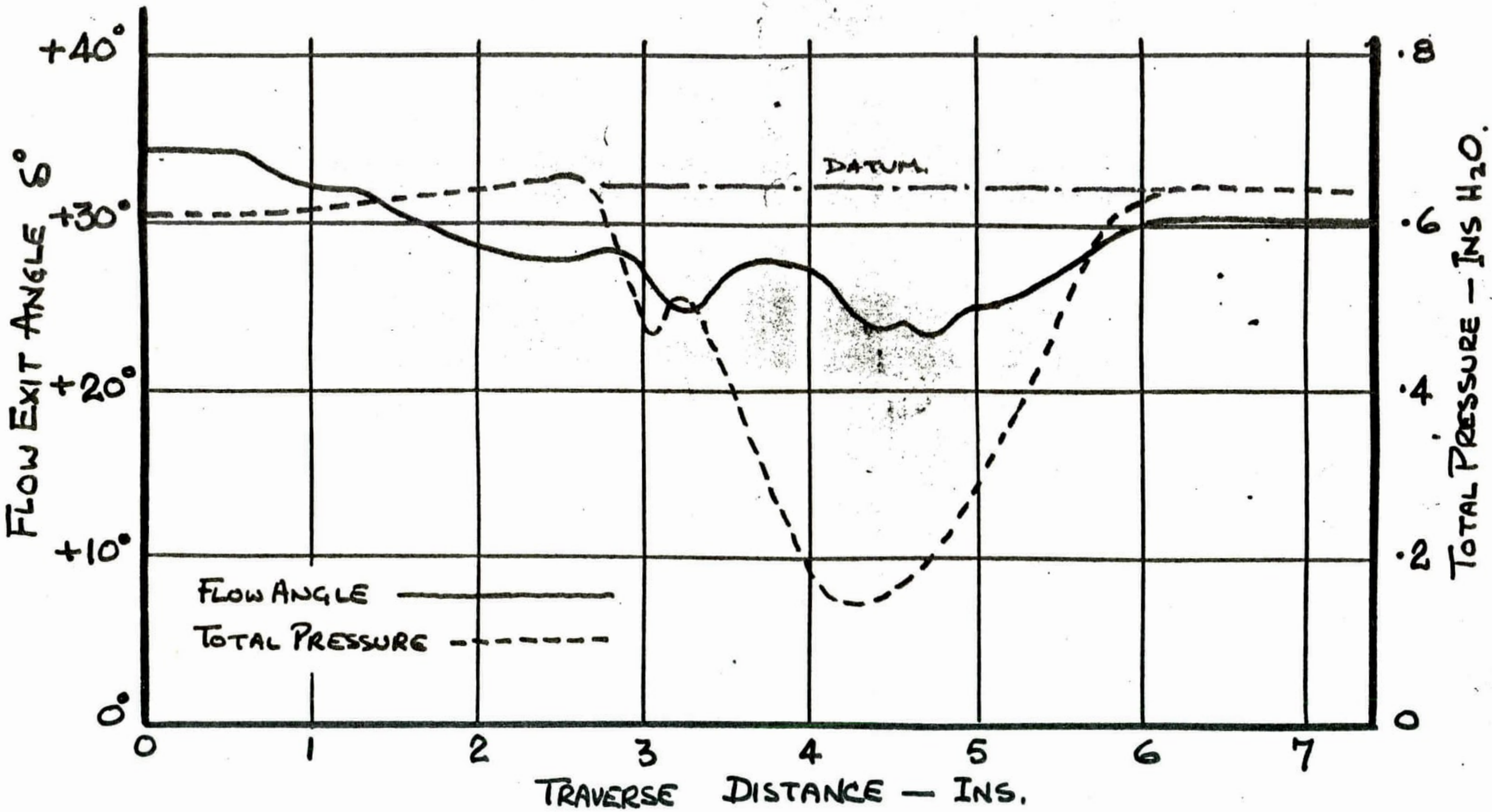

75° CAMBER. 4 SLOTS. BLADE "F". +8° α

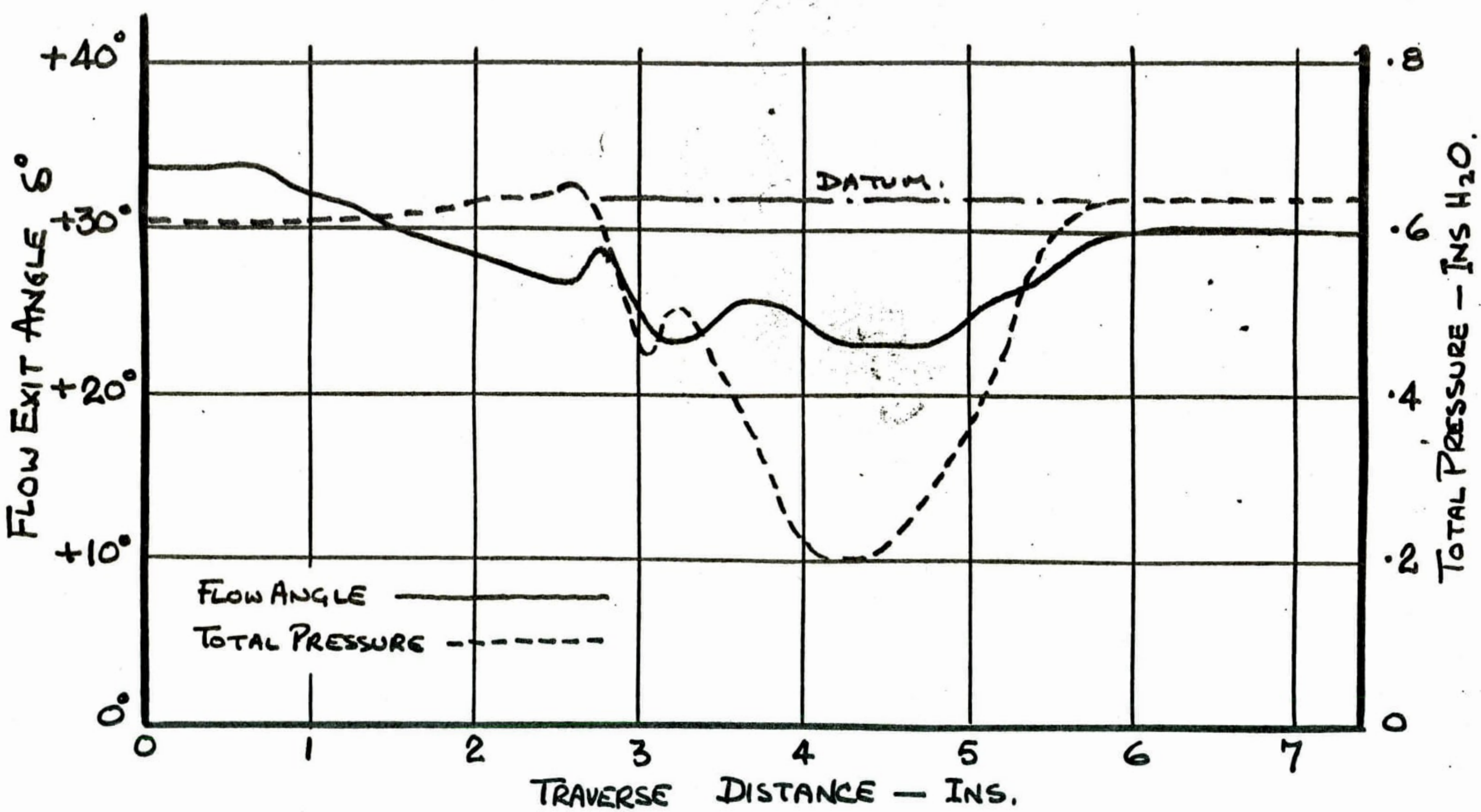

75° CAMBER. 4 SLOTS. BLADE "F". +6° α

F2

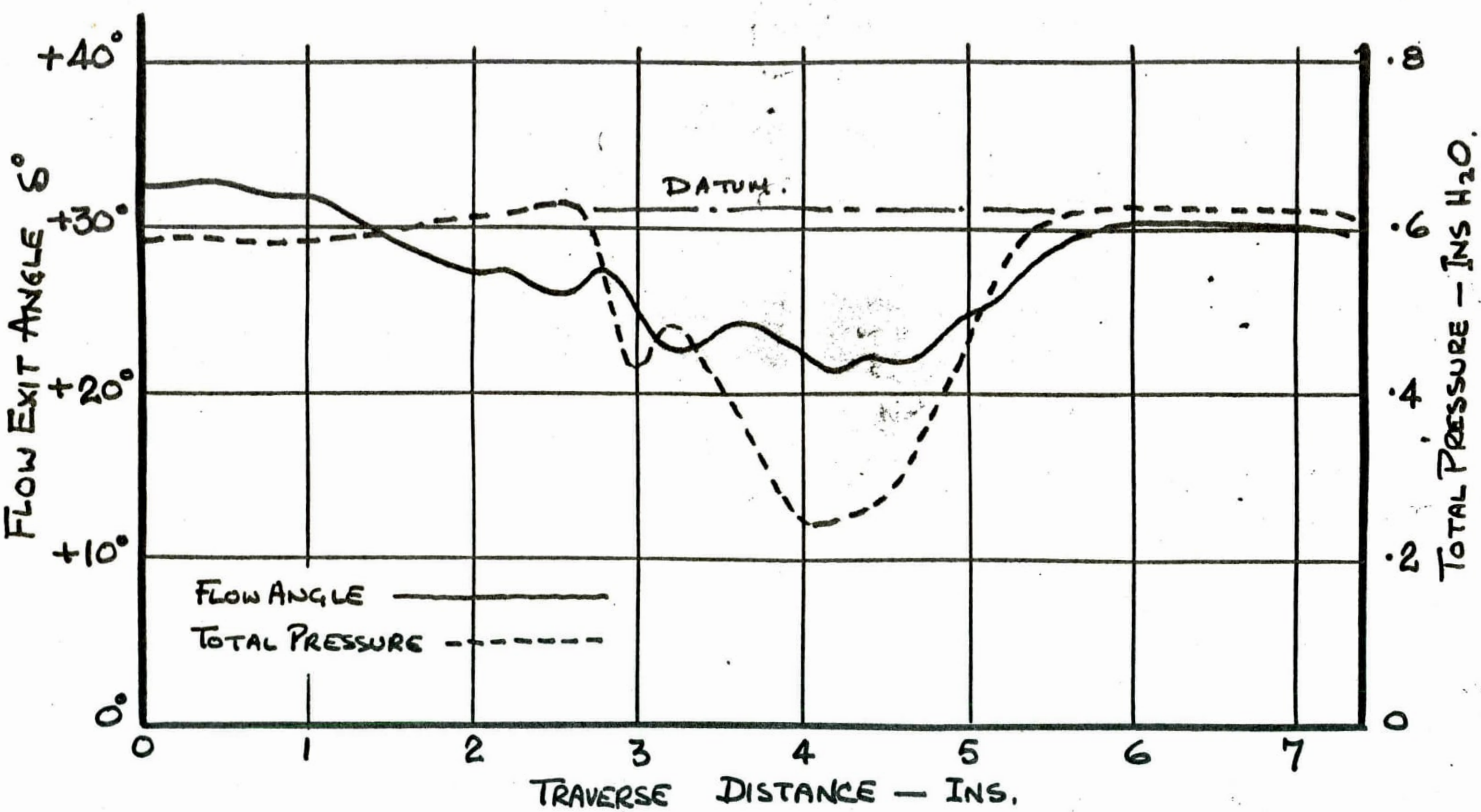

75° CAMBER. 4 SLOTS. BLADE "F". +4° α

F3

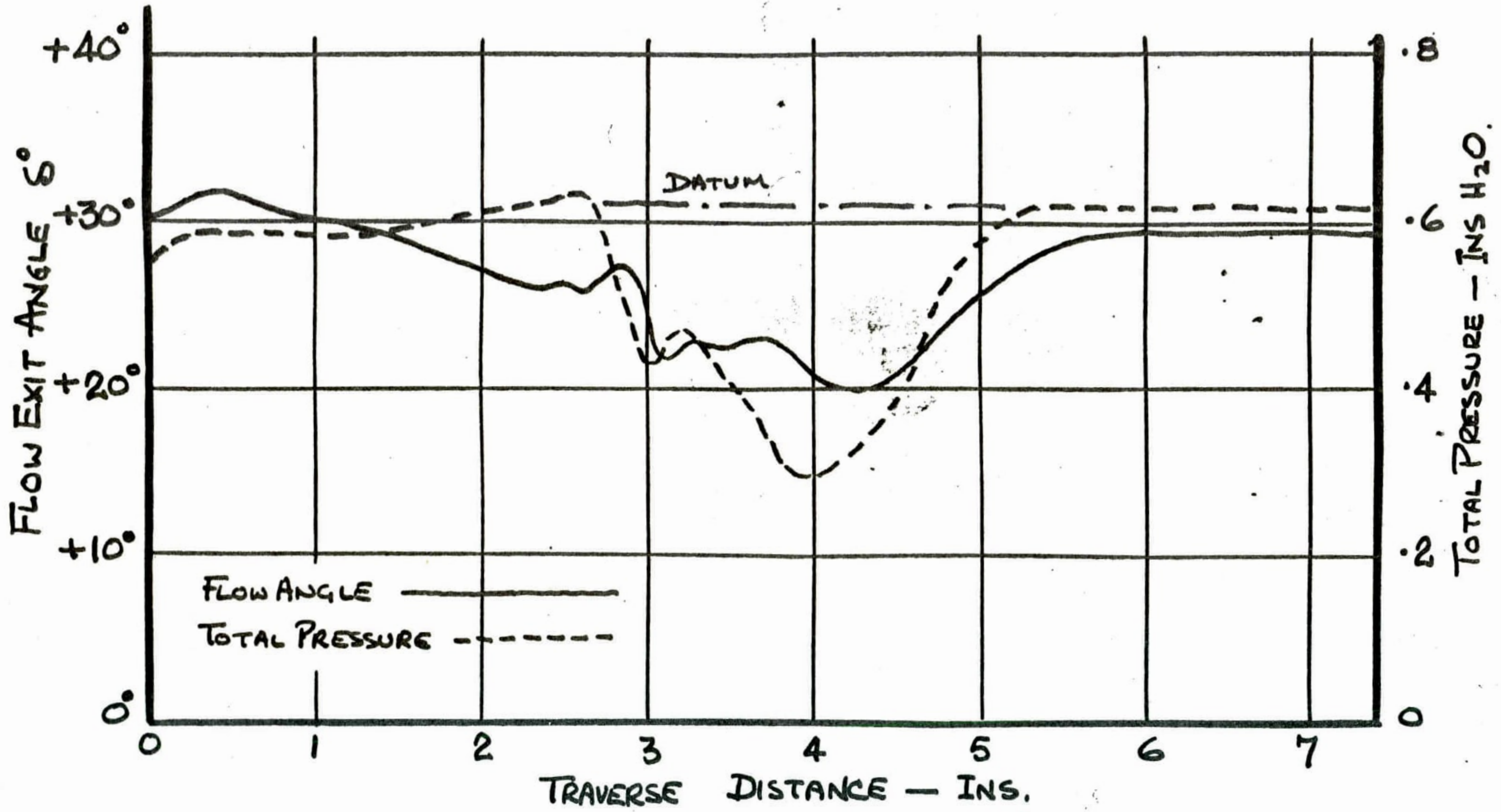

75° CAMBER. 4 SLOTS. BLADE "F". +2°α

F4

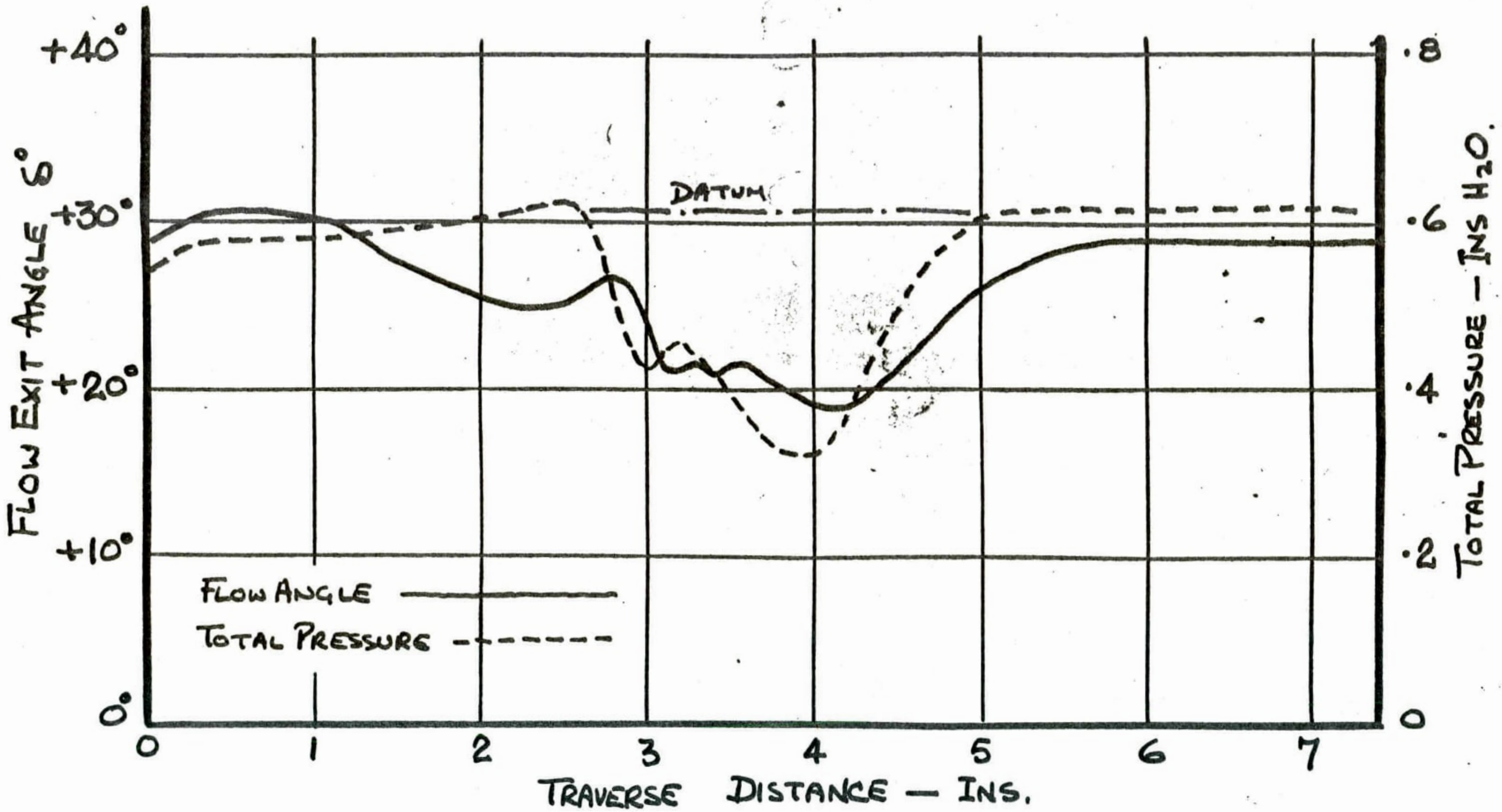

75° CAMBER. 4 SLOTS. BLADE "F". 0 °α

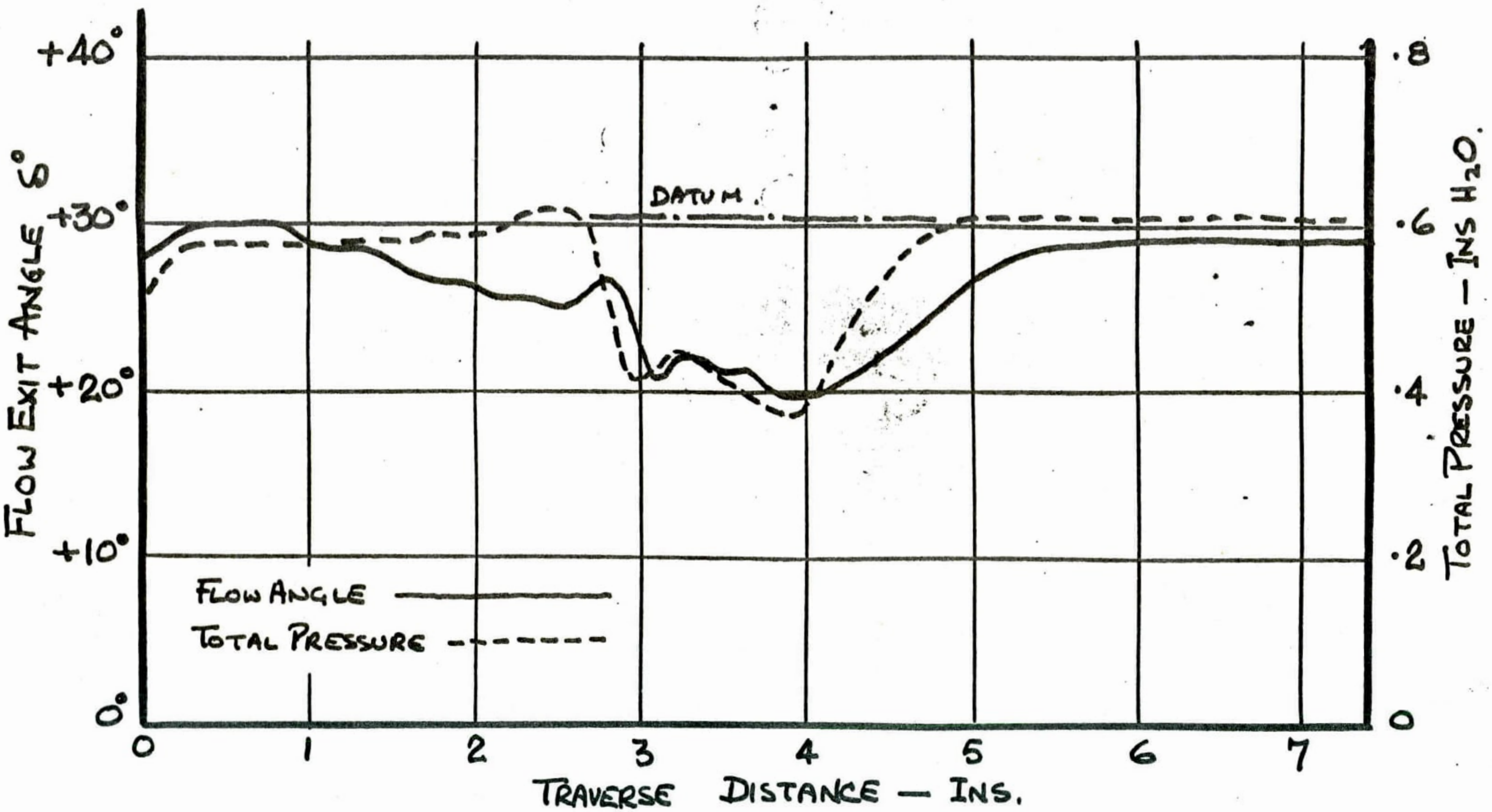

75°CAMBER. 4 SLOTS. BLADE "F". −2 °α

F6

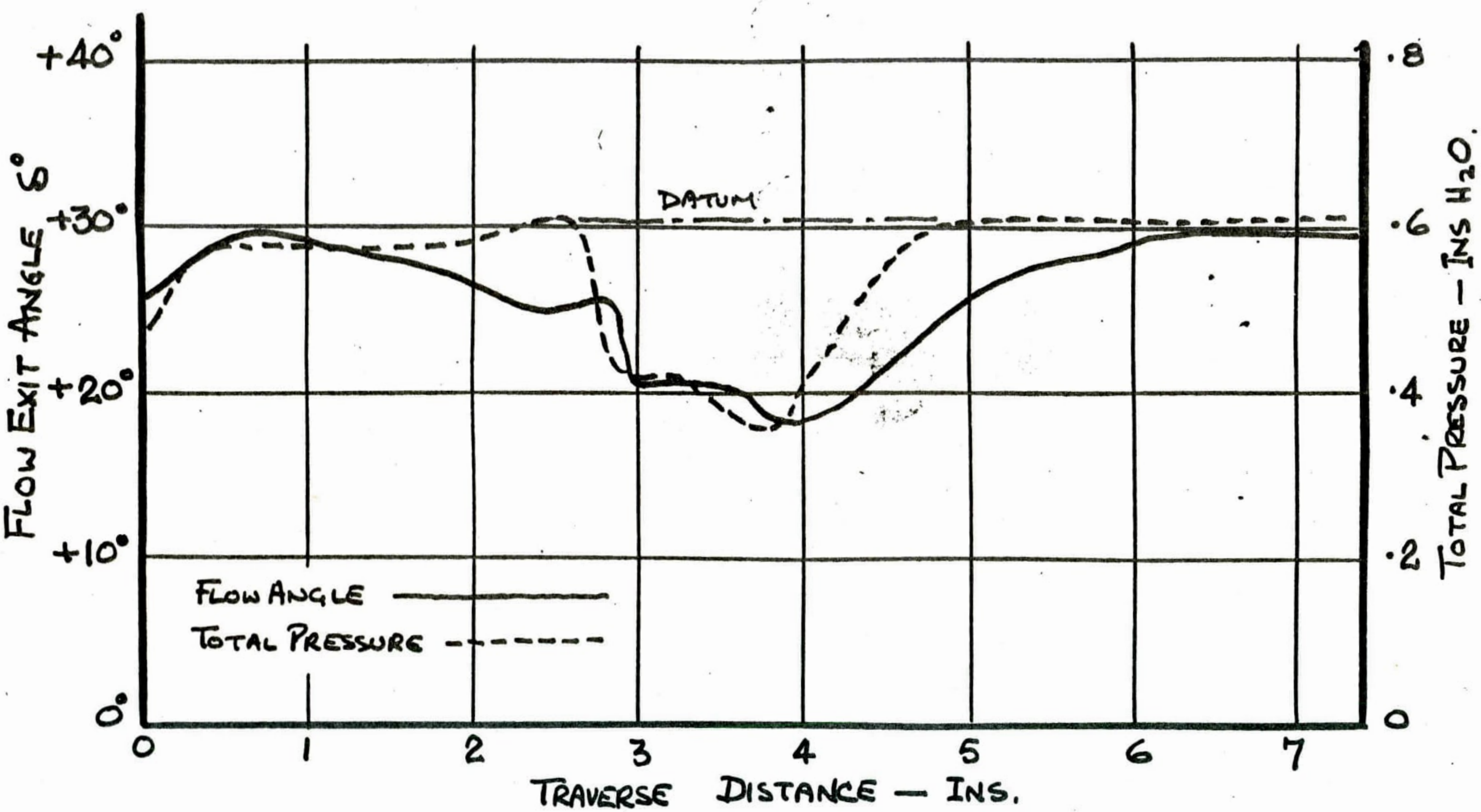

75° CAMBER. 4 SLOTS. BLADE "F". −4° α

F7

BLADE "G" 3 SLOTS

75° CAMBER

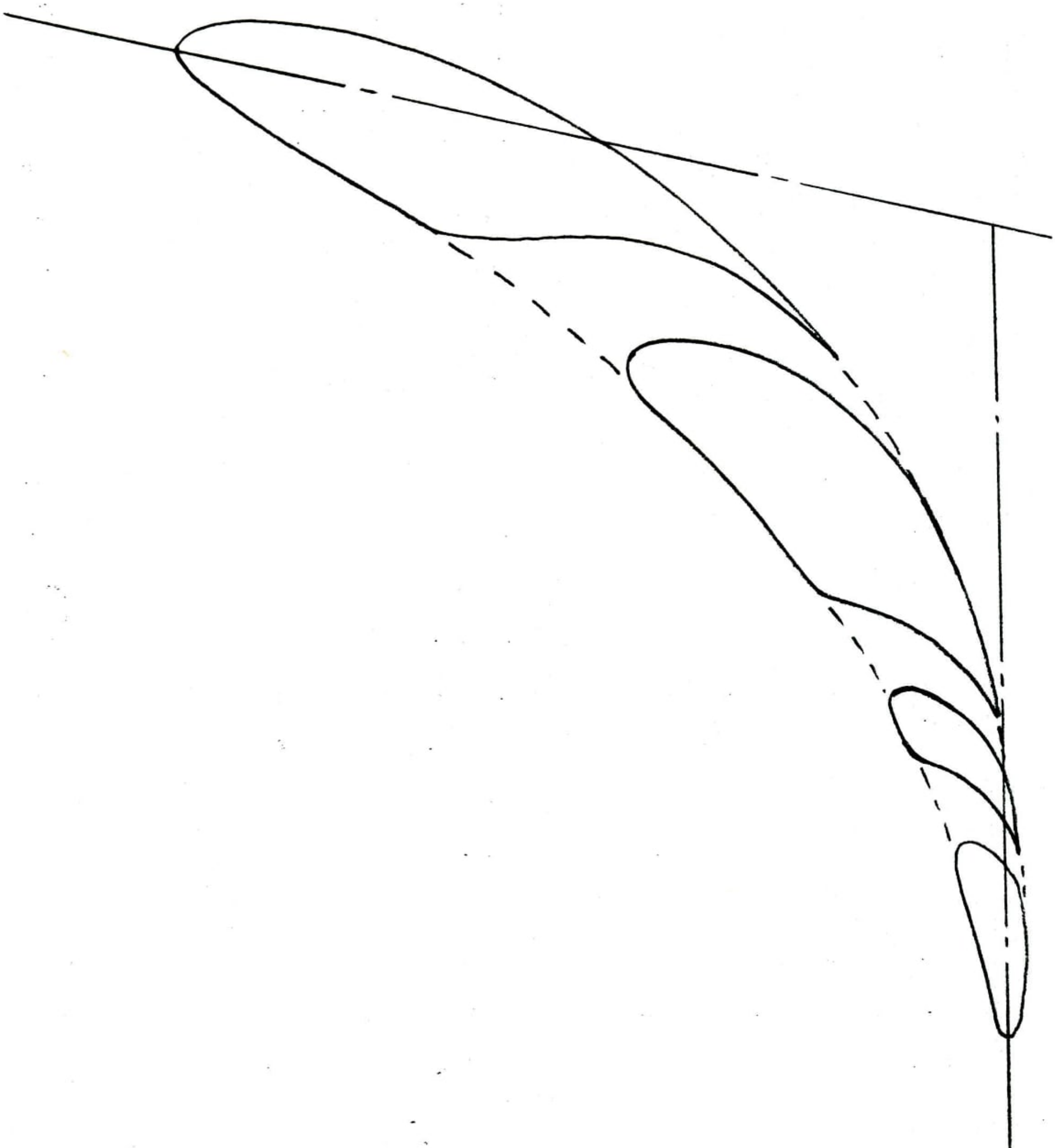

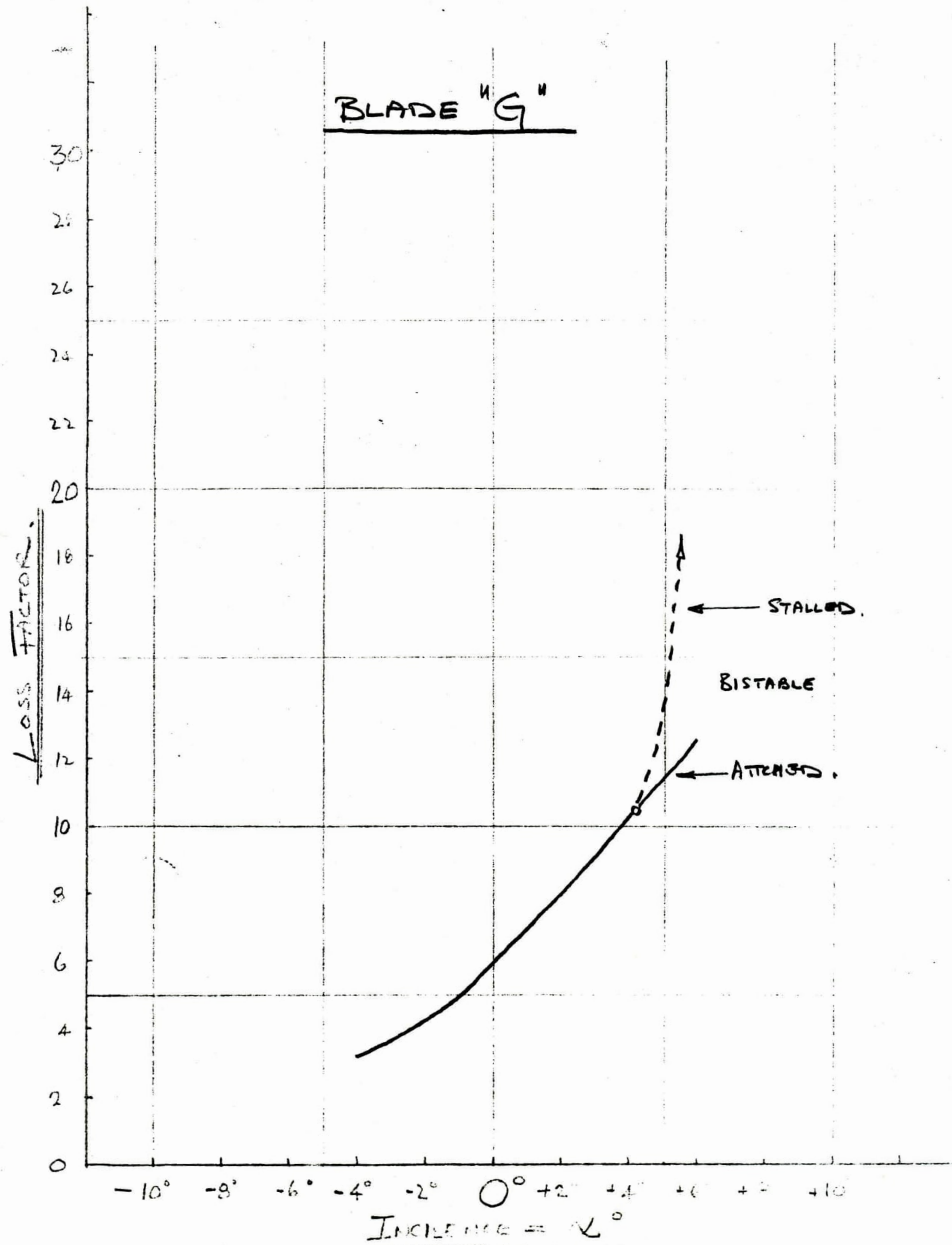
BLADE "G"
LOSS FACTOR
INCIDENCE = α°
STALLED.
BISTABLE
ATTACHED.
30
26
24
22
20
18
16
14
12
10
8
6
4
2
0
-10°
-8°
-6°
-4°
-2°
0°
+2
+4
+6
+8
+10

GA

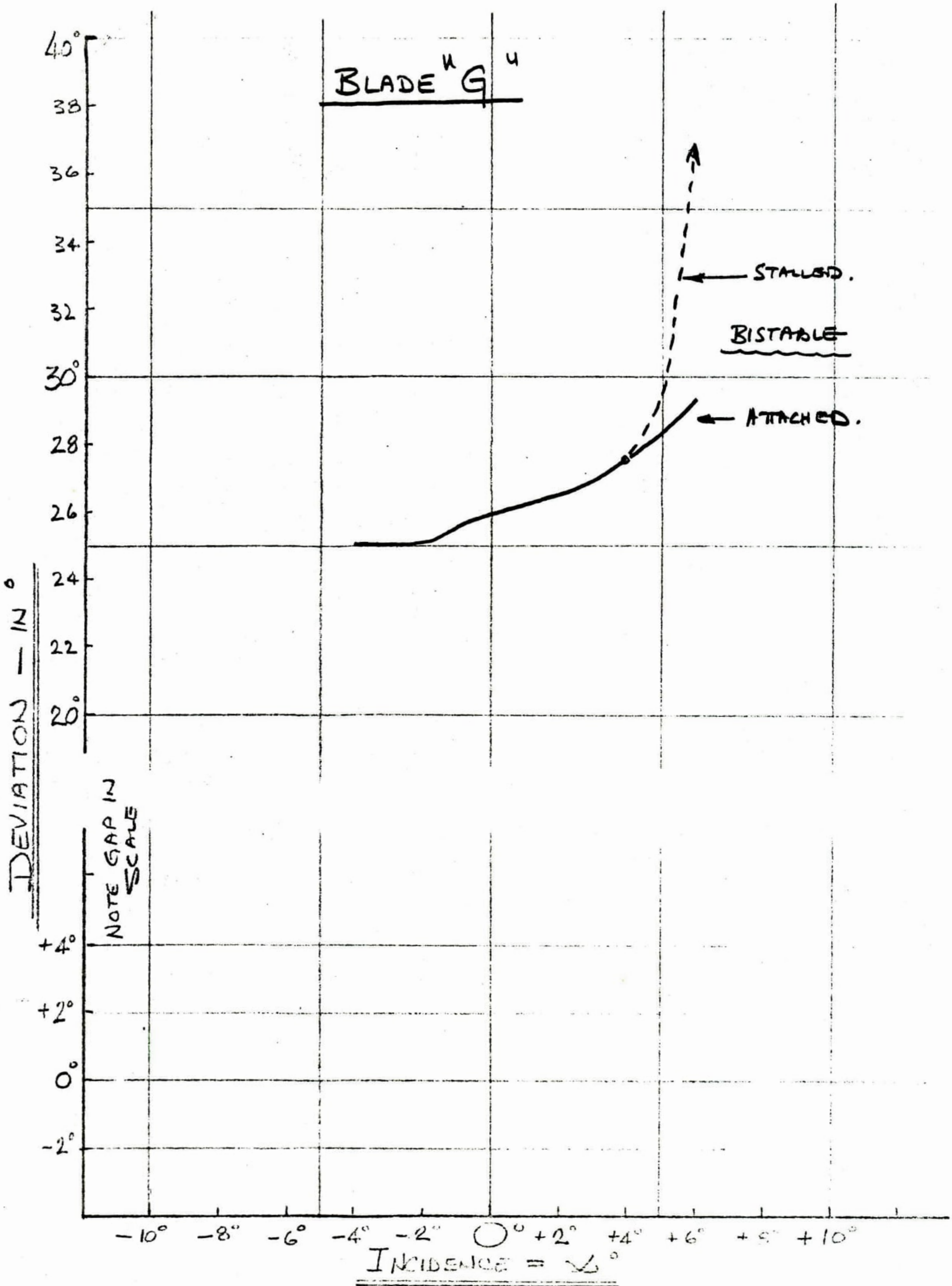
BLADE "G"
STALLED.
BISTABLE
ATTACHED.
DEVIATION — IN °
NOTE GAP IN SCALE
40°
38
36
34
32
30°
28
26
24
22
20°
+4°
+2°
0°
-2°
-10° -8° -6° -4° -2° 0° +2° +4° +6° +10°
INCIDENCE = α °

Gb

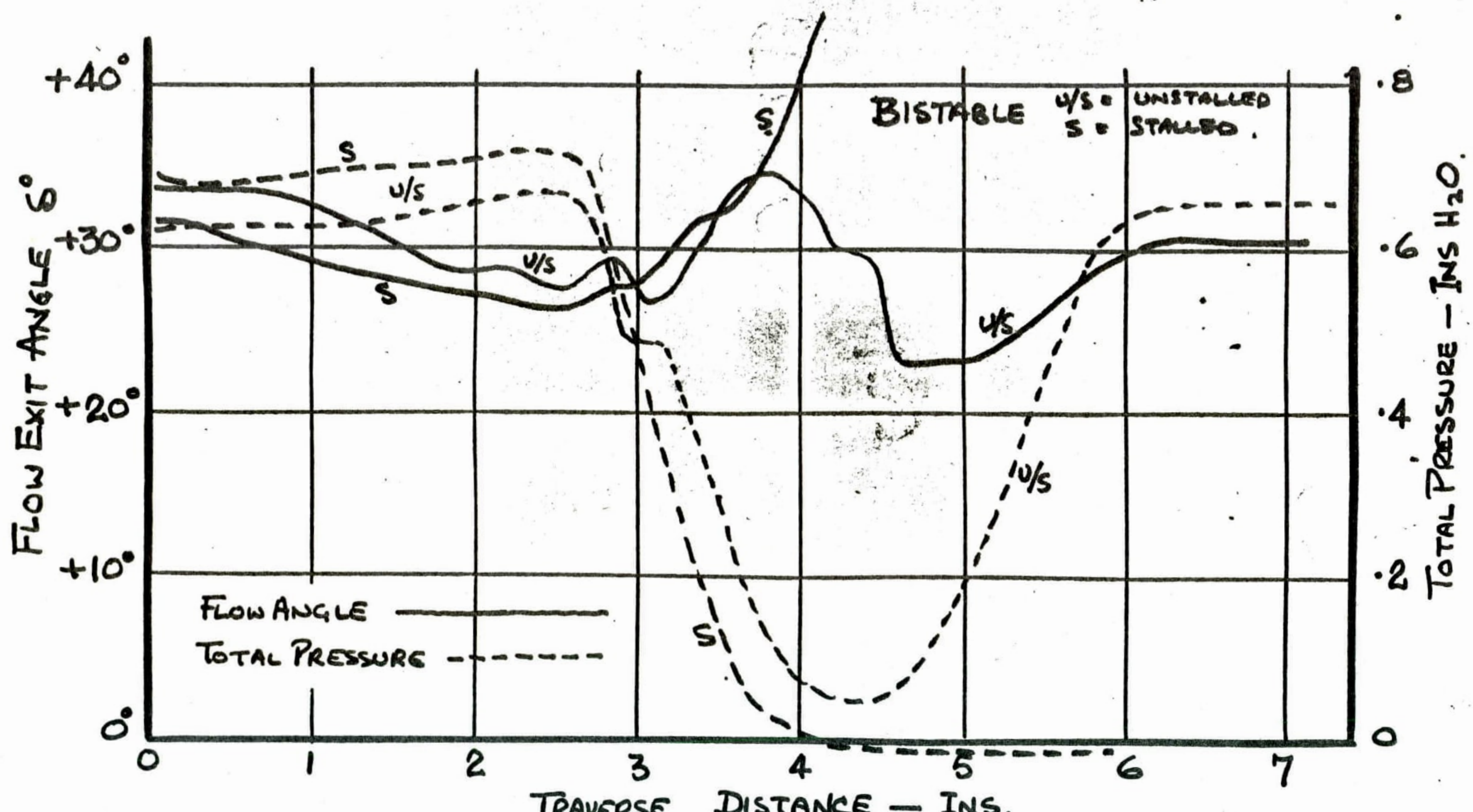

75° CAMBER. 3 SLOTS. BLADE "G". +6° α

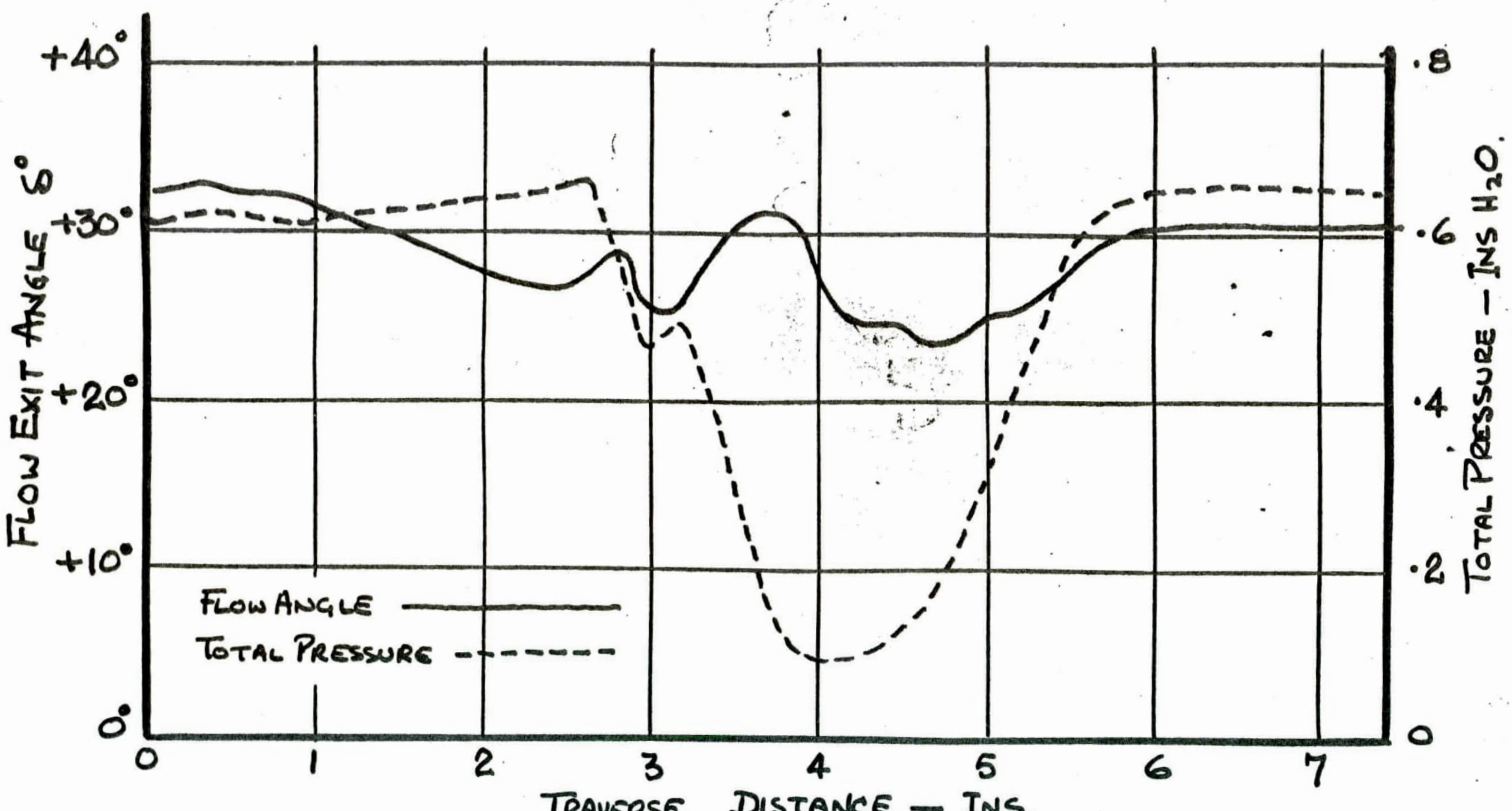

75° CAMBER. 3 SLOTS. BLADE "G". +4.° α

G2

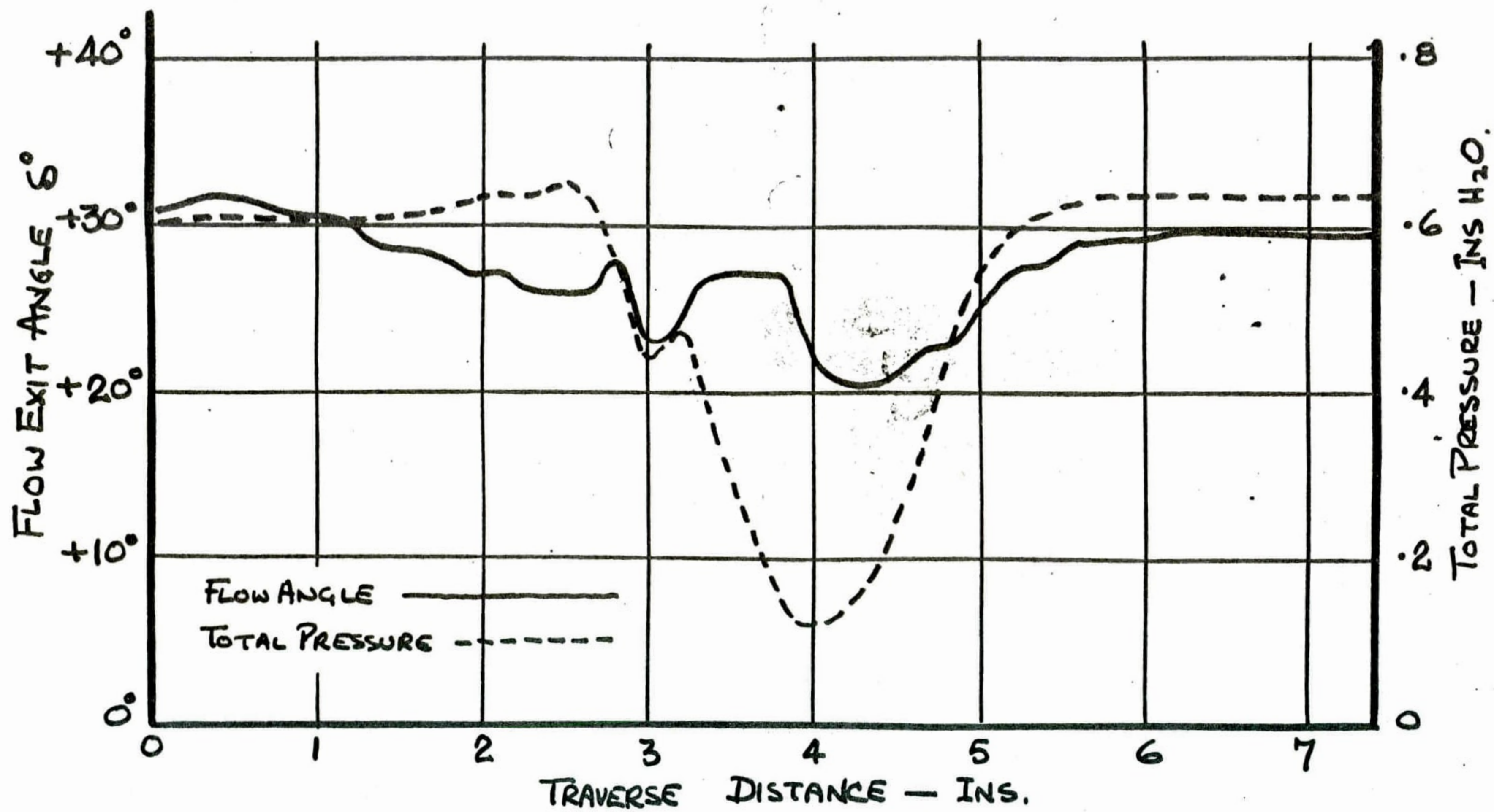

75° CAMBER. 3 SLOTS. BLADE "G". +2 °α

G3

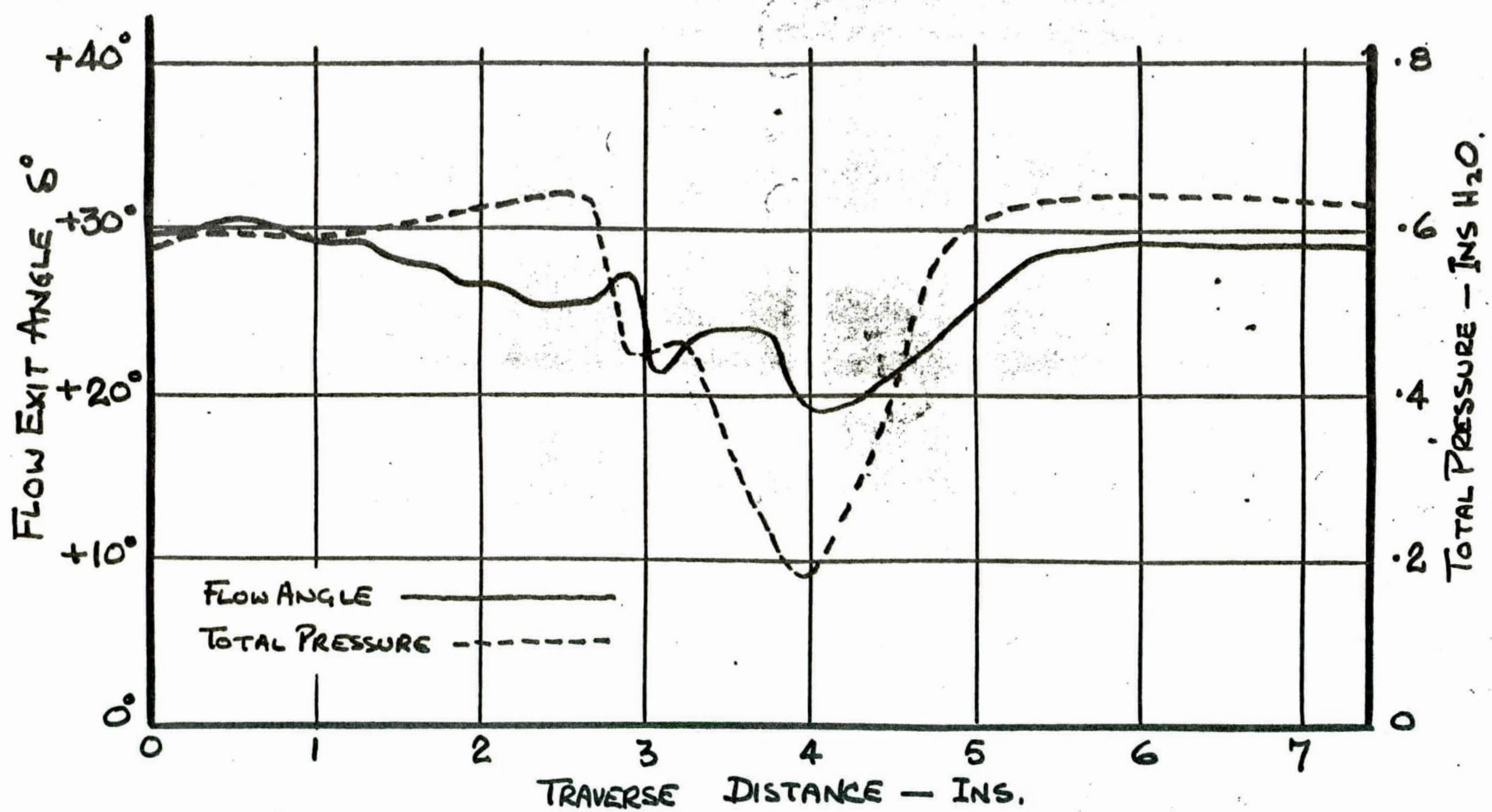

75° CAMBER. 3 SLOTS. BLADE "G". 0 °α

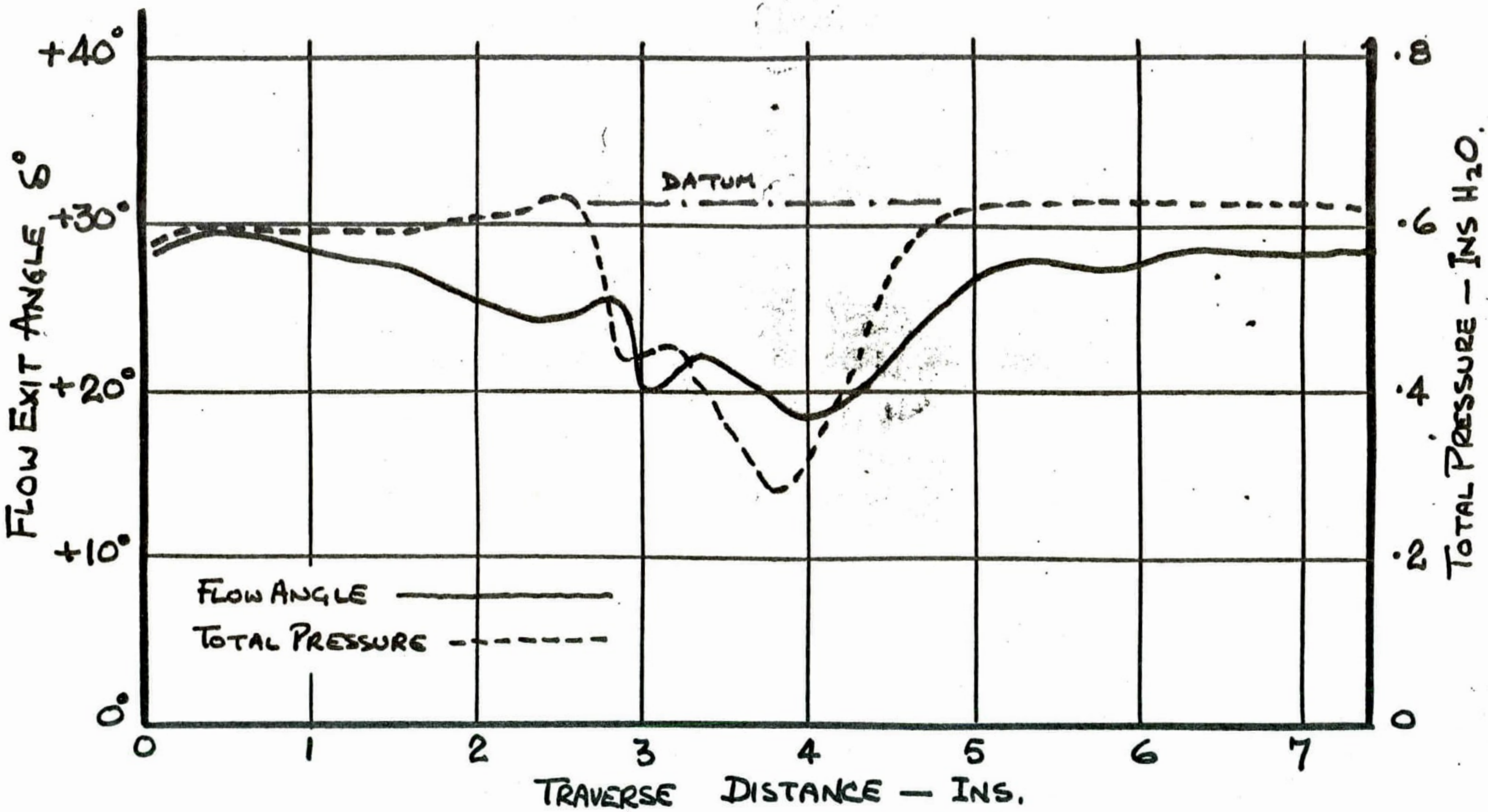

75° CAMBER. 3 SLOTS. BLADE "G". −2°α

G5

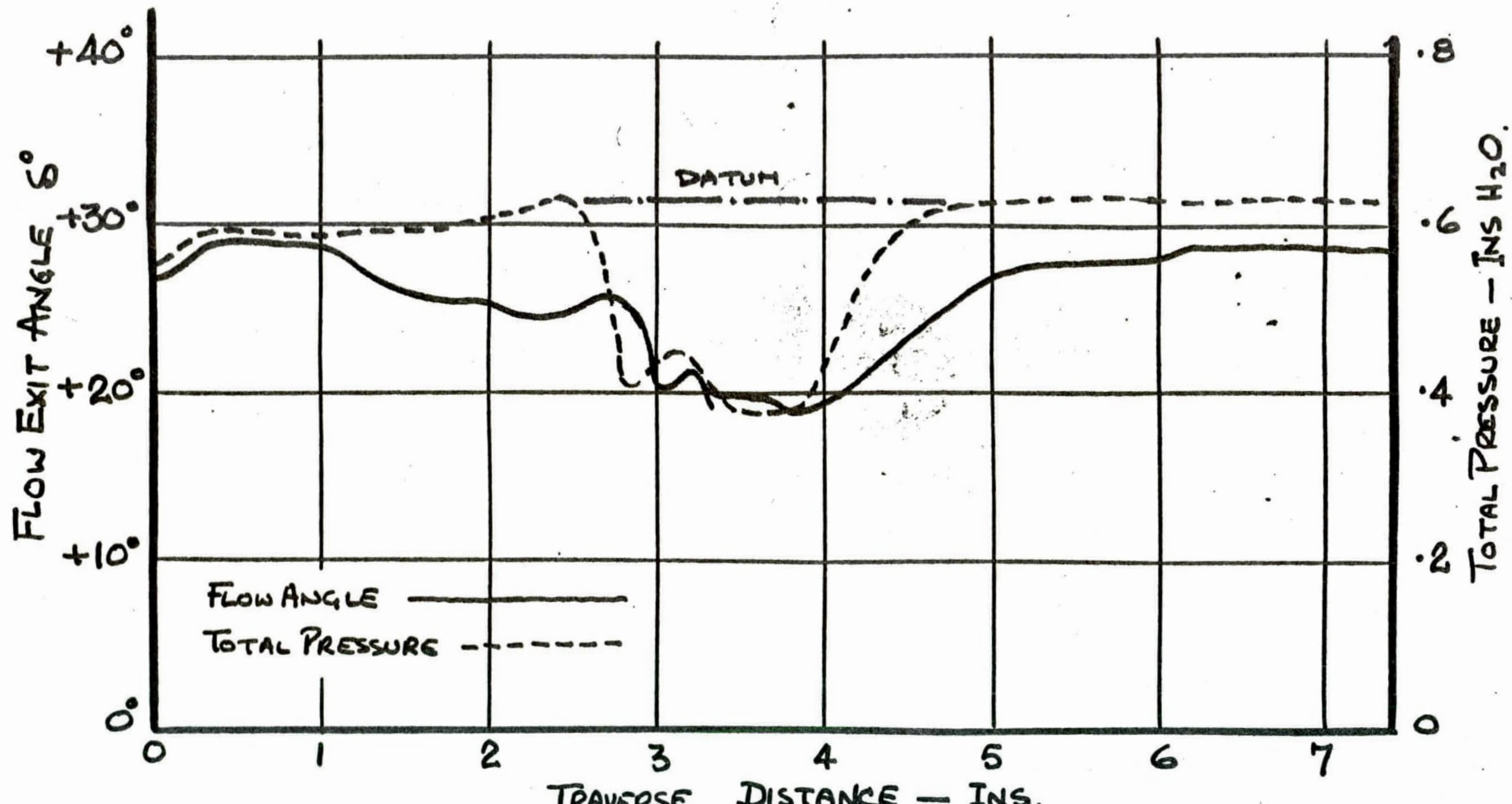

75° CAMBER. 3 SLOTS. BLADE "G". −4.°α

G6

BLADE "H"   2 SLOTS.
75° CAMBER.

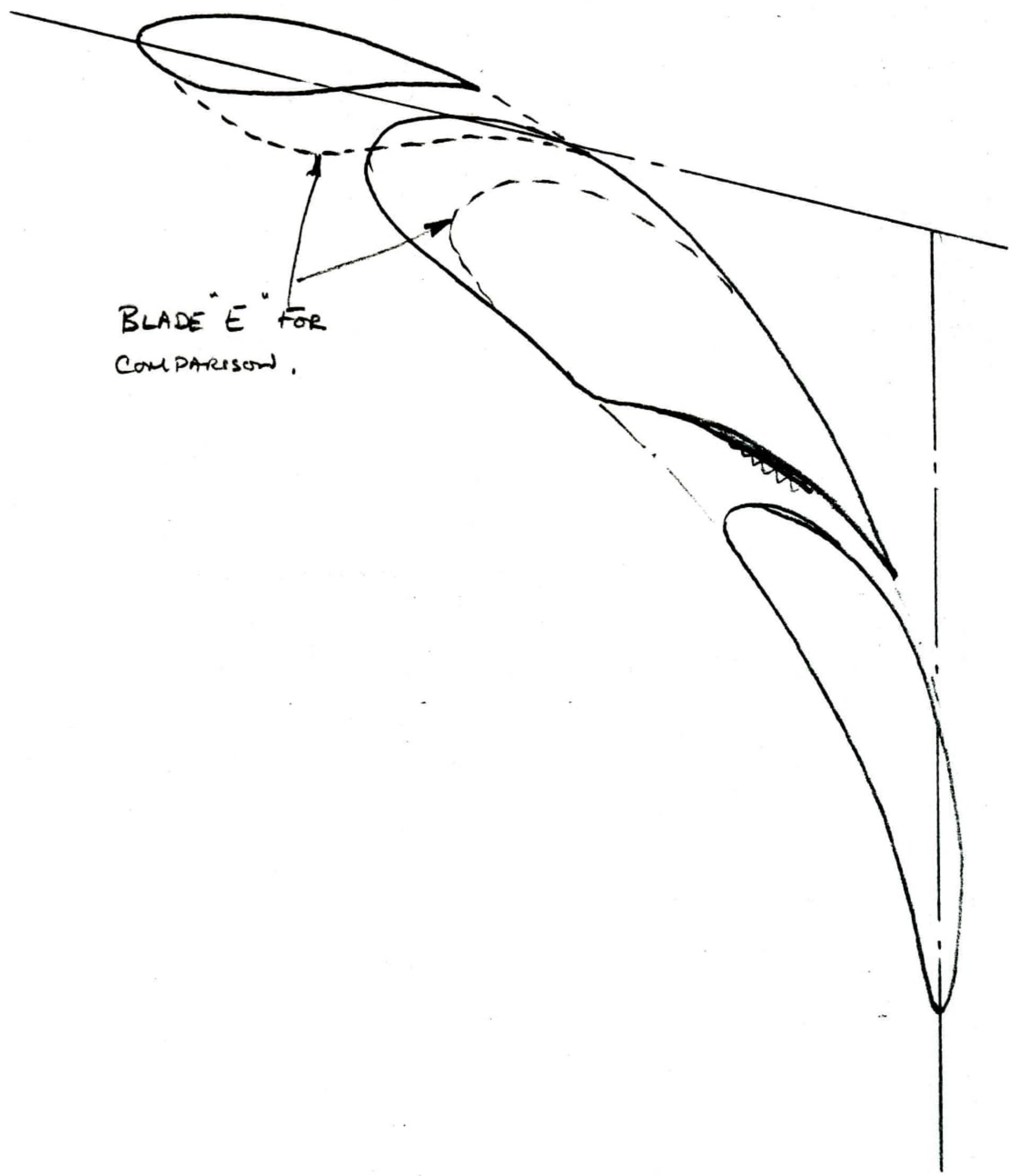

H.

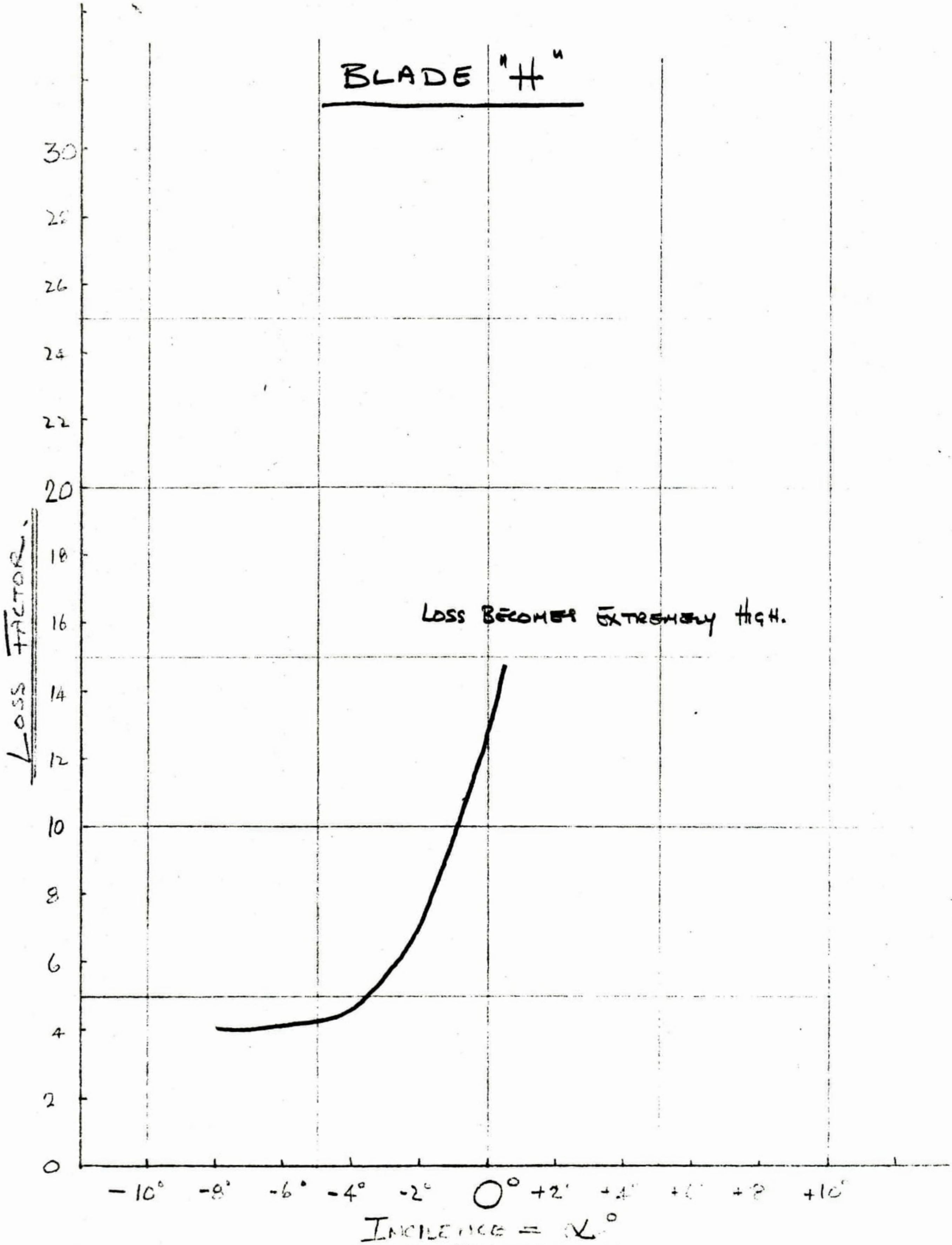
BLADE "H"
LOSS FACTOR.
LOSS BECOMES EXTREMELY HIGH.
INCIDENCE = α°
0
2
4
6
8
10
12
14
16
18
20
22
24
26
28
30
-10°
-8°
-6°
-4°
-2°
0°
+2°
+4°
+6°
+8°
+10°

Ha

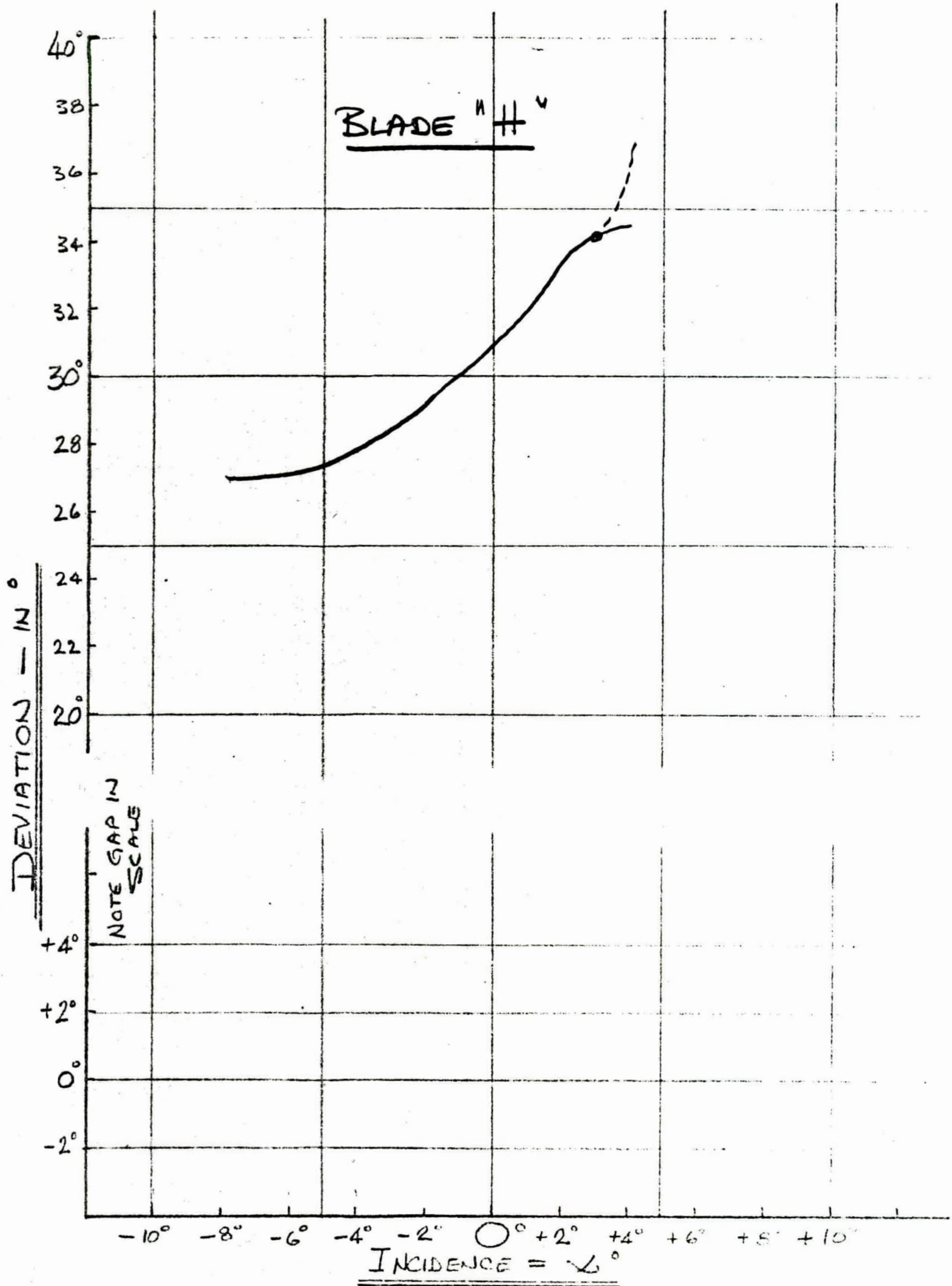

BLADE "H"
DEVIATION — IN °
NOTE GAP IN SCALE
40°
38
36
34
32
30°
28
26
24
22
20°
+4°
+2°
0°
-2°
-10°
-8°
-6°
-4°
-2°
0°
+2°
+4°
+6°
+8°
+10°
INCIDENCE = ∠°

Hb

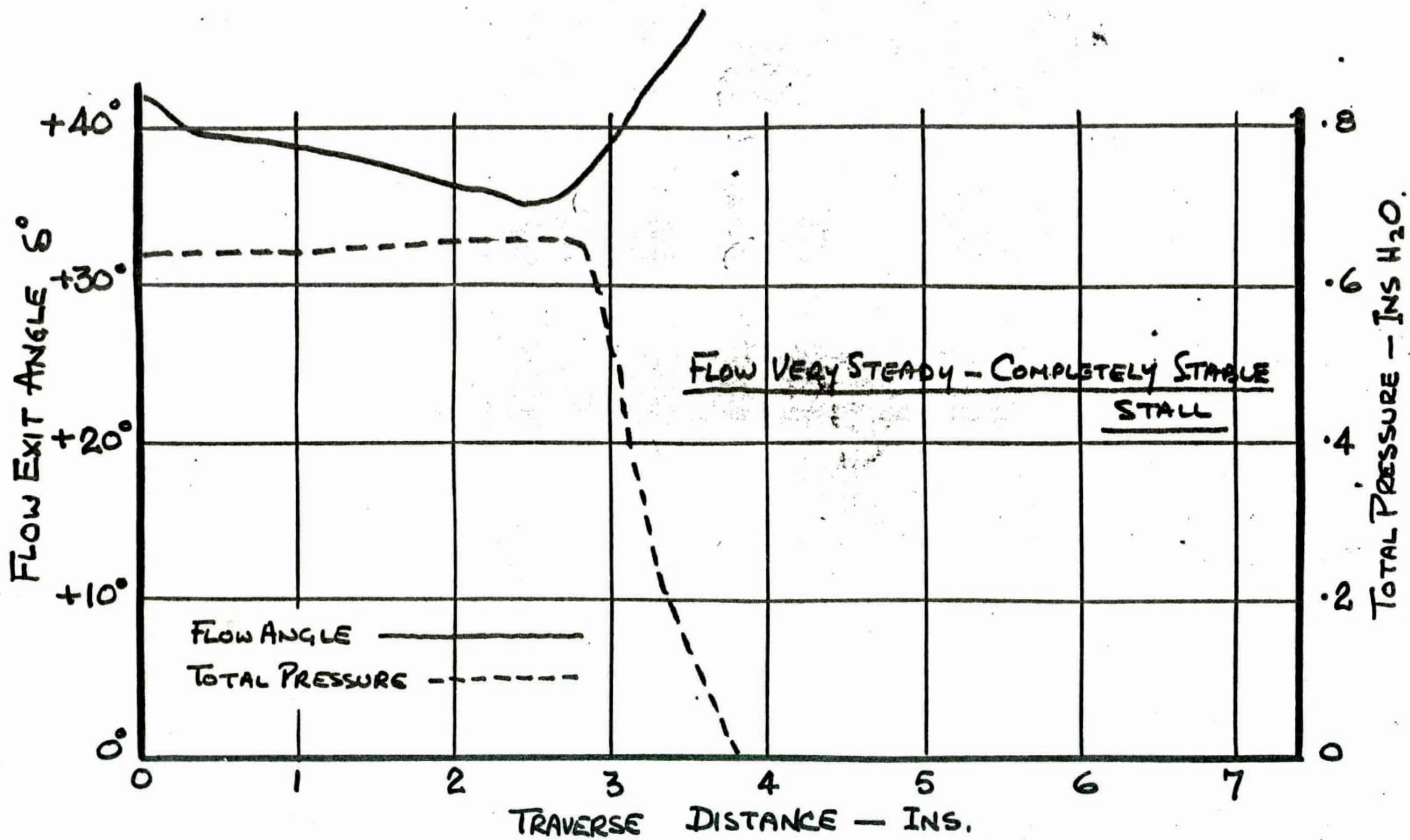

75° CAMBER. 2 SLOTS. BLADE "H". +6° α

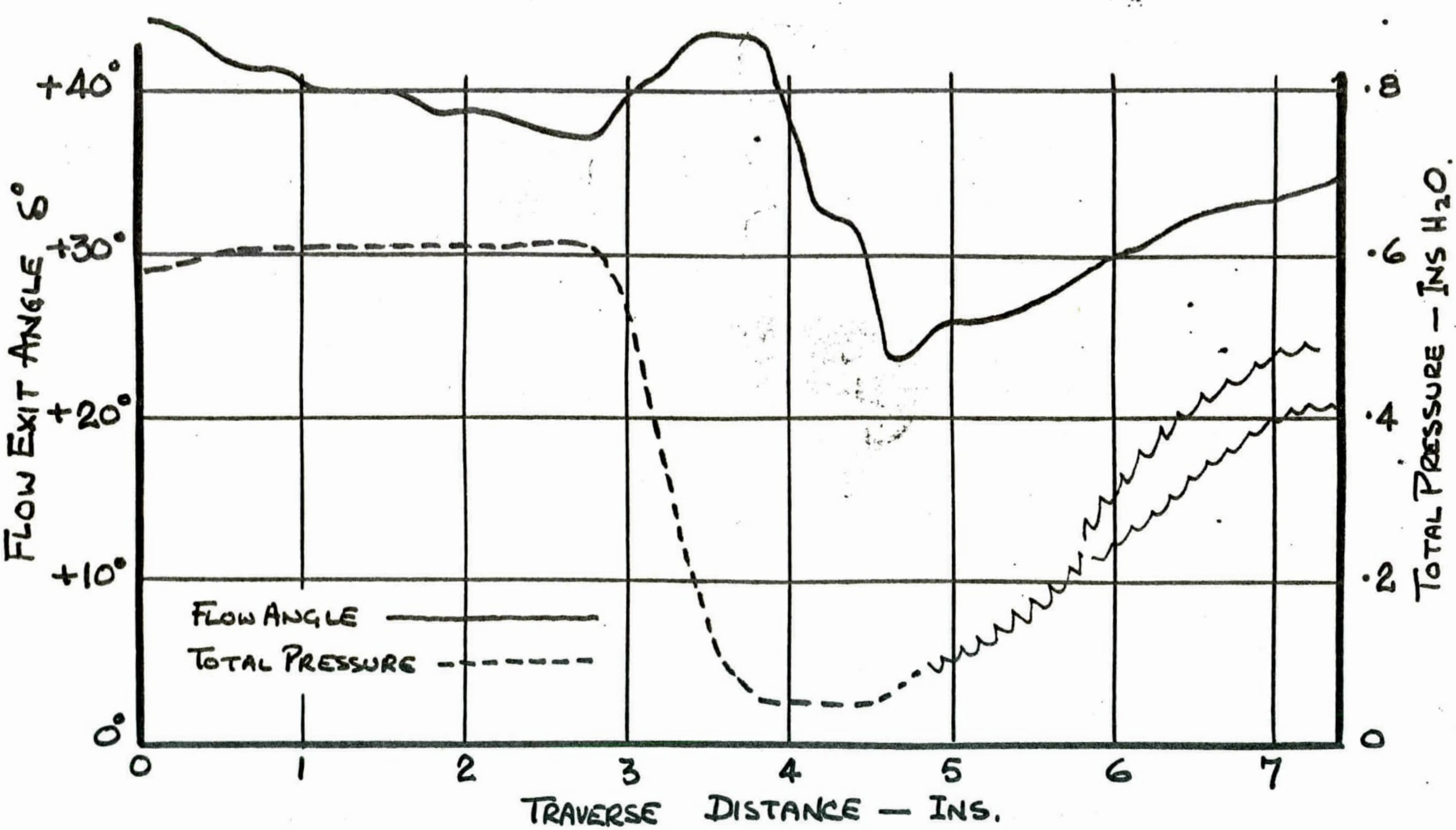

75° CAMBER. 2 SLOTS. BLADE "H". +4°α

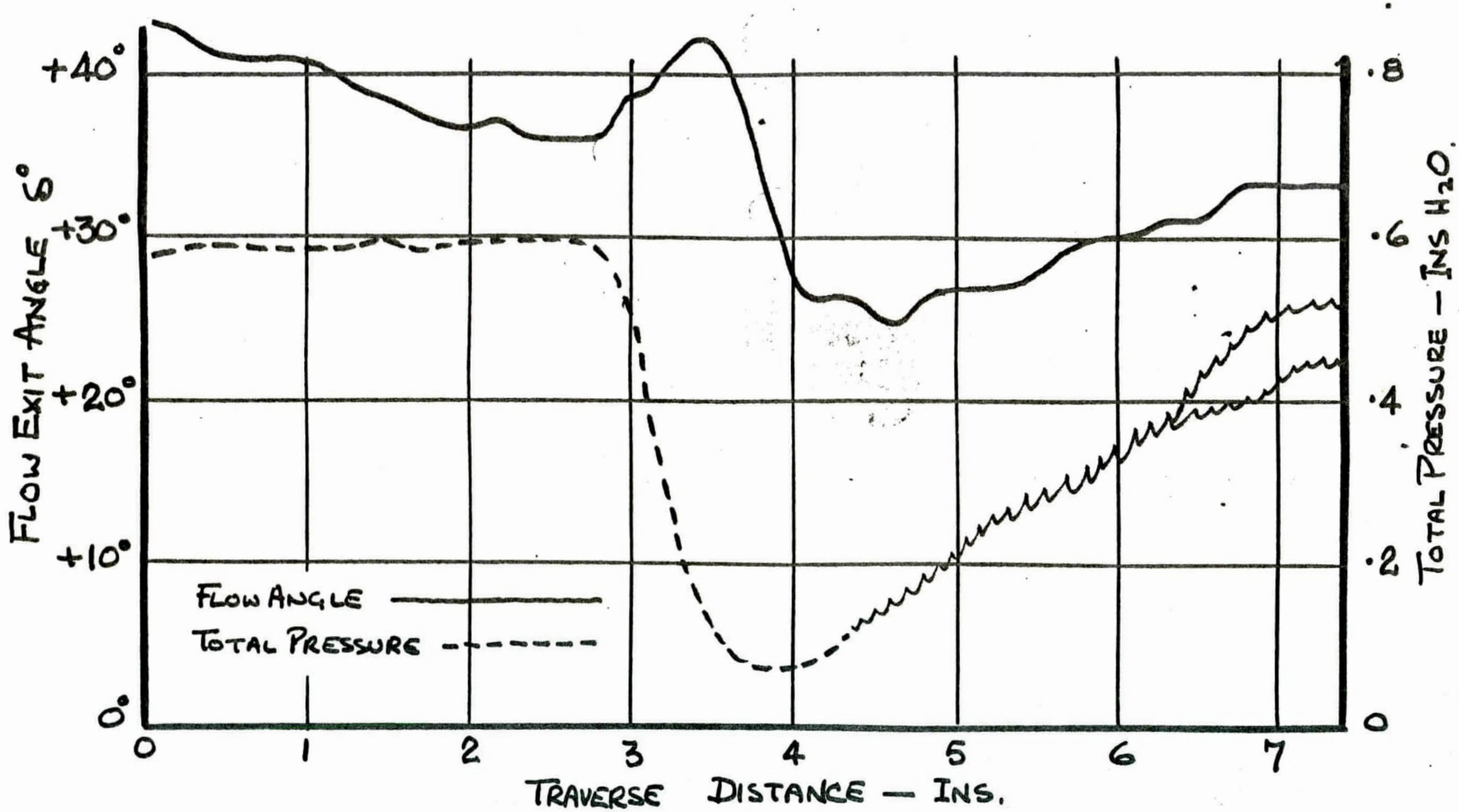

75° CAMBER. 2 SLOTS. BLADE "H". +2 °α

H3

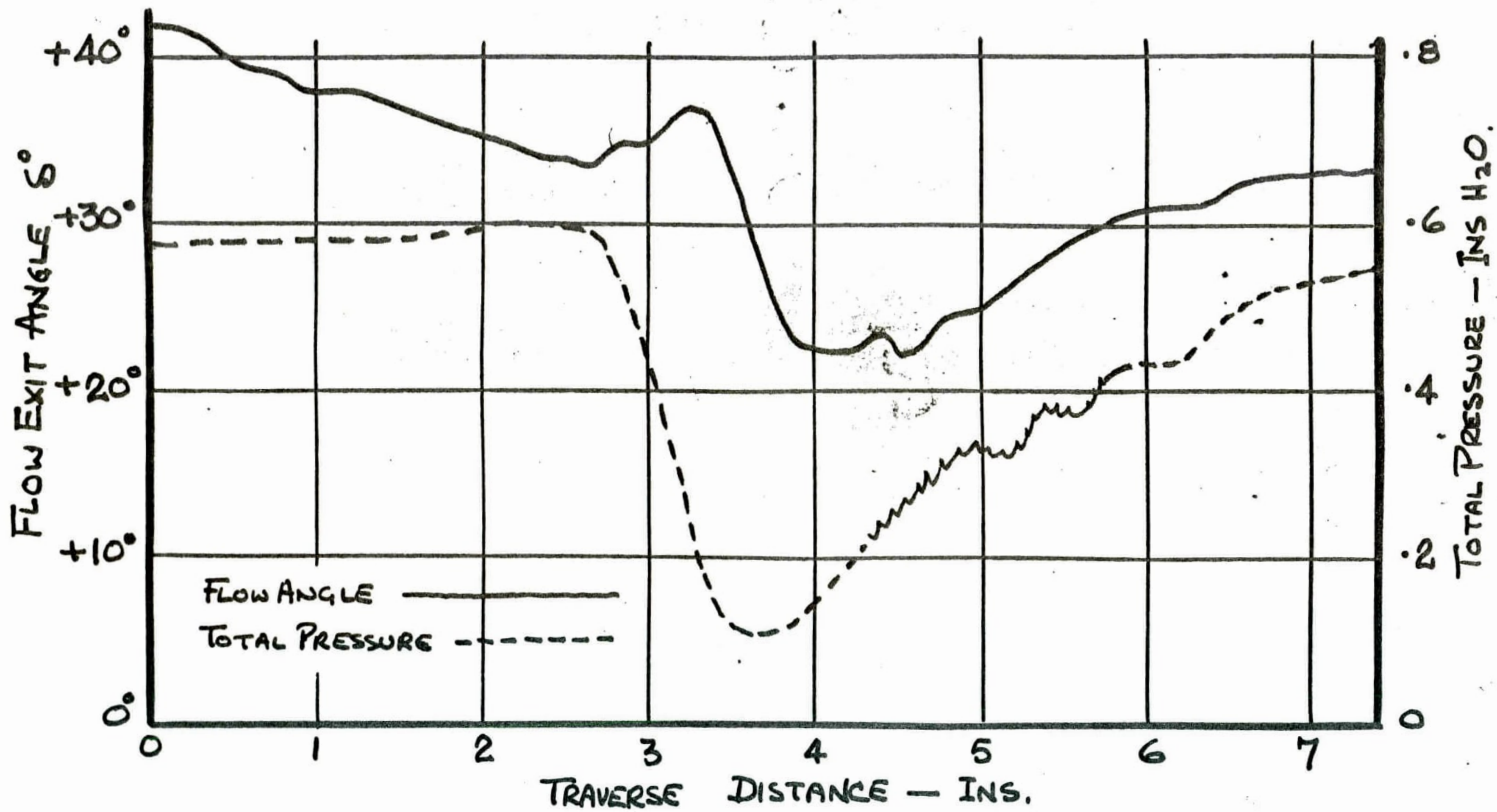

75° CAMBER. 2 SLOTS. BLADE "H". 0 °α

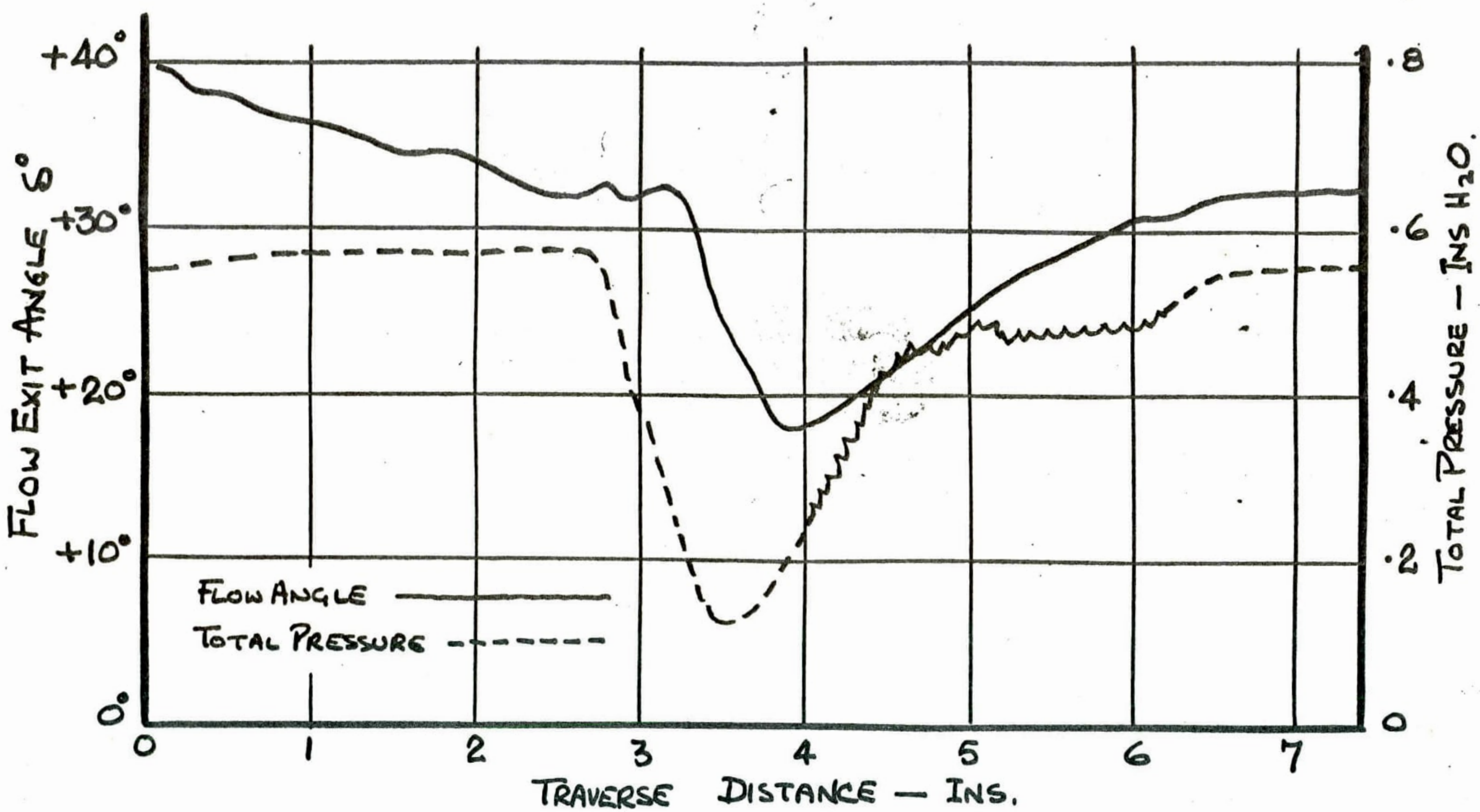

75° CAMBER. 2 SLOTS. BLADE "H". −2°α

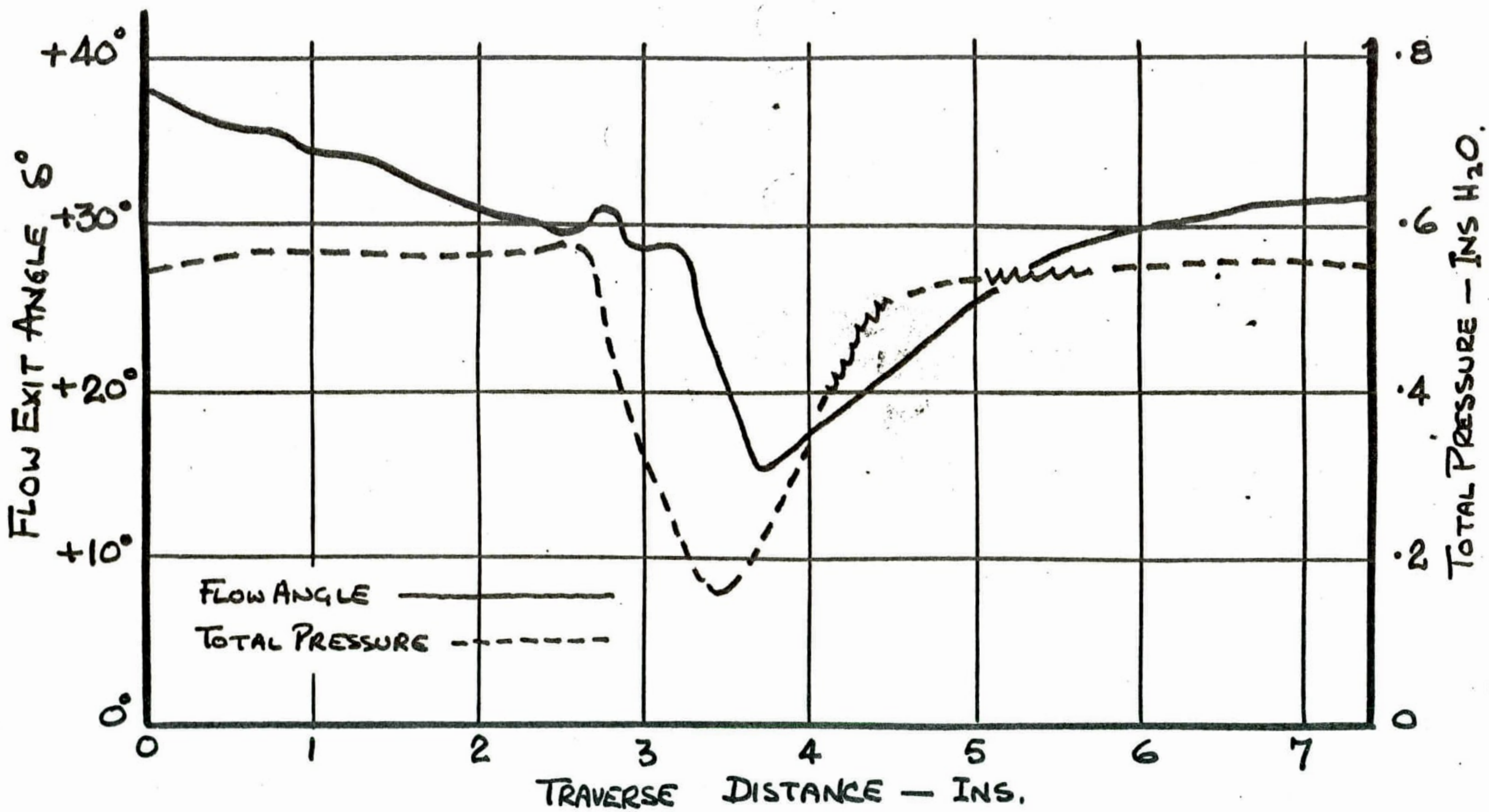

75° CAMBER. 2 SLOTS. BLADE "H". −4 °α

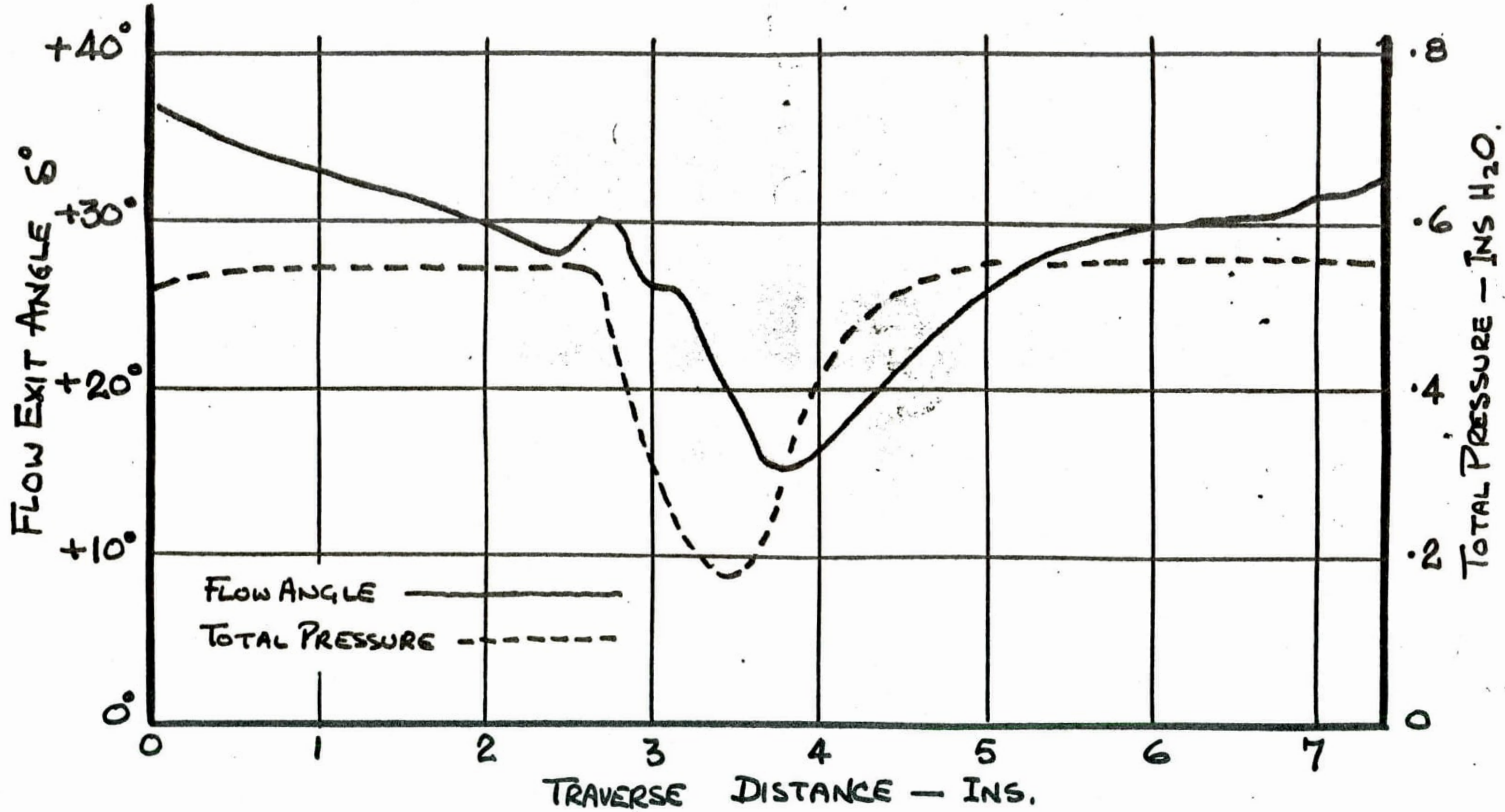

75° CAMBER. 2 SLOTS. BLADE "H". −8° α

BLADE "I" 2 SLOTS.
75° CAMBER

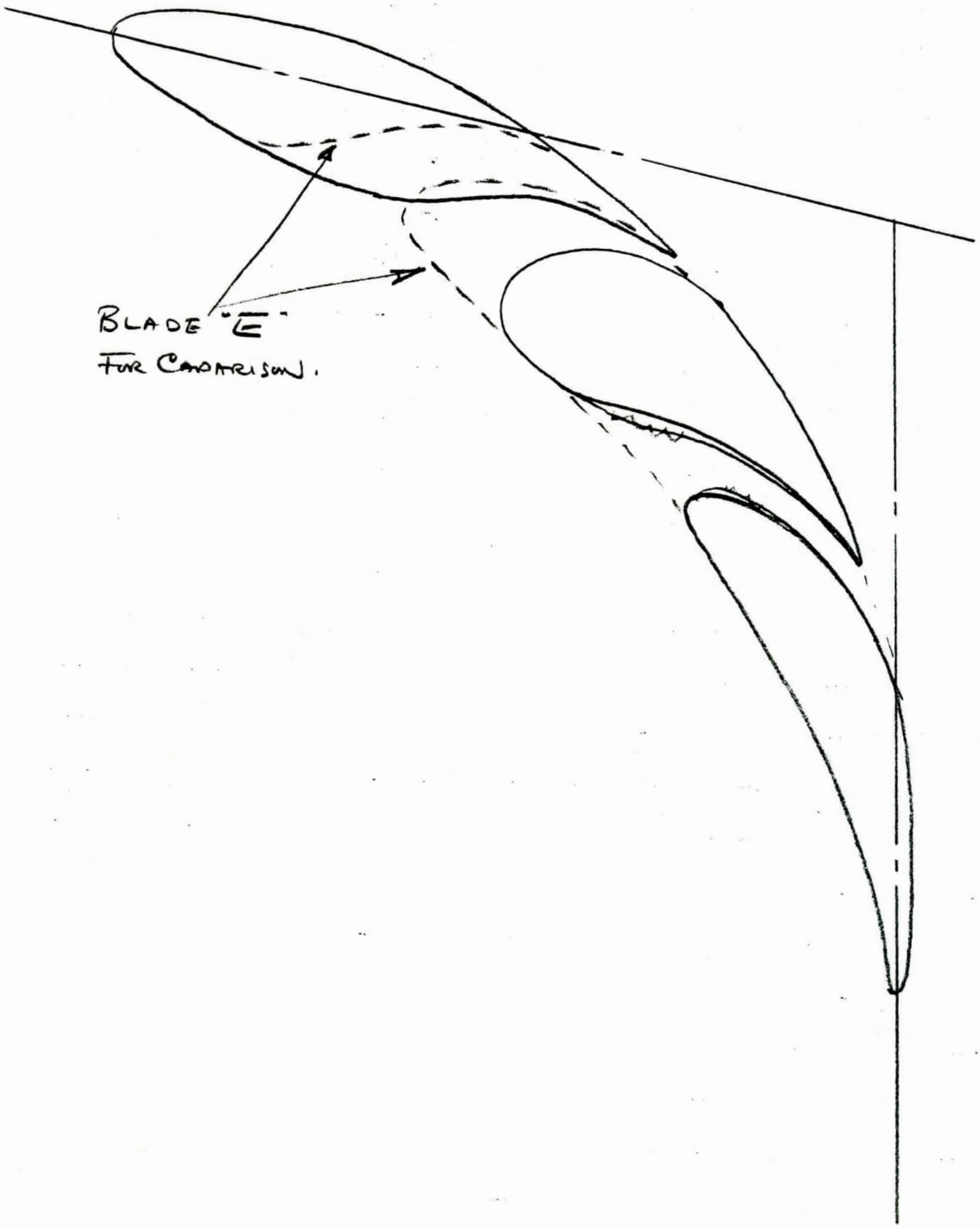

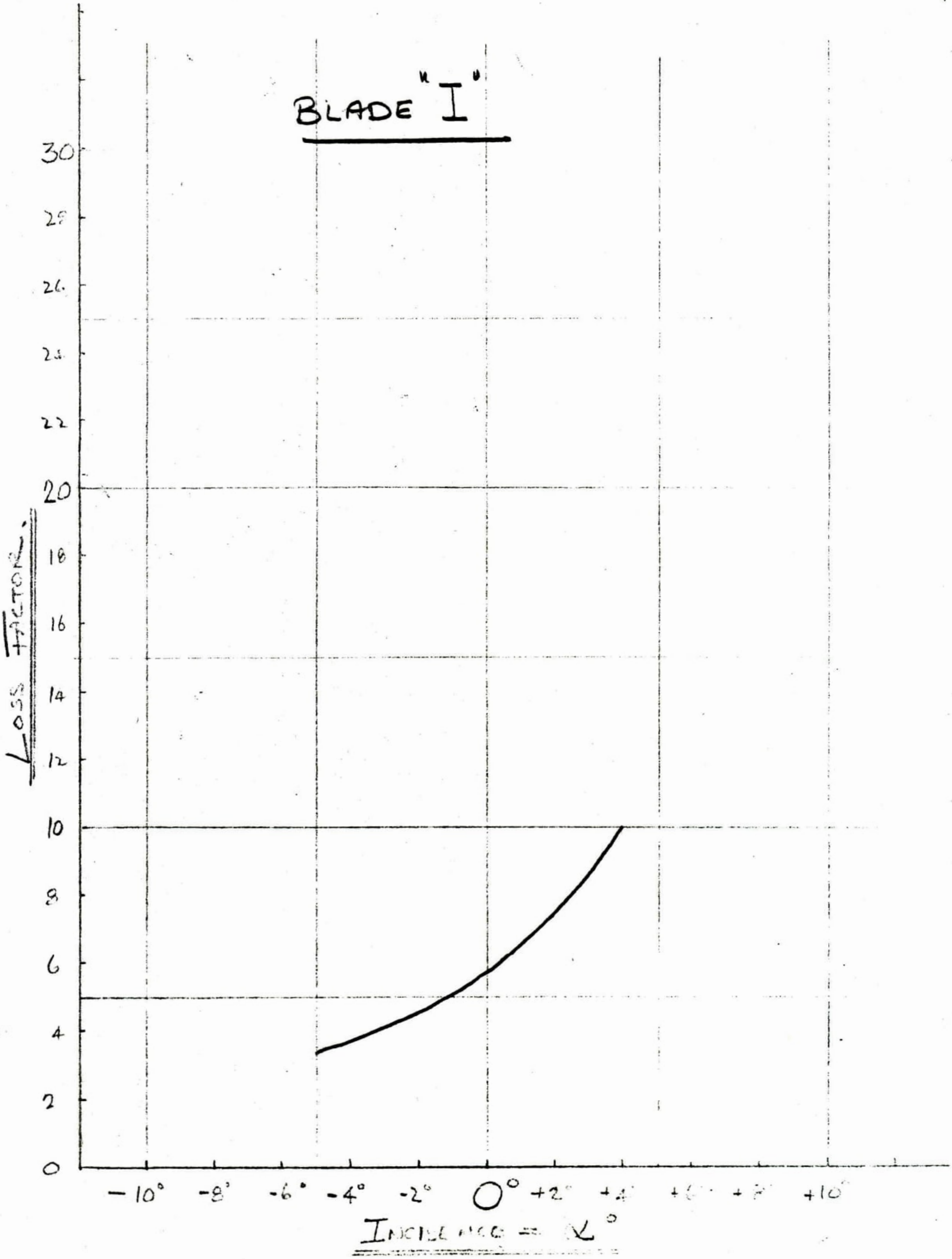

Ia

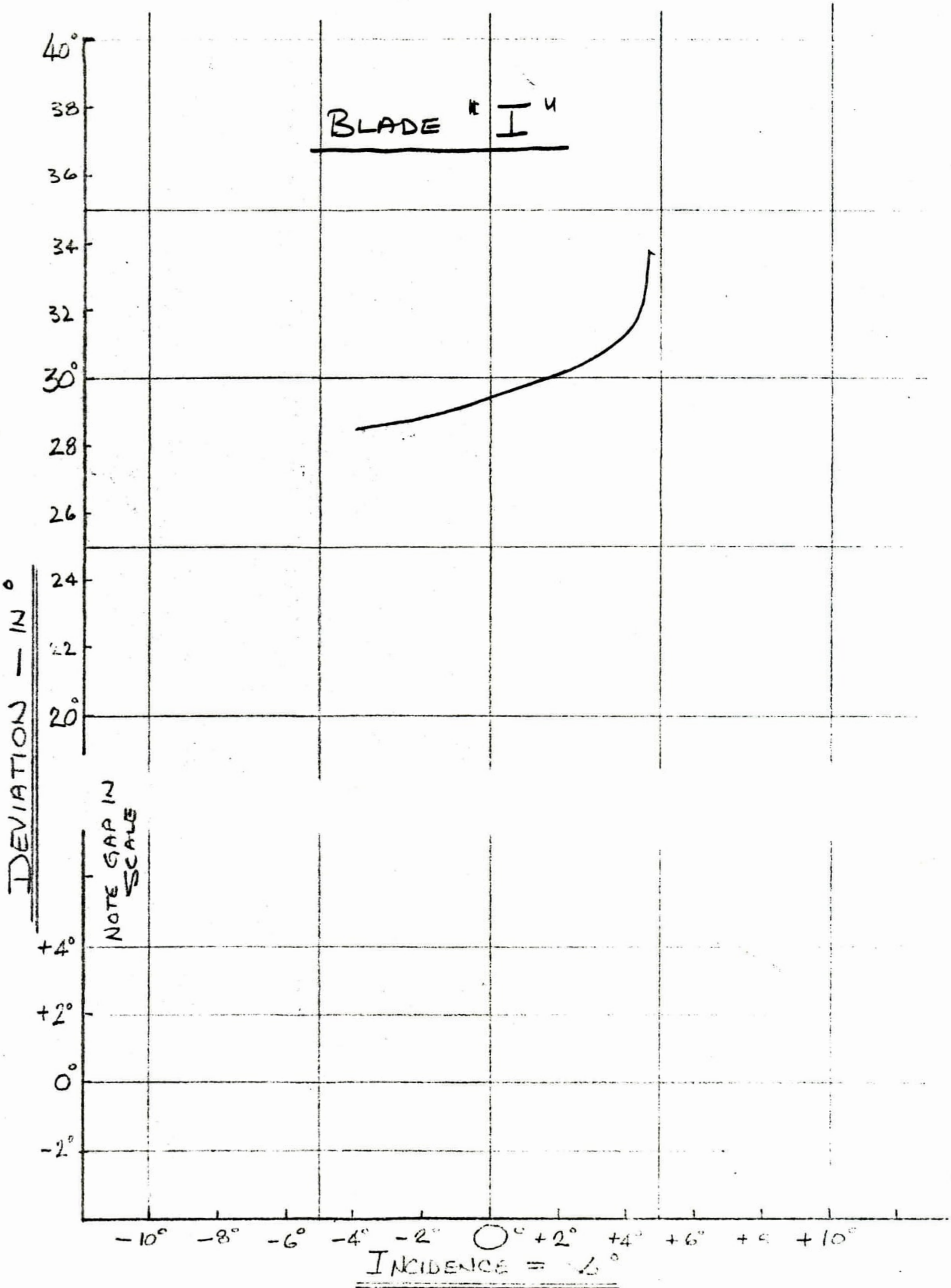
BLADE "I"
40°
38
36
34
32
30°
28
26
24
22
20°
+4°
+2°
0°
-2°
DEVIATION — IN °
NOTE GAP IN SCALE
-10° -8° -6° -4° -2° 0° +2° +4° +6° +10°
INCIDENCE = ∠°

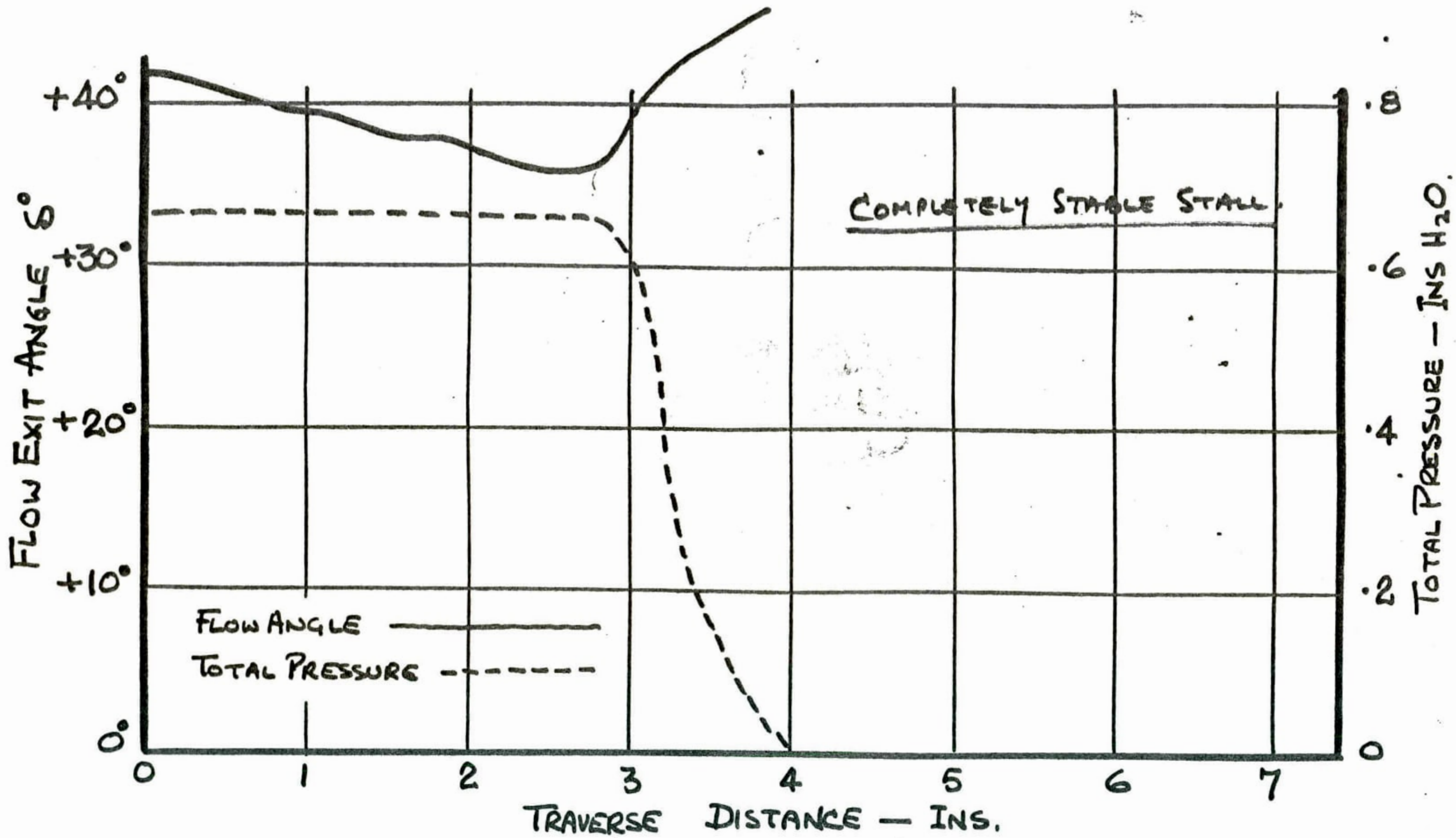

75° CAMBER. 2 SLOTS. BLADE "I". +6°α

I1

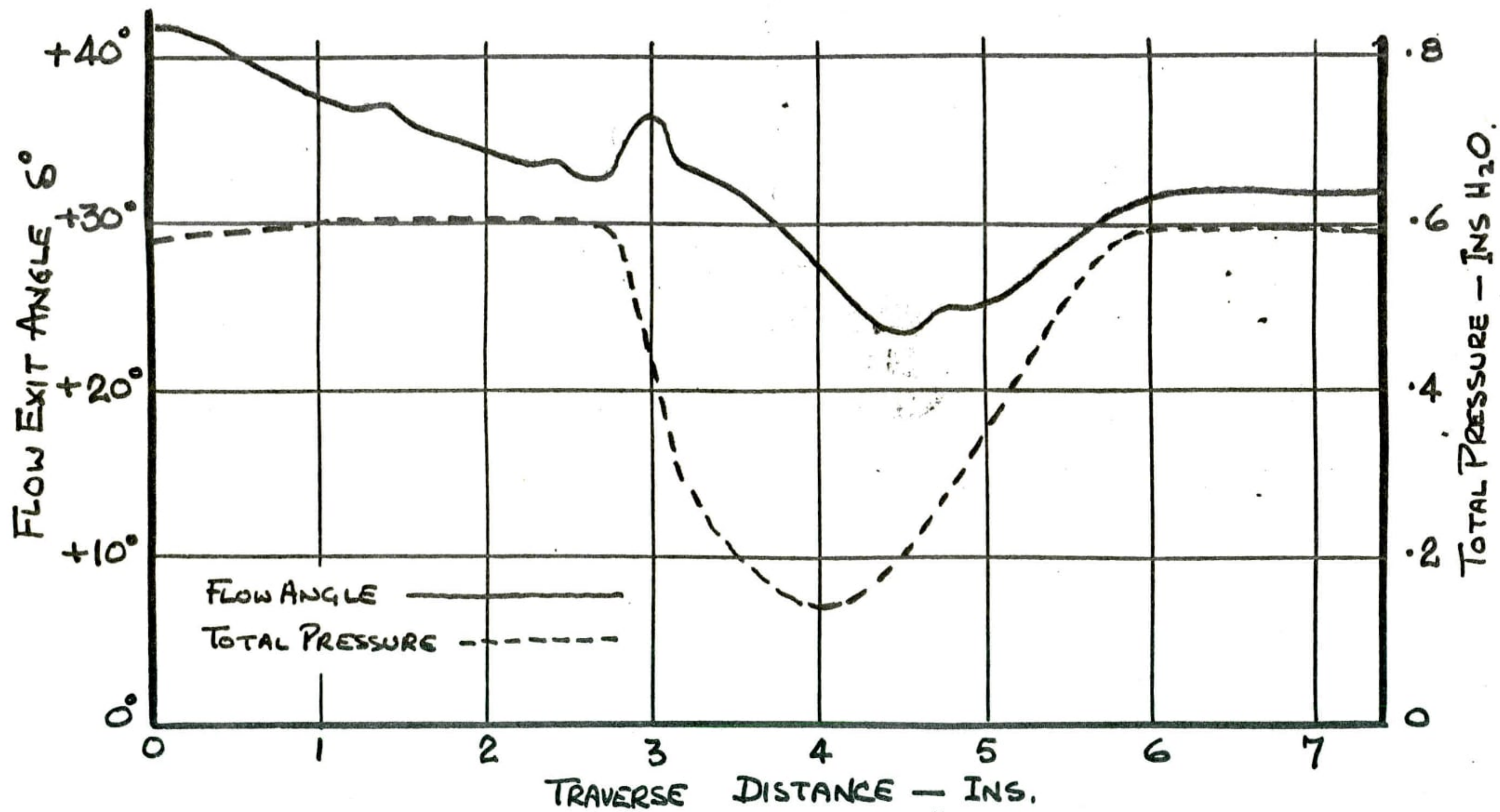

75° CAMBER. 2 SLOTS. BLADE "I". +4° α

I_2

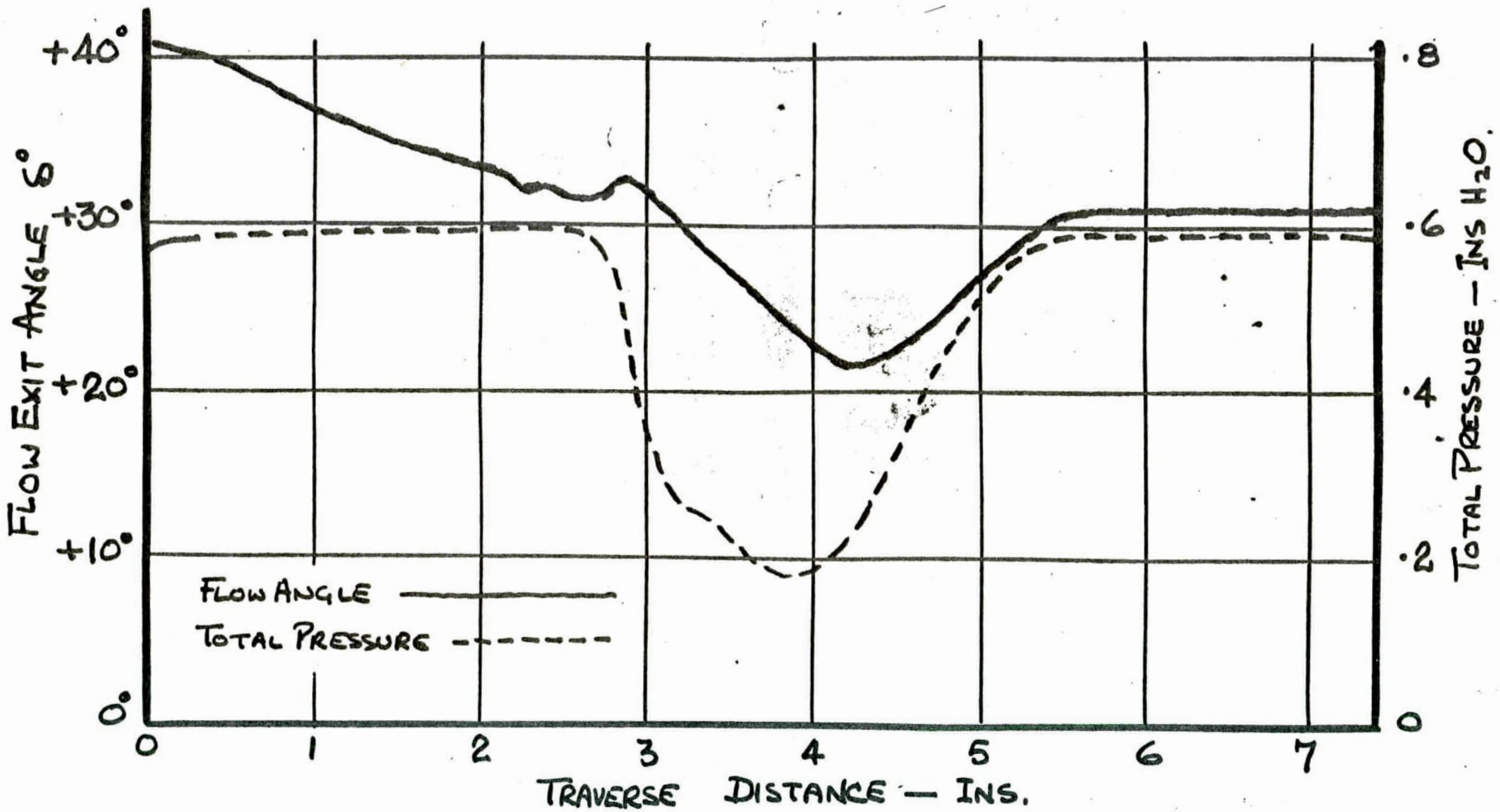

75° CAMBER. 2 SLOTS. BLADE "I". +2°α

I3

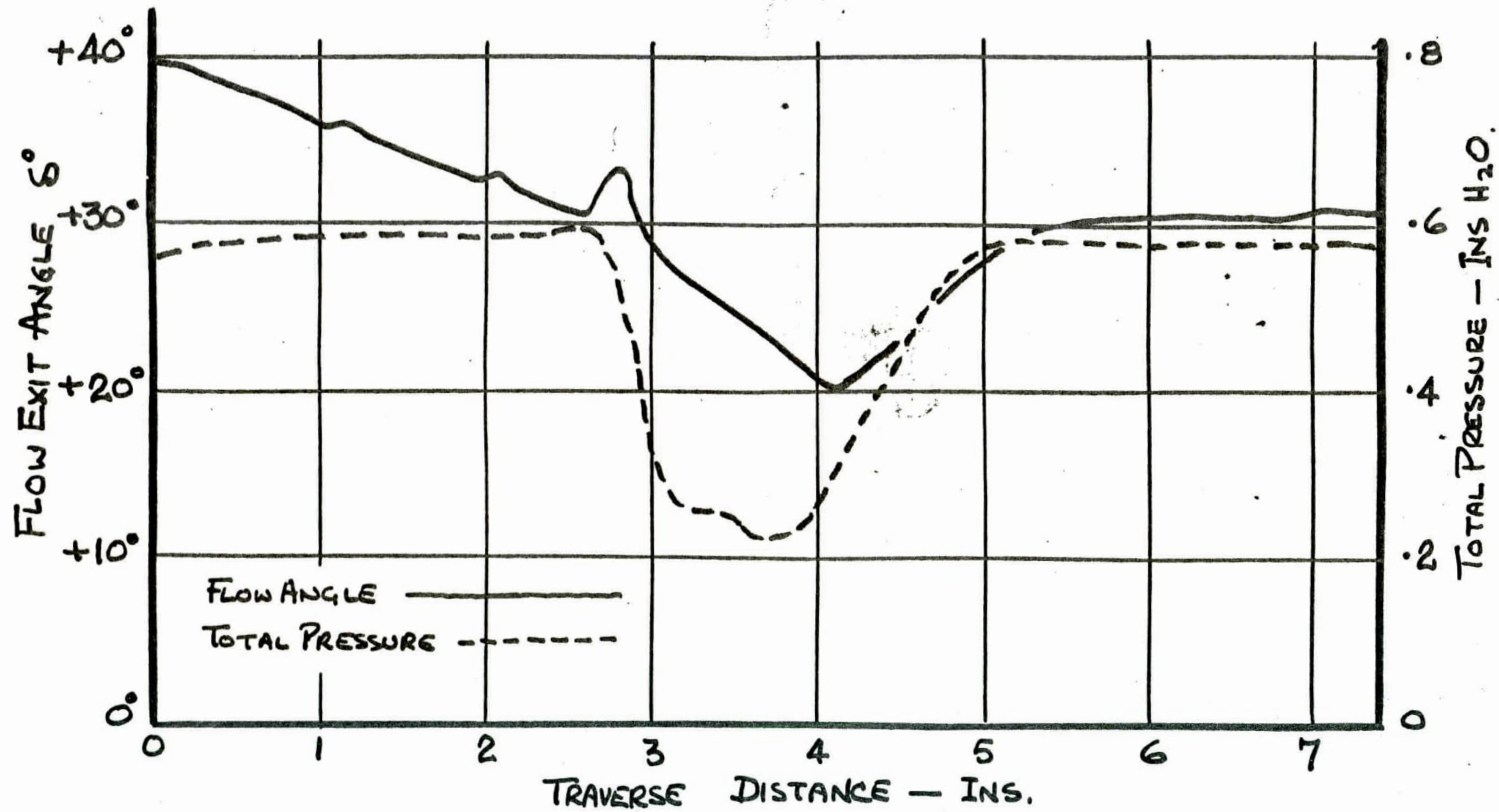

75° CAMBER. 2 SLOTS. BLADE "I". 0° α

I_4

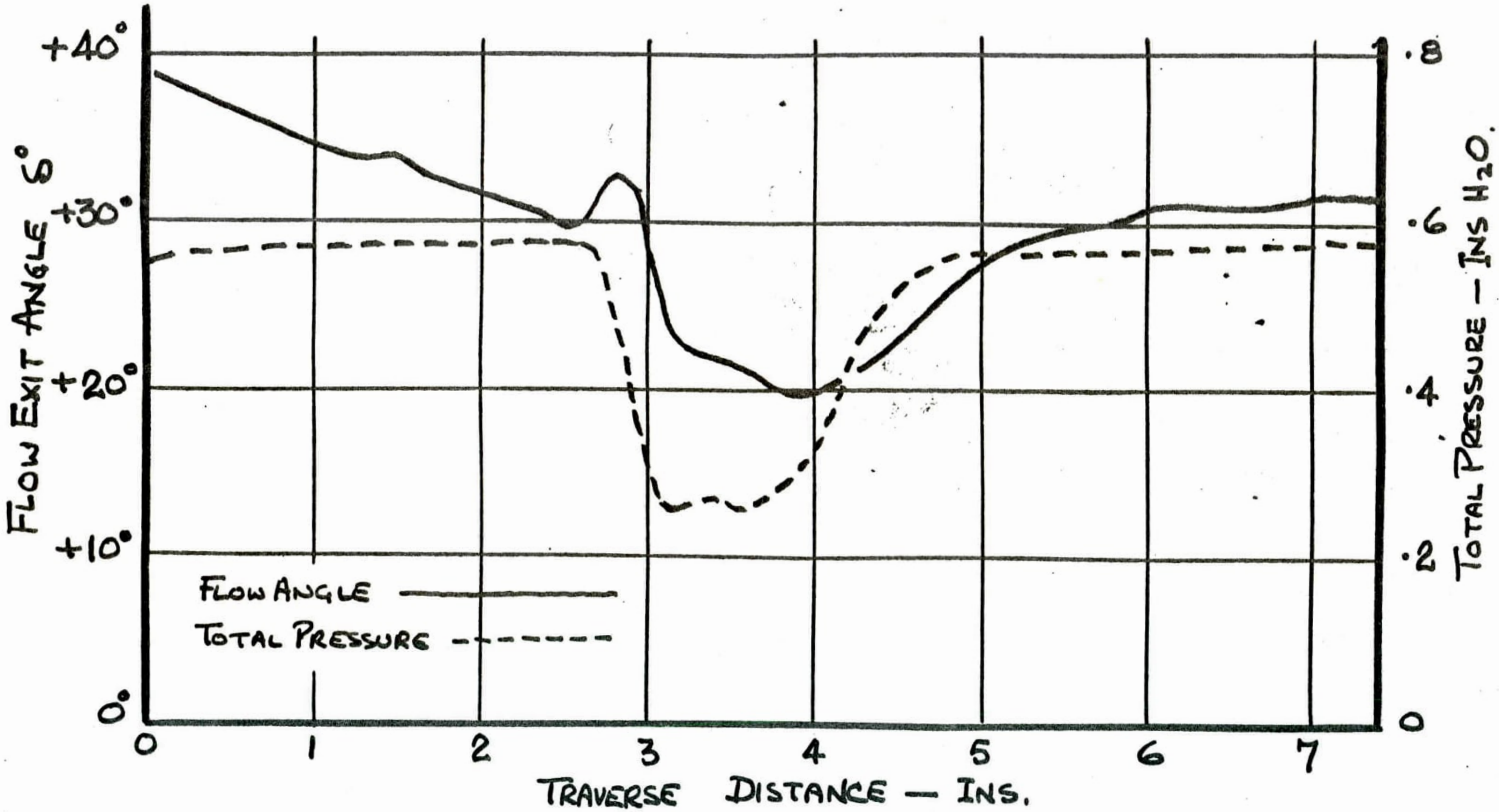

75° CAMBER. 2 SLOTS. BLADE "I". −2° α

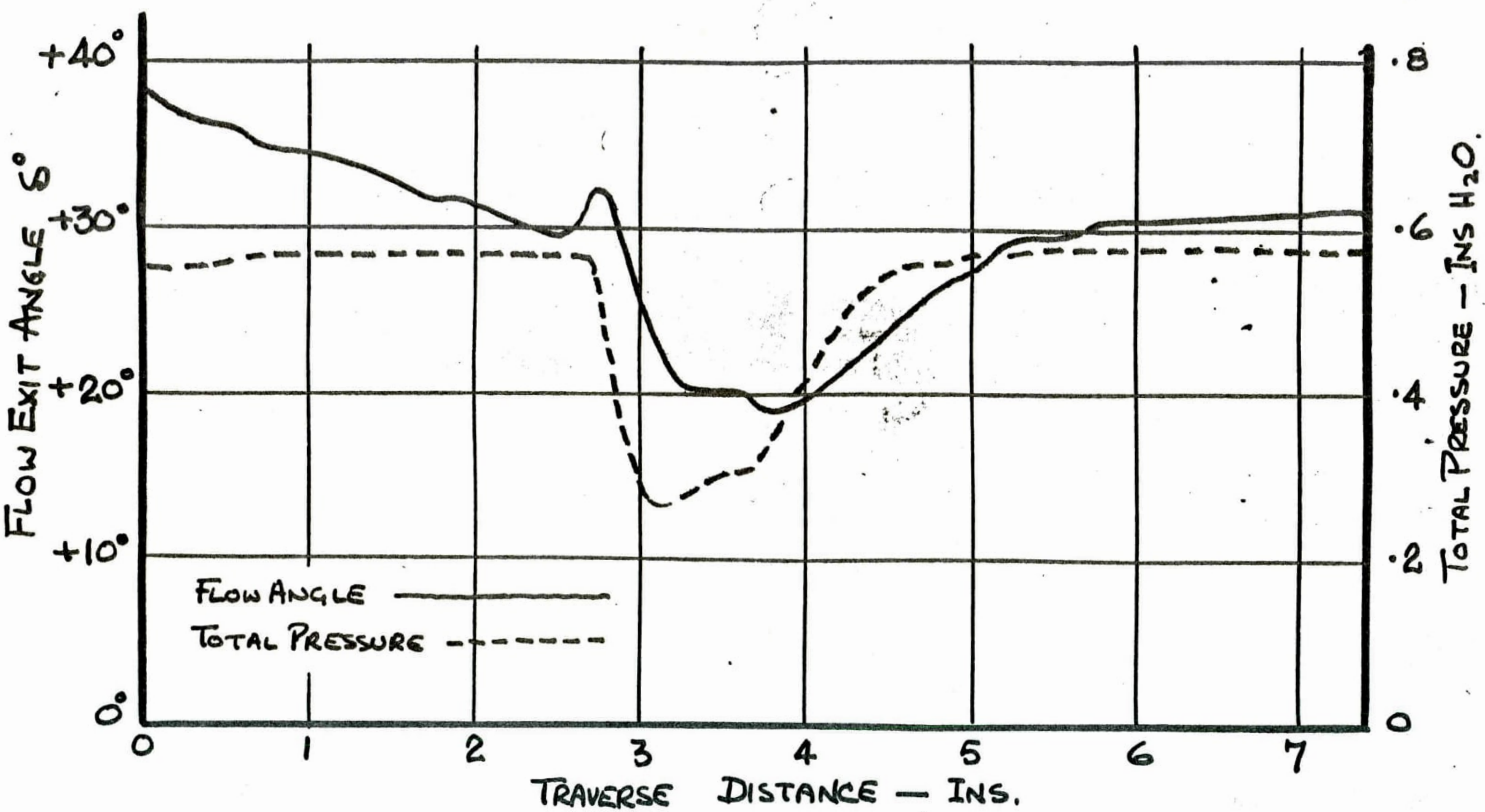

75° CAMBER. 2 SLOTS. BLADE "I". −4° α

BLADE "J" 2 SLOTS

75° CAMBER

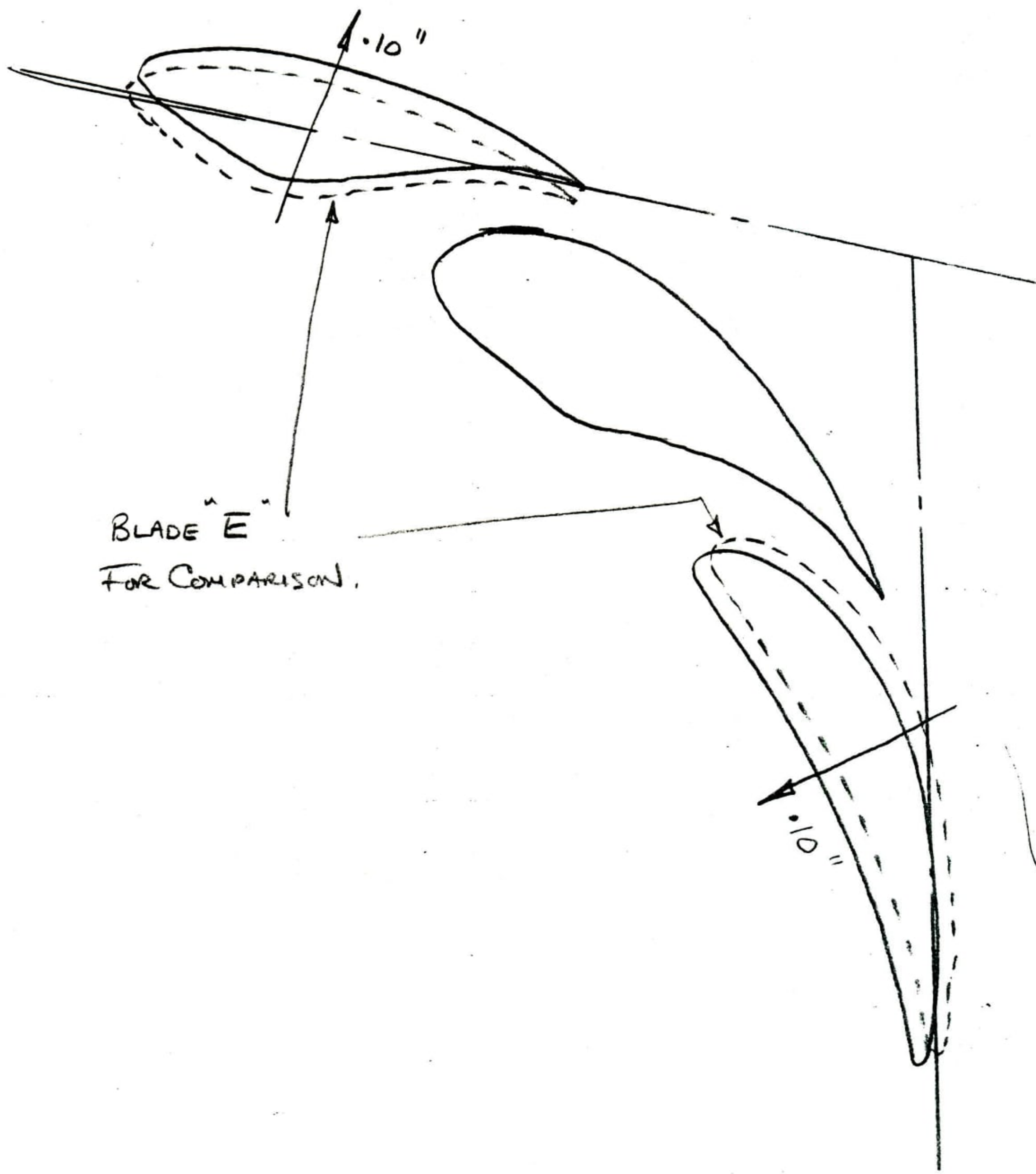

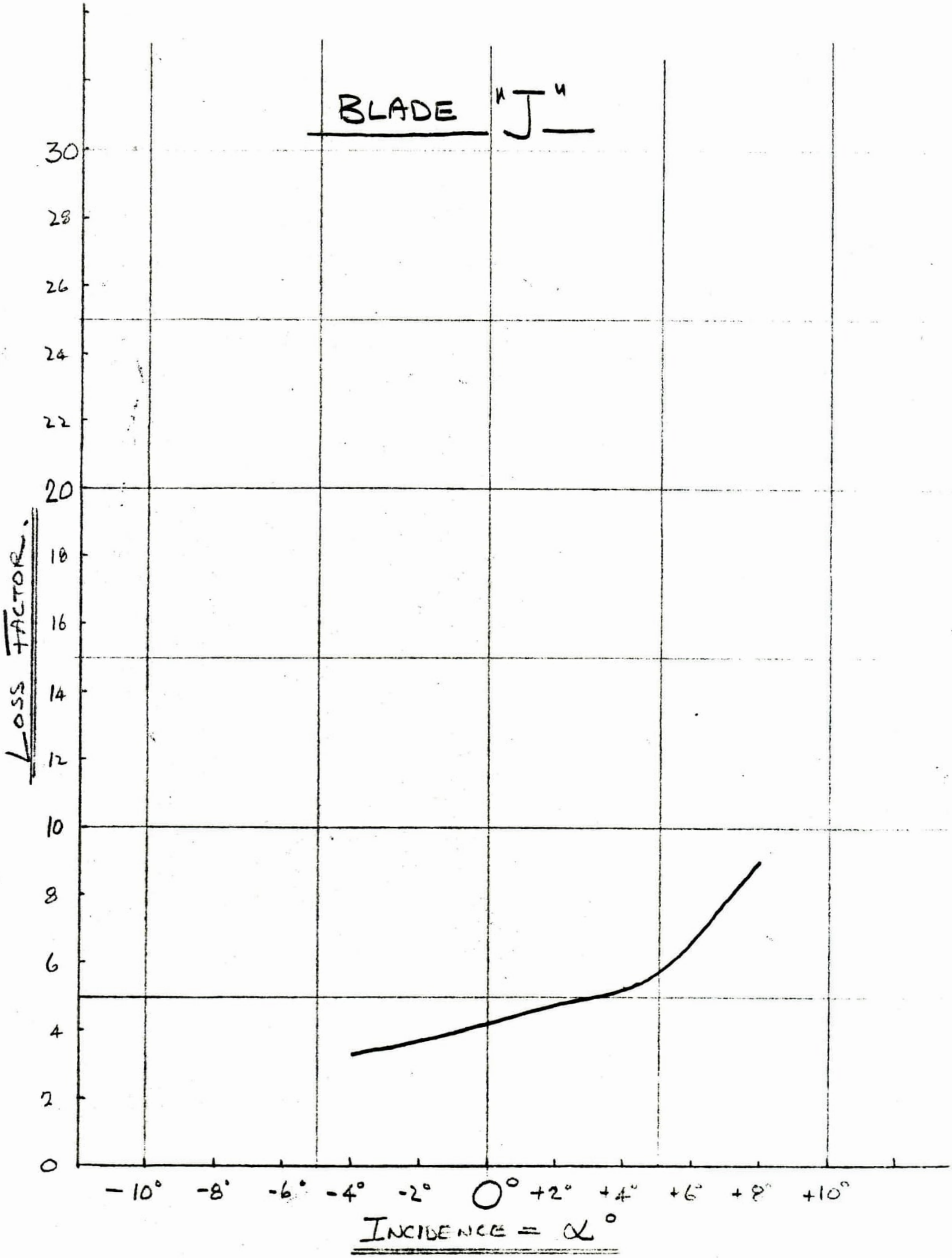
BLADE "J"
LOSS FACTOR
30
28
26
24
22
20
18
16
14
12
10
8
6
4
2
0
-10°
-8°
-6°
-4°
-2°
0°
+2°
+4°
+6°
+8°
+10°
INCIDENCE = α°

Ja

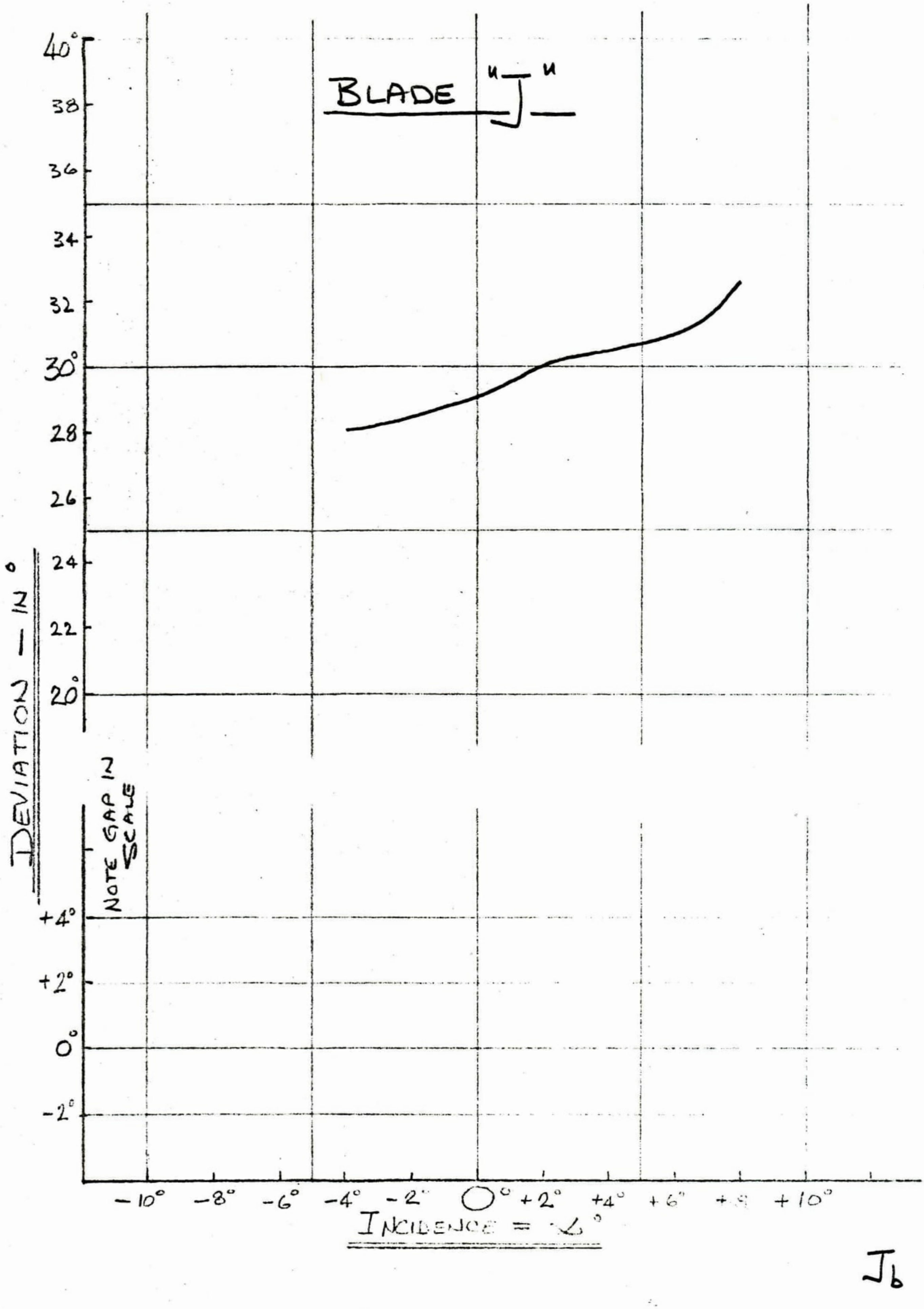

BLADE "J"
40°
38
36
34
32
30°
28
26
24
22
20°
DEVIATION — IN °
NOTE GAP IN SCALE
+4°
+2°
0°
-2°
− 10° −8° −6° −4° − 2° 0° +2° +4° +6° +8 +10°
INCIDENCE = ∠°

Jb

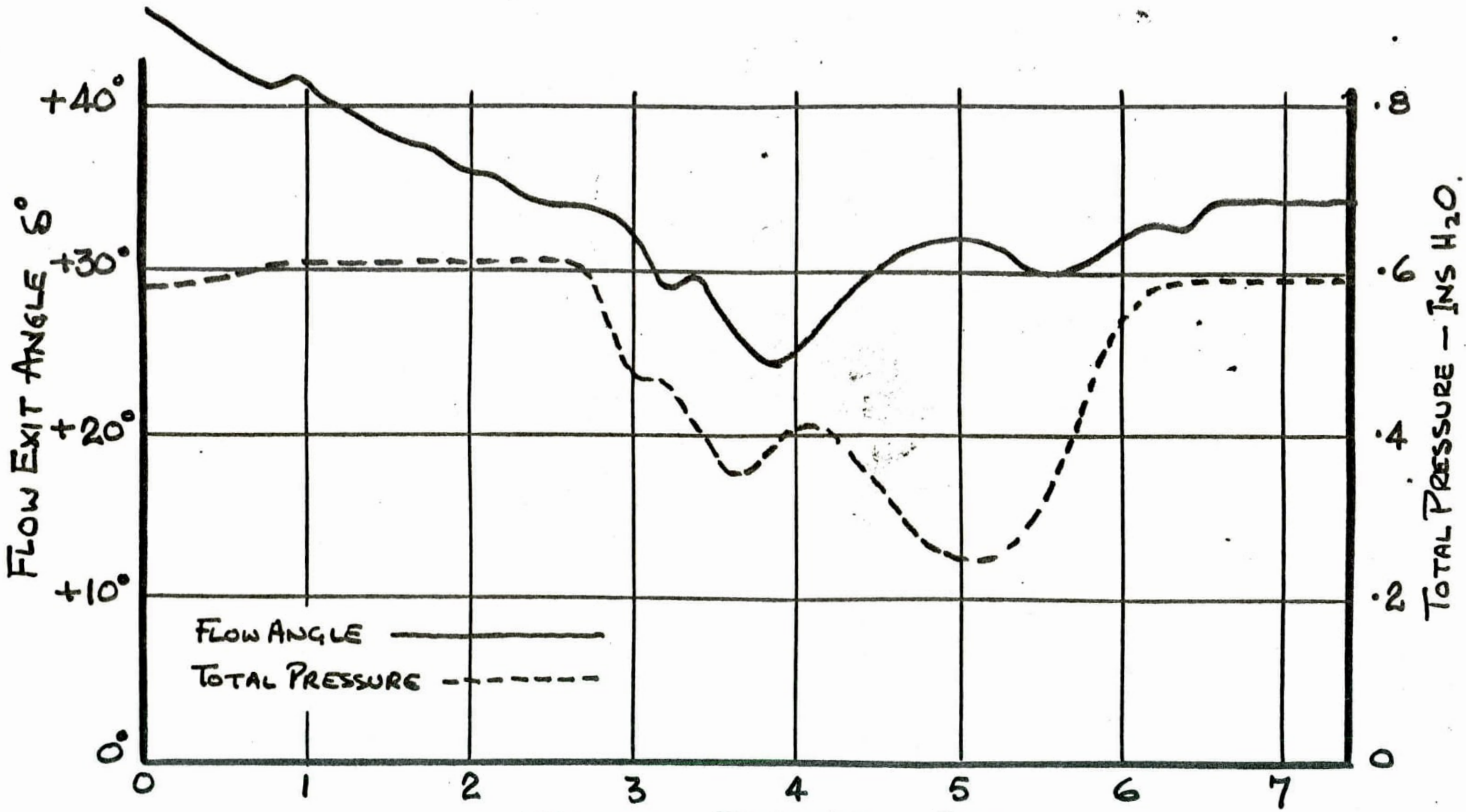

75° CAMBER. 2 SLOTS. BLADE "J". + 8° α

J1

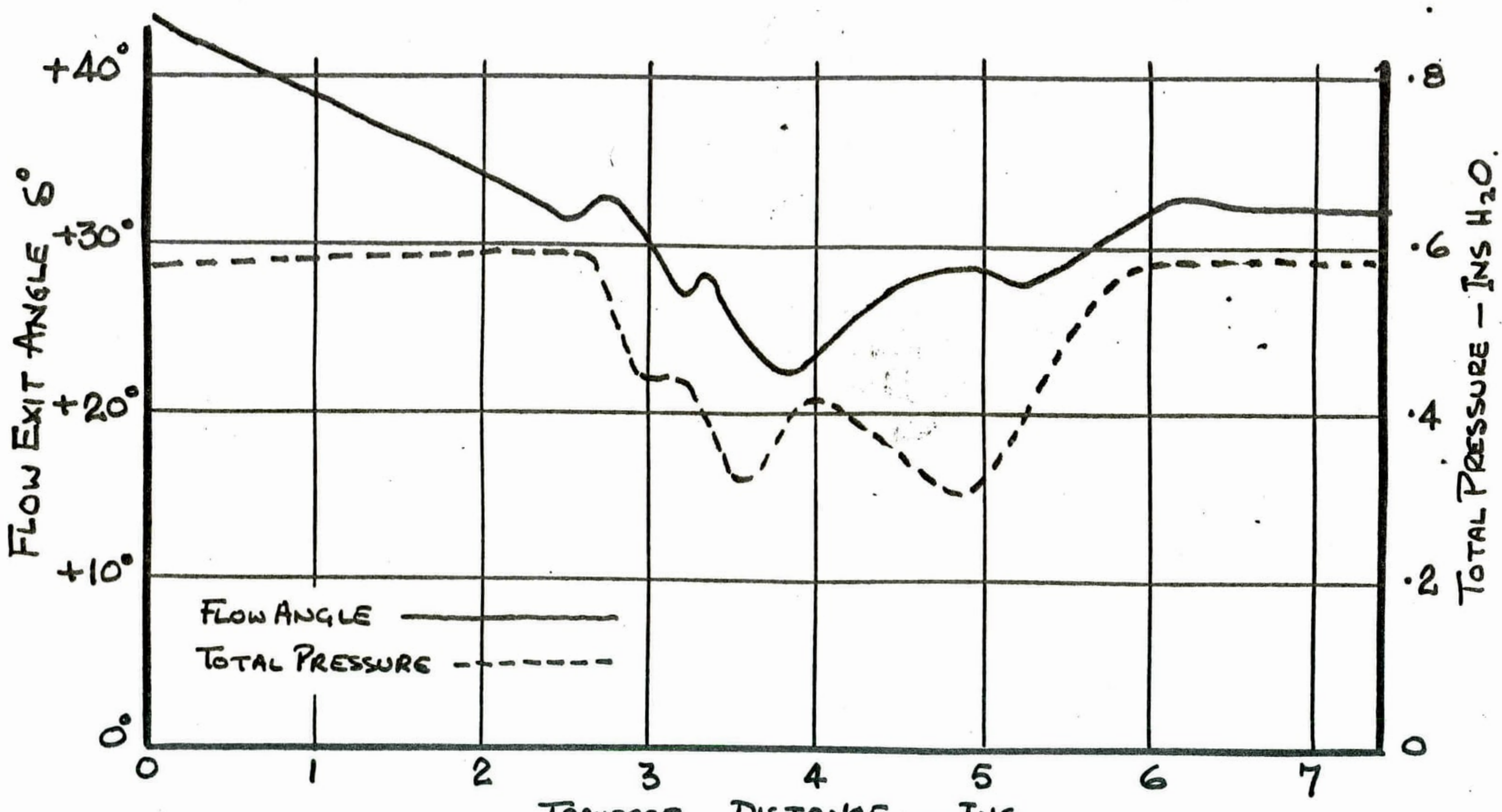

75° CAMBER. 2 SLOTS. BLADE "J". +6 °α

J_2

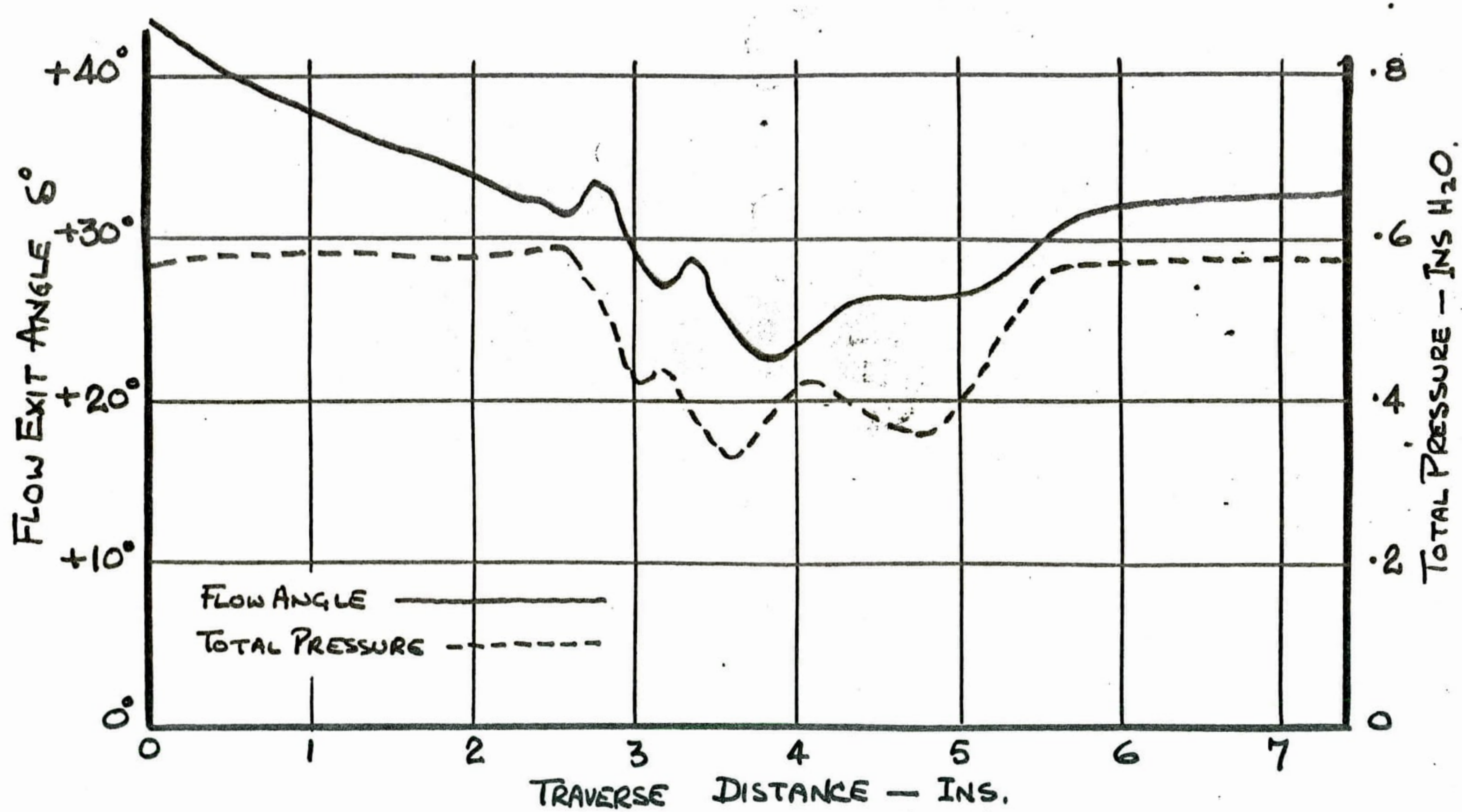

75° CAMBER. 2 SLOTS. BLADE "J". +4.° α

J3

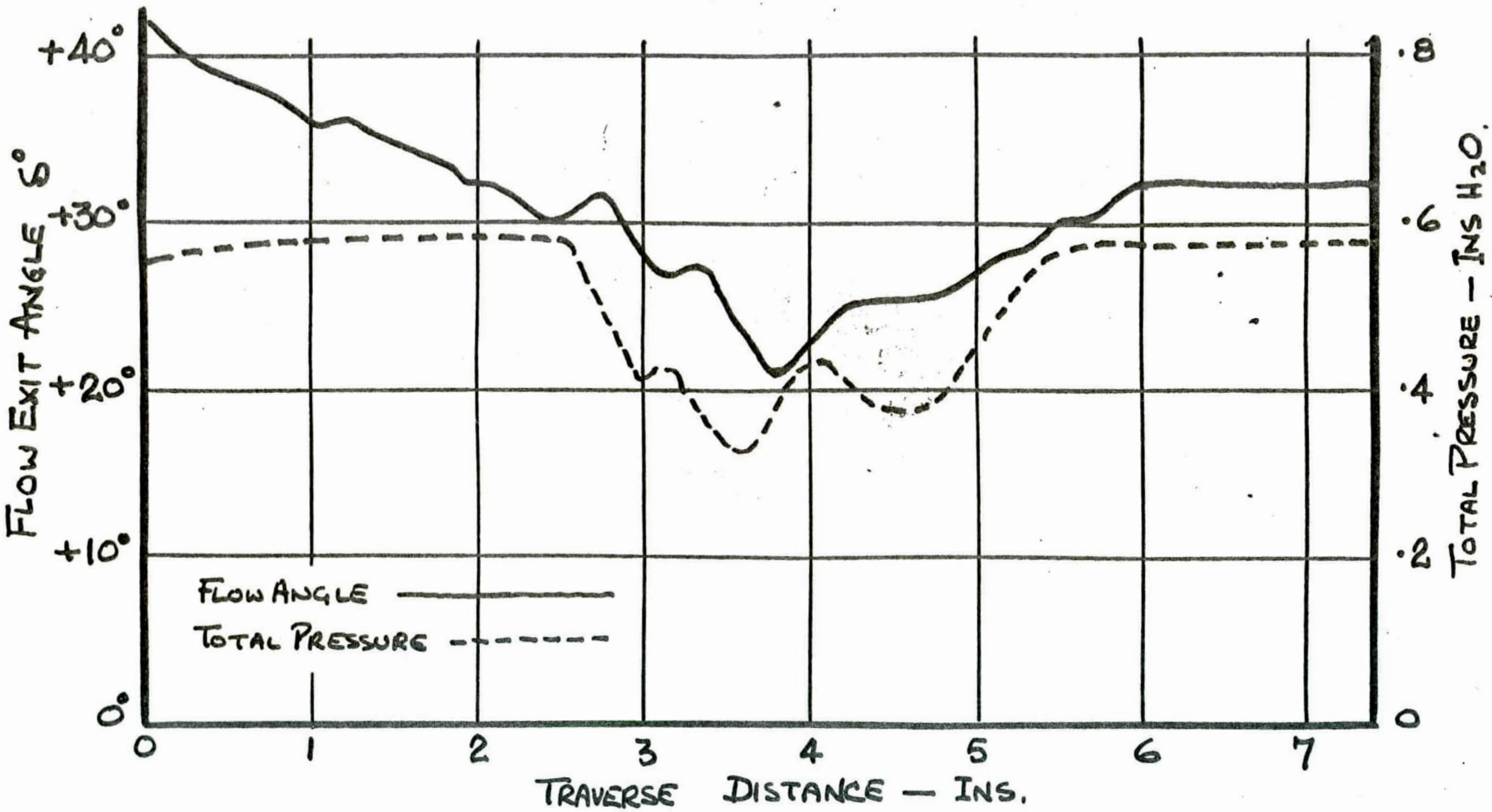

75° CAMBER. 2 SLOTS. BLADE "J". +2° α

J4

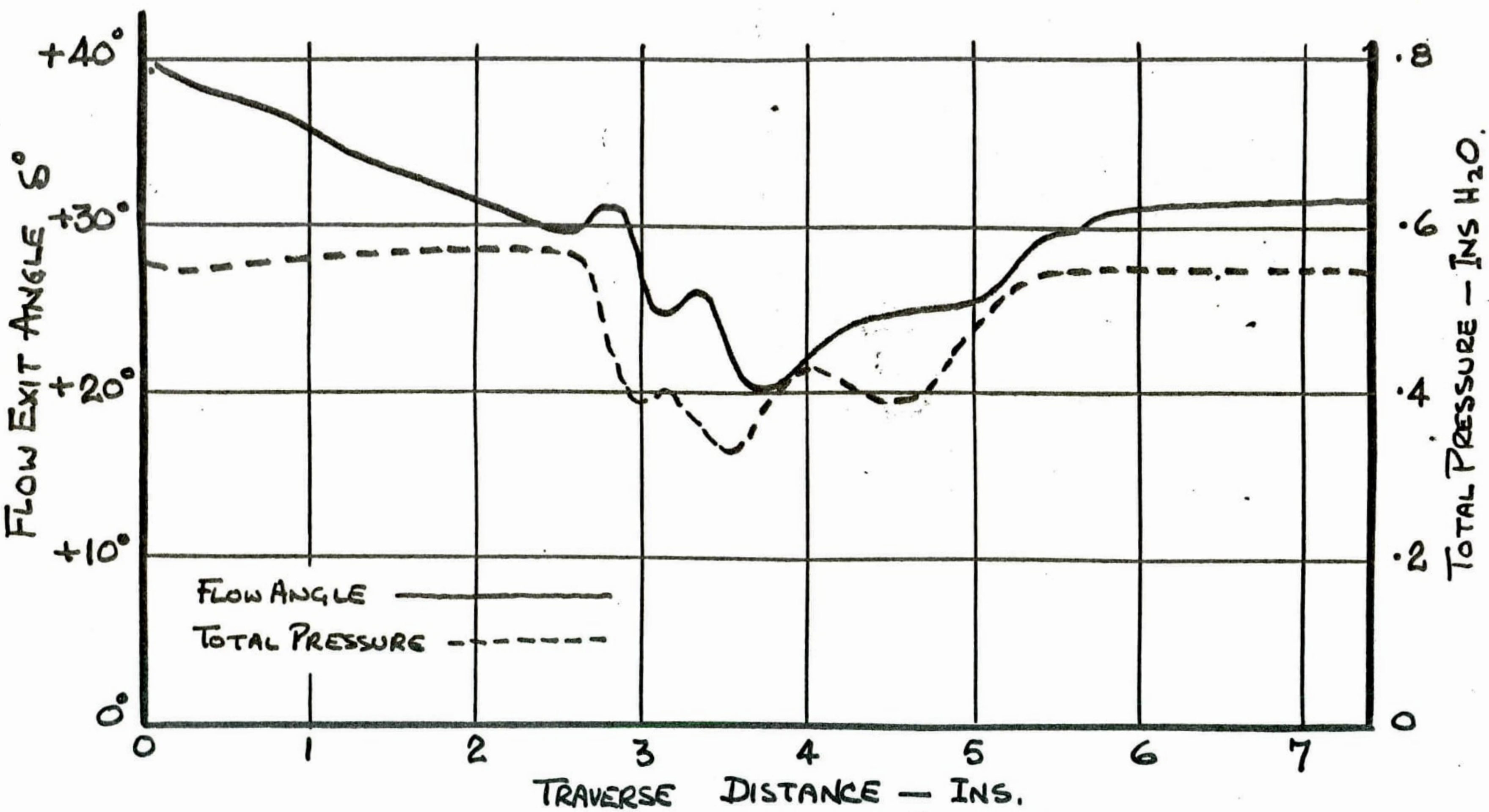

75° CAMBER. 2 SLOTS. BLADE "J". 0 °α

J5

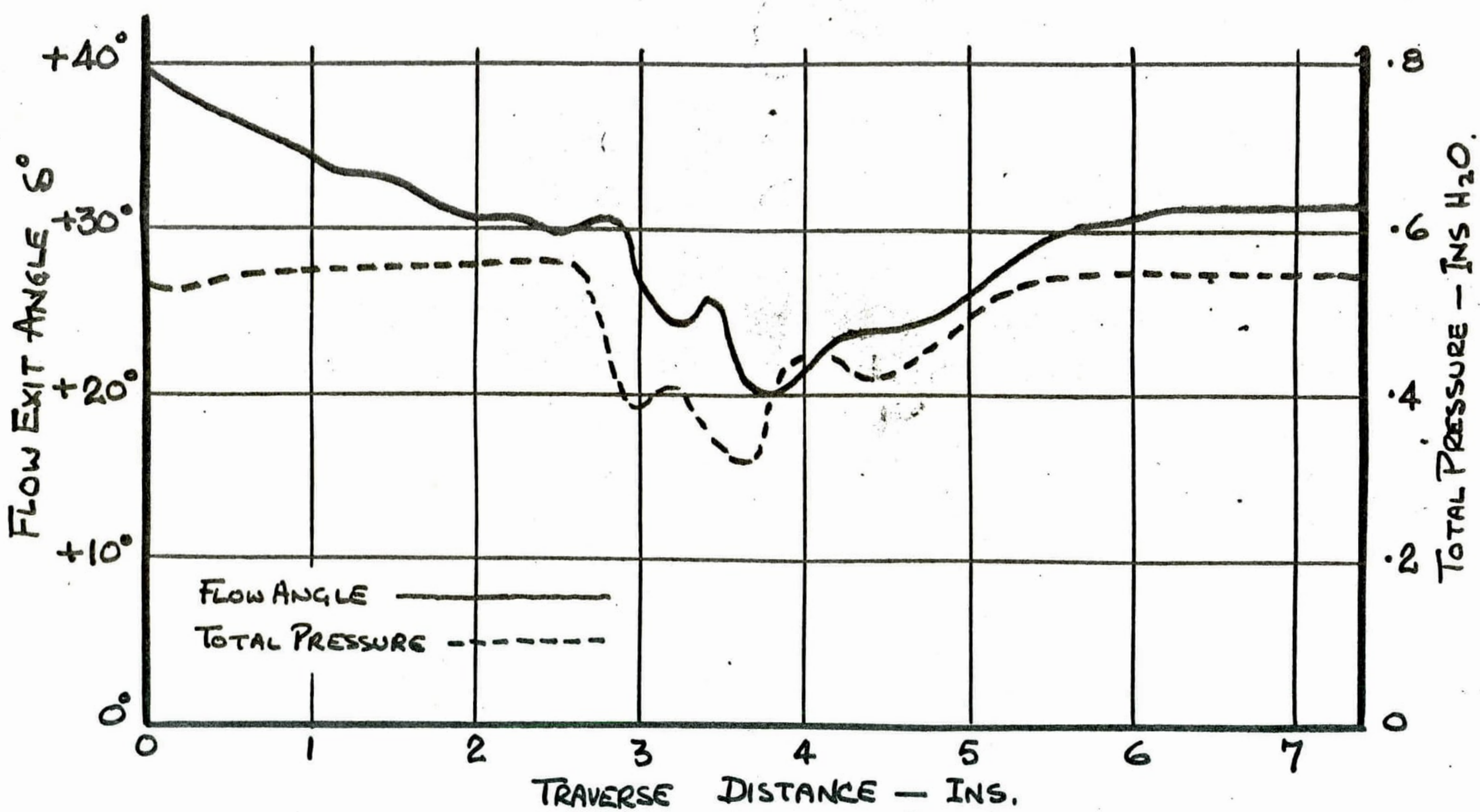

75° CAMBER. 2 SLOTS. BLADE "J". −2° α

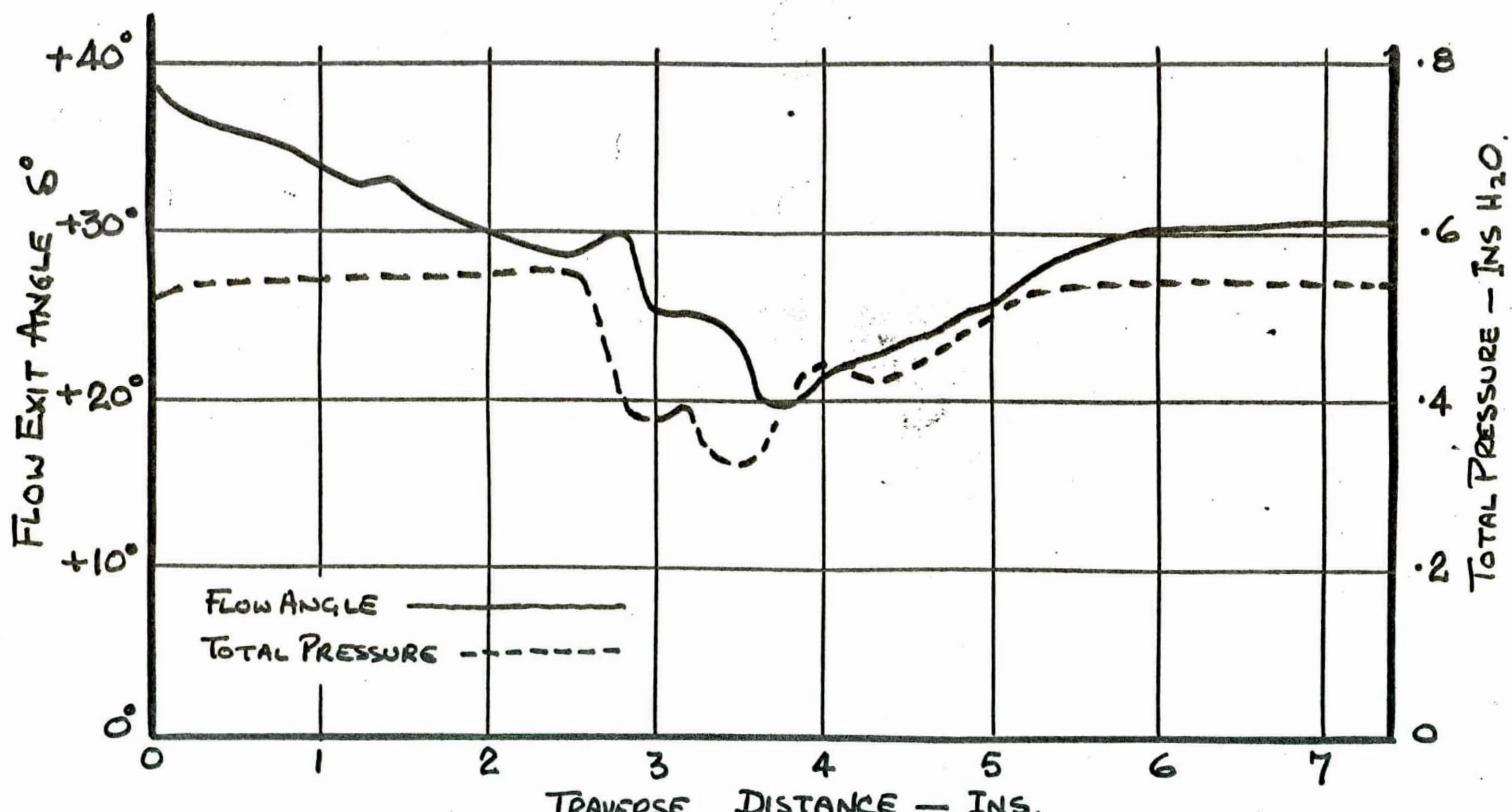

75° CAMBER. 2 SLOTS. BLADE "J". −4° α

J7

BLADE "K" 2 SLOTS.
75° CAMBER.

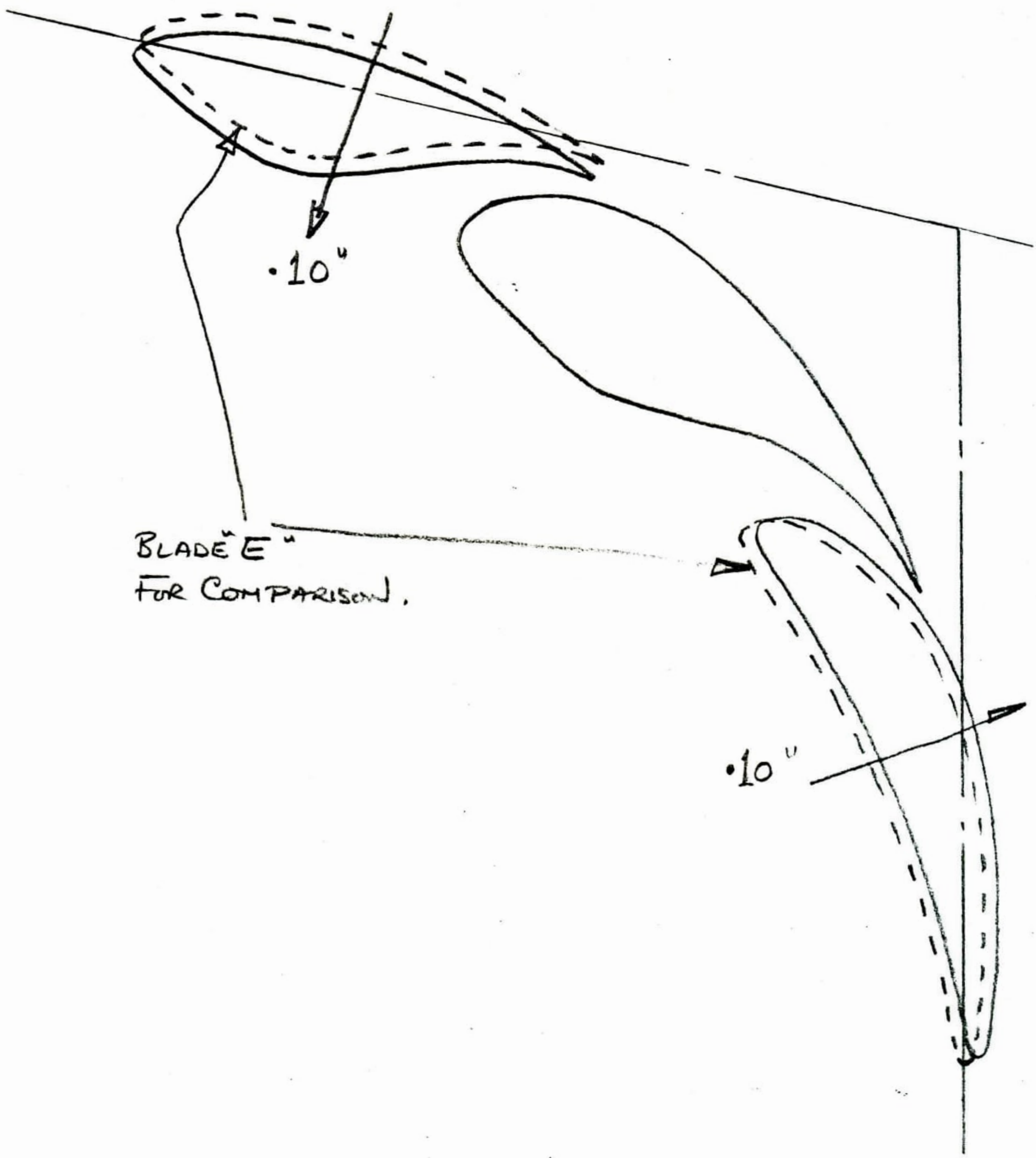

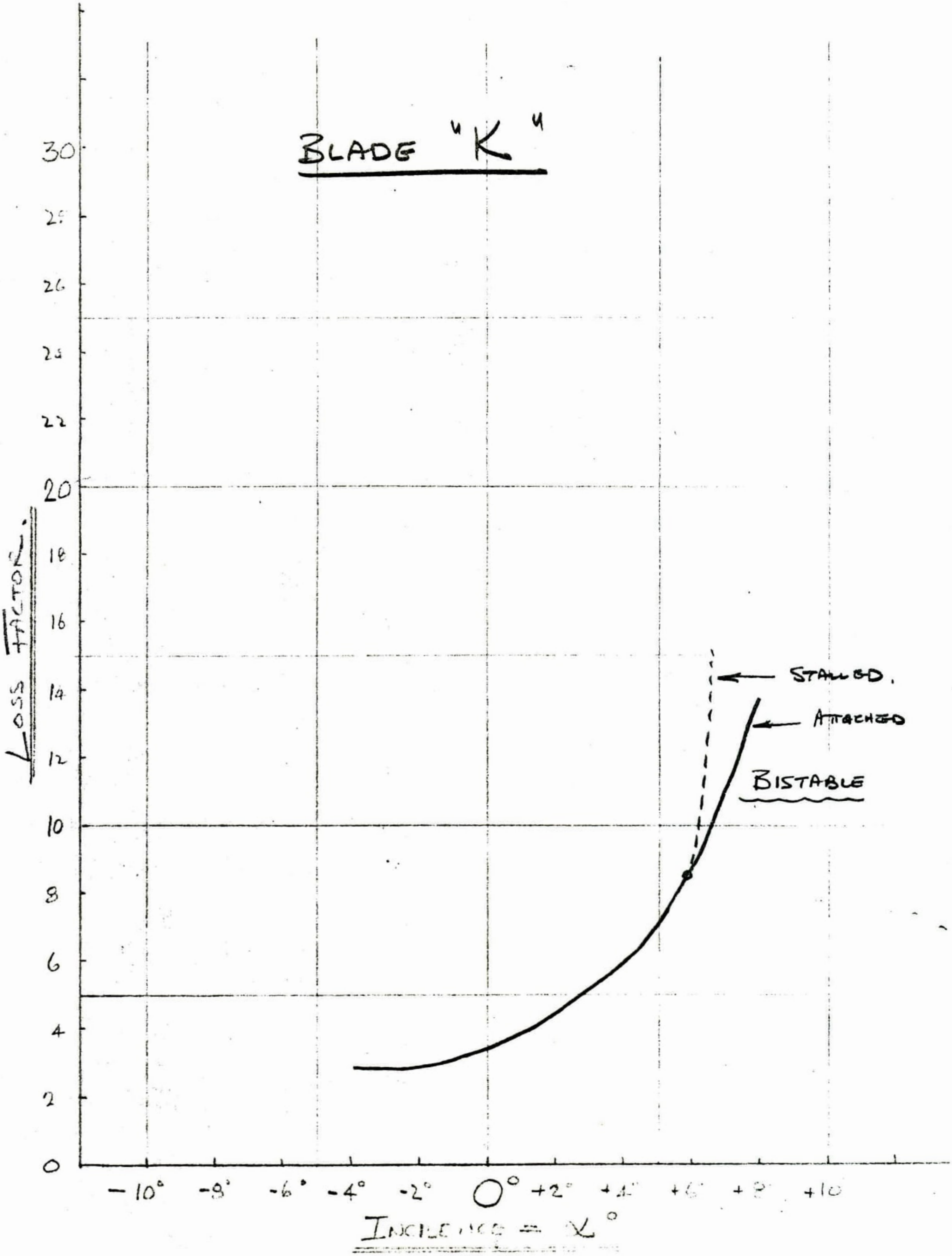
BLADE "K"
LOSS FACTOR.
30
20
18
16
14
12
10
8
6
4
2
0
STALLED.
ATTACHED
BISTABLE
− 10°
-8°
-6°
-4°
-2°
0°
+2°
+10
INCIDENCE = α°

Ka

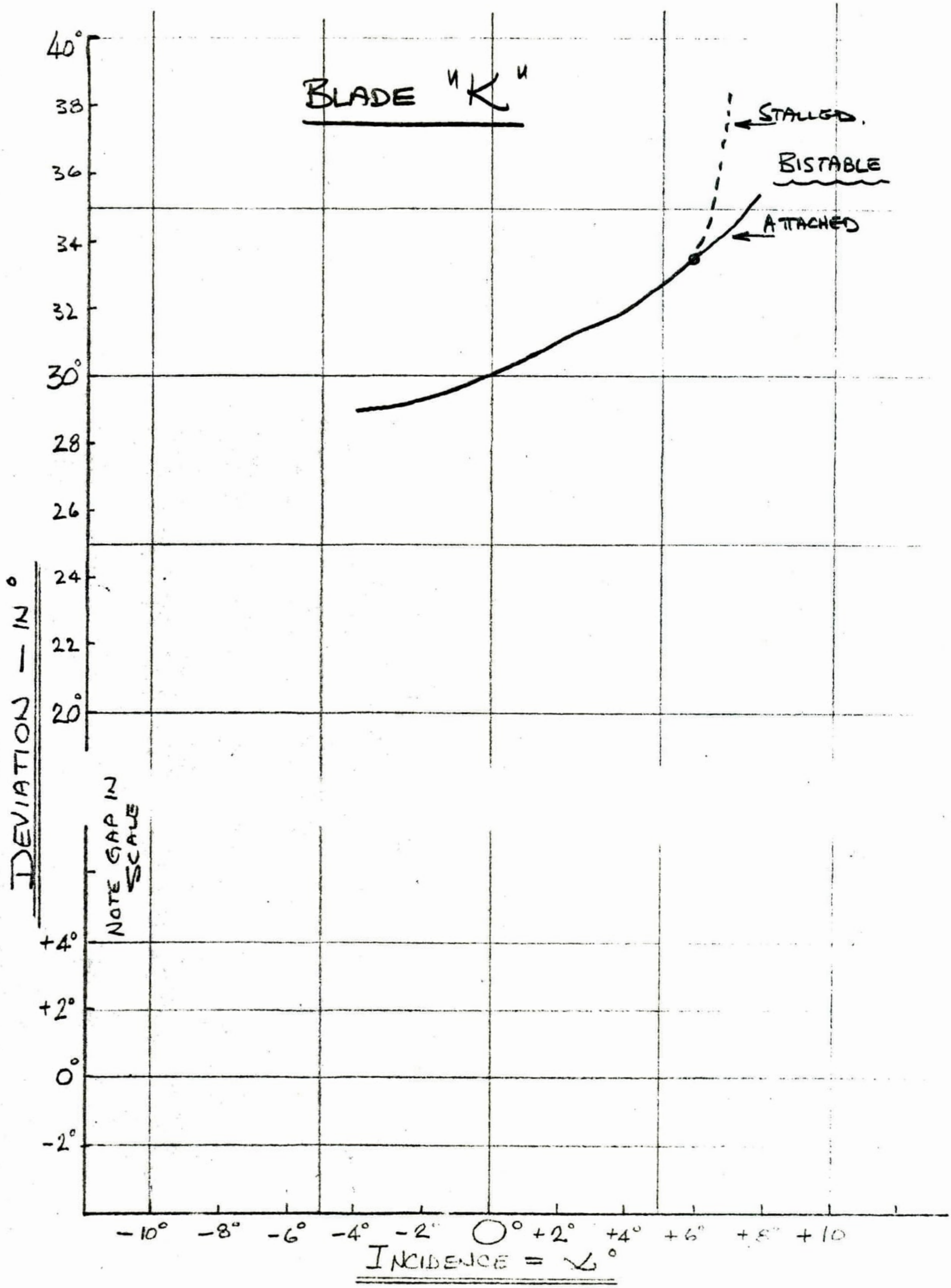

BLADE "K"
STALLED.
BISTABLE
ATTACHED
40°
38
36
34
32
30°
28
26
24
22
20°
DEVIATION – IN °
NOTE GAP IN SCALE
+4°
+2°
0°
-2°
-10°
-8°
-6°
-4°
-2°
0°
+2°
+4°
+6°
+8°
+10
INCIDENCE = ∠ °

Kb

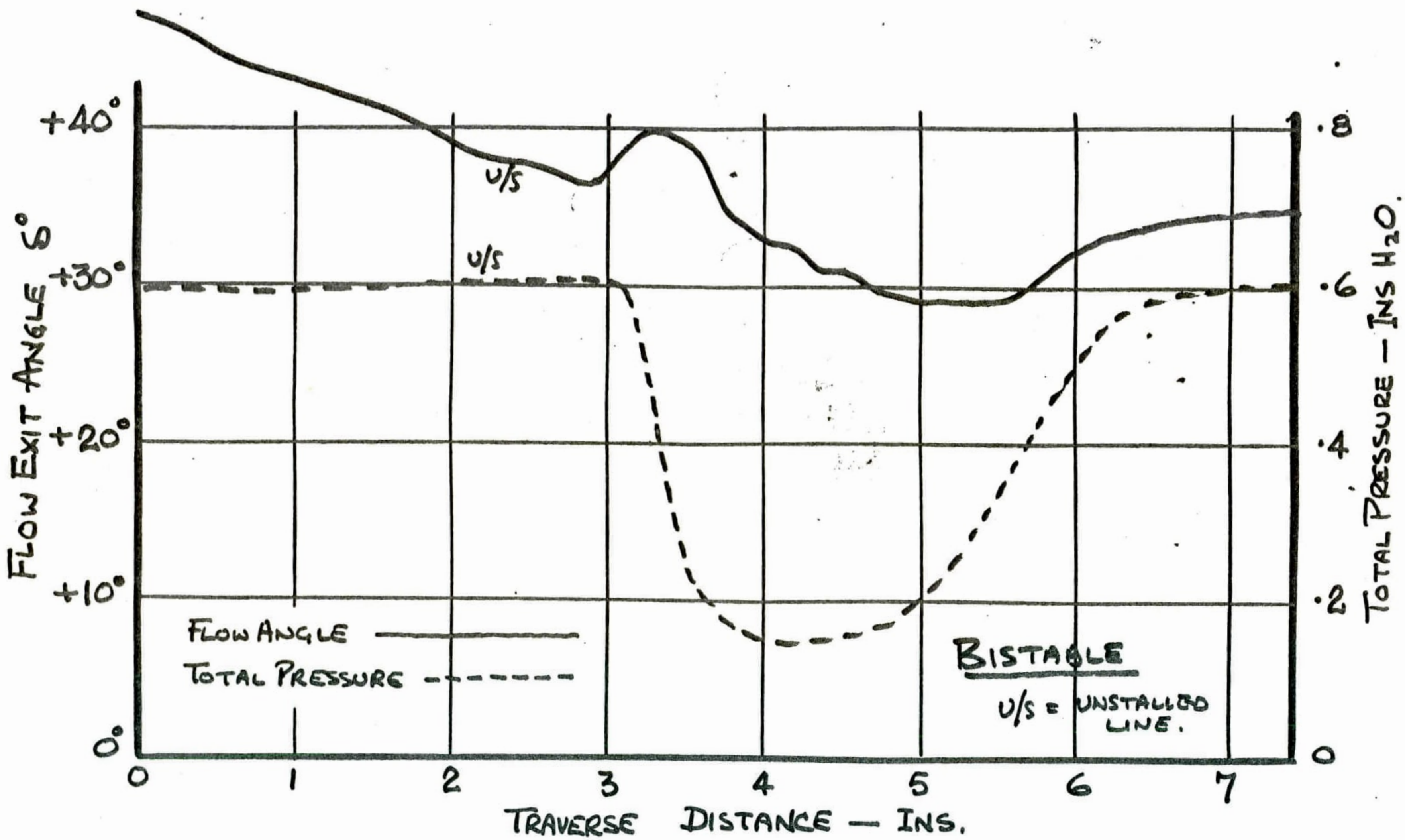

75° CAMBER. 2 SLOTS. BLADE "K". +8° α

K1

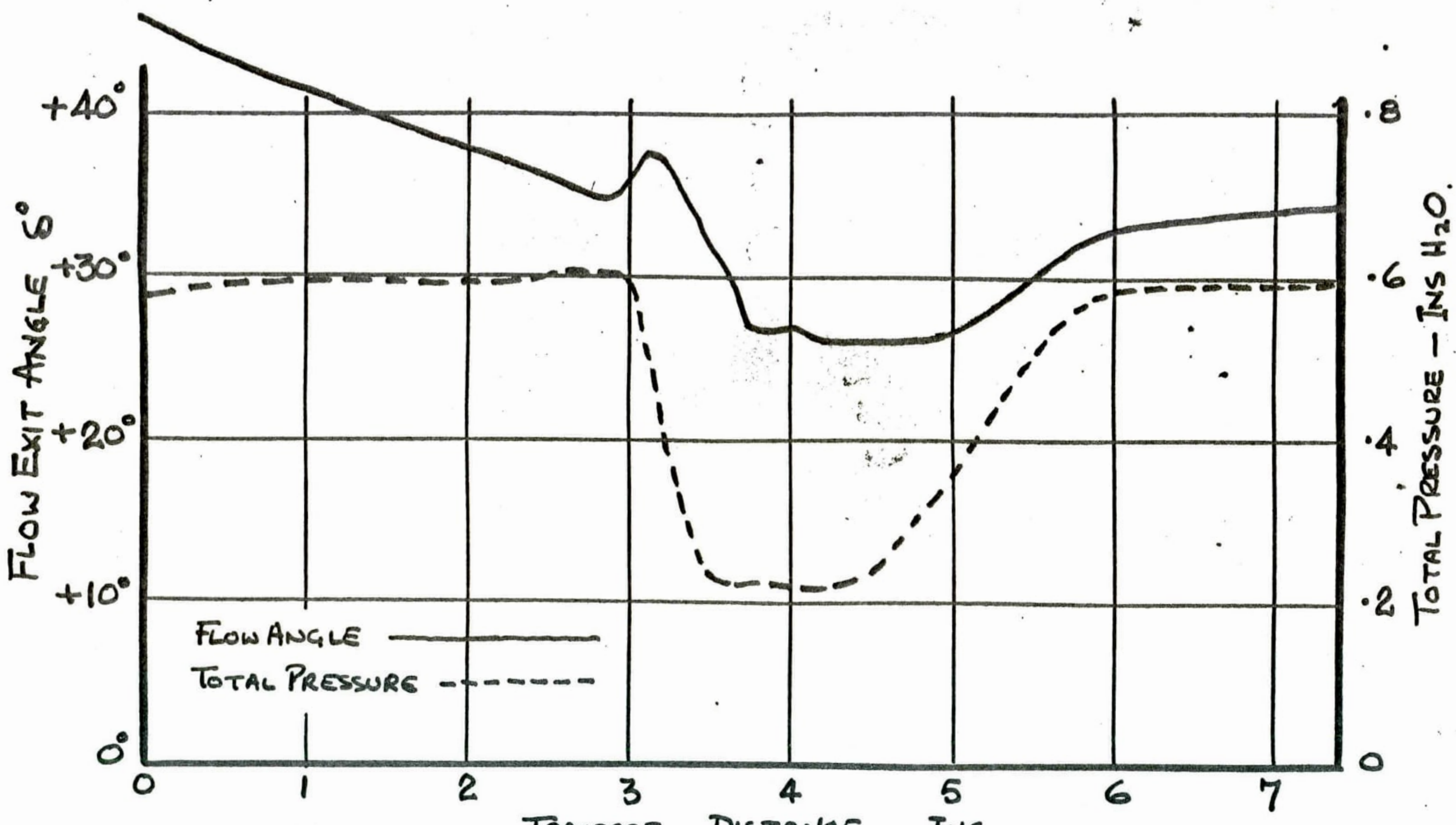

75° CAMBER. 2 SLOTS. BLADE "K". +6° α

K2

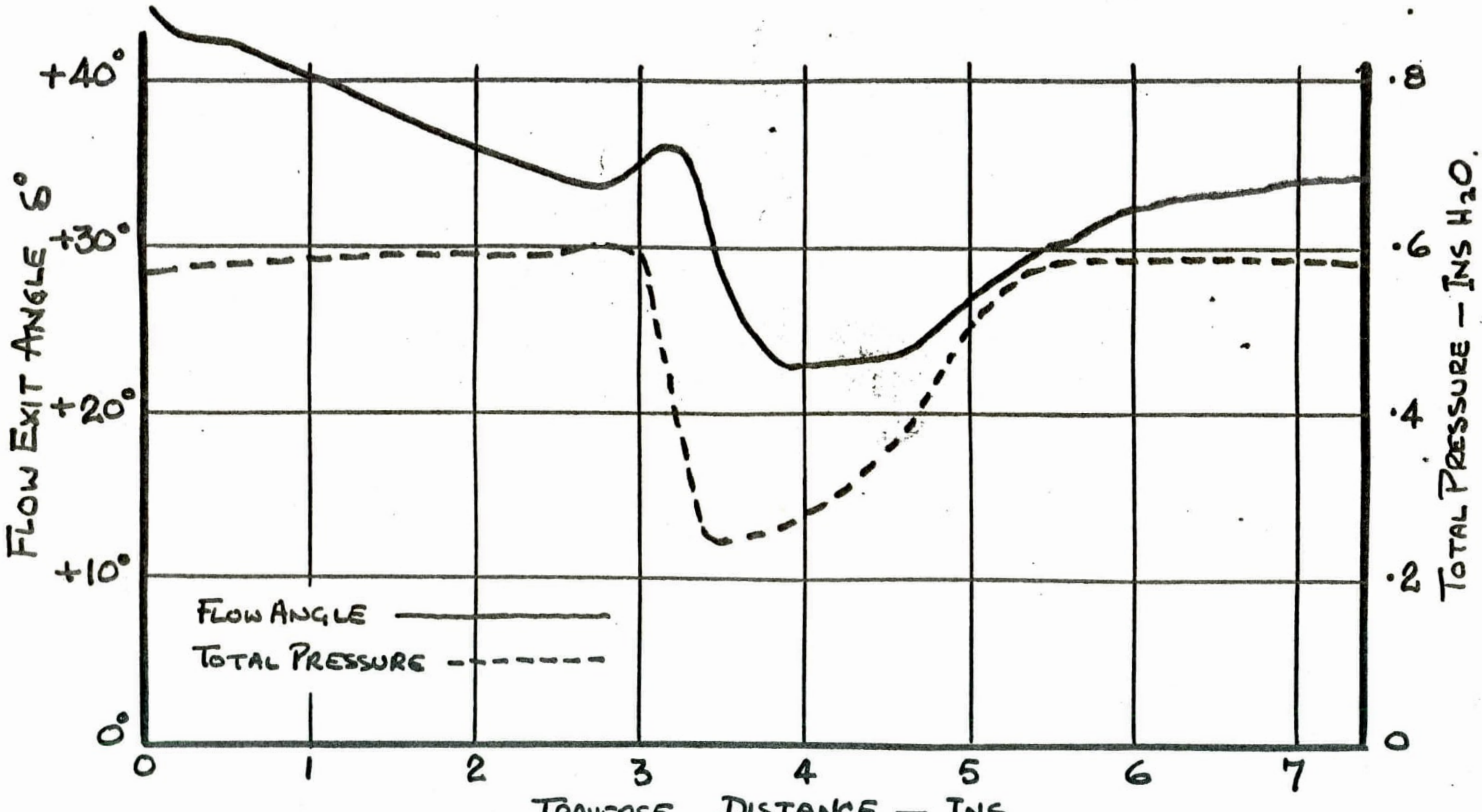

75° CAMBER. 2 SLOTS. BLADE "K". +4° α

K3

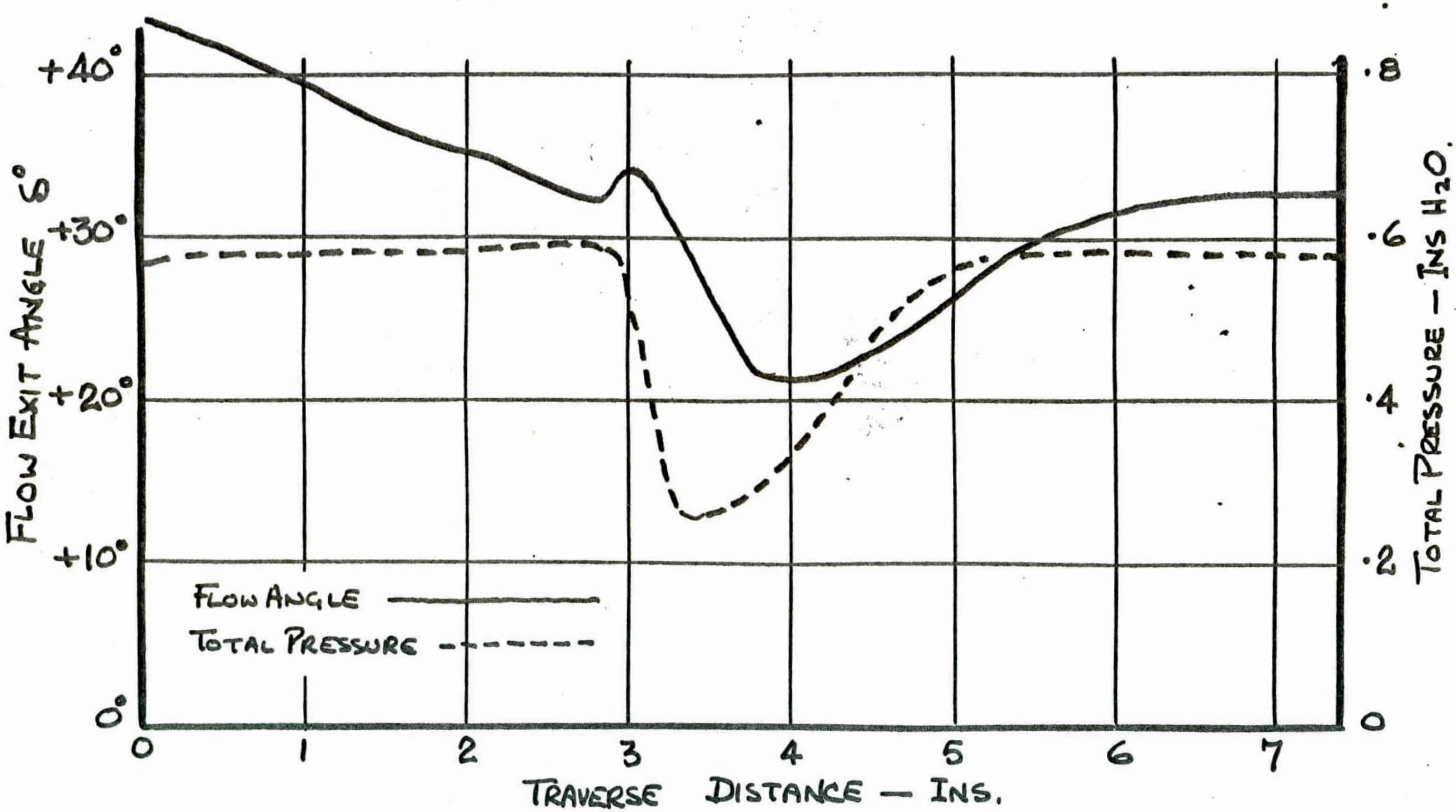

75° CAMBER. 2 SLOTS. BLADE "K". +2° α

K4

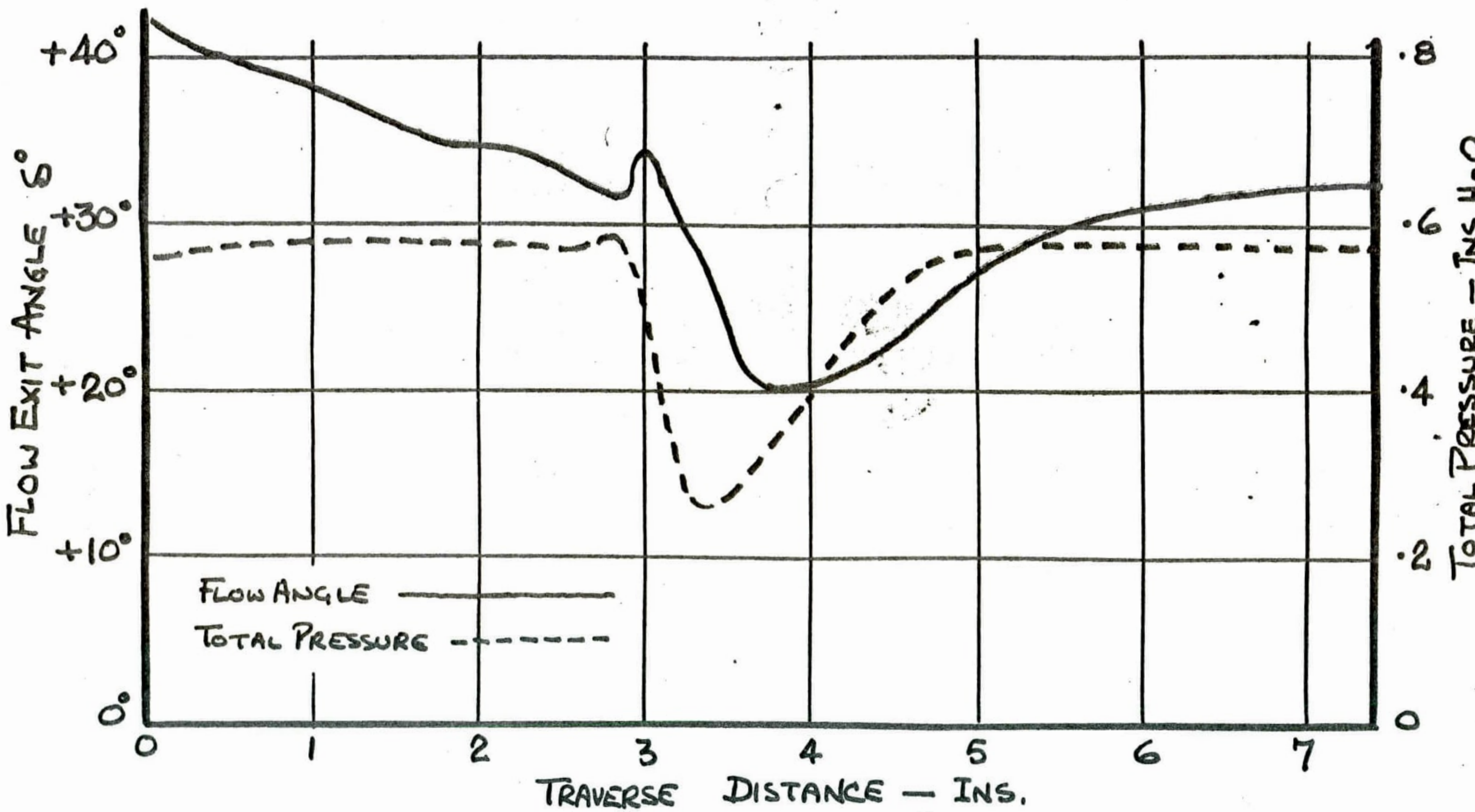

75° CAMBER. 2 SLOTS. BLADE "K". 0 °α

K5

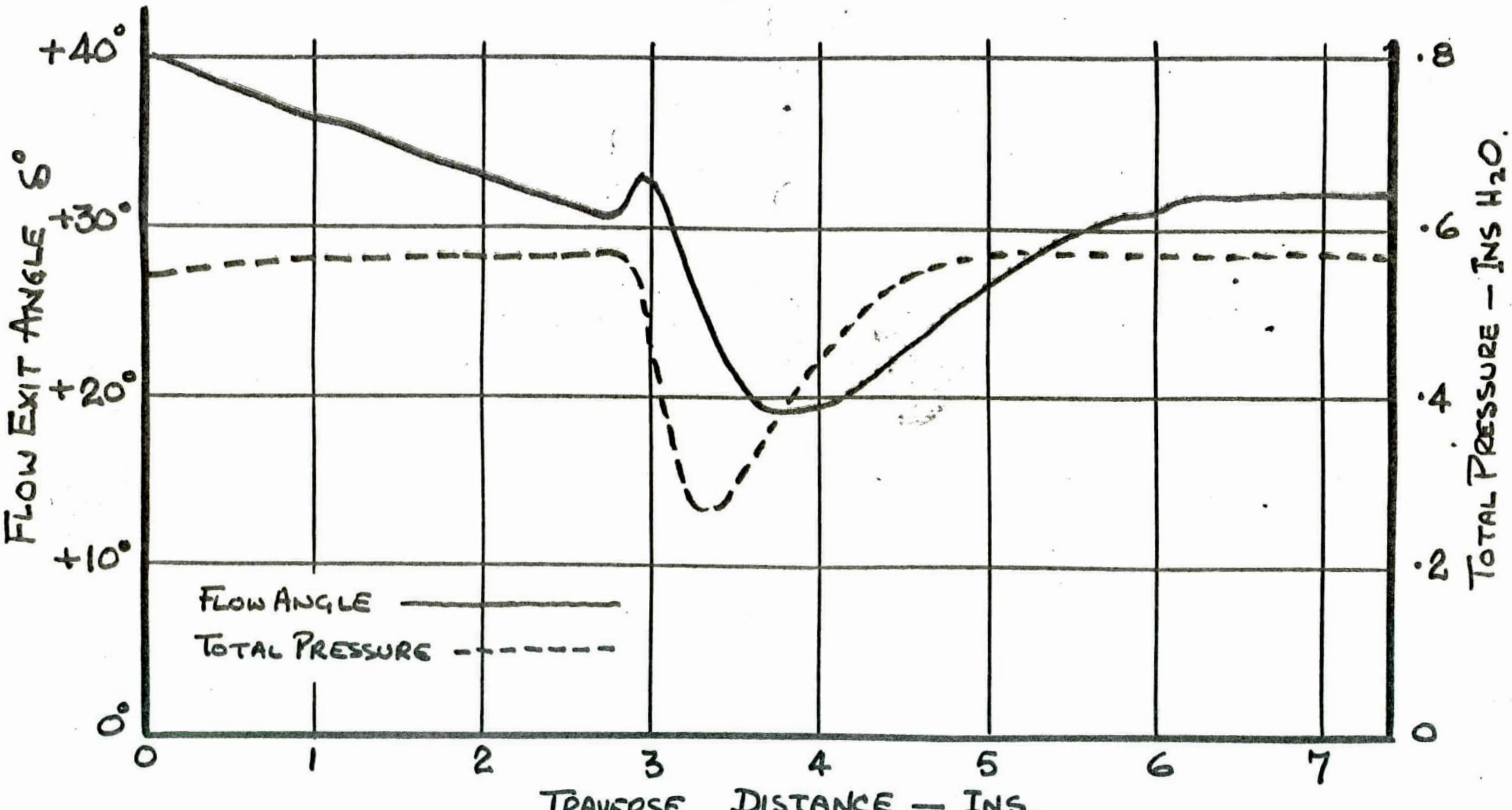

75° CAMBER. 2 SLOTS. BLADE "K". −2°α

K6

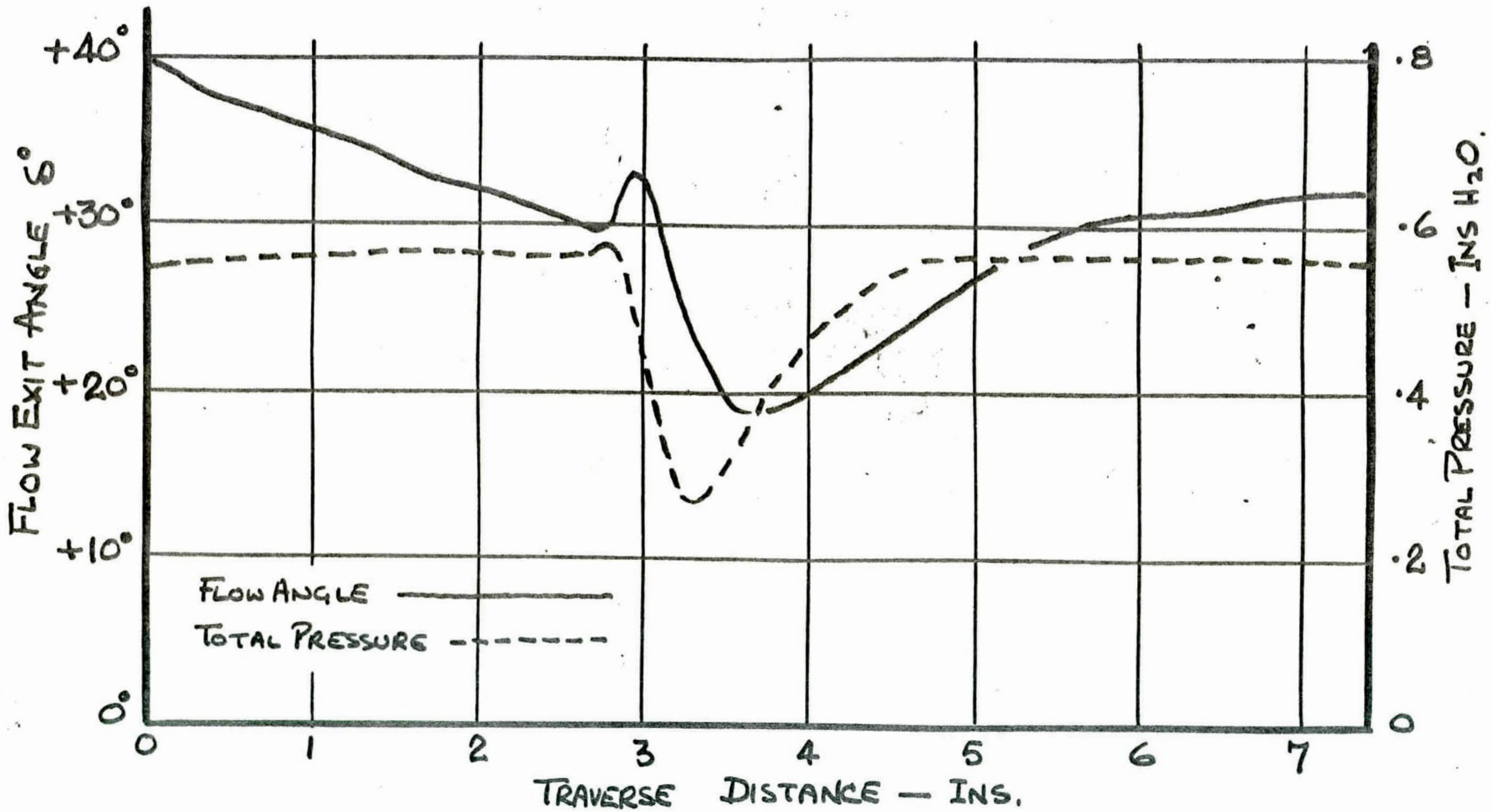

75° CAMBER. 2 SLOTS. BLADE "K". −4°α